Chapter 1

Introduction and Literature Review

1.1 Introduction

1.1.1 Significance of this topic

The global soil carbon pool (2500 gigatons [Gt]) is 3.3 times the size of the atmospheric pool (760 Gt) and 4.5 times that of the biotic pool (560 Gt; Lal et al., 2004). Organic carbon represents approximately 60% of global soil carbon (Six et al., 2006), and at least 50% of this carbon has traditionally been categorized as the chemically resistant component known as humic substances (HS; Otto et al., 2005). Therefore, soil organic matter (SOM) contains huge amounts of carbon and plays an important role in regulating anthropogenic changes to the global carbon cycle. It also plays essential roles in soil quality and agricultural productivity (Sollins et al., 2006; Kindler et al., 2009), water quality (Lal et al., 2004), immobilization and transport of nutrients and anthropogenic chemicals (Linn et al., 1993), while also concealing exciting opportunities for the discovery of novel compounds for potential use in industry and medicine (Flaig, 1997 in Kelleher and Simpsom, 2006). It may also be a precursor for some fossil fuels, especially buried anaerobically as peat (Knicker and Lüdemann, 1995).

Soil quality can be defined as the capacity of the soil to carry out ecological functions that support terrestrial communities (including agroecosystems and humans), resist erosion and reduce negative impacts on associated air and water resources. Specific SOM functions important in agricultural productivity include: 1) chelation and provision of mineral nutrients available to plant roots in time, space, and form; 2) retention of water in sufficient quantities and with appropriate potential energy to be available for root uptake; 3) improving the buffering properties of soil; 4) provision of a network of interconnected pores sufficient to provide pathways for low physical resistance to root growth and meet plant root needs by supplying oxygen, removing CO_2 and toxic gases; and 5) support plant growth-promoting soil organisms. High levels of SOM are also associated with reduced erosion and runoff and soil aggregation (Weil and Magdoff, 2004).

Despite these critical roles and potential, many uncertainties exist regarding the size of the labile and refractory SOM pool, carbon dynamics within the SOM pool, and the role of SOM in carbon sequestration. For instance, the size and capacity of the SOM pool to sequester additional amounts of carbon is not known. Moreover, our

understanding of SOM's specific contribution to soil function has not advanced notably in over five decades and remains primarily descriptive in nature (Wander, 2004). In addition, many studies that investigate SOM turnover and stability neglect its chemical nature and inherent variability. Consequently, detailed studies of SOM structure and distinction between microbial and plant inputs are required to improve our fundamental understanding of SOM stability as well as its roles in carbon cycling and sustainable agriculture.

A recent issue of *Science* described SOM as "the most complicated biomaterial on the planet" and stated that "there is mounting evidence that the essential features of soil will emerge only when the relevant physical and biochemical approaches are integrated", and "this will require better molecular tools" (Young and Crawford, 2004). At present, it is not fully understood which organic components are accessible to soil microbes, which are physically protected, and which are chemically recalcitrant. With respect to global warming, if we are to understand how this vast terrestrial pool (with over 4 times the carbon than all life on Earth) will react to increases in the mean annual temperature, we must first understand the organic constituents as well as their chemistry, physical organization and intimate relationship with soil biota. The same is true with respect to agriculture and other land uses, and it is critical that we understand the key chemical, physical and biological properties that give rise to stable soils and avoid perturbing these in order to implement truly sustainable practices.

Humic substances are a large, operationally defined fraction of SOM and represent the largest pool of recalcitrant organic carbon in the terrestrial environment. It has traditionally been thought that HS consist of novel categories of cross-linked macromolecular structures that form a distinct class of chemical compounds (Stevenson, 1994). In recently published work, advanced Nuclear Magnetic Resonance (NMR) approaches were used to conclude that most of the humic material in soils is a very complex mixture of microbial and plant biopolymers and their degradation products and <u>not</u> a distinct chemical category as is traditionally thought (Kelleher and Simpson, 2006).

Furthermore, Simpson et al. (2007) challenged the concept that extractable SOM is comprised mainly of humic materials. The contribution of microbial biomass to SOM has been accepted to vary between 1-5% and is often associated with the labile, readily

degradable component (Alef and Nannipieri, 1995). However, it has been discovered that microbial presence far exceeds presently accepted values and that large contributions of microbial peptide/protein are found in the HS fraction. Considering the amounts of fresh cellular material in soil extracts, we believe the contributions of micro-organisms in the terrestrial environment are seriously underestimated. If this is the case then efforts to manage soils to increase their carbon storage capacity (as suggested by the IPCC in 1996) may be a possible means of slowing the rate of atmospheric CO_2 increase (IPCC, 1996).

The Kyoto Protocol sets the agenda for reducing carbon emissions, with carbon trading already in existence especially in Europe. To assist countries in achieving the emissions reduction targets, offsets through the creation of soil and vegetation sinks will be recognised on company or country balance sheets. The huge amounts of carbon stored in soils could result in the commodification and trading of this carbon. Without an accurate knowledge of the role played by and contribution of microbial biomass to SOM we will be unable to assess our responsibilities under these agreements and the extent of our contribution to climate change. Furthermore, the industrial and environmental technology market in the EU could grow exponentially in value over the next decade.

There has been an inseparable co-existence of the microbial biosphere and human communities that has had both benefits and dangers (Hallsworth et al., 2003). The beneficial aspects of micro-organisms can be exploited to our advantage and for the good of the environment but to do so, there is a need for detailed knowledge. Clearly, the use of micro-organisms and resulting bio-products in industrial technologies has considerable potential for the generation of wealth across the globe for many years to come. The knowledge accrued will contribute to providing environmental solutions exploitable by industry. Because the contribution of both living and dead microbial biomass has been underestimated then it is important to understand how it degrades in soil and does it degrade in a similar way to plant materials.

1.1.2 Understanding of the issues and their impacts on the global environment

It is well established that the global soil C far exceeds the combined atmospheric and biotic C pools (Hedges et al., 2000; Lal et al., 2004), and that organic carbon in the form of SOM represents the most abundant and ubiquitous natural organic product in

the biosphere (van Bergen et al., 1997). SOM is a complex, heterogeneous mixture of material from various sources that exist along a continuum of decomposition and stabilization in the soil profile (Crow et al., 2006). One of the most important functions of SOM is arguably its critical role in regulating anthropogenic changes to the global emission or sequestration of atmospheric and biospheric CO_2 (Kindler et al., 2009). Moreover, it is believed that SOM may represent all or part of the elusive "missing C sink" (Gleixner et al., 2001). The emission of CO_2 from terrestrial OM is recognized as one of the largest C fluxes of global C cycling (Schlesinger and Andrews, 2000), and the quantification of labile OM pools is considered imperative for determining future increases in CO_2 fluxes from anthropogenic disturbances or global warming (Otto et al., 2005).

1.1.3 Microbes and microbial degradation

Microbial biomass is an important component of the total living soil biomass (Findlay et al., 1989; Wander et al., 1995; Six et al., 2006), and represents a significant component of the total terrestrial C and N (Kögel-Knabner, 2002). Microbial biomass and its residues in soil are important source material for SOM formation (Kögel-Knabner, 2002), contributing to productivity, and are responsible for driving the biogeochemical cycling of biologically important elements; carbon, hydrogen, nitrogen, oxygen, phosphorus and sulphur on Earth (Vestal and White, 1989; Zak et al., 2003). Furthermore, microorganisms and various by-products of their metabolism have been noted to play an important role in the formation of soil aggregates and in soil structure maintenance (Wander et al., 1995). It has been estimated that one gram of forest soil contains an estimated 4×10^7 microbial cells, where as one gram of cultivated soils and grasslands contains an estimated 2×10^9 microbial cells (Daniel, 2005). Therefore, changes in microbial biomass composition and function will directly influence rates of soil C and N cycling (Zak et al., 2003). In fact, recent studies suggest that microbes may ultimately ''define'' a soil by introducing multi-scaled structure and order to soil components (Young and Crawford, 2004). Because of their importance and vast diversity, understanding the full contribution of micro-organisms to environmental processes remains a great challenge in contemporary environmental sciences.

Microbial biomass decomposition is dynamic and complex involving physical, chemical and biological processes and can be summarized as a rapid loss of labile fractions followed by the slow degradation of more recalcitrant microbial components.

In general recalcitrance increases in the order of protein < polysaccharide < lipid, and the fate of each compound class can be predicted based on their chemical characteristics (Baldock et al., 2004). Biomacromolecules exhibit conspicuous differences in degradation, and the ratio of labile to recalcitrant pools cannot be assumed to stay constant and this is due in part to the complexities of some biopolymers. Concomitant with microbial decomposition, stabilization of the decomposition products occurs, leading to the formation of refractory SOM, which resists further chemical modification for several hundred years (Knicker and Lüdemann, 1995; Derenne and Largeau, 2001). Derenne and Largeau (2001) hypothesized that some macromolecules exhibit a high intrinsic resistance to degradation, whereas in other cases, such a resistance is acquired through extensive transformation to incomplete combustion and recondensation reactions.

Although the cell wall polysaccharides of microorganisms are relatively easily decomposed, the basic units such as glucosamime, galactosamine or muramic acid are found in soils after hydrolysis (Stevenson, 1994) and they accumulate during litter decomposition (Coelho et al., 1997). Bacteria also produce a host of other structural components such as lipoteichonic acid and lipopolysaccharides. However, little is known about the fate of these compounds in soils (Kögel-Knabner, 2002). Fungi, as well as some bacteria synthesize black- to brown-coloured pigments, with only partly known compositions, called melanins. Little is also known about their fate or decomposition in soils, but they are considered recalcitrant due to their aromatic structure (Kögel-Knabner, 2002; Knicker, 2004). The same is true for algenans and bacteran, insoluble, non-hydrolyzable aliphatic polyether components of a number of algae and bacteria, which are selectively preserved in sediments (Derenne and Largeau, 2001). It is believed that these compounds are derived from the condensation of complex lipids and are located in the cell wall (Simpson et al., 2006). These microbial compounds may be relatively resistant to biodegradation and thus have high potential to accumulate in soils (Augris et al., 1998). As a consequence, detailed understanding of the biodegradation pathways of the microbial component at the molecular-level, and their role as precursors for SOM will aid in the prediction of the effects of climate change on soil carbon storage (Kelleher et al., 2006).

1.1.4 Soil organic matter

Soil organic matter is composed of a continuum of materials of varying chemical complexity (Kindler et al., 2009) with huge amounts of C and N, and plays an important role in regulating anthropogenic changes to the global C and N biogeochemical cycles (Lal et al., 2004). It is therefore widely accepted that relatively small changes in the size and the turnover rates of soil C and N pools may potentially bring about substantial effects on atmospheric concentrations and global C and N cycling at large (von Lützow et al., 2006; Belay-Tedla et al., 2009). Thus, it is no surprise that the dynamics of soil organic C and N stabilization are of great interest in environmental research. This is especially true for the emission of CO_2 from SOM to the atmosphere as a result of perturbation caused by global warming (Trumbore et al., 1990; Gleixner et al., 2002) and nutrient cycling and soil structure maintenance (Saggar et al., 1994; Parfitt et al., 1999; Rillig et al., 2007), an important resource in agricultural productivity (Belay-Tedla et al., 2009; Kindler et al., 2009).

It has been generally accepted that the C and N in SOM is predominantly plant derived (Kögel-Knabner, 2002; Six et al., 2006). However, only a small fraction of the yearly litter and root input becomes part of the stable OM pool, with most of it becoming integrated into microbial biomass after repeated processing (Dijkstra et al., 2006). Although the conversion of plant derived C and N, first into soil microbial biomass and later into SOM has been demonstrated (Pelz et al., 2005; Bottner et al., 2006; Kindler et al., 2009), not much information is available about the precise contribution of microbial biomass C and N and its constituents to the formation of SOM. The living microbial biomass in soil is only a relatively small pool, but significant contribution to SOM formation can be inferred since a major amount of the C input into soil is cycled through microbial metabolism (Kindler et al., 2009).

Therefore, on the basis of such evidence, it would appear that microbes are a major source of SOM. In fact, in a recent study using high resolution NMR spectroscopy, Simpson et al. (2007) demonstrated that microbial biomass contributes >50% of the extractable SOM fraction, ~45% of the humin fraction and accounted for >80% of the soil N, a much grater contribution than previously tought (Alef and Nannipieri, 1995). Kindler et al. (2006) demonstrated that 56% of total C derived from dying bacterial cells (*Escherichia coli*) added to soil was mineralized to CO_2 after 244 days, whereas 44% of the bulk microbial C remained in the soil although 99.9% of the

added cells died during the first 28 days. The authors estimated that the carbon remaining in the soil was distributed equally to the non-living SOM and the soil microbial food web. If this is the case then efforts to investigate the transformation dynamics of individual biochemical groups, carbohydrates, proteins (Knicker et al., 1996) and lipids (Caradec et al., 2004; Moriceau et al., 2009) of soil microbial biomass are needed to enhance our understanding of the transformation of microbially derived C and N.

The decomposition of SOM is dynamic and complex, involving physical, chemical and biological processes (Baldock et al., 2004). SOM pools are chemically divided into a labile pool with a small size and rapid turnover and a recalcitrant fraction with large size and slow turnover (McLauchlan and Hobbie, 2004) that are probably important precursors of HS and fossil OM (Derenne and Largeau, 2001). Each type of biomolecule present in decomposing residues has a characteristic biochemical recalcitrance defined by the strength of intra- and inter-molecular bonds, the degree of polymerization and regularity of structural units in polymers, and the content of aromatic and aliphatic groups (Baldock et al., 2004). Biochemical recalcitrance can also result form a range of condensation reactions between labile precursors such as non-enzymatic browning between carbohydrates and amino groups to form hydroxymethylfurfurals according to the Maillard reaction (Knicker, 2007).

In soils, the composition of organic materials is controlled primarily by two factors: (1) the chemical composition of the net carbon inputs (its quantity and quality; Baldock et al., 1992; Chotte et. al., 1998) and (2) the nature and magnitude of the decomposition process (von Lützow et al., 2006; Six et al., 2006). Studies have shown that the biological stability of OM in soil is controlled by the chemical structure of the OM and the existence of various mechanisms of protection offered by soil matrix and soil minerals (Derenne and Largeau, 2001). Chemical structure is important because of its direct influence on the rate of decomposition of OM and its importance in defining the strength with which mineral and organic soil components interacts (Baldock and Skjemstad, 2000). Rillig et al. (2007) suggest that ultimately, organic compounds may persist in soil as a result of their inherent chemical recalcitrance, inaccessibility due to physical protection, or stabilization due to intermolecular interactions with minerals, inorganic solutes and other organic compounds. The C and N fluxes are largely dominated by the small but highly bio-reactive labile pool, while long-term C and N

storage is often dominated by the chemically recalcitrant fraction (Trumbore et al., 1990). One of the key characteristics of the labile SOM pool is that it serves as a direct source of readily available nutrients, exerting considerable control on ecosystem functioning (Belay-Tedla et al., 2009). Together with the recalcitrant fraction, information on the labile pool could improve detection and prediction of changes in soil C and N dynamics that may not be readily evident with the traditional monitoring of total C and N content (Belay-Tedla et al., 2009).

Many studies that investigate SOM turnover and stability neglect its chemical nature and inherent variability. Therefore, detailed studies of SOM structure and distinction between microbial and plant inputs is required to improve our fundamental understanding of SOM cycling as well as carbon cycling on a global level. This is particularly important, as the structure of SOM is significantly impacted by the carbon input source, since the microbial and the plant derived biomass residues differ significantly in their molecular structures, and the nature of the precursor material will determine the stability, aggregation, reactivity and other properties of SOM (Kindler et al., 2009). A good understanding of decomposition at the molecular-level will aid in the prediction of the effects of climate changes on soil carbon storage (Kelleher et al., 2006).

1.1.5 Dissolved organic matter

Dissolved organic matter (DOM) represents an active OM reservoir in soils (Tanoue et al., 1995) and is often defined operationally as that organic matter, which passes through a 0.45-μm filter (Bowen et al., 2009). It often represents less than 0.25% of the total SOM but is an important fraction in soil environments (Kalbitz et al., 2001). The global DOM pool contains ~700 x 10^{15} g of carbon, this amount is significant when compared to the ~750 x 10^{15} g C contained in atmospheric CO_2 and the annual flux of ~7.0 ± 1.1 x 10^{15} g of CO_2 in the atmosphere (Powell et al., 2005). It is therefore considered to contribute significantly to the C and N cycle in terrestrial ecosystems, to soil formation and to pollutant transport. In some ecosystems dissolved organic N represent the major form of N (Michalzik and Matzner, 1999). It also contributes to the mobilization and transport of nutrients, acidity and hazardous compounds. In addition, DOM changes the properties of soil surfaces by inducing weathering and sorptive interactions, and it controls the colloidal properties of particles. The extent of these interactions is a function of the concentration but also of the chemical composition of

the DOM (Kaiser et al., 2001). Despite these roles, the exact processes contributing to the production and loss of DOM are not yet fully understood, making it difficult for any predictions about the effects of changing environmental conditions on its properties and dynamics (Kaiser et al., 2001).

DOM can enter the soil as soluble organic material leached from the surfaces of leaves, stems and plant litter and be generated within the soil through the decomposition of OM, and the release of both microbial metabolites and plant root exudates (Guggenberger et al., 1994). It may be lost from soils as a result of its utilization as a substrate by soil organisms, leaching from the profile by percolating water and, in limited quantities, the uptake of selected organic molecules by plant roots. Studies on forest ecosystems have shown that the amount of DOM released from forest floors and organic layers have been attributed to changes in microbial activity (Guggenberger et al., 1998; Tipping et al., 1999). Kaiser et al. (2001) demonstrated that varying microbial activity does not only affect the amount of released DOM but also its composition. The balance between the different loss and production processes for DOM is moderated by the soil's DOM storage capacity by sorption to mineral and organic surfaces (Guggenberger and Kaiser, 2003), making it difficult to account for DOM dynamics from determination of the soluble DOM pool and the CO_2 flux as it is mineralised.

Radiocarbon dating has shown the average age of DOC to be over 1000 years, but two distinct fractions comprise the DOM pool. Over 99% of DOC is very labile and undergoes a very high turnover rate, most likely as nutritional source for microbial loop. Turnover rates for this labile DOM fraction can vary from less than a day to more than 1000 years (Powell et al., 2005). Refractory DOM fraction in water columns has been shown to be as old as 6000 years old and consist of selectively preserved constituents, mainly marine derived polymeric materials (Williams and Druffel, 1988). Powell et al. (2005) suggested over 70% of marine DOM resides in the deep ocean is bio-refractory and contributes to its limited bioavailability.

Two main theories have been proposed to explain the existence of refractory DOM: physical protection and selective preservation (Hedges et al., 2000). The physical protection model states that the refractory nature of a DOM molecule is a result of its microenvironment rather than its structure. Therefore, DOM molecules that are adsorbed onto particulate surfaces, entrapped within cell membrane fragments, or

encapsulated within liposome-like structures are protected from degradation (Hedges et al., 2001). Physically protected DOM molecules may be shielded by their matrix from normal photolytic and chemolytic conditions and be protected from enzymatic attack because the cleavage sites are not accessible to enzymes (Hedges et al., 2001).

The selective preservation theory attributes the refractory nature of particular DOM molecules to their structure, which is thought to provide an inherent protection from degradation. This inherent protection can be fundamental to the molecule in its initial state (for example, natural enzyme resistance) or in altered or modified form as a result of other biochemical transformation processes (Tanoue et al., 1995). Powell et al. (2005) suggest that microorganisms can also produce DOM that is resistant to decomposition through degradation of high-molecular-weight biomolecules into low molecular weight DOM components. This is further supported by the detection of bacterial porins (outer membrane channel proteins of gram-negative bacteria) and OmpA protein homologues in seawater, suggesting that microorganisms can directly produce refractory DOM (Yamada and Tanoue, 2003). Porins are known to have extraordinary resistance to enzymatic cleavage that is largely due to their structure, which is a tightly wound β-barrel whose hydrophilic loops do not contain residues recognized by most enzymes (Cowan et al., 1992).

1.1.6 Lipids as a source of soil organic carbon

It is well established that a large part of the stable OM in soils is composed of microbially and faunally derived compounds (Kögel-Knabner, 2002; Six et al., 2006; Kindler et al., 2009). These compounds can be divided into several classes of biomolecules including polysaccharides (e.g. cellulose, chitin, and peptidoglycan), protein, lipid/aliphatic materials and lignin (Kögel-Knabner, 2002). Lipids are a heterogeneous group of organic substances, operationally defined as being insoluble in water but extractable with non-polar solvents (Wiesenberg et. al., 2004). Lipids constitute an important biochemical class in living organisms, and are the major organic C pools in microbial biomass, making up 5 to 20% of the total C (Wakeham et al., 1997; Oursel et al., 2007). Soil lipids consist of a wide variety of organic compounds such as fatty acids, *n*-alkyl hydrocarbons (alkenes and alkanes), *n*-alkyl alcohols, to more complex cyclic terpenoids and steroids, fats, waxes and resins, as well as phospholipids (Jandl et al., 2002) and are an important component of SOM (Sun et al., 2000). In soils, lipids originate from both plants and animals as products of decomposition, and

exudation, as well as from various other pedogenic sources, including fungi, bacteria and mesofauna (Bull et al., 2000). Of the classes of lipids, fatty acids are the most abundant and probably the most investigated (Jandl et al., 2002). The composition of accumulated lipids in soils is influenced by a wide range of processes, including bioturbation, oxidation, microbial degradation and hydrolysis (Naafs et al., 2004). Many lipids are reactive and subject to readily discernable modifications to their original molecular structure as a consequence of degradation reactions, thus allowing biogeochemical reaction sequences to be studied (Colombini et al., 2005b).

Lipid analysis is a useful method to study the dynamics of SOM because specific lipid classes provide useful information about their sources. For example, triglycerides are storage compounds, and phospholipids exist as structural and functional components of biological membranes (Sun et al., 2004). The degradation of lipid classes of algae has been studied in soils and other environments (Caradec et al., 2004; Sun et al., 2004). For example, Moriceau et al. (2009) compared the degradation property of each lipid class of algal lipid associated with the biogenic silica-carbon interaction during degradation experiments of diatom *Skeletonema marinoi*. However, the degradation dynamics of lipids, particularly in clay-microbial complexes have been studied insufficiently. Laboratory studies of the degradation of *n*-alkanes in soils indicated that the *n*-alkanes are oxidized to *n*-alkanols and ultimately to their *n*-alkanoic acids (Amblés et al., 1994). Furthermore, unsaturated and especially polyunsaturated fatty acids easily undergo oxidation processes localized at the double bonds via radical reactions with the inclusion of oxygen in the acyl chain, carbon-carbon bond cleavage, and the formation of lower molecular weight species (Colombini et al., 2005b). Cross-linking and polymerization reactions also occur, leading to the formation of polymeric network especially in the case of highly unsaturated oils. α,ω-Dicarboxylic fatty acids and ω-hydrocycarboxylic acids are products if these processes (Colombini et al., 2005a). The natural degradation process of lipids could be accelerated or modified if the material has been exposed to oxidizing conditions or to high temperatures. Thus, the nature of the degradation products depends on the composition of the original material (Colombini et al., 2005b).

Other lipids are relatively stable to biogeochemical transformation, allowing these compounds to survive degradation (Wakeham et al., 1997). As a result of their good potential of preservation in the environment and the specific structure of some lipids, they are widely used as biomarkers in geochemical studies for determining the

source, fate, alteration and historical changes of organic matter (Sun et al., 2000; Grossi et al., 2003), thus aiding the understanding of the processes that underpin carbon cycling in soils (Nierop and Verstraten, 2004). Lipids deposited in different environments degrade at different rates (Sun and Wakeham, 1994). Solid state ^{13}C NMR data on total soil samples indicate that aliphatic moieties accumulate during decomposition, whereas aromatic compounds increase, decrease or remain unchanged (Baldock et al., 2004).

It is interesting to note that there are no data to support a classification of fatty acids as refractory non-biodegradable compounds; they are regularly detected in old non-living SOM fractions (Kindler et. al., 2009). This can only be explained by stabilization of fatty acid residues in SOM, either by chemical or physical protection processes (von Lützow et al., 2006). Kindler et al. (2006) suggest that the concentration of microbial biomass compounds such as fatty acids within the non-living SOM cannot simply be translated to the quantitative contribution of microbial biomass to SOM formation without information on carbon pool sizes and turnover times. The turnover of biogenic molecules in soil is determined by their integration within complex biotic structures. In living cells, repair mechanisms and aggregation prevent the cell biomass components from being decomposed (Kindler et al., 2009). Even after the death of a cell, molecules integrated within a complex cell wall structure may be stabilized and protected against enzymatic degradation by chemical bonding, physical sorption and encapsulation as described for proteins (Knicker and Hatcher, 1997). Although such effects have been suggested, they have not been accounted for in most degradation studies, which usually employ pure compounds that are not embedded into a matrix (Kindler et al., 2009).

1.1.7 Soil organic nitrogen

The cycling of nitrogen in soils is particularly important since it is inextricably linked to that of carbon. Moreover, organic nitrogen comprises >96% of total soil nitrogen and there is great interest in realistically estimating potentially available nitrogen to predict fertilizer requirenents and improve nitrogen use efficacy. This has significant environmental implications – particularly the contribution of SOM-nitrogen pool to N_2O emissions, eutrophication and NO_3 contamination of groundwater. Although soils are the most significant terrestrial sink for nitrogen, current understanding of organic nitrogen pools and nitrogen cycling cannot account for some mechanisms and sinks that stabilize nitrogen additions from fertilizers. Differentiating

microbial from other forms of organic nitrogen is therefore vital if we are to provide better estimates of its availability and apply fertilizer in a sustainable manner.

Proteins are by far the most abundant N-containing substances in many organisms (Zang et al., 2001), and account for upto 85% of the organic N found in SOM (Tanoue, 1995; Simpson et al., 2007). Proteins also constitute an important component of high molecular-weight dissolved OM (Powell et al., 2005). The two main categories of amino-N compounds in soils are intact proteins released for various extracellular functions and detrital proteins and polypeptides–plant and microbial constituents in various stages of transformation (Murase et al., 2003; Rillig et al., 2007). Other N-containing compounds in the soil are amino sugars and compounds formed by abiotic interactions, such as protein–tannin complexes and Maillard reaction products, as well as various heterocyclic pyrolysis products (Knicker, 2007). The analysis of proteins in environmental samples allows us to understand and relate the functional contribution of certain proteins to biogeochemical processes, and to identify source organisms for specific enzyme activity (Schulze, 2005).

Approximately one third of the organic-N in soil in the form of proteins may be liberated as α-amino N by acid or alkaline hydrolysis (Bremner, 1950). Amino acids either in a monomeric or polymeric (protein) state provide the largest input of organic N into most soils (Stevenson, 1982). In general, amino acids constitute 5 to 10% of soil organic C and account for 22 to 46% of the organic N (Amelung et al., 2006). Further, the major labile soil nitrogen fraction consists of N in the form of peptide bonds (Knicker, 2000); hence, the pool of soil proteins and polypeptides may be most representative of soil organic N. In addition, amino acids also provide a ready source of C and N for soil microbial biomass (Vinolas et al., 2001). It can be expected that amino acid in soil will vary spatially and temporally depending on vegetation cover, land management strategy and environmental conditions (Vinolas et al., 2001). It has been suggested that greater microbial activity in warmer soils results in higher turnover of proteinaceous material and a selective preservation of the sorbed basic amino acids, whereas other studies have indicated that acidic amino acids are enriched in hot compared to cold climates (Stevenson, 1982). While in sediments, the amino acid composition may be altered by increased turnover of proteins (Dauwe and Middelburg, 1998).

In soils, inorganic N is rapidly immobilized into microbial cells as a part of SOM, and the newly immobilized N is still highly available for plant uptake. It is assumed that amino sugars should constitute a significant part of the newly immobilized organic matter, because amino sugars in soil are mainly of microbial origin (He et al., 2006). These compounds are part of the cell walls of bacteria, fungi and actinomycetes (Glaser and Gross, 2005), and constitute between 5 and 10% of the organic nitrogen in soils (Coelho et al., 1997). Bacterial cell wall contains a peptidoglycan, constructed of the glucose derivatives of *N*-acetyl glucosamine and muramic acid (Glaser and Gross, 2005; He et al., 2005). In gram-positive bacteria, as much as 90% of the cell wall consists of peptidoglycan, whereas in gram-negative bacteria, this figure is only 5–20% (Glaser et al., 2004). Amino sugars occur in soil as structural components of a broad group of macromolecules such as mucopolysaccharides, and mucopeptides, mostly as glucosamine and galactosamine (Coelho et al., 1997). Other amino sugars such as muramic acid, mannosamine and fucosamine have been detected (He et al., 2005), but their contribution to the total amino sugar is not significant.

Amino sugars are usually not found in plants and originate almost exclusively from microbial biomass (Scholle et al., 1993). Therefore, analyses of amino sugars are useful in the assessment of both living and dead biomass and can provide clues to the microbial contribution to SOM dynamics (Zhang and Amelung, 1996; Liang et al., 2007). Turrión et al. (2002) demonstrated that the amino sugar pattern can be used as an indicator of the origin of different microbial C and N residues in soil. The concentrations and ratios of amino sugars and muramic acid are also routinely used to estimate microbial contributions to SOM (Zhang and Amelung, 1996; Glaser et al., 2004). He et al. (2005) suggested that the dynamics of amino compounds provide significant information on the transformation of soil N, and the amino sugars routinely studied to monitor the microbial contribution to SOM turnover are glucosamine, galactosamine, muramic acid, and mannosamine. It has also been suggested that, amino sugars are expected to function not only as a source of N for plants and microorganisms, but also promoters of good soil structure (Coelho et al., 1997).

Traditionally, proteins have been considered relatively labile in the environment with poor preservation potential (Nguyen and Harvey, 2003). This lability is conferred by the high sensitivity of the amide linkages present in peptides (Derenne and Largeau, 2001; Roth and Harvey, 2006). However, Rillig et al. (2007) reported that the mean

resident time of N in the soil has been calculated as 50 years in contrast to 26 years for C. The authors further suggest that a part of this discrepancy may be attributed to the reprocessing of N by soil microorganisms, the mechanisms that stabilize N-containing organic compounds may also differ in part from those that stabilize non-N-containing organic compounds. The recent development of solid state CP MAS ^{15}N-NMR on natural samples revealed substantial amounts of N in the form of amide functions in various samples such as recent sediments, soils, and composts (Michalzik and Matzner, 1999). Direct evidence has also been reported for the preservation of proteins or at least proteinaceous moieties in natural environments. This includes reports of intact membrane proteins (porins) in dissolved and particulate organic matter (POM) shown to be preserved at depths. Recent evidence also exists for the preservation of high molecular mass proteinaceous materials or at least proteinaceous moieties in aquatic environments over relatively short geologic time scales (Nguyen and Harvey, 1997; Kelleher et al., 2007). In an experiment measuring the chirality of several amino acids, Amelung et al. (2006) reported ages of soil proteins in the range of hundreds of years.

Detailed examination of algal detritus and sediments has shown that hydrophobic and hydrogen-bond interactions are important stabilizing forces which lead to the aggregation and preservation of proteinaceous materials over longer timescales (Nguyen and Harvey, 2001; Roth and Harvey, 2006). Several characteristics and processes may increase protein resistance to degradation by altering their structure to occlude the peptide bond (Rillig et al., 2007). Nguyen and Harvey (2001) demonstrate that high-molecular-mass aggregated proteins remain susceptible to enzymatic attack after their extraction from the organic matrix (Nguyen and Harvey, 2001). This supports the concept of ‘encapsulation’ (Knicker and Hatcher, 1997), which argues that organic materials incorporated within the sedimentary organic matrix are protected from bacterial hydrolysis. Such organic matrix is usually composed of highly aliphatic material (Yamashita and Tanoue, 2004). Moreover proteins preserved in humic extracts have been demonstrated by the release of amino acids by acid hydrolysis (Bremner, 1950). Other mechanisms suggested for protein preservation or recycling include abiotic processes such as condensation reactions which result in reduced bioavailability (Hedges, 1978; Nagata and Kirchman, 1997) and sorption to mineral surfaces which impede microbial attack (Hedges and Hare, 1987; Kirchman et al., 1989).

Several characteristics and processes may increase protein resistance to degradation by altering their structure to occlude the peptide bond (Rillig et al., 2007). For example, glycosylation, the covalent linkage of specific polysaccharides to specific amino acids, is an enzymatically mediated intracellular modification of proteins that occur prior to secretion (Varki, 1993). Glycosylation is known to increase in vitro protein stability against proteolytic enzymes up to ten-folds (West, 1986; Varki, 1993).

Protein stability can be further enhanced by interactions with other soil molecules, specifically polyphenolics and carbohydrates. One of the oldest known mechanisms of protein stabilization involves those plant polyphenols commonly referred to as tannins (Nierop et al., 2006). Proteins can react with tannins and related polyphenols to form soluble and insoluble products through reversible non-covalent processes such as hydrogen bonding and hydrophobic interactions (Nyman, 1985; Hagerman et al., 1998). The degree of solubility of these complexes and their resistance to enzymatic degradation vary significantly with the type of protein and tannin, ratio of protein to tannin, ionic strength and pH (Hagerman and Robbins, 1987). Another common plant phenolic that interacts with protein is lignin (Rillig et al., 2007). To this effect, several studies have demonstrated to formation of lingo-protein condensation products form mixtures of alkali lignin and casein-N (Waksman and Iyer, 1932).

In addition to their ability to increase protein stabilization intrinsically (glycosylation), soil carbohydrates may also stabilize proteins through extrinsic interactions (Rillig et al., 2007). Glycation, or the Maillard reaction, is the non-enzymatic covalent bonding of a sugar aldehyde to an amino group. This is particularly true for the side-chain amino groups of lysine and arginine residues (Knicker, 2007). Several studies have demonstrated that glycation significantly increased the stability of proteins relative to the non-glycated form (Jakas and Horvat, 2004). Phytates, another group of protein-complexing carbohydrates, consist of a sugar core (inositol) in which each hydroxyl is phosphorylated. Phytate-protein complexes are formed by weak electrostatic bonds between the negatively charged phosphates and positively charged basic amino acid residues, as well as through cation-bridging of phosphates to carbohydrates (Rillig et al., 2007).

1.1.8 Stable carbon isotope biogeochemistry

The study of the biogeochemistry of SOM is particularly important because of its intense productivity and related biogeochemical cycles (Faganeli et al., 2009). The ratios of the stable isotopes of elements important to biological systems such as those of carbon, nitrogen, oxygen, hydrogen and sulphur ($^{13}C/^{12}C$, $^{15}N/^{14}N$, $^{18}O/^{16}O$, $^{2}H/^{1}H$ and $^{34}S/^{32}S$, respectively) give information regarding many biological processes and transformations within global biogeochemical cycles (Rieley, 1994). Several authors have suggested that measurements of the stable isotope composition of individual compounds provide an added dimension to biological, geochemical (Blair et. al., 1985) and biogeochemical processes occurring in peat, soil and sediments (Kracht and Gleixner, 2000; Lichtfouse, 2000). The stable C and N isotopes, for instance, are frequently used as reliable indicators of soil microbial and biogeochemical processes (Santruckova et al., 2000; Gleixner et al., 2002). Moreover, a complete understanding of these processes can only be achieved through knowledge of the isotopic composition of the source organic matter (Gleixner et al., 2002) and the corresponding fractions in microbial transformation (He et al., 2006; Faganeli et al., 2009).

The natural abundance ^{13}C and ^{15}N content of the SOM is usually higher than that of the plant and fresh litter input. Additionally, older, more decomposed SOM is ^{15}N- and, less consistently, ^{13}C-enriched compared to more recent organic compounds (Dijkstra et. al., 2006). Several possible mechanisms have been suggested to explain shifts in stable isotope composition. Isotopically depleted materials may be used by microorganisms, while the leftover isotopically enriched material may end up in the SOM. Alternatively, the microbial biomass itself may be the origin of the isotopically enriched material. The latter possibility is in line with ^{13}C and especially ^{15}N shifts observed in food web studies (Dijkstra et al., 2006).

It has been suggested that changes in the isotopic signature of individual compounds reflect biochemical conversion (synthesis or degradation) of corresponding source molecules (Blair et al., 1985; Macko et al., 1991). Most notably, differences in decomposition rates among compounds that vary in $\delta^{13}C$ can cause carbon isotope fractionations in SOM (Agren et al., 1996). In contrast, constant values indicate "preservation" of source molecules (Kracht and Gleixner, 2000). Variations in $\delta^{13}C$ values in microbial biomass have been attributed to species composition (Boschker et al., 1999), and perhaps more importantly, kinetic isotope effects (Sharp, 2007). Kinetic

isotope effects are common in both nature and in the laboratory, and their magnitudes are comparable to, and sometimes much larger than, those of equilibrium isotope effects. Kinetic isotope effects are normally associated with fast, incomplete, or unidirectional processes such as diffusion, dissociation reactions, and almost all biological reactions (Sharp, 2007).

Angers et al. (1995) demonstrated that the ^{13}C enrichment of microbial biomass by about 2‰ relative to that of the corresponding total soil C is indicative of an isotope effect due to microbial degradation and may be of huge importance in soil. The authors also suggest that this isotope effect could be induced by selective assimilation of different soil carbon pools or ^{13}C fractionation during microbial metabolism, particularly during respiration where the released CO_2 is depleted in ^{13}C. The process of microbial reworking of organic matter can also potentially alter the stable carbon isotopic composition of individual organic molecules that are produced by multiple sources (Keil and Fogel, 2001). However, the processes that contribute to isotope fractionation are not well understood, and little is known about differences in the degree of fractionation during decomposition from SOM pools of different ecosystems (Crow et al., 2006).

Free and bound lipids from a variety of biological precursors are key components of organic matter in soils and sediments (Lichtfouse et al., 1995). Although soil lipids only represent ~10% of SOM (Stevensen, 1994), these and other solvent-extractable compounds have been the main components studied in isotope fractionation. As a result of their unique chemical properties and advantages over other types of biomarkers, phospholipid fatty acids (PLFAs) have also been widely used to study microbial sediments. They include several compounds, mainly methyl-branched fatty acids that are found only in bacteria. It should be noted however, that PLFAs are readily turned over when an organism dies (Boschker et al., 1999), and may not be applicable in a degradation study. Isotope ratios of bacteria in aquatic systems have also been studied using extracted DNA from estuarine water samples (Coffin et al., 1990).

The stable isotope analysis of individual amino acids from living systems and detritus materials is a powerful method for probing the transformation dynamics in various ecological systems (Silfer et al., 1991). Pelz et al. (1998) demonstrated that carbon isotopic ratios of the bacterial amino acid, D-alanine can be used to study sources

of OM assimilated by bacteria in sediments and soils. However, the isotopic behaviour of the majority of soil compounds remains unknown (Gleixner et al., 2002). Adequate recognition of these microbial inputs will allow a better understanding of ecological systems where CO_2-recycling plays a major role, since the isotopic composition of bulk organic matter may not always reflect this process (Hartgers et al., 2000).

1.1.9 Phosphorus and the global biogeochemical cycling of carbon

Element phosphorus (P) is usually present in the biosphere in its highest oxidation state (+5) as inorganic orthophosphate (Pi), with biogenic organophosphorus compounds generally found as esters of phosphoric acid (Quinn et al., 2007). However, Pi has not always been the predominant P species on the planet, and the occurrence of phosphonic acids-organophosphate analogues in which the carbon-oxygen-phosphorus ester bond is replaced by a direct carbon-phosphorus linkage – has been recognised for over 40 years (Quinn, 2000). The existence of C-P compounds is a reflection of the reducing atmosphere on the primitive earth, and that phosphonates preceded phosphates in early life forms (Jia et al., 1999). In the period immediately after their discovery, biogenic C-P compounds were thought to be molecular vestiges; however, it is now known that they are widely distributed in contemporary biological materials, and that a number of pathways for their synthesis exist (Quinn et al., 2007).

Phosphonates may occur either as ‘free’ molecules or more frequently in peptide, glycan or lipid conjugates such as the 2-aminoethylphosphoric acid and phosphonoalanine components of membrane phospholipids (Sannigrahi et al., 2006). Their presence in outer-membrane structures may protect cells from enzymatic attack or confer additional rigidity (Clark et al., 1998) because C-P bonds are resistant to chemical hydrolysis, thermal decomposition and photolysis, as well as phosphatase activity (Quinn et al., 2007). The quantitative importance of biogenic phosphonates as a P source in the terrestrial biosphere has not yet been established; however, phosphonate-P is known, for example, to make up 25% of dissolved, high-molecular P in water column of the pacific (Clark et al., 1998) and other oceans (Kolowith et al., 2001). In soils, the OM pool includes many compounds that contain both C and P and thus the global biogeochemical cycling of P must be considered in conjunction with that of C. Furthermore, the crucial balance between carbon dioxide and oxygen in the atmosphere is largely controlled by primary productivity, which is in turn linked to the availability of limiting nutrients such as N and P (Sannigrahi et al., 2006). Recent reports also

suggest that P may be critical in limiting primary productivity and nitrogen fixation in oligotrophic ocean regions (Sanñudo-Wilhelmy et al., 2001). Therefore, a fundamental knowledge of C-P chemistry is paramount to understanding the coupled C and P cycles.

Biogenic soil P exists in a multitude of chemical forms, which differ widely in their behaviour in the soil environment (Turner et al., 2003b). Organic P is also a major component of total soil P. Organic P compounds in soil extracts are usually dominated by monoester P compounds, whereas diester P compounds are more abundant in plant materials and bacterial cells. Fungi tend to contain a significant proportion of their total P in inorganic forms, i.e. as orthophosphates or as polyphosphates, and their organic P is dominated by monoester P (Bünemann et al., 2008). Differences in microbial community composition may also influence the chemical composition of organic P in soil (Makarov et al., 2002). Nonetheless, the chemical nature and dynamics of soil organic P remain highly enigmatic and the role of organic P forms in biogeochemical cycles is not well understood (Turner et al., 2003a; Kögel-Knabner, 2006) despite constituting up to 90% of total P in some soils, providing a source of P for plant uptake (Turner et al., 2003a,b), and influencing biological processes, such as litter decomposition and microbial activity (Lair et al., 2009). Significantly, a large proportion of the organic P in most soils remains unidentified (Turner et al., 2003a,b).

Phosphorus originating from plant, animal, and microbial sources occurs in a range of complex compounds, which exhibit significantly different behaviour in the soil environment. This leads to the rapid degradation and disappearance of some compounds, but the stabilisation and persistence of others (Turner et al., 2003a). For example, mononucleotides and other monophosphate esters are degraded within hours of release (Turner et al., 2003a), on the other hand, inositol phosphates react strongly in most soils and accumulate to form the major classes of organic P (Turner et al., 2002). Makarov et al. (2002) have also been demonstrated that diester forms of soil organic P was more labile and more readily mineralized than monoesters, suggesting that organic P in diester compounds is an important source of P for plants and that these compounds play an important role in P transformation of ecosystems.

In the developed world, the use of phosphate fertilizers has declined since the last decades of the twentieth century; however, in the developing world, their use is continuously increasing, which results in increasing global consumption (Lair et al.,

2009). A large proportion of inorganic phosphorus applied to soil as fertilizers is rapidly immobilized after application and becomes unavailable to plants (Nautiyal, 1999). Indeed the continued application of P fertilizers and manures in amounts exceeding plant requirements leads to an accumulation of P in top soils under agriculture (Kögel-Knabner, 2006). This accumulation increases the risk of P fluxes from soils to aquifers and surface water bodies entailing the threat of eutrophication (a measure of algal biomass; Lair et al., 2009). This excess algal biomass is known cause toxicity, clogging of water filters, unsightly water bodies, reduced biodiversity and low oxygen concentrations in stratified waters. The consequent relationship between P and eutrophication makes the management of phosphorus inputs into rivers and lakes very important (Andrews et al., 2004). Moreover, the biological properties conferred by the C-P bond have also led to the introduction of a wide range of synthetic organophosphonates as pesticides, herbicide, fungicides and antibiotics into the environment over the last 50 years. Much of this anthropogenic production eventually reaches soils and natural waters. Despite extensive research (simulated by environmental concerns) the extent to which they enter the biogeochemical C-P cycle is poorly understood (Quinn et al., 2007).

1.1.10 Silicon and the global carbon cycle

Silicon (Si) is the second-most abundant element in the earth's crust (28%), occurring in more than 370 rock-forming minerals, and is one of the basic components in most soils. Although a quantitatively important element in soils, Si has received relatively little research attention compared with other elements (Sommer et al., 2006). More importantly, Si distinctly influences global C cycle (Treguer et al., 1995), namely through (1) weathering processes and (2) Si fluxes into the oceans (van Breemen and Buurman, 2002). During the weathering processes of primary silicates, CO_2 is consumed, for example, by the following reaction: $\mathbf{CaAl_2Si_2O_8 + 2CO_2 + 8H_2O \rightarrow Ca^{2+} + 2Al(OH)_3 + 2H_4SiO_4 + 2HCO_3^-}$. The resulting HCO_3^- is stored as carbonates in marine biogeosystems. Thus, processes of silicate weathering take part in the regulation of atmospheric CO_2 (Sommer et al., 2006). The relationship between CO_2 and silicate weathering is observable within short periods of time, and enhanced silicate weathering under conditions of experimentally elevated atmospheric CO_2 has been reported (Schlesinger, 2001 in Sommer et al., 2006).

Soils are the main reactor of terrestrial biogeosystems in which chemical processes interact with biological processes. Soils contain very different Si pools which can be subdivided into mineral and biogenic pools according to their origin (Sommer et al., 2006). Mineral Si pools in soils consists of three major phases, which are (1) primary minerals inherited from parent material, (2) secondary minerals developed through soil formation, mainly clay minerals, and (3) secondary micro-crystalline (e.g. quartz) to poorly ordered phases (Opal A, allophone), which also result from soil formation (Sommer et al., 2006). Biogenic Si pools in soils can be subdivided into phytogenic (including phytoliths), microbial and protozoic Si. It must be emphasized that knowledge about size, properties and transformation of theses pools is very limited for almost all soils (Sommer et al., 2006). Microorganisms influence Si transformation in soils through the (1) decomposition of plant material, which releases Si from plant tissues and (2) active mineral dissolution (van Breemen and Buurman, 2002). It has also been suggested that cell membranes of microorganisms may function as seed crystals for Si precipitation ("biomineralization", Kawano and Tomita, 2001), this phenomenon is well known in biogeosystems such as geothermal springs with Si supersaturation (Inagaki et al., 2003). Phytogenic Si is precipitated in roots, stems, branches, leaves, or needles of plants (Sommer et al., 2006).

Global C sequestration in oceans is inextricably linked with the global cycling of Si (Treguer et al., 1995; Ragueneau et al., 2000). This results from the fact that diatoms–which need Si for their cell walls (Skeleton)–constitute approximately 50% of the oceans' biomass (Tréguer and Pondaven, 2000). The greater the Si supply to oceans, the higher the export flux of C to marine sediments and ultimately, the more C removed from atmospheric CO_2 (Treguer et al., 1995).

1.1.11 Ultraviolet induced degradation of soil organic matter

The amount of solar ultraviolet-B radiation (UV-B, 280-315 nm) radiation reaching the Earth's surface has increased significantly as a consequence of changes in radiation interception due to decreased cloudiness, increased stratospheric ozone depletion, reduced vegetative cover, or high radiation interception at the soil surface (Pancotto et al., 2005; Austin and Vivanco, 2006). The most pronounced stratospheric ozone depletion occurs every year over Antarctica during the austral spring (September–November) because of the annual formation of the 'ozone hole' (Pancotto et al., 2005). Further ozone depletion will result in the exposure of sparsely vegetated soils to

enhanced UV-B and blue light doses and may have a more significant effect on the carbon balance in these environments. This is of special significance as it has been estimated that close to 40% of the terrestrial land surface is currently classified as arid or semi-arid. Furthermore it is expected that human-induced global changes will affect key controls on the carbon cycle in these ecosystems. As a result, factors affecting rates of photochemical mineralization could have consequences for the potential of C sequestration in these and other ecosystems (Austin and Vivanco, 2006).

Ultraviolet-B radiation has been shown to play an important role in the turnover of OM in aquatic ecosystems and oceans: photochemical reactions change the quality of DOM (Mopper et al., 1991) and produce dissolved inorganic carbon and volatile CO_2, CO and carbonyl sulphides (Austin and Vivanco, 2006). Light also acts as the energy source for priming refractory organic materials for further degradation (Kovac et al., 1998) and the formation of novel photoproducts (Kieber et al., 1989). Photochemical chemical production of pyruvate from DOM in ocean surface waters, for example, is believed to be a critical transformation to permit biological degradation of recalcitrant DOM (Kieber et al., 1989; Austin and Vivanco, 2006). Dissolved inorganic carbon (in the form of CO) is quantitatively one of the most important photoproducts observed during photochemical degradation of DOM (Mopper et al., 1991); however, other studies have indicated that the indirect effects of photochemical mineralization on the lability of OM, and not direct production of photoproducts, are the most important influences of solar radiation on carbon cycle in aquatic ecosystems (Kieber et al., 1989; Mopper et al., 1991). It must also be emphasized that solar radiation other than UV-B [ultraviolet-A (UV-A) and/or short wavelength visible radiation] has been implicated in the photodegradation of OM (Anesio et al., 1999; Schade et al., 1999; Austin and Vivanco, 2006).

Photodegradation has been demonstrated as a dominant control of above ground litter decomposition in semi-arid ecosystems and that UV-B, accounting for up to 50% of the C lost due to photochemical mineralization of litter (Austin and Vivanco, 2006), a much higher effect than previously thought (Pancotto et al., 2003). However, studies detailing the direct effects of solar radiation on C turnover in terrestrial ecosystems are limited (Austin and Vivanco, 2006), although the production of CO_2 from sterilized litter subjected to radiation treatments (Anesio et al., 1999) and the detection of CO as a photoproduct from live and senescent plants in short-term incubations in grassland have

been reported (Schade et al., 1999). Several studies have also demonstrated the effects of UV-B radiation on litter decomposition through changes in the chemical composition of the litter or through changes in the microbial community characteristics (Johnson et al., 2002; Pancotto et al., 2005). In contrast, fewer studies have evaluated the effects of solar radiation on soil microbial biomass decomposition, the process by which OM is cycled in soils. Johnson et al. (2002) demonstrated that unlike the plant community, soil microbial biomass is highly sensitive to elevated UV-B radiation and CO_2 concentrations. The authors further suggest that the impact of UV-B treatment on the accumulation of N in the microbial biomass may have far reaching implications for the supply of N to plants, because the productivity of many semi-natural ecosystems is limited by N. More importantly the effect of photochemical mineralization is that it may represent a short circuit in the global carbon cycle, with a substantial proportion of carbon sequestered in plant and microbial biomass being lost directly to the atmosphere without cycling through soil organic matter pools (Austin and Vivanco, 2006).

1.1.12 Photodegradation of microbial components

In order to better understand the biogeochemical cycle of C in soils, it is essential to determine the relative contribution of soil microbes and to study the processes that are responsible for the alteration of this C pool (Christodoulou et al., 2009). Lipids which constitute one of three main classes of OM in microbial biomass (Oursel et al., 2007), are well suited for such studies: they are less labile than carbohydrates and proteins and are thus frequently used as biomarkers to determine the source and the alteration state of OM (Sun et al., 2000; Grossi et al., 2003). Most studies of the degradation of major biochemical components of OM focus on biotic degradation processes, but the effect of abiotic processes (photooxidation and autoxidation) which are competitive with microbially mediated reactions has been virtually ignored (Kovac et al., 1998; Christodoulou et al., 2009).

It has been demonstrated that the chlorophyll phytyl side-chain, sterols, unsaturated fatty acids can be photodegraded quickly in senescent or dead cells of phytoplankton, cyanobacteria, and purple sulphur bacteria (Rontani, 1998; Rontani et al., 2003, Rontani et al., 2009). Photosensitized oxidation of monounsaturated fatty acids involves a direct reaction of $^1O_2$ with the carbon double bond by a concerted “ene” addition (Marchand and Rontani, 2001) and leads to the formation of hydroperoxides at each unsaturated carbon. Thus oleic acid produces a mixture of 9- and 10-

hydroxyperoxides with allylic *trans* double bond (Frankel et al., 1979). These two hydroperoxides may undergo highly stereo selective radical allylic rearrangement to 11- and 8-*trans* hydroperoxides, respectively (Marchand and Rontani, 2001). Hydroperoxides derived from type II photosensitized oxidation of $C_{16:1}$ Δ9, $C_{18:1}$ Δ9, and $C_{18:1}$ Δ11 fatty acids during irradiation of killed cells of *Dunaliella* sp. may either be reduced to the corresponding hydroxyacids after homolytic cleavage or cleaved to ω-oxocarboxylic acids and aldehydes after heterolytic cleavage (Rontani, 1998). The induction of free radical-mediated oxidation (autoxidation) processes result from the homolytic cleavage of photochemically produced hydroperoxides catalyzed by specific metal ions (Christodoulou et al., 2009).

Proteins encounter a large variety of potential routes for degradation that are usually divided into physical and chemical mechanisms (Miller et al., 2003). The most prominent chemical pathways are hydrolytic (e.g., deamidation) and oxidative reactions (Miller et al., 2003). Several studies have demonstrated that the sulfhydryl groups and aromatic amino acids of membrane proteins are susceptible to direct UV-A (Kerwin and Remmele, 2006), UV-B-induced photooxidation or indirect degradative processes mediated by endogenous photosensitizers, free radicals, and other reactive compounds produced during UV-B radiation (Caldwell, 1993). Under UV exposure conditions, proteins will degrade to varying extents depending on the protein and the mechanism of degradation (Kerwin and Remmele, 2006).

The peptide backbone, tryptophan (Trp), tyrosine (Tyr), phenylalanine (Phe) and cysteine (Cys–Cys disulfide bonds) are the primary targets of photodegradation in proteins (Kerwin and Remmele, 2006). Primary or type I photodegradation begins with adsorption of light resulting in excitation of an electron to higher energy singlet state (Kerwin and Remmele, 2006). Adsorption occurs either through the peptide backbone or by amino acid side chains of Trp, Try, and Cys-Cys. Excitation to the higher energy states is followed by one of a number of processes influenced by the solution pH, temperature, polarity, nearby side chains and protein structure (Bent and Hayon, 1975; Miller et al., 2003). These processes include relaxation to the ground state, formation of a triplet state, and reaction with oxygen to form peroxy radicals. Additionally, in proteins both Try and Phe can transfer their excited state energy to Trp. While Trp is in relatively low abundance in proteins, it has the highest molar absorption coefficients and

is therefore of huge significance in the photodegradation pathway (Kerwin and Remmele, 2006).

The conformation of a protein can also play an essential role in the photodegradation process. Changes in the protein conformation due to factors such as pH, ligands or salts can influence the sites of energy transfers which form reactive radicals (Kerwin and Remmele, 2006). The position of Trp residues within the protein, whether buried or exposed, or its position relative to other amino acids in the primary amino acid sequence and to the three-dimensional structure are all key factors in the photocatalyzed degradation process (Rao et al., 1990; Silvester et al., 1998). It has been proposed that some of the phytotoxic effects of UV-induced radiation may result from UV-induced membrane damage (Murphy, 1983).

Primary oxidation may also be accompanied by indirect oxidation of the protein via the formation of reactive oxygen species such as peroxy radicals and singlet oxygen (Kerwin and Remmele, 2006). Peroxy radicals are known to play a significant role in the protein degradation process as they are known to react with methionine residues to form methionine sulfoxide (Scislowski and Davis, 1987), with cysteine to form various sulfones and acids (Kerwin and Remmele, 2006) and with Trp to form kyneurenine and other hydroxylated derivatives which also act a photosensitizers (Kerwin and Remmele, 2006). The basic amino acid residue, histidine (His) is also extremely susceptible to attack by active oxygen if contaminating metal ions are complexed with the hystidyl residue. The interaction of contamination metal ions with peroxide in a Fenton type reaction to produce hydroxyl radicals capable of chemically modifying a number of amino acids, including His to form 2-oxo-His has also been demonstrated (Schoneich, 2000).

1.1.13 Clay-organo interactions

The sorption of OM to soil minerals is an important process in the natural environment (Feng et al., 2005) with significant geochemical implications (Hedges and Keil, 1999). The mineralogy, surface charge characteristics, and precipitation of amorphous Fe and Al oxides on clay mineral surfaces give clay minerals the capacity to adsorb OM (Baldock and Skjemstad, 2000). In soils and marine sediments, a significant proportion of the OM present interacts with mineral particles (Baldock et al., 2004). Christensen (2001) demonstrated that 50-70% of OM in temperate, arable soils exists

within clay-sized organo-mineral particles. Hedges and Keil (1999) also provided evidence that a major fraction of OM carried to estuaries by rivers is tightly associated with the surfaces of suspended minerals. Soil minerals also provide a solid phase for the adsorption of important individual biological molecules such as proteins (Fu et al., 2007) and nucleic acids (Nannipieri et al., 2003). For example, the adsorption of the purified Bt toxin to microbial proteins to clay minerals (montmorillonite and kaolinite) has been demonstrated (Fu et al., 2007).

Moreover, expandable clays such as smectites have been shown to have a high affinity for protein adsorption (Safari Sinegani et al., 2005), and the adsorption of enzymes and amino acids on both external and internal surfaces of montmorillonite has been reported (Miao et al., 2005; Safari Sinegani et al., 2005). In some cases, extracellular enzymes adsorbed by clay minerals or entrapped by humic molecules preserve their activity by being protected against proteolysis, thermal and pH denaturation (Huang et al., 2003; Nannipieri et al., 2003), while in other cases, inhibition of enzyme activity result from the association (Kelleher et al., 2003). Enzymes accumulating in soil are important, as they participate in the biological cycles of elements and play an important role in the transformation of organic mineral compounds (Safari Sinegani et al., 2005). The extent of organo-mineral interactions are said to increase with decreasing particle size in response to an increased area of relative mineral surfaces and the presence of multivalent cations, various oxides and hydroxides (Baldock et al., 2004). The chemical structure of organic materials is also of importance in defining the strength with which mineral and organic soil components interacts (Baldock and Skjemstad, 2000).

1.1.14 Mechanism of clay-organic matter interactions

The precise mode or combination of mechanisms for OM sorption is currently a topic of debate; however, several studies have provided insights into the relationship between organic matter and mineral surfaces (Simpson et al., 2006). Collectively, these studies indicate (1) the sorption of soluble organic matter to clay surface is competitive, as higher molecular weight compounds are preferentially sorbed, (2) the adsorption of organic matter increases inversely with pH, and (3) the number of OM coatings varies with concentration (Wershaw et al., 1995, 1996a,b). OM can be sorbed to clay-based minerals through ligand exchange between the carboxyl functional groups of organic

matter and the hydroxyl groups bonded to structural Al exposed on spherule surfaces (Parfitt et al., 1997).

Wershaw and Pinckney (1980) postulated that decayed organic materials are often bound to clay surfaces by amino acids or proteins, based on the observation that deamination of organo-mineral complexes with nitrous acid released organic material from clay. In particular, positively charged amino acids such as lysine can be strongly adsorbed to cation exchange sites of clay minerals in comparison to net neutral and negatively charged amino acids such as glycine and glutamate. Generally, peptidic compounds sorb strongly to a wide variety of clays, with strength of bonding varying over several orders of magnitude depending on the protein (Rillig et al., 2007). The mechanisms of such interactions may involve electrostatic interactions, ligand exchange and physisorption (Rillig et al., 2007). In addition to ion exchange, the type of clay, the nature of charge-compensating ions on the clay, water content, and the tertiary structure and size of the biomolecules have been shown to be important (Franchi et al., 1999). This may significantly affect their bioavailability as has been demonstrated for other low molecular weight C substrates (Jones and Edwards, 1998). Ultimately, the mineralogy, surface charge characteristics, and precipitation of amorphous Fe and Al oxides on clay mineral surfaces give clay minerals the capacity to adsorb OM. Such adsorption reactions provide a mechanism of stabilizing OM against biological attack (Baldock and Skjemstad, 2000).

1.1.15 Mechanism of organic matter protection

It is the general concensus that clay-organo association stabilizes soil organic carbon (Hsieh, 1996; Parfitt et al., 1997) in the global C cycle (Ladd et al., 1985; Spain, 1990) and influences transport and bioavailability of nutrients and contaminants in soils and waters (Hedges and Keil, 1999). Baldock and Skjemstad (2000) suggest hat the extent to which OM progresses through the stages of decomposition will depend on the presence of protection mechanisms capable of enhancing biological stability. Mineral particles capable of protecting OM will perturb the progression from less to more chemically recalcitrant material during decomposition. This is evidenced by the several positive correlations obtained between the content of initial soil organic C and clay content and between the amount of residual substrate C retained in a soil and clay content (Ladd et al., 1985; Spain, 1990). Christensen (2001) further suggested that the mechanisms responsible for the preservation and turnover of OM in soils and sediments

are due not only to the intrinsic chemical recalcitrance of the substrates, but also, and perhaps more importantly, to the nature of the association of OM with soil's mineral components creating physical barriers between substrates and decomposers. These suggestions are supported by the findings of Hedges et al. (1997) who provided evidence that terrestrial OM adsorbed to fine suspended riverine sediment material accumulated in coastal marine sediments, whereas DOM discharged by rivers into the open sea is subjected to rapid oxic biodegradation and/or photolysis (Opsahl and Benner, 1997).

Various schemes for the protection of OM from decomposition have been proposed. In one such scheme three major mechanisms have been identified for the protection of OM from degradation and include; biological recalcitrance (Kothawala et al., 2008), reduced accessibility for biological degradation (Sollins et al., 1996), and interactions with soil minerals (Wagai et al., 2009). The consequence of biological recalcitrance is selective stabilization which leads to the relative accumulation of recalcitrant molecules. A parallel mechanism to reduced accessibility for biological degradation is that of spatial inaccessibility. This is the spatial localization of OM that influences access by microbes and enzymes. Inaccessibility is caused by occlusion of OM by aggregation, intercalation with phyllosilicates, hydrophobicity and encapsulation in organic macromolecules (von Lützow et al., 2006).

Pure clays demonstrate hydrophilic properties; however, the association of organic material, particularly fatty acids with clay minerals increases their hydrophobicity (Doerr et al., 2000). Hydrophobic interactions are driven by the exclusion of non-polar residues (e.g. aromatic or alkyl C) from water to force the non-polar groups together (von Lützow et al., 2006). Hydrophobicity reduces the surface wettability and thus the accessibility of OM for microorganisms. This results in a decrease of decomposition rates, as the absence of water directly restricts the living conditions of decomposing microorganisms (Jandl et al., 2004). In addition to the direct effect of hydrophobicity on microbial accessibility, hydrophobicity also enhances aggregate stability thereby contributing to the occlusion of OM as a stabilizing mechanism (von Lützow et al., 2006). There is clear evidence to suggest that aggregation protects OM from degradation, because C mineralization increases when soil aggregates have become disrupted (Six et al., 2000, 2002).

In contrast, Baldock et al. (2004) have suggested a model for biological degradation based on biological recalcitrance, biological capability and capacity of the decomposer community and physical protection. This model suggests that the biological recalcitrant chemical structures are alkyl C and charred OM and that the other mechanisms are responsible for the protection of potentially labile molecules and lead to the variable chemical structure observed for soil OM. Baldock and Skjemstad (2000) also suggested that where no protection mechanisms are operative, biological stability will be entirely controlled by the recalcitrance offered by the chemical structure of the OM. It has been proposed that adsorption and aggregation can retard decomposition processes but molecular recalcitrance appears to be the only mechanism by which soil OM can be stabilized for extended periods of time (Krull et al., 2003). Mayer et al. (2004) proposed two broad categories for the stabilization of OM in soils and sediments, namely organic recalcitrance and abiotic exclusion. Ultimately, the cycling of OM in soils is influenced by a combination of chemical, physical and biological processes (Kothawala et al., 2008).

The precise mechanisms for C stabilization in soils and the extent of organic coverage on soil mineral surfaces or the factors controlling it are unknown (Wagai et al., 2009). Our lack of understanding of the processes that maintain soil OM pools makes soil OM management difficult and uncertain (von Lützow et al., 2006). This requires a fundamental understanding of the mechanisms regulating OM and mineral surface interactions (Simpson et al., 2006). Of particular importance but great complexity are the questions of how strongly SOM may bind to mineral surfaces, how such bonds form and eventually break, and how the mechanism of attachment of SOM to mineral surfaces affect the residence time in soils (Kleber et al., 2007). To gain further insights into these processes, direct microscopy, elemental X-ray analysis, X-ray diffraction patterns and advanced NMR approaches are applied to investigate clay-organo complexes to determine the mechanism of interaction and the stabilizing effect of the mineral on OM degradation. Direct microscopy allows the characterization of physical features of clay-organo associations, while XRD patterns and elemental X-ray analysis of SEM images showed spatial co-variations of organic materials with the mineral (Wagai et al., 2009). Several studies have applied an NMR approach to investigate whole soils (Simpson et al., 2002), and the sorption of organic materials to mineral surfaces in soils (Wershaw et al., 1996a; Parfitt et al., 1999; Feng et al., 2005, 2006). More recently, Simpson et al. (2006) employed novel advanced NMR approaches to

investigate the interactions of model and natural mixtures with a mineral, elucidating which organic species bind preferentially to clay mineral surfaces.

1.1.16 Clay-microbial interactions

In soils, clay minerals play a significant role in the sorption of microorganisms (Chaerun et al., 2005) which are present as single cells or multicell colonies associated with mineral surfaces. These interactions have profound impacts on the physical, chemical and biological properties of soils such as mineral weathering, organic matter decomposition and elemental cycling (Jiang et al., 2007). An important process in microbe-mineral interactions is biomineralization (microbially-mediated synthesis of minerals). The interactions between bacteria and soil particles also play important roles in the mobility of a wide variety of contaminants including heavy metals (Cheung et al., 2007). However, few studies focus on the adsorption of soil bacteria on clay minerals which are the most active inorganic colloidal components in soils, and the interaction mechanisms between them are still not known (Jiang et al., 2007).

Bacterial cell walls represent a significant proportion of the total surface area exposed to soil (Fein et al., 1997). These surfaces are predominantly electronegative (Urrutia Mera and Beveridge, 1993) as are their polymeric exudates such as mucopolysaccharides and capsules which often provide nucleation sites and a favourable chemical microenvironment for bio-mineral complexes (Ueshima and Tazaki, 2001). Sherbert (1978) demonstrated that several anionic functional groups, including, carboxylic, hydroxyl and phosphate sites are present in bacterial cell walls and are responsible for the anionic characteristic and mineral binding ability of the cell wall. Microbial attachment to minerals may occur via a cation-bridging mechanism in which multivalent metal cations complex with a functional group (e.g., COO^-) which in turn bridges with ionic silicates to form large aggregates (Tazaki, 2005). Theng and Orchard (1995) also suggested that multivalent cations might have served as cation bridges in the interaction between clays and microbial extracellular polymeric substances.

In gram-positive organisms at circumneutral pH, the walls also possess a certain number of electropositive amino groups that are available for reaction with soluble anions. These are the D-alanine residue of teichoic acid, the amino sugar of the glycan, and the amino function of the diaminopimelic acid from the peptide portion of the

peptidoglycan. In addition the proton motive force exudes H^+ into the wall which neutralizes many of the electronegative sites. These metabolically active cells would then have more accessible electropositive sites in their walls for interaction with environmental anions such as SiO_3^{2-} (Urrutia Mera and Beveridge, 1993).

1.1.17 Clay minerals

Clay minerals are the main colloidal soil fraction (Lombardi et al., 2002). Their physico-chemical properties are fundamentally influenced by their atomic structure, texture, composition and surface reactivity (Bakhti et al., 2001). Although clay minerals share a basic set of structural and chemical characteristics, each clay mineral has its own unique set of properties that determines how it will interact with other chemical species (Costanzo, 2001). The size and aspect ratio, for example, of kaolinite are larger than those of montmorillonite. Consequently, the interactions at the interface between kaolinite and organic molecules are very different from those of smectite-organic systems (Itagaki et al., 2001).

Montmorillonite is a 2:1 phyllosilicate mineral consisting of two tetrahedral silicate layers sandwiching a central alumina octahedral layer (Miao et al., 2005). It is classified as a dioctahedral mineral meaning that along the *b* axis there is one vacant site in every three octahedral positions, unlike trioctahedral aluminosilicates which have a fully occupied octahedral sheet. The imperfection of the crystal lattice and the isomorphic substitution of Al^{3+} atom in the octahedral layer by Mg^{2+} and Fe^{2+} and Si^{4+} atoms in the tetrahedral layer by Al^{3+} induce a net negative charge located mainly in the silicate octahedral layers (Sainz-Diaz et al., 2000). These charges are compensated for by hydrated alkali or alkaline earth cations situated in the gallery. Montmorillonite clay mineral also combines unique swelling, a large surface area, intercalation and cation exchange capacity (CEC; Bakandritsos et al., 2006). In contrast, kaolinite is a non-expandable layer silicate (1:1 clay mineral). However, it is unique because the interlayer is sandwiched by OH groups on one side and oxide layers on the other side which may induce specific guest orientation (Itagaki et al., 2001). Kaolinite clay mineral is without layer charge and interlayer spaces and exhibit low surface area, low CEC and consequently low bonding affinities (Wattel-Koekkoek et al., 2001).

1.1.18 Project objectives

The broad objectives of this project were to investigate the molecular properties and degradation dynamics of major biochemical components (proteins, carbohydrates and lipids) of soil microbial biomass and to delineate the contribution of labile and recalcitrant microbial biomass constituents to the SOM pool. An additional objective was to investigate the adsorption mechanisms of microbially derived OM to clay minerals and the preservation of labile OM by clays, thereby enhancing our understanding of carbon and nitrogen nutrient cycles particularly as they relate to agriculture and environmental sustainability. Further, attempts were made to identify stable biomarkers that can be used to follow the fate of microbially derived carbon and nitrogen in the environment and to detect novel compounds (degradation products) that may have potential applications in industry and medicine. More specific objectives of the project were to:

1. Characterize the microbial diversity of the culturable fraction of two arable Irish field sites.
2. Propagate isotopically labelled ($^{13}C/^{15}N$) soil microbial biomass and elucidate the compositions and aspects of the chemical structures of soil microbial biomass degraded under ambient and UV conditions.
3. Investigate the sorption and preservation of major microbial biomolecules by kaolinite and montmorillonite clay minerals.
4. Investigate the dynamics of microbially derived fatty acids and amino acids degraded under ambient and UV conditions.
5. Determine the composition of the refractory protein pool of soil microbial biomass degraded under ambient and UV conditions, and yield clues to their phylogenetic origin.

To achieve these objectives, soil microbial biomass was exclusively propagated in a minimal medium and the culturable microbial community characterized using 16S rRNA amplification and sequencing. Microbial biomass amended with or without montmorillonite and kaolinite clay minerals was also propagated with isotopically labelled (^{13}C and ^{15}N) substrates. Increasing the relative abundance of ^{13}C and ^{15}N through labelling the culture medium greatly enhances NMR sensitivity and therefore provides extremely detailed information on the molecular make-up of the OM. Enriched microbial biomass and clay-microbial complexes were degraded under ambient and intense UV-A UV-B radiation. Elucidation of the compositions and

aspects of the chemical structures of the fresh and degraded microbial biomass, clay-microbial interaction and OM stabilization by clay minerals were investigated by solution state multidimentional NMR. Additionally, SEM-EDS and XRD were used to provide some insights into these interactions. High resolution LC-TOF-MS, MALDI-TOF, GC-MS and GC-IRMS were also employed to investigate the transformation dynamics of major soil microbial biomolecules and relate this molecular level information to the labile and recalcitrant microbially derived OM and its contribution to the carbon and nitrogen biogeochemical cycles. GC-MS and advanced multidimentional NMR techniques allowed us to identify and trace microbial biomarkers and as well as novel degradation products.

1.2 References

Ågren, G. J., Bosatta, E., and Balesdent, J. 1996. Isotope discrimination during decomposition of organic carbon: a theoretical analysis. *Soil Science Society of America Journal* 60, 1121–1126.

Alef, K., and Nannipieri, P. 1995. *Methods in applied soil microbiology and biochemistry*. Academic Press, London.

Ambles, A., Jambu, P., Parlanti, E., Joffre, J., and Riffe, C. 1994. Incorporation of natural monoacids from plant residues into an hydromorphic forest podzol. *European Journal of Soil Science* 45, 175–82.

Amelung, W., Zhang, X., and Flach, K. W. 2006. Amino acids in grassland soils: climatic effects on concentrations and chirality. *Geoderma* 130, 207–217

Andrews, J. E., Brimblecombe, P., Jickells, T. D., Liss, P. S., and Reid, B. J. 2004. *An introduction to environmental chemistry*. 2nd Ed.; Blackwell Science, Malden, MA.

Anesio, A. M., Tranvik, L. J., and Granéli, W. 1999. Production of inorganic carbon from aquatic macrophytes by solar radiation. *Ecology* 80, 1852–1859.

Angers, D. A., Voroney, R. P., and Cote, D. 1995. Dynamics of soil organic matter and corn residues affected by tillage practices. *Soil Science Society of America Journal* 59, 1311–1315.

Augris, N., Balesdent, J., Mariotti, A., Derenne, S., and Largeau, C. 1998. Structure and origin of insoluble and non-hydrolyzable, aliphatic organic matter in forest soil. *Organic Geochemistry* 28, 119–124.

Austin, A. T., and Vivanco, L. 2006. Plant litter decomposition in a semi-arid ecosystem controlled by photodegradation. *Nature* 422, 555–558.

Bakandritsos, A., Simopoulos, A., and Petridis, D. 2006. Iron changes in natural and Fe(III) loaded montmorillonite during carbon nanotube growth. *Nanotechnology* 17, 1112–1117.

Bakhti, A., Derriche, Z., Iddou, A., and Larid, M. 2001. A study of the factors controlling theee adsorption of Cr(III) on modified montmorillonites. *European Journal of Soil Science* 52, 683–692.

Baldock, J. A., and Skjemstad, J. O. 2000. Role of the soil matrix and minerals in protecting natural organic materials against biological attack. *Organic Geochemistry* 31, 697–710.

Baldock, J. A., Massiello, C. A., Gelinas, Y., and Hedges, J. L. 2004. Cycling and composition of organic matter in terrestrial and marine ecosystems. *Marine Chemistry* 92, 39–64.

Baldock, J. A., Oades, J. M., Waters, A. G., Peng, X., Vassallo, A. M., and Wilson, M. A. 1992. Aspects of the chemical structure of soil organic materials as revealed by solid-state ^{13}C NMR spectroscopy. *Biochemistry* 16, 1–42.

Belay-Tedla, A., Zhou, X., Su, B., Wan, S., and Luo, Y. 2009. Labile, recalcitrant, and microbial carbon and nitrogen pools of tallgrass prairie soil in the US Great Planes subjected to experimental warming and clipping. *Soil Biology & Biochemistry* 41, 110–116.

Bent, D. V., and Hayon, E. 1975. Excited state chemistry of aromatic amino acids and related peptides. III. Tryptophan. *Journal of American Chemical Society* 97, 2612–2619.

Blair, N., Leu, A., Muñoz, E., Olsen, J., Kwong, E., and Des Marais, D. 1985. Carbon isotope fractionation in heterotrophic microbial metabolism. *Applied and Environmental Microbiology* 50, 996–1001.

Boschker, H. T. S. deBrouwer, J. F. C., and Cappenberg, T. E. 1999. The contribution of macrophyte-derived organic matter to microbial biomass in salt-marsh sediments: Stable carbon isotope analysis of microbial biomarkers. *Limnology and Oceanography* 44, 309–319.

Bottner, P., Pansu, M., Sarmiento, L., Hervé, D., Callisaya-Bautista, R., and Metselaar, K. 2006. Factors controlling decomposition of soil organic matter in fallow systems of high tropical Andes: a field simulation approach using ^{13}C- and ^{15}N-labeled plant material. *Soil Biology & Biochemistry* 38, 2162–2177.

Bowen, S. R., Gregorich, E. G., and Hopkins, D. W. 2009. Biochemical properties and biodegradation of dissolved organic matter from soils. *Biology and Fertility of Soils* 45, 733–742.

Bremner, J. M. 1950. The Amino-acid composition of protein material in soil. *Biochemistry Journal* 47, 538–542.

Bull, I. D., van Bergen, P. F., Nott, C. J., Poulton, P. R., and Evershed, R. P. 2000. Organic geochemical studies of soils from the Rothamsted classical experiments-V. The fate of lipids in different long-term experiments. *Organic Geochemistry* 31, 389–408.

Bünemann, E. K., Marschner, P., Smernik, R. J., Conyers, M., and McNeill, A. M. 2008. Soil organic phosphorus and microbial community composition as affected by 26 years of different management strategies. *Biology and Fertility of Soils* 44, 717–726.

Caldwell, C. R. 1993. Ultraviolet-induced photodegradation of cucumber (*Cucumis sativus* L.) microsomal and soluble protein tryptophanyl residues in vitro. *Plant Physiology* 101, 947–953.

Caradec, S., Grossi, V., Gilbert, F., Guigue, C., and Goutx, M. 2004. Influence of various redox conditions on the degradation of microalgal triacylglycerols and fatty acids in marine sediments. *Organic Geochemistry* 35, 277–287.

Chaerun, S. K., Tazaki, K., Asada, R., and Kogure, K. 2005. Interaction between clay minerals and hydrocarbon-utilizing indigenous microorganisms in high concentrations of heavy oil: implications for bioremediation. *Clay Minerals* 40, 105–114.

Cheung, H.-Y, Chan, G.K.-L., Cheung, S.-H., Sun, S.-Q., and Fong, W.-F. 2007. Morphological and chemical changed in the attached cells of *Pseudomonas aeruginosa* as primary biofilms develop on aluminium and CaF_2 plates. *Journal of Applied Microbiology* 102, 701–710.

Chotte, J. L., Ladd, J. N., and Amato, M. 1998. Sites of microbial assimilation, and turnover of soluble and particulate ^{14}C-labelled substrate decomposing in a clay soil. *Soil Biology & Biochemistry* 30, 205–218.

Christensen, B. T. 2001. Physical fractionation of soil and structural and functional complexity in organic matter turnover. *European Journal of Soil Science* 52, 345–353.

Christodoulou, S., Marty, J.-C., Miquel, J.-C., Volkman, J. K., and Rontani, J.-F. 2009. Use of lipids and their degradation products as biomarkers for carbon cycling in the northwestern Mediterranean Sea. *Marine Chemistry* 113, 25-40.

Clark, L. L., Ingall, E. D., and Benner, R. 1998. Marine phosphorus is selectively remineralized. *Nature* 393, 426.

Coelho, R. R. R., Sacramento, D. R., and Linhares, L. F. 1997. Amino sugars in fungal melanins and soil humic acids. *European Journal of Soil Science* 48, 425–429.

Coffin, R. B., Velinsky, D. J., Devereux, R., Price, W. A., and Cifuentes, L. A. 1990. Stable carbon isotope analysis of nucleic acids to trace sources of dissolved substrates used by estuarine bacteria. *Applied and Environmental Microbiology* 56, 2012–2020.

Colombini, M. P., Giachi, G., Modugno, F., and Ribechini, E. 2005a. Characterization of organic residues in pottery vessels of the roman age Antinoe (Egypt). *Microchemical Journal* 79, 83–90.

Colombini, M. P., Modugno, F., and Ribechini, E. 2005b. Organic mass spectrometry in archaeology: evidence for *Brassicaceae* seed oil in Egyptian ceramic lamps. *Journal of Mass Spectrometry* 40, 890–898.

Costanzo, P. M. 2001. Baseline studies of the clay minerals society source clays: introduction. *Clays and Clay Minerals* 49, 372–373.

Cowan, S. W., Schirmer, T., Rummel, G., Steiert, M., Ghosh, R., Pauptit, R. A., J. N. Jansonius, J. N., and Rosenbusch, J. P. 1992. Crystal structures explain functional properties of two *E. coli* porins. *Nature* 358, 727–733.

Crow, S. E., Sulzman, E. W., Rugh, W. D., Bowden, R. D., and Lajtha, K. 2006. Isotopic analysis of respired CO_2 during decomposition of separated soil organic matter pools. *Soil Biology & Biochemistry* 38, 3279–3291.

Daniel, R. 2005. The metagenomics of soil. *Nature Reviews Microbiology* 3, 470–478.

Dauwe, B., and Middelburg, J. J. 1998. Amino acids and hexosamines as indicators of organic matter degradation state in North Sea sediments. *Limnology and Oceanography* 43, 782–798.

Derenne, S., and Largeau, C. 2001. A review of some important families of refractory macromolecules: Composition, origin, and fate in soils and sediments. *Soil Science* 166, 833–847.

Dijkstra, P., Ishizu, A., Doucett, R., Hart, S. C., Schwartz, E., Menyailo, O. V., and Hungate, B. A. 2006. ^{13}C and ^{15}N Natural abundance of soil microbial biomass. *Soil Biology & Biochemistry* 38, 3257–3266.

Doerr, S. H., Shakesby, R. A., and Walsh, R. P. D. 2000. Soil water repellency: its causes, characteristics and hydro-geomorphological significance. *Earth Science Reviews* 51, 33–65.

Faganeli, J., Ogrinc, N., Kovac, N., Kukovec, K., Falnoga, I., Mozetic, P., and Bajt. O. 2009. Carbon and nitrogen isotope composition of particulate organic matter in relation to mucilage formation in the north Adriatic Sea. *Marine Chemistry* 114, 102–109.

Fein, J. B., Daughney, C. J., Yee, N., and Davis, T. A. 1997. A chemical equilibrium model for metal adsorption onto bacterial surfaces. *Geochimica et Cosmochimica Acta* 61, 3319–3328.

Feng, X., Simpson, A. J., and Simpson, M. J. 2005. Chemical and mineralogical controls on humic acid sorption to clay mineral surfaces. *Organic Geochemistry* 36, 1553–1566.

Feng, X., Simpson, A. J., and Simpson, M. J. 2006. Investigating the role of mineral-bound humic acid in phenanthrene sorption. *Environmental Science and Technology* 40, 3260–3266.

Findlay, R. H., King, G. A., and Watling, L. 1989. Efficacy of phospholipid nnalysis in determining microbial biomass in sediments. *Applied and Environmental Microbiology* 55, 2888–2893.

Franchi, M., Bramanti, E., Morassi Bonzi, L., Luigi Orioli, P., Vettori, C., and Gallori, E. 1999. Clay-nucleic acid complexes: characterization and implications for the preservation of genetic materials in primeval habitats. *Origins of Life and Evolution of the Biosphere* 29, 279–315.

Frankel, E. N., Neff, W. E., and Bessler, T. R. 1979. Analysis of autoxidized fats by gas chromatography-mass spectrometry: V. Photosensitized oxidation. *Lipids* 14, 961–967.

Fu, Q., Dong, Y., Hu, H., and Huang, Q. 2007. Adsorption of the insecticidal protein of *Bacillus thuringiensis* subsp. *Kurstaki* by soil minerals: effects of organic acid ligands. *Applied Clay Sciences* 37, 201–206.

Glaser, B., and Gross, S. 2005. Compound-specific stable-isotope $\delta^{13}C$ analysis of individual amino sugars – a tool to quantify timing and amount of soil microbial residue stabilization. *Rapid Communication in Mass Spectrometry* 19, 1409–1416.

Glaser, B., Turrión, M.-B., and Alef, K. 2004. Amino sugars and muramic acid-biomarkers for soil microbial community structure analysis. *Soil Biology & Biochemistry* 36, 399–407.

Gleixner, G. Czimczki, C., Kramer, K., Luhker, B. M., and Schmidt, M. W. I. 2001. Plant compounds and their turnover and stabilization as soil organic matter. In: Schulze, M., Heimann, M., Harrison, S., Holland, E., Lloyd, J., Prentice, I. C., and Schimel, D. (Eds.), *Global biogeochemical cycles in the climate system*. Academic Press, San Diego, pp. 201–215.

Gleixner, G., Poirier, N., Bol, R., and Balesdent, J. 2002. Molecular dynamics of organic matter in a cultivated soil. *Organic Geochemistry* 33, 357–366.

Grossi, V., Caradec, S., and Gilbert, F. 2003. Burial and reactivity of sedimentary microbial lipids in bioturbated Mediterranean coastal sediments. *Marine Chemistry* 81, 57–69.

Guggenberger G., and Kaiser, K. 2003. Dissolved organic matter in soil: challenging the paradigm of sorptive preservation. *Geoderma* 113, 293–310.

Guggenberger, G., Christensen, B. T., and Zech, W. 1994. Land use effect on the composition of organic matter in particle-size separates of soil: 1 lignin and carbohydrate signature. *European Journal of Soil Sciences* 45, 449–458.

Guggenberger, G., Kaiser, K. and Zech, W. 1998. Organic colloids in forest soils: 1. Biochemical mobilization in the forest floor. *Physics and Chemistry of the Earth* 23, 141–146.

Hagerman, A. E., and Robbins, C. T. 1987. Implication of soluble tannin–protein complexes for tannin analysis and plant defense mechanisms. *Journal of Chemical Ecology* 13, 1243–1258.

Hagerman, A. E., Rice, M. E., and Ritchard, N. T. 1998. Mechanisms of protein precipitation for two tannins, pentagalloyl glucose and epicatechin$_{16}$ (4→8) catechin (procyanidin). *Journal of Agricultural and Food Chemistry* 46, 2590–2595

Hallsworth J. E., Heim S., and Timmis K. N. 2003. Chaotropic solutes cause water stress in *Pseudomonas putida*. *Environmental Microbiology* 5, 1270–1280.

Hartgers, W. A., Schouten, S., Lopez, J. F., Sinninghe Damsté, J. S., and Grimalt, J. O. 2000. ^{13}C-contents of sedimentary bacterial lipids in shallow sulfidic monomictic lake (Lake Cisó, Spain). *Organic Geochemistry* 31, 777–786.

He, H., Xie, H., and Zhang, X. 2006. A novel GC/MS technique to assess ^{15}N and ^{13}C incorporation into soil amino sugars. *Soil Biology & Biochemistry* 38, 1083–1091.

He, H., Xie, H., Zhang, X., Wang, Y., and Wu, Y. 2005. A gas chromatographic/mass spectrometric method for tracing the microbial conversion of glucose into amino sugars in soil. *Rapid Communication in Mass Spectrometry* 19, 1993–1998.

Hedges, J. I. 1978. The formation and clay mineral reactions of melanoidins. *Geochimica et Cosmochimica Acta* 42, 69–76.

Hedges, J. I., and Hare, P. E. 1987. Amino acid adsorption by clay minerals in distilled water. *Geochimica et Cosmochimica Acta* 51, 255–259.

Hedges, J. I., and Keil, R. G. 1999. Organic geochemical perspectives on estuarine processes: sorption reactions and consequences. *Marine Chemistry* 65, 55–65.

Hedges, J. I., Baldock, J. A., Gélinas, Y., Lee, C., Peterson, M., and Wakeham, S. G. 2001. Evidence for non-selective preservation of organic matter in sinking marine particles. *Nature* 409, 801–804.

Hedges, J. I., Eglinton, G., Hatcher, P. G., Kirchman, D. L., Arnosti, C., Derenne, S., Evershed, R. P., Kögel-Knabner, I., de Leeuw, J. W., Littke, R., Michaelis, W., and Rullkötter, J. 2000. The molecularly-uncharacterized component of nonliving organic matter in natural environments. *Organic Geochemistry* 31, 945–958.

Hedges, J. I., Keil, R. G., and Benner, R. 1997. What happens to terrestrial organic matter in the ocean? *Organic Geochemistry* 27, 195–212.

Hsieh, Y. P. 1996. Soil organic carbon pools of two tropical soils inferred by carbon signatures. *Soil Science Society of America Journal* 60, 117–1121.

Huang, Q., Zhao, Z., and Chen, W. 2003. Effects of several low-molecular weight organic and phosphate on the adsorption of acid phosphatase by soil colloids and minerals. *Chemosphere* 52, 571–579.

Inagaki, F., Motomura, Y., and Ogata, S. 2003. Microbial silica decomposition in geothermal hot waters. *Applied Microbiology and Biotechnology* 60, 605–611.

IPCC (1996) *Cimate Change 1995. Impacts, adaptations and mitigation of climate change*. Scientific-technical analyses, Cambridge University Press, Cambridge, U.K.

Itagaki, T., Komori, Y., Sugahara, Y., and Kurodda, K. 2001. Synthesis of a kaolinite-poly(β-alanine) intercalating compound. *Journal of Materials Chemistry* 11, 3291–3295.

Jakas, A., and Horvat, S. 2004. The effect of glycation on the chemical and enzymatic stability of the endogenous opioid peptide, leucine-enkephalin, and related fragments. *Bioorganic Chemistry* 32, 516–526.

Jandl, G., Leinweber, P., Schulten, H.-R., and Eusterhues, K. 2004. The concentrations of fatty acids in organo-mineral particle-size fractions of a Chernozem. *European Journal of Soil Science* 55, 459–469.

Jandl, G., Schulten, H.-R., and Leinweber, P. 2002. Quantification of long-chain fatty acids in dissolved organic matter and soils. *Journal of Plant Nutrition and Soil Science* 165, 133–139.

Jia, Y., Lu, Z. B., Huang, K., Herzberg, O., and Dunaway- Mariano, D. 1999. Insight into the mechanism of phosphoenolpyruvate mutase catalysis derived from site-directed mutagenesis studies of active site residues. *Biochemistry* 38, 14165–14173.

Jiang, D., Haung, Q., Cai, P., Rong, X., and Chen, W. 2007. Adsorption of *Pseudomonas putida* on clay minerals and iron oxide. *Collides and Surfaces B*: *Biointerfaces* 54, 217–221.

Johnson, D., Campbell, C. D., Lee, J. A., Callaghan, T. V., and Gwynn-Jones, D. 2002. Artic microorganisms respond more to elevated UV-B radiation than CO_2. *Nature* 416, 82–83.

Jones, D. L., and Edwards, A. C. 1998. Influence of sorption on the biological utilization of two simple carbon substrates. *Soil Biology & Biochemistry* 30, 1895–1902.

Kaiser, K., Guggenberger, G., Haumaier, L., and Zech, W. 2001. Seasonal variation in the chemical composition of dissolved organic matter in organic forest floor layer

leachates of old-growth Scots pine (*Pinus sylvestris* L.) and European beech (*Fagus sylvatica* L.) stands in northeastern Bavaria, Germany. *Biochemistry* 55, 103–143.

Kalbitz, K., Solinger, S., Park, J.-H., Michalzik, B., and Matzner, E. 2001. Controls on the dynamics of dissolved organic matter in soils: a review. *Soil Science* 165, 277–304.

Kawano, M., and Tomita, K. 2001. Microbial biomineralization in weathered volcanic ash deposit and formation of biogenic minerals by experimental incubation. *American Mineralogist* 86, 400–410.

Keil, R. G. and Fogel, M. L. 2001. Reworking of amino acid in marine sediments: stable carbon isotope composition of amino acids in sediments along the Washington coast. *Limnology and Oceanography* 46, 14–23.

Kelleher, B. P., and Simpson, A. J. 2006. Humic substances in soils: are they really chemically distinct? *Environmental Science and Technology* 40, 4605–4611.

Kelleher, B. P., Oppenheimer, S. F., Han, F. X., Willeford, K. O., Simpson, M. J., Simpson A. J. and Kingery, W. L. 2003. Dynamic systems and phase plane analysis of protease-clay interactions. *Langmuir* 19, 9411–9417.

Kelleher, B. P., Simpson, A. J., Rogers, R. E., Dearman, J., and Kingery, W. L. 2007. Effects of organic matter from sediments on the growth of marine gas hydrates. *Marine Chemistry* 103, 237–249.

Kelleher, B. P., Simpson, M. J., and Simpson, A. J. 2006. Assessing the fate and transformation of plant residues in the terrestrial environment using HR-MAS NMR spectroscopy. *Geochimica et Cosmochimica Acta* 70, 4080–4094.

Kerwin, B. A., and Remmele, R. L. Jr. 2006. Protect from light: Photodegradation and protein biologics. *Journal of Pharmaceutical Sciences* 96, 1468–1479.

Kieber, D. J., McDaniel, J., and Mopper, K. 1989. Photochemical source of biological substrates in sea water: implications for carbon cycling. *Nature* 341, 637–639.

Kindler, R., Miltner, A., Richnow, H.-H., and Kästner, M. 2006. Fate of gram-negative bacterial biomass in soil—mineralization and contribution to SOM. *Soil Biology & Biochemistry* 38, 2860–2870.

Kindler, R., Miltner, A., Thullner, M., Richnow, H.-H., and Kästner, M. 2009. Fate of bacterial biomass derived fatty acids in soil and their contribution to soil organic matter. *Organic Geochemistry* 40, 29–37.

Kirchman, D. L., Henry, D. L., and Dexter, S. C. 1989. Adsorption of proteins to surfaces in seawater. *Marine Chemistry* 27, 201–217.

Kleber, M., Sollins, P., and Sutton, R. 2007. A conceptual model of organo-mineral interactions in soils: self-assembly of organic molecular fragments into zonal structures on mineral surfaces. *Biogeochemistry* 85, 9–24.

Knicker, H. 2000. Biogenic nitrogen in soils as revealed by solidstate carbon-13 and nitrogen-15 nuclear magnetic resonance spectroscopy. *Journal of Environmental Quality* 29, 715–723.

Knicker, H. 2004. Stabilization of N-compounds in soil and organicmatter-rich sediments – what is the difference? *Marine Chemistry* 92, 167–195.

Knicker, H. 2007. Vegetation fires and burnings; how do they affect the nature and stability of soil organic nitrogen and carbon? – A review. *Biogeochemistry* 85, 91–118.

Knicker, H., and Hatcher, P. G. 1997. Survival of protein in an organicrich sediment: possible protection by encapsulation in organic matter. *Naturwissenschaften* 84, 231–234.

Knicker., H., and Lüdemann, H.-D. 1995. N-15 and C-13 CPMAS and solution NMR studies of N-15 enriched plant material during 600 days of microbial degradayion. *Organic Geochemistry* 23, 329–341.

Knicker., H., Scaroni, A. W., and Hatcher, P. G. 1996. ^{13}C and ^{15}N NMR spectroscopic investigation on the formation of fossil algal residues. *Organic Geochemistry* 24, 661–669.

Kögel-Knabner, I. 2002. The molecular organic composition of plant and microbial residues as inputs in soil organic matter. *Soil Biology & Biochemistry* 34, 139–162.

Kögel-Knabner, I. 2006. Chemical structure of organic N and organic P in soil. In: Nannipieri, P., and Smalla, K. (Eds), *Nucleic acids and proteins in soil*. Springer-Verlag Berlin Heidelberg, pp. 23–48.

Kolowith, L. C., Ingall, E. D., and Benner, R. 2001. Composition and cycling of marine organic phosphorus. *Limnology and Oceanography* 46, 309–320.

Kothawala, D. N., Mooe, T. R., and Hendershot, W. H. 2008. Adsorption of dissolved organic carbon to mineral soils: a comparison of four isotherm approaches. *Geoderma* 148, 43–50.

Kovac, N., Faganeli, J., Sket, B., and Bajt, O. 1998. Characterization of macroaggregates and photodegradatoin of their water soluble fraction. *Organic Geochemistry* 29, 1623–1634.

Kracht, O., and Gleixner, G. 2000. Isotope analysis of pyrolysis products from *Sphagnum* peat and dissolved organic matter from bog water. *Organic Geochemistry* 31, 645–654.

Krull, E. S., Baldock, J. A., and Skjemstad, J. O. 2003. Importance of mechanisms and processes of the stabilisation of soil organic matter for modelling carbon turnover. *Functional Plant Biology* 30, 207–222.

Ladd, J. N., Amato, M., and Oades, J. M. 1985. Decomposition of plant materials in Australian soils: III. Residual organic and microbial biomass C and N from isotope-labelled legume materials and soil organic matter decomposing under field conditions. *Australian Journal of Soil Research* 23, 603–611.

Lair, G. J., Zehetner, F., Khan, Z. H., and Gerzabek, M. H. 2009. Phosphorus sorption-desorption in alluvial soils of a young weathering sequence at the Danube River. *Geoderma* 149, 39–44.

Lal, R., Griffin, M., Apt, J., Lave, L., and Morgan M. G. 2004. Ecology – managing soil carbon. *Science* 304, 393–393.

Liang, C., Zhang, X., Rubert IV, K. F., and Balser, T. C. 2007. Effect of plant materials on microbial transformation of amino sugars in three soil microcosms. *Biology and Fertility of Soils* 43, 631–639.

Lichtfouse, E. 2000. Compound-specific isotope analysis. Application to archaeology, biomedical sciences, biosynthesis, environment, extraterrestrial chemistry, food science, forensic science, humic substances, microbiology, organic geochemistry, soil science and sport. *Rapid Communication in Mass Spectrometry* 14, 1337–1344.

Lichtfouse, E., Berthier, G., Houot, S., Barriuso, E., Bergheaud, V., and Vallaeys, T. 1995. Stable carbon isotope evidence for the microbial origin of C_{14}-C_{18} *n*-alkanoic acids in soils. *Organic Geochemistry* 23, 849–852.

Linn, D. M., Carski, T. H., and Brusseau, M. L. 1993. *Sorption and degradation of pesticides and organic chemicals in soil*. Soil Science Society of America, Madison, WI.

Lombardi, K. C., Guimarães, J. L., Mangrich, A. S., Mattoso, N., Abbate, M., Schreiner, W. H., and Wypych, F. 2002. Structural and morphological characterization of the PP-0559 kaolinite from the Brazilian Amazon Region. *Journal of Brazilian Chemical Society* 13, 270–275.

Macko, S. A., Angel, M. H., Hartley, G., Hatcher, P., Helleur, R., Jackman, P., and Silfer, J. 1991. Isotopic compositions of individual carbohydrates as indicators of early diagenesis of organic matter. *Chemical Geology* 93, 147–161.

Makarov, M. I., Haumaier, L., and Zech, W. 2002. Nature of soil organic phosphorus: an assessment of peak assignments in the diester region of ^{31}P NMR spectra. *Soil Biology & Biochemistry* 34, 1467–1477.

Marchand, D., and Rontani, J.-F. 2001. Characterization of photo-oxidation and autoxidation products of phytoplanktonic monounsaturated fatty acids in marine particulate matter and recent sediments. *Organic Geochemistry* 32, 287–304.

Mayer L. M., Schick, L. L., Hardy, K., Wagai, R., and McCarthy, J. 2004. Organic matter content of small mesopores in sediments and soils. *Geochimica et Cosmochimica Acta* 68, 3863–3872.

McLauchlan, K. K., and Hobbie, S. E. 2004. Comparison of labile soil organic matter fractionation techniques. *Soil Science Society of America Journal* 68, 1616–1625.

Miao, S., Liu, Z., Han, B., Zhang, J., Yu, X., Du, J., and Sun, Z. 2005. Synthesis and characterization of TiO_2-montmorillonite nanaocomposites and their application for removal of methylene blue. *Journal of Materials Chemistry* 16, 579–584.

Michalzik, B., and Matzner, E. 1999. Dynamics of dissolved organic nitrogen and carbon in a Central European Norway spruce ecosystem. *European Journal of Soil Science* 50, 579–590.

Miller, B. L., Hageman, M. J., Thamann, T. J., Barròn, L. B., and Schöneich, C. 2003. Solid-state photodegradation of bovine somatotropin (bovine growth harmone): evidencce for tryptophan-mediated photooxidation of disulfide bonds. *Journal of Pharmaceutical Sciences* 92, 1698–1709.

Mopper, K., Zhou, X., Kieber, R. J., Kieber, D. I., Sikorski, R. J., and Jones, R. D. 1991. Photochemical degradation of dissolved organic carbon and its impact on oceanic carbon cycle. *Nature* 353, 60–62.

Moriceau, B., Goutx, M., Guigue, C., Lee, C., Armstrong, R., Duflos, M., Tamburini, C., Charrière, B., and Ragueneau, O. 2009. Si–C interactions during degradation of the diatom *Skeletonema marinoi*. *Deep-Sea Research II* 56, 1381–1395.

Murase, A., Yoneda, M., Ueno, R., and Yonebayyashi, K. 2003. Isolation of extracellular proteins from greenhouse soil. *Soil Biology & Biochemistry* 35, 733–736.

Murphy, T. M. 1983. Membranes as targets of ultraviolet radiation. *Plant Physiology* 58, 381-388.

Naafs, D. F. W., van Bergen, P. F., de Jong, M. A., Oonincx, A., and de Leeuw, J. W. 2004. Total lipid extracts from characteristic soil horizons in a podzol profile. *European Journal of Soil Science* 55, 657–669.

Nagata, T., and Kirchman, D. L. 1997. Roles of submicron particles and colloids in microbial food webs and biogeochemical cycles within marine environments. In: Jones, T. (Ed.), *Advances in microbial ecology*. Plenum, New York, pp. 81–103.

Nannipieri, P., Ascher, J., Ceccherini, M. T., Landi, L., Pietramellara, G., and Renella, G. 2003. Microbial diversity and soil function. *European Journal of Soil Science* 54, 655–670.

Nautiyal, C. S. 1999. An efficient microbiological growth medium for screening phosphate solubilizing microorganisms. *FEMS Microbiology Letters* 170, 265–270.

Nguyen, R. T., and Harvey, H. R. 1997. Protein and amino acid cycling during phytoplankton decomposition in oxic and anoxic waters. *Organic Geochemistry* 27, 115–128.

Nguyen, R. T., and Harvey, H. R. 2001. Protein preservation in marine systems: hydrophobic and other non-covalent associations as major stabilizing forces. *Geochimica et Cosmochimica Acta* 65, 1467–1480.

Nguyen, R. T., and Harvey, H. R. 2003. Preservation via macromolecular associations during *Botryococcus braunii* decay: proteins in the Pula Kerogen. *Organic Geochemistry* 34, 1391–1403.

Nierop, K. G. J., and Verstraten, J. M. 2004. Rapid molecular assessment of the bioturbation extent in sandy soil horizons under pine using ester-bound lipids by on-line thermally assisted hydrolysis and methylation-gas chromatography/mass spectrometry. *Rapid Communication in Mass Spectrometry* 18, 1081–1088.

Nierop, K. G. J., Verstaten, J. M., Tietma, A., Westervald, J. W., and Wartenbergh, P. E. 2006. Short- and long-term tannin induced carbon, nitrogen and phosphorus dynamics in Corsican pine litter. *Biogeochemistry* 79, 275–296.

Nyman, B. F. 1985. Protein-proanthocyanidin interactions during extraction of Scots pine needles. *Phytochemistry* 24, 2939–2944.

Opsahl, S., and Benner, R. 1997. Distribution and cycling of terrigenous dissolved organic matter in the ocean. *Nature* 386, 480–482.

Otto, A., Chubashini, S., and Simpsom, M. J. 2005. A comparison of plant and microbial biomarkers in grassland soils from the Prairie Ecozone of Canada. *Organic Geochemistry* 36, 425–448.

Oursel, D., Loutelier-Bourhis, C., Orangr, N., Chevalier, S., Norris, V., and Lange, C. M. 2007. Identification and relative quantification of fatty acids in *Escherichia coli* membranes by gas chromatography/mass spectrometry. *Rapid Communications in Mass Spectrometry* 21, 3229–3233.

Pancotto, V. A., Sala, O. E., and Cabello, M. 2003. Solar UV-B decreases decomposition in herbaceous plant litter in Tierra del Fuego, Argentina: potential role of an altered decomposer community. *Global Change Biology* 9, 1465–1474.

Pancotto, V. A., Sala, O. E., Robson, M., Caldwell, M. M., and Scopel, A. L. 2005. Direct and indirect effects of solar ultraviolet-B radiation on long-term decomposition. *Global Change Biology* 11, 1982–1989.

Parfitt, R. L., Theng, B. K. G., Whitton, J. S., and Shepherd, T. G. 1997. Effects of clay minerals and land use on organic matter pools. *Geoderma* 75, 1–12.

Parfitt, R. L., Yuan, G., and Theng, B. K. G. 1999. A ^{13}C-NMR study of the interactions of soil organic matter with aluminium and allophane in podzols. *European Journal of Soil Science* 50, 695–700.

Pelz, O., Abraham, W. R., Saurer, M., Siegwolf, R., and Zeyer, J. 2005. Microbial assimilation of plant-derived carbon in soil traced by isotope analysis. *Biology and Fertility of Soils* 41, 153–162.

Pelz, O., Cifuentes, L. A., Hammer, B. T., Kelly, C. A., and Coffin, R. B. 1998. Tracing the assimilation of organic compounds using δ^{13}C analysis of unique amino acids in the bacterial peptidoglycan cell wall. *FEMS Microbiology Ecology* 25, 229–240.

Powell, M. J., Sutton, J. N., Del Castillo, C. E., and Timperman, A. T. 2005. Marine proteomics: generation of sequence tags for dissolved proteins in sea water using tandem mass spectrometry. *Marine Chemistry* 95, 183–198.

Quin, L. D. 2000. *A guide to organophosphorus chemistry*. John Wiley & Sons, New York, NY.

Quinn, J. P., Kulakova, A, N., Cooley, N, A., and McGrath, J. W. 2007. New ways to break an old bond: the bacterial carbon-phosphorus hydrolases and their role in the biogeochemical phosphorus cycling. *Environmental Microbiology* 9, 2392–2400.

Ragueneau, O., Tréguer, P., and Leynaert, A. 2000. A review of the Si cycle in the modern ocean: recent progress and missing gaps in the application of biogenic opal as a paleoproductivity proxy. *Global and Planetary Change* 26, 317–365.

Rao, S. C., Rao, C. M., and Balasubramanian, D. 1990. The conformational status of a protein influences the aerobic photolysis of its tryptophan residues: Melittin, beta-lactoglobulin and the crystallins. *Photochememistry and Photobiology* 51, 357–362.

Rieley, G. 1994. Derivatisation of organic compounds prior to gas chromatographic-combustion-isotope ratio mass spectrometric analysis: identification of isotope fractionation processes. *Analyst* 119, 915–919.

Rillig, M. C., Caldwell, B. A., Wösten, H. A. B., and Sollins, P. 2007. Role of proteins in soil carbon and nitrogen storage: controls of persistence. *Biogeochemistry* 85, 25–44.

Rontani, J.-F. 1998. Photodegradation of unsaturated fatty acids in sescent cells of phytoplankton: photoproduct structural identification and mechanistic aspects. *Journal of Photochemistry and Photobiology A*: *Chemistry* 114, 37–44.

Rontani, J.-F., Koblížek, M., Beker, B., Bonin, P., and Kolber, Z. S. 2003. On the origin of *cis*-Vaccenic acid photodegradation products in the marine environment. *Lipids* 38, 1085–1092.

Rontani, J.-F., Zabeti, N., and Wakeham, S. G. 2009. The fate of marine lipids: biotic vs. abiotic degradation of particulate sterols and alkenones in the Northwestern Mediterranean Sea. *Marine Chemistry* 113, 9–18.

Roth, L. C., and Harvey, R. 2006. Intact protein modification and degradation in estuarine environments. *Marine Chemistry* 102, 33–45.

Safari Sinegani, A. A., Emtiazi, G., and Shariatmadari, H. 2005. Sorption and immobilization of cellulose on silicate clay minerals. *Journal of Colloid and Interface Science* 290, 39–55.

Saggar, S., Tate, K. R., Feltham, C. W.,Childs, C. W., and A. Parshotam, A. 1994. Carbon turnover in a range of allophanic soils amended with ^{14}C-labelled glucose. *Soil Biology & Biochemistry* 26, 1263–1271.

Sainz-Diaz, C. I., Timon, V., Botella, V., and Hernendez-Laguna, A. 2000. Isomorphic substitution effect on the vibration frequencies of hydroxyl groups in molecular cluster models of the clay octahedral sheet. *Americal Mineralogist* 85, 1038–1045.

Sannigrahi, P., Ingall, E. D., and Benner, R. 2006. Nature and dynamics of phosphorus-containing components of marine dissolved and particulate organic matter. *Geochimica et Cosmochimica Acta* 70, 5868–5882.

Sanñudo-Wilhelmy, S. A., Kustka, A. B., Gobler, C. J., Hutchins, D. A., Yang, M., Lwiza, K., Burns, J., Capone, D. G., Raven, J. A., and Carpenter, E. J. 2001. Phosphorus limitation of nitrogen fixation by *Trichodesmium* in the central Atlantic Ocean. *Nature* 411, 66–69.

Santruckova, H., Bird, M. I., and Lloyd, J. 2000. Microbial processes and carbon isotope fractionation in tropical and temperate grassland soils. *Functional Ecology* 14, 108–114.

Schade, G. W., Hormann, R. M., and Crutzen, P. J. 1999. CO emissions from degrading plant matter. *Tellus B* 51, 899–908.

Schlesinger, W. H., and Andrews, J. A., 2000. Soil respiration and the global carbon cycle. *Biogeochemistry* 48, 7–20.

Scholle, G., Joergensen, R. G., Schaefer, M., and Wolters, V. 1993. Hexosamines in the organic layer of two beech forest soils: effects of mesofauna exclusion. *Biology and Fertility of Soils* 15, 301–307.

Schoneich, C. 2000. Mechanisms of metal-catalyzed oxidation of histidine to 2-oxo-histidine in peptides and proteins. *Journal of Pharmaceutical and Biomedical Analysis* 21, 1903–1097.

Schulze, W. X. 2005. Protein analysis in dissolved organic matter: what proteins from organic debris, soil leachate and surface water can tell us – a prospective. *Biogeosciences* 2, 75–86.

Scislowski, P. W., and Davis, E. J. 1987. Sulfur oxidation of free methionine by oxygen free radicals. *FEBS Letters* 224, 177–181.

Sharp, Z. 2007. *Principles of stable isotope geochemistry*. Pearson Prentice Hall, New Jersey.

Sherbert, G. V. 1978. *The biophysical characterization of the cell surface*. Academic Press, London.

Silfer, J. A., Engel, M. H., Macko, S. A., and Jumeau, E. J. 1991. Stable carbon isotope analysis of amino acid enantiomers by conventional isotope ration mass spectrometry and combined gas chromatography/isotope ratio mass spectrometry. *Analytical Chemistry* 63, 370–374.

Silvester, J. A., Timmins, G. S., and Davies, M. J. 1998. Phytodynamically generated bovine serum albumen radicals: evidence of damage transfer and oxidation at cysteine and tryptophan residues. *Free Radical Biology and Medicine* 24, 754–766.

Simpson, A. J. 2002. Determining the molecular weight, aggregation structures, and interactions of natural organic matter using diffusion ordered spectroscopy. *Magnetic Resonance in Chemistry* 40, S72–S82.

Simpson, A. J., Simpson, M. J., Kingery, W, L., Lefebvre, B. A., Moser, A., Williams, A. J., Kvasha, M., and Kelleher, B. P. 2006. The application of ^{1}H high-resolution magic-angle spinning NMR for the study of clay–organic associations in natural and synthetic complexes. *Langmuir* 22, 4498–4508.

Simpson, A. J., Simpson, M. J., Smith, E., and Kelleher, B. P. 2007. Microbially derived inputs to soil organic matter: are current estimates too low? *Environmental Science and Technology* 41, 8070–8076.

Six, J., Conant, R. T., Paul, E. A., and Paustian, K. 2002. Stabilization mechanisms of soil organic matter: implications for C-saturation of soils. *Plant and Soil* 241, 155–176.

Six, J., Elliott, E. T., and Paustian, K. 2000. Soil macroaggregate turnover and microaggregate formation: a mechanism for C sequestration under no-tillage agriculture. *Soil Biology & Biochemistry* 32, 2099–2103.

Six, J., Frey, S. D., Thiet, R. K., and Batten, K. M. 2006. Bacterial and fungal contribution to carbon sequestration in agroecosystems. *Soil Science Society of America Journal* 70, 555–569.

Sollins, P., Homann, P., and Caldwell, B. A. 1996. Stabilisation and destabilisation of soil organic matter: mechanisms and controls. *Geoderma* 74, 65–105.

Sollins, P., Swanston, C., Kleber, M., Filley, T., Kramer, M., Crow, S., Caldwell, B. A., Lajtha, K., and Bowden, R. 2006. Organic C and N stabilization in a forest soil: evidence from sequential density fractionation. *Soil Biology & Biochemistry* 38, 3313–3324.

Sommer, M., Kaczorek, D., Kuzyakov, Y., and Breuer, J. 2006. Silicon pools and fluxes in soils and landscape-a review. *Journal of Plant Nutrition and Soil Science* 169, 310–329.

Spain, A. 1990. Influence of environmental conditions and some soil chemical properties on the carbon and nitrogen contents of some Australian rainforest soils. *Australian Journal of Soil Research* 28, 825–839.

Stevenson, F. 1994. *Humus chemistry, genesis, composition, reaction*. Wiley & Sons, New York.

Stevenson, F. J. 1982. Organic forms of soil nitrogen. In: Stevenson, F. J. (Ed.), *Nitrogen in agricultural soils*. American Society of Agronomy Inc., Madison, WI, pp. 67–22.

Sun, M.-Y., and Wakeham, S. G. 1994. Molecular evidence for degradation and preservation of organic matter in the anoxic Black Sea Basin. *Geochimica et Cosmochimica Acta* 58, 3395–3406.

Sun, M.-Y., Shi, Y., and Lee, R. F. 2000. Lipid-degrading enzyme activities associated with distribution and degradation of fatty acids in the mixing zone of Altamaha estuarine sediments. *Organic Geochemistry* 31, 889–902.

Sun, M.-Y., Zou, L., Dai, J., Ding, H., Culp, R. A., and Scranton, M. I. 2004. Molecular carbon isotopic fractionation of algal lipids during decomposition in natural oxic and anoxic seawaters. *Organic Geochemistry* 35, 895–908.

Tanoue, E. 1995. Detectionof dissolved protein molecules in oceanic waters. *Marine Chemistry* 51, 239–252.

Tanoue, E., Nishiyama, S., Kamo, M., and Tsugita, A. 1995. Bacterial membranes: possible source of major dissolved proteins in seawater. *Geochimica et Cosmochimica Acta* 59, 2643–2648.

Tazaki, K. 2005. Microbial formation of halloysite-like mineral. *Clays and Clay Minerals* 53, 224–233.

Theng, B. K. G., and Orchard, V.A. 1995. Interactions of clays with microorganisms and bacterial survival in soil: a physicochemical perspective. In: Huang, J. Berthelin, P. M., Bollag, J. M., McGill, W. B., and Page, A. L. (Eds.), *Environmental impact of soil components*. CRC Press, Florida, pp. 123–139.

Tipping, E., Woof, C., Rigg, E., Harrison, A. F., Ineson, P. Taylor, K., Benham, D., Poskitt, J., Rowland, A. P., Bol, R., and Harkness, D. D. 1999. Climate influence on the leaching of dissolved organic matter from upland UK moorland soils, investigated by field manipulation experiments. *Environment International* 25, 83–95.

Tréguer, P., and Pondaven, P. 2000. Silicon control of carbon dioxide. *Nature* 406, 358–359.

Tréguer, P., Nelson, D. M., and Van Bennekom, A. J. 1995. The silica balance in the world ocean: a reestimate. *Science* 268, 375–379.

Trumbore, S. E., Bonani, G., and Wolfli, W. 1990. The rates of carbon cycling in several soils from AMS ^{14}C measurements of fractionated soil organic matter. In: Bouwman, A. F. (Ed.), *Soils and the greenhouse effect*. John Wiley, New York, NY, pp. 405–414.

Turner, B. L., Mahieu, N., and Condron, L. M. 2003a. The phosphorus composition of temperate pasture soils determined by NaOH-EDTA extraction and solution state ^{31}P NMR spectroscopy. *Organic Geochemistry* 34, 1199–1210.

Turner, B. L., Mahieu, N., and Condron, L. M. 2003b. Phosphorus-31 nuclear magnetic resonance spectral assignments of phosphorus compounds in soil NaOH-EDTA extracts. *Soil Science Society of America Journal* 67, 497–510.

Turner, B. L., Paphazy, M. J., Haygarth, P. M., and McKelvie, I. A. 2002. Inositol phosphates in the environment. *Phylosophical Transactions of the Royal Society of London B* 357, 449–469.

Turrión, M.-B., Glaser, B., and Zech, W. 2002. Effects of deforestation on contents and distribution of amino sugars within particle-size fractions of mountain soils. *Biology and Fertility of Soils* 35, 49–53.

Ueshima, M., and Tazaki, K. 2001. Possible role of microbial polysaccharides in nontronite formation. *Clays and Clay Minerals* 49, 292–299.

Urrutia Mera, M., and Beveridge, T. J. 1993. Mechanism of silicate binding to the bacterial cell wall in *Bacillus subtilis*. *American Society for Microbiology* 175, 1936–1945.

van Bergen, P. F., Bull, I, D., Poulton, P. R., and Evershed, R. P. 1997. Organic geochemical studies of soils from the Rothamsted Classical Experiments-I. Total lipid extracts, solvent insoluble residues and humic acid from Broadbalk Wilderness. *Organic Geochemistry* 26, 117–135.

Van Breemen, N., and Buurman, P. 2002. *Soil formation*. Kluwer Academic Publishers, Norwell, MA.

Varki, A. 1993. Biological roles of oligosaccharides: all of the theories are correct. *Glycobiology* 3, 97–130.

Vestal, J. R., and White, D. C. 1989. Lipid analysis in microbial ecology. *BioScience* 39, 535–541.

Vinolas, L. C., Healey, J. R., and Dones, D. L. 2001. Kinetics of soil microbial uptake of free amino acids. *Biology and Fertility of Soils* 33, 67–74.

von Lützow, M., Kögel-Knabner, I., Ekschmitt, K., Matzner, E., Guggenberger, G., Marschner, B., and Flessa, H. 2006. Stabilization of organic matter in temperate soils: mechanisms and their relevance under different soil conditions—a review. *European Journal of Soil Science* 57, 426–445.

Wagai, R., Mayer, L. M., and Kitayama, K. 2009. Extent and nature of organic coverage of soil mineral surfaces assessed by gas sorption approach. *Geoderma* 149, 152–160.

Wakeham, S. G., Hedges, J. I., Lee, C., Peterson, M. L., and Herns, P. J. 1997. Compositions and transport of lipid biomarkers through the water column and surficial sediments of the equatorial Pacific Ocean. *Deep-Sea Research II* 44, 2131–2162.

Waksman S. A., and Iyer, K. R. N. 1932. Contribution to our knowledge of the chemical nature and origin of humus: I on the synthesis of the ‘‘humus nucleus’’. *Soil Sci*ence 34, 43–69.

Wander, M. 2004. Soil organic matter functions and their relevance to soil functions. In: Magdoff, F., and Weil, R. R. (Eds.), *Soil organic matter in sustainable agriculture*. CRC Press, NY, pp. 67–102.

Wander, M. M., Hedrick, D. S., Kaufman, D., Traina, S. J., Stinner, B. R., Kehrmeyer, S. R., and White, D. C. 1995. The functional significance of the microbial biomass in organic and conventionally managed soils. *Plant and Soil* 170, 87–97.

Wattel-Koekkoek, E. J. W., van Genuchten, P. P. L., Buurman, P., and van Lagen, B. 2001. Amount and composition of clay-associated soil organic matter in a range of kaolinitic and smectitic soils. *Geoderma* 99, 27–49.

Weil, R. R., and Magdoff, F. 2004. Significance of soil organic matter to soil quality and health. In: Magdoff, F., and Weil, R. R. (Eds.), *Soil organic matter in sustainable agriculture*. CRC Press, NY, pp. 1–44.

Wershaw, R. L., and Pinckney, D. J. 1980. Isolation and characterization of clay-humic complexes In: Baker, R. A. (Ed.), *Contaminants and sediments*. Ann Arbor Science, Michigan.

Wershaw, R. L., Leenheer, J. A., Sperline, R. P., Song, Y., Noll, L. A., Melvin, R. L., and Rigatti, G. P. 1995.Mechanism of formation of humus coatings on mineral surfaces 1. Evidence for multidentate binding of organic acids from compost leachate on alumina. *Colloids and Surfaces A: Physicochemical and Engineering Aspects* 96, 93–104.

Wershaw, R. L., Llaguno, E. C., and Leenheer, J. A. 1996b. Mechanism of formation of humus coatings on mineral surfaces 3. Composition of adsorbed organic acids from compost leachate on alumina by solid-state ^{13}C NMR. *Colloids and Surfaces A: Physicochemical and Engineering Aspects* 108, 213–223.

Wershaw, R. L., Llaguno, E. C., Leenheer, J. A., Sperline, R. P., and Song, Y. 1996a. Mechanism of formation of humus coatings on mineral surfaces 2. Attenuated total reflectance spectra of hydrophobic and hydrophilic fractions of organic acids from compost leachate on alumina. *Colloids and Surfaces A: Physicochemical and Engineering Aspects* 108, 199–211.

West, C. M. 1986. Current ideas on the significance of protein glycosylation. *Molecular and Cellular Biochemistry* 72, 3–20.

Wiesenberg, G. L. B., Schwark, L., and Schmidt, M. W. I. 2004. Improved automated extraction and separation procedure for soil lipid analyses. *European Journal of Soil Science* 55, 349–356.

Williams, P. M., and Druffel, E. R. M. 1988. Dissolved organic matter in the ocean: comments on a controversy. *Oceanography* 1, 14–17.

Yamada, N., and Tanoue, E. 2003. Detection and partial characterization of dissolved glycoproteins in oceanic waters. *Limnology and Oceanography* 48, 1037–1048.

Yamashita, Y., and Tanoue, E. 2004. Chemical characteristics of amino acid-containing dissolved organic matter in seawater. *Organic Geochemistry* 35, 679–692.

Young, I. M. and Crawford, J. W. 2004. Interactions and self-organization in the soil-microbe complex. *Science* 304, 1634–1637.

Zak, D. R., Holmes, W. E., White, D. C., Peacock, A. D., and Tilman, D. 2003. Plant diversity, soil microbial communities, and ecosystem function: are there any links? *Ecology* 84, 2042–2050.

Zang, X., Nguyen, R. T., Harvey, H. R., Knicker, H., and Hatcher, P. G. 2001. Preservation of proteinaceous material during the degradation of the green alga *Botryococcus braunii*: a solid state 2D ^{15}N ^{13}C NMR spectroscopy study. *Geochimica et Cosmochimica Acta* 65, 3299–3305.

Zhang, X., and Amelung, W. 1996. Gas chromatographic determination of muramic acid, glucosamine, mannosamine, and galactosamine in soils. *Soil Biology & Biochemistry* 28, 1201–1206.

Chapter 2

Microbial Characterization

Microbial characterization

2.1 Introduction

Soil is a complex and dynamic biological system with up to 90% of the processes in soil mediated by microbes. The microbial population in soil is diverse and contains up to 6000 bacterial genomes per gram of soil (Nannipieri et al., 2003). Furthermore, it has recently been reported that soil microbial presence far exceeds currently accepted values and large contributions of microbial peptide/protein are found in the humic substance fraction of soils (Simpson et al., 2007). Investigating microbial diversity is important as it is believed that differences in microbial community composition may also influence the chemical composition of organic materials in soil (Makarov et al., 2002). Moreover, the structure of SOM is significantly impacted by the carbon input source, since the microbial and the plant derived biomass residues are believed to differ significantly in their molecular structures (Kindler et al., 2009). In these contexts, the study of soil microbiology ecology is vital to our understanding of natural processes such as C and N cycling and their associated impacts on agricultural productivity and climate change.

Molecular markers, such as the 16S rRNA gene, have been extensively applied to detect, identify and measure microbial diversity from environmental samples (Peixoto et al., 2002). In most cases, the 16S rRNA is amplified from total DNA extracted from a sample by employing polymerase chain reaction (PCR). Universal primer pair 27f and 1525r (Lane, 1991), that allow amplification of nearly complete 16S rRNA genes from the majority of known bacteria have been used to study the types of bacteria present (composition), the number of types (richness), and the frequency of distribution or the relative abundance of types (structure) in a diverse range of habitats (Dunbar et al., 199; Osborne et al., 2005). In this chapter, the near complete 16S rRNA gene sequences of 40 isolates were determined and analysed for two soils used in subsequent studies.

2.2 Materials and Method

2.2.1 Soil and sampling

Soil samples were collected from two Irish field sites (Church and Big Bull Park) at the Teagasc, Oakpark Crops Research Centre, Carlow in February 2007. The soils, a light clay-loam (Big Bull Park) and heavy clay-loam (Church) were under similar management practices and agricultural regimes, and have been subjected to intensive tillage for over 20 years. The agricultural management practices and physico-chemical properties of these fields are summarized in ***Table 2.2.1.1***. Sampling was carried out according to a modified version of the protocol described by Joseph et al. (2003). Composite samples (each composite sample composed of three samples) were collected at eight locations along transect lines following a 'Z' pattern. A 25-mm-diameter clean metal core was used to sample 100-mm long soil cores from the A horizon, which were transferred to sterile polyethylene bags and sealed at the collection sites. Soil cores were transported at the ambient temperature and processed within 24 h of collection. The upper 30 mm of each core was discarded, and large pieces of roots and stones were removed from the remainder, which was sieved through a stainless steel sieve with a 2-mm aperture (IMPACT Laboratory Test Sieve, UK). Sieved samples were pooled, homogenized and stored at 4°C at its field moisture content for further analysis.

Characteristics	**Oakpark soils**	
Origin	Church	Big Bull Park
Management history	Intensive tillage for over 20 years	
Texture		
% sand	38.0	45.0
% silt	22.0	25.0
% clay	40.0	30.0
Total C (%)	5.33	4.17
Total N (%)	0.42	0.14
pH in H_2O	6.9	6.7

Table 2.2.1.1: Origin, management history and physico-chemical properties of soils for microbial characterization. Information provided by Oakpark Crops Research.

2.2.2 Media and growth conditions

Microbial cultivation was carried out according to a modified version of the protocol described by Janssen et al. (2002). Approximately 1 g of either soil was added to 100-ml aliquots of sterile distilled water in 250-ml conical flasks and dispersed by

stirring with Teflon-coated magnetic bars (8 mm in diameter, 50 mm long) on a magnetic stirrer for 15 min at 400 rpm. One-millilitre aliquots of soil suspension were added to 9-ml portions of dilute nutrient broth (DNB), containing gL^{-1}: Lab-Lemco' Powder 1.0; Yeast Extract 2.0; Peptone 5.0; and Sodium Chloride 5.0, at a concentration of 0.08 g per litre of distilled water (Oxoid Ltd., Hampshire, England). Diluted soil suspensions were mixed by vortexing at approximately 150 rpm for 10 s, and used to prepare serial dilutions containing 10^{-2} to 10^{-4} g of soil suspension. One hundred-microlitre (100 µl) aliquots of each dilution series was plated on duplicate LB agar plates containing 0.5% dripstone, 0.25% yeast extract, 0.1% D-glucose, 0.25% NaCl and 1.5% agar. Serially inoculated LB plates were incubated at RT for 48 h and all isolated colonies were selected from the 10^{-4} dilution of each soil type and used to inoculate 3.0 ml of LB broth. Cultures were incubated at RT for 48 h. All samples were done in duplicates.

2.2.3 Total DNA isolation and PCR amplification

Total bacterial DNA was isolated from pure cultures according to the manufacturer's instructions (UltraClean™ DNA Extraction Kit, Mo Bio Laboratories). The region of the 16S rRNA between nucleotide position 27 and 1525 (*Escherichia coli* 16S rRNA gene sequence numbering), corresponding to almost the entire 16S rRNA gene, was targeted for PCR amplification from total genomic DNA. The amplification was primed with universal 16S rDNA primers 27f 5'-AGAGTTTGATCMTGGCTCAG-3'and 1525r 5'-AAGGAGGTGWTCCARCC-3' (Lane, 1991). PCR reaction was prepared in a fifty microlitre (50 µl) reaction volume containing 2 ng of genomic DNA template, 0.2 mM concentrations of dNTPs, 1x GoTaq® Flexi Buffer[1], 0.2 µM of each primer, 1.5 mM $MgCl_2$, 2.5 U of GoTaq® DNA Polymerase (Promega, Madison USA).

Amplification profiles consisted of an initial denaturation of one cycle of 95ºC for 2 min, followed by 30 cycles of denaturation at 95ºC for 1 min, annealing at 60ºC for 1 min, and elongation at 72º for 2 min, 1 cycle of final extension at 72ºC for 10 min (Biometra® TGradient, AnaChem, UK). PCR amplification products were electrophoresed in 1.0% (wt/vol) agarose gels in 1x TAE buffer, stained with ethidium bromide (0.5µg/ml), destained in 1 mM $MgSO_4$ and photographed using a gel documentation system (PharmaciaBiotech). A 1Kb DNA Ladder was used as the standard marker (Promega, Madison USA).

2.2.4 Nucleotide sequence and phylogenetic analysis

The resulting PCR amplified products were purified by gel extraction (QIAGEN®, Valencia, CA) and sequenced by commercial providers using primer pair 27f and 1525r (Macrogen, Korea). Partial 16S rRNA gene sequences were edited using EditSeq (DNASTAR, Madison, WI USA), and contiguous 16S rRNA gene sequences assembled using SeqMan II (DNASTAR). The resulting sequences were submitted to the SEQUENCE MATCH program of the Ribosomal Database Project (RDP [Maidak et al., 1997]) and to the advanced BLAST search program of the National Centre for Biotechnology Information (NCBI [Altschul et al., 1997]) and the closest database relatives of all sequences retrieved for comparison, using the FASTA algorithm (Pearson and Lipman, 1988). Isolates exhibiting less than 95% similarity to an existing GenBank sequence were checked for chimeric artefacts by the CHIMERA_CHECK program at the Ribosomal Database Project II (RDP-II [Maidak et al., 2001]), using the default settings. The 16S rRNA gene sequences which were determined have been deposited into the Genbank under the accession numbers shown in ***Tables 2.3.2.1*** and ***2.3.2.2***.

The low similarity of some isolate sequences to known organisms' sequences made classification into phyla based solely on these searches difficult: therefore, all isolate sequences were subjected to phylogenetic analysis with representative sequences of known phyla. Alignments of isolate sequences and reference organisms were created using the MegAlign module of DNASTAR, and only sequence data corresponding to *E. coli* bases 63 to 633 were considered for the phylogenetic trees (Furlong et al., 2002). Trees were constructed using PAUP* Version 4.0 (Swofford, 1998). Phylogeny was by a distance method where a phylogenetic tree was constructed by the Neighbour Joining (NJ) method. A bootstrap analysis yielding bootstrap percentages was performed for each data set using 1000 bootstrap replicates and a 70% confidence level to evaluate the statistical significance of branching. The resulting phylogenetic tree was visualised using TreeView (Page, 1996).

2.3 Results and Discussion

2.3.1 PCR amplification

In order to assess the richness and relative abundance of bacteria considered in this study, totals of 21 and 19 bacterial 16S rDNA isolates of approximately 1.5 kb long, were amplified and sequenced from pure cultures of a heavy and light clay loam agricultural soil, respectively. The approximately 1.5 kb amplified fragment represented almost the entire 16S rRNA gene sequence (***Figures 2.3.1.1*** and ***2.3.1.2***).

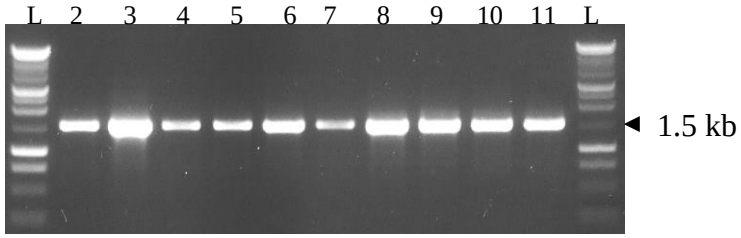

Figure 2.3.1.1: Polymerase chain reaction (PCR) product of Teagasc heavy clay loam soil bacterial 16S rRNA genes generated from universal 16S primer pair 27f and 1525r. Lane L, 1 kb ladder (Promega); lanes 2-11, Teagasc heavy clay loam soil bacterial 16S rRNA gene.

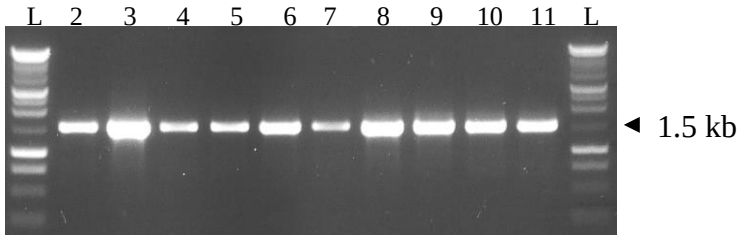

Figure 2.3.1.2: Polymerase chain reaction (PCR) product of Teagasc light clay loam soil bacterial 16S rRNA genes generated from universal 16S primer pair 27f and 1525r. Lane L, 1 kb ladder (Promega); lanes 2-11, Teagasc heavy clay loam soil bacterial 16S rRNA gene.

2.3.2 Nucleotide sequence and phylogenetic analysis

Isolate sequences from the heavy clay loam soil were analysed and compared with their closest database relatives. Of the 21 sequences analysed, 12 (57.1%) had similarity values greater than 95% compared with the available sequences from the database, while 3 (14.3%) showed similarity values between 90% and 95%, and 6 (28.6%) revealed nucleotide similarities ranging between 83% and 87%. Of the 19 light clay loam sequences analysed, 9 (47.4%) had similarity values higher than 95% when compared with the available sequences from the GenBank, 6 (31.6%) had similarity values between 90% and 95%, while 4 (21%) revealed a similarity index of 86% to 87%. Further sequence analysis indicated that the isolates from both soils were affiliated

with two major phylogenetic (candidate) groups of the eubacterial domain, which included members of *Proteobacteria* comprising the *β* and γ subdivisions and *Firmicutes* phyla.

The Isolates of the heavy clay loam soil were dominated by members of the phylum *Proteobacteria* (81%) with the *γ*- and *β*- subdivisions accounting for approximately 57 and 24%, respectively. The *Firmicutes* were less abundant, accounting for 21% of the total heavy clay loam isolates. Sequences belonging to the *γ-Proteobacteria* (47.4%) and *β-Proteobacteria* (26.3%) comprised approximately 74% of the total isolates from the light clay loam soil. The *Firmicutes* (26%) represented the remaining light clay loam isolates. All isolates of the *γ-Proteobacteria* from the heavy and light clay loam soils (12 and 9 isolates, respectively) were associated with the family *Pseudomonadaceae* and, particularly, to the genus *Pseudomonas*, with sequence similarities of 85-99 % and 87-99%, respectively. Isolates of the *β-Proteobacteria* of both soils (five isolates each) were grouped within the family *Oxalobacteraceae* of the order *Burkholderiales* and represented by the genus *Janthinobacterium*, with sequence similarities of 84-99% and 86-99%, respectively. The *Firmicutes* isolates of the heavy clay loam soil (four isolates) were all of the family *Bacillaceae* and associated with the *Bacillus* spp., with a sequence similarity of 83-99%. The *Firmicutes* isolates of the light clay loam soil (5 isolates) were grouped within the class *Bacilli* and the families: *Bacillaceae* (4 isolates) and *Staphylococcaceae* (1 isolate), and were represented by the *Bacillus* spp. and *Staphylococcus* spp., respectively, with a sequence similarity of 87-98%. All of these taxa are typical of soil microbial environment and the rhizosphere in particular. Isolate sequences examined with CHIMERA_CHECK were divided into two fragments. The results revealed that there was no significant difference between the highest binary association coefficient (S_ab) value of a full length sequence and its associated fragments, which indicated that the sequences were not chimeric.

In this study, 570 nucleotides of the almost complete 16S rRNA sequences of 21 heavy clay loam and 19 light clay loam soil isolates were used for phylogenetic analysis. Phylogenetic trees were constructed on the basis of these sequences and reference sequences obtained from the database (***Figures 2.3.2.1*** and ***2.3.2.2***). Both trees had three main clusters, with > 70% bootstrap support. The first cluster of the heavy clay loam soil isolates contained 12 (57%) isolates and grouped with known organisms of the *γ-Proteobacteria* subdivision. The second and third clusters contained

five (24%) and four (19%) isolates and grouped with known organisms of the *β-Proteobacteria* subdivision and the *Firmicutes* phyla, respectively. The first and second clusters of the light clay loam soil isolates contained five (~26%) and four (~21%) isolates and grouped with known organisms of the *Firmicutes* phyla and the *β-Proteobacteria* subdivision, respectively. The third cluster of the light clay loam soil isolates contained 10 (~53%) isolates that grouped with known organisms of the *γ-Proteobacteria* subdivision. These results were consistent with the initial assignment of both sets of isolates into candidate divisions based sequence matches from the RDP-II and nucleotide sequence similarities with known sequences from the database.

This work presents a molecular study of the diversity of microorganisms cultured from two agricultural soils. The overall phylogenetic distribution of the bacterial isolates obtained from both soils indicated similar patterns of abundance and diversity in their community structures. The *γ-Proteobacteria* isolates from both soils was the dominant group, accounting for up to one half of the total number of isolates. Isolates of the *β-Proteobacteria* division were slightly less abundant in the heavy clay loam soil, while isolates of the *Firmicutes* division from both soils were of similar abundance. Except for a single isolate for the light clay loam soil associated with the *Staphylococcus* spp., all isolates of both soils were associated with the *Pseudomonas* species, *Janthinobacterium* species and *Bacillus* species.

The results confirmed an abundance of sequence types of the *γ-Proteobacteria*, and the predominance of the sequence types related to *Pseudomonas* spp. and support the potential functional importance of this bacterial group in cultivated soils. Many plant-symbiotic and plant associated bacteria are affiliated to the *Proteobacteria* (Gremion et al., 2003) and are producers of secondary metabolites such as hydrogen cyanide, siderophores and antibiotics and may inhibit the growth of other organisms, particularly gram-positive and sensitive gram-negative organisms (Brown, 1995; Vassey, 2003). Siderophores are low molecular weight compounds involved in sequestering ferric iron from soil, making it available to plants, but unavailable to other microorganisms (Anith et al., 2004). Furthermore, *Pseudomonas* species are capable of utilizing a broad spectrum of growth substances and can grow well in the presence of other organisms. Additionally, many pseudomonads are resistant to antibiotics (Palleroni, 1992) produced by *Bacilli*, a group which constituted relatively significant

proportions of both sets of isolates. A combination of these characteristics may account for the dominance of *Pseudomonas* species among the isolates from both soils.

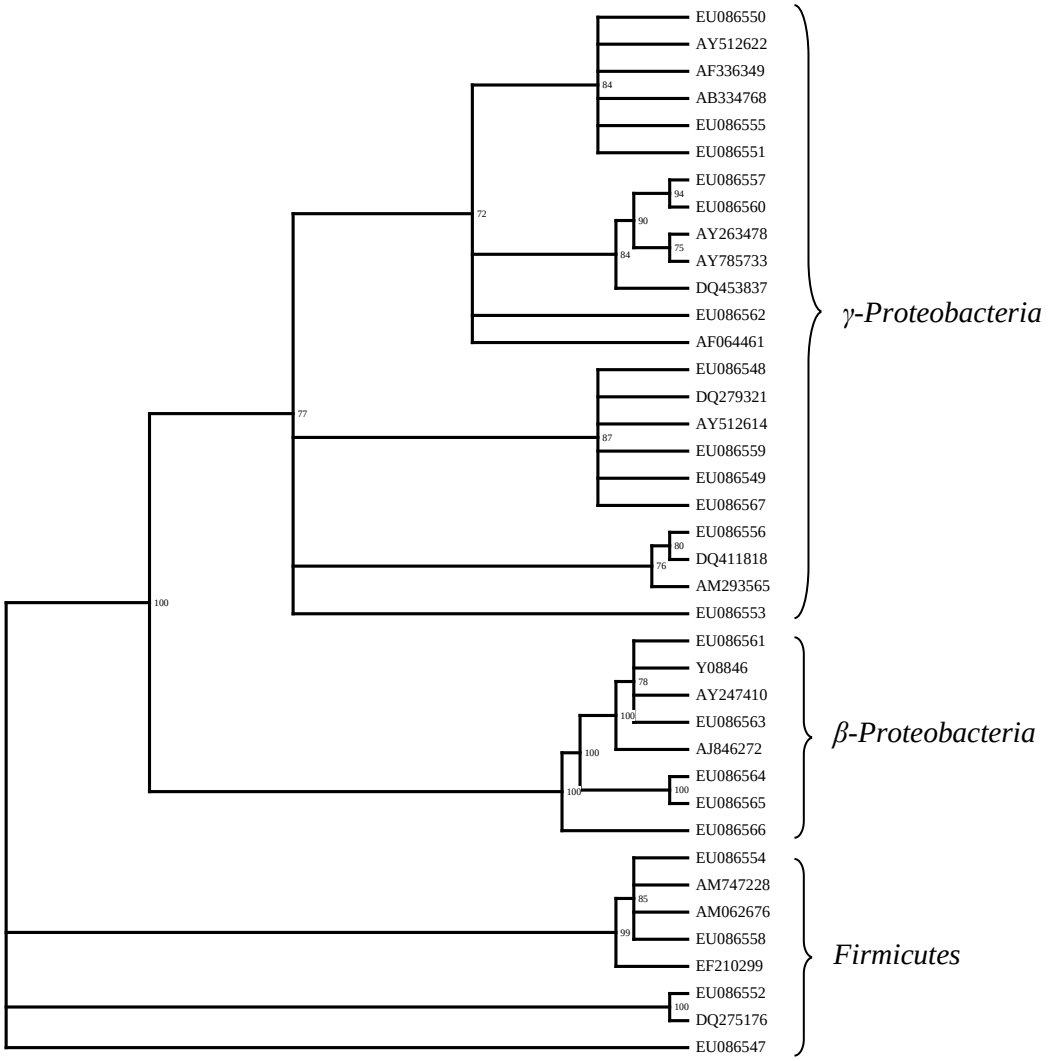

Figure 2.3.2.1: Unrooted NJ phylogenetic tree showing the relationship between isolates of a heavy clay loam agricultural soil form Teagasc and reference organisms from the database. The tree was constructed using a total of 570 aligned positions of the 16S rRNA gene, corresponding to *E. coli* positions 63 to 633. Branch lengths are proportional to genetic distances inferred, while the vertical position is arbitrary. Bootstrap values are indicated as percentages of 1000 bootstrap samples, and only values > 70% are shown. Isolates are clustered with the *γ-Proteobacteria*, *β-Proteobacteria* and the *Firmicutes* phyla. GenBank accession numbers are as follows: Bacterium THCL 1 to 21 **EU086547** to **EU086567**, *B. weihenstephanensis* **AM062676**, *B. thuringiensis* **EF210299**, *B. drentensis* strain WN575 **DQ275176**, *B. mycoides* strain SDA NFMO448 **AM747228**, *Janthinobacterium* sp. HHS7 **AJ846272**, *J. lividum* **Y08846**, *J. lividum* **AY247410**, *Pseudomonas* sp. TM4_4 **DQ279321**, *P. fluorescens* strain A1XB1-4 **AY512614**, *P. veronii* **AB334768**, *P. veronii* strain A1YB2-4 **AY512622**, *P. fluorescens* **AF336349**, *Pseudomonas* sp. K93.3 **DQ453837**, *Pseudomonas* sp. PALXIL01 **DQ411818**, *Pseudomonas* sp. SE22#2 **AY263478**, *P. frederiksbergensis* isolate OUCZ24 **AY785733**, *P. cedrella* **AF064461**, *P. reinekei* **AM293565**.

Sample	Accession No.	Homologue
THCL1	EU086547	*Bacillus weihenstephanensis* KBAB4
THCL2	EU086548	*Pseudomonas* sp. TM4_4
THCL3	EU086549	*Pseudomonas* sp. TM4_4
THCL4	EU086550	*Pseudomonas fluorescens* SBW25
THCL5	EU086551	*Pseudomonas fluorescens* SBW25
THCL6	EU086552	*Bacillus* sp. BF47
THCL7	EU086553	*Pseudomonas* sp. F78 16S
THCL8	EU086554	*Bacillus cereus* strain REG200
THCL9	EU086555	*Pseudomonas* sp. L1-11-07
THCL10	EU086556	*Pseudomonas* sp. PALXIL01
THCL11	EU086557	*Pseudomonas* sp.
THCL12	EU086558	*Bacillus* sp. TAD111
THCL13	EU086559	*Pseudomonas* sp. WR5-34
THCL14	EU086560	*Pseudomonas* sp. PR3-5
THCL15	EU086561	*Janthinobacterium* sp. WPCB148
THCL16	EU086562	*Pseudomonas* sp. NZ081
THCL17	EU086563	*Janthinobacterium lividum* strain DSM
THCL18	EU086564	*Janthinobacterium lividum* isolate Acam
THCL19	EU086565	*Janthinobacterium lividum* isolate Acam
THCL20	EU086566	*Janthinobacterium* sp. HHS7
THCL21	EU086567	*Pseudomonas reinekei*

Table 2.3.2.1: GenBank accession numbers and homologues of 16S rRNA gene sequences of Teagasc heavy clay-loam soil isolates.

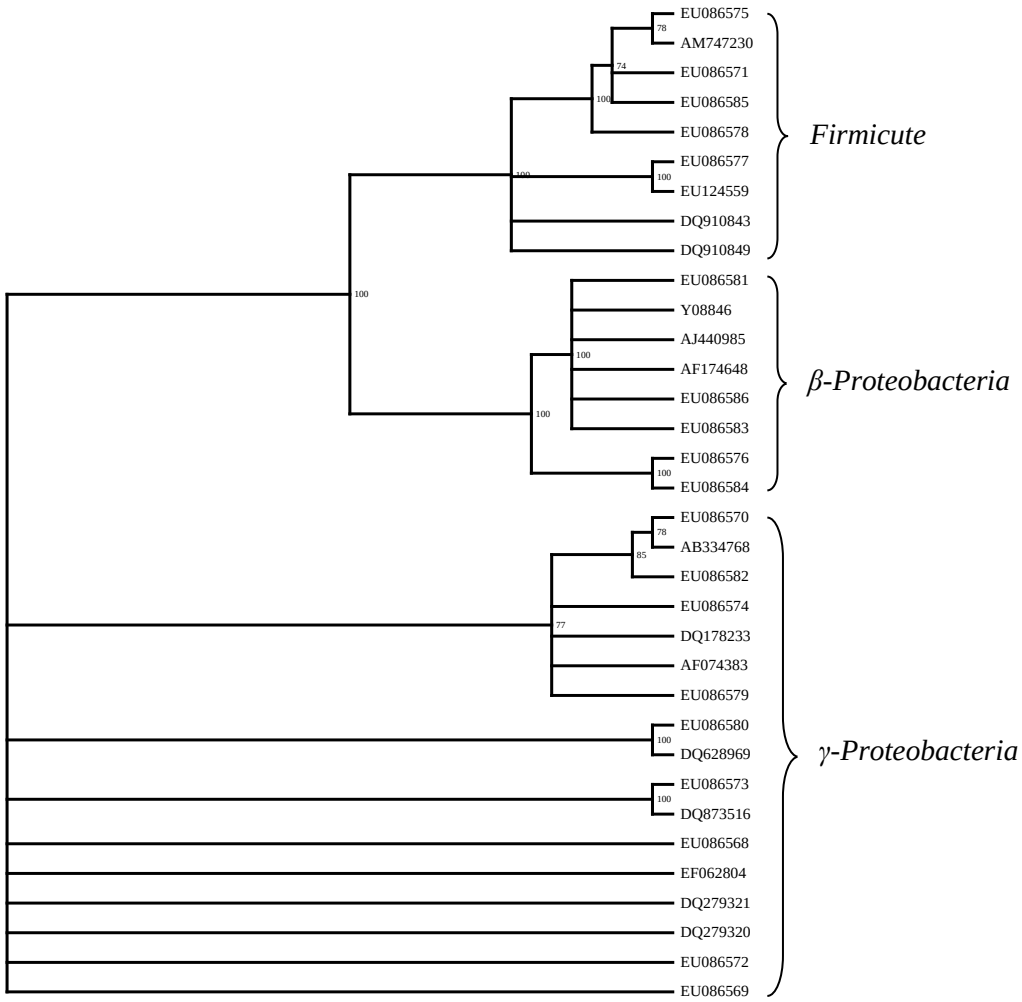

Figure 2.3.2.2: Unrooted NJ phylogenetic tree showing the relationship between isolates of a light clay loam agricultural soil form Teagasc and reference organisms from the database. The tree was constructed using a total of 570 aligned positions of the 16S rRNA gene, corresponding to *E. coli* positions 63 to 633. Branch lengths are proportional to genetic distances inferred, while the vertical position is arbitrary. Bootstrap values are indicated as percentages of 1000 bootstrap samples, and only values > 70% are shown. Isolates are clustered with the *γ-Proteobacteria*, *β-Proteobacteria* and the *Firmicutes* phyla. GenBank accession numbers are as follows: Bacterium TLCL 1 to 19 **EU086568** to **EU086586**, Antarctic bacterium strain R-7687 **AJ440985**, *B. weihenstephanensis* strain WSBC 10204 **AM747230**, *B. simplex* strain OSS 24 **EU124559**, *J. lividum* **AF174648**, *J. lividum* **Y08846**, *Pseudomonas* sp. MY1408 **EF062804**, *Pseudomonas* sp. TM3_3 **DQ279320**, *P. veronii* **AB334768**, *Pseudomonas* sp. TM4_4 **DQ279321**, *Pseudomonas* sp. IST102 **DQ873516**, *P. putida* strain PC36 **DQ178233**, *P. migulae* **AF074383**, *Pseudomonas* sp. PSA A4(4) **DQ628969**, *Staphylococcus* sp. SK1-1-2 **DQ910843**, *Virgibacillus* sp. SK1-3-11 **DQ910849.**

Sample	Accession No.	Homologue
TLCL1	EU086568	*Pseudomonas putida*
TLCL2	EU086569	*Pseudomonas putida*
TLCL3	EU086570	*Pseudomonas* sp. W15Feb38
TLCL4	EU086571	*Bacillus weihenstephanensis* KBAB4
TLCL5	EU086572	*Pseudomonas* sp. TM3_3
TLCL6	EU086573	*Pseudomonas* sp. IST102
TLCL7	EU086574	*Pseudomonas* sp. An1
TLCL8	EU086575	*Bacillus weihenstephanensis* KBAB4
TLCL9	EU086576	*Janthinobacterium lividum* isolate Acam
TLCL10	EU086577	*Bacillus simplex* strain REG129
TLCL11	EU086578	*Pseudomonas* sp. CL3.1
TLCL12	EU086579	*Pseudomonas migulae* strain CT14
TLCL13	EU086580	*Pseudomonas* sp. BAM288
TLCL14	EU086581	*Janthinobacterium* sp. J3
TLCL15	EU086582	*Pseudomonas* sp. TB4-4-I
TLCL16	EU086583	*Janthinobacterium lividum* strain DSM
TLCL17	EU086584	*Janthinobacterium lividum* isolate Acam
TLCL18	EU086585	*Bacillus flexus* strain RARE-3
TLCL19	EU086586	*Janthinobacterium lividum*

Table 2.3.2.2: GenBank accession numbers and homologues of 16S rRNA gene sequences of Teagasc light clay-loam soil isolates.

Some members of the *Bacillus* species are also producers of secondary metabolites (Glick, 1995) previously discussed, however, they were less abundant when compared with isolates of the *Pseudomonas* species from both soils. The discrepancy in abundance may be due in part to the fact that *Bacillus* species often sporulate under adverse environmental conditions (Rajalakshmi and Shethna, 1980) and may require special pre-propagation treatments to encourage the germination of these spores. Such treatments could be undertaken to address these problems in future work.

While the community composition of both soils appeared typical of the microbial profile of the rhizosphere, a greater bacterial diversity might be expected from a nutrient-enriched root zone facilitated by root exudates. The identification of members

of the *α-Proteobacteria* has been reported in many studies; however, this group of bacteria was not identified in the current study. The absence of this group may be due to the fact that it is mainly composed of slow growing bacterial species. In addition, many of the members of the *α-Proteobacteria* respond to changes in environmental conditions by entering a viable by non-culturable state. Moreover, the *α-Proteobacteria* may require specific physicochemical conditions not found in simple growth media (Barbieri et al., 2007). One suggestion for future work is to try and optimize the media and growth conditions to maximize the species richness of the culturable soil microbial fraction. Alternatively, microbes (culturable and non-culturable) may be extracted from soils; however, while this method favours microbial diversity studies, it must be understood that it is equally difficult to separate microbes from soil particles. Therefore, great care must be exercised to ensure that only microbial biomass is being considered for degradation.

It is unlikely that cultivation-based diversity studies will reflect the true microbial community structure present *in situ* because of inherent qualitative and quantitative biases. However, the bacterial isolates obtained can be considered as, and provide relative measures of the natural bacterial diversity of both soil communities (Barbieri et al., 2007). It is also interesting to note that the diversity results presented in this chapter show some degree of similarity (an abundance of *Proteobacteria* and *Firmicutes*) to culture-independent studies of the bacterial community tightly associated to the gut wall of earthworms and within soil samples taken from pairs of two adjacent fields (arable and pasture) located at Johnstown Castle Estate, Wexford, Co. Wexford; Lyons Estate, Celbridge, Co. Kildare; and Teagasc, Oakpark Crops Research Centre, Carlow (Thakuria et al., 2010). Moreover, Simpson et al. (2007) suggested that the microbial fingerprint of cultivable biomass is similar to that of microbes extracted from soils, and although only a small fraction of the total population can be cultured, the cultivable fraction is representative (at the biochemical input level) of the microbes that cannot be cultured.

The biochemical contribution of the culturable microbial fraction of the light clay-loam Oakpark soil to SOM is considered in greater details in subsequent chapters. In addition, the 16S rDNA sequences obtained from the bacterial isolates extended the taxonomic database of bacteria associated with agricultural soil, and more specifically the soils used in this work, for comparative systematic studies. In a recent study using

culture-independent approaches, Thakuria et al. (2008) demonstrated significant variations in the microbial diversity of Irish soils. Considering the taxonomic and metabolic diversity of soil microbes and the fact that microbes are inextricably linked to the chemical structure, location, and rates of decomposition of SOM, we would like to suggest that the focus of future work should be directed at characterizing the spatial and temporal scales of influence of soil microbial biomass on SOM structure and composition in Irish soils and indeed soils across Europe.

2.4 References

Altschul, S. F., Madden, T. L., Schäffer, A. A., Zhang, J., Zhang, Z., Miller, W., and Lipman, D. 1997. Gapped BLAST and PSI-BLAST: A new generation of protein database search programs. *Nucleic Acids Research* 25, 3389–3402.

Anith, K. N., Momol, M. T., Kloepper, J. W., Marois, J. J., Olson, S. M., and Jones J. B. 2004. Efficacy of plant growth-promoting rhizobacteria, acibenzolars-*S*-methyl, and soil amendments for integrated management of bacterial wilt on tomato. *Plant Disease* 88, 669–673.

Barbieri, E., Guidi, C., Bertaux, J., Frey-Klett, P., Garbaye, J., Ceccaroli, P., Saltarelli, R., Zambonelli, A., and Stocchi, V. 2007. Accurance and diversity of bacterial communities in *Tuber magnatum* during truffle maturation. *Environmental Microbiology* 9, 2234–2246.

Brown, G. G. 1995. How do earthworms affect microfloral and faunal diversity? *Plant and Soil* 170, 209–231.

Dunbar, J., Takala, S., Barns, S. M., Davis, J. A., and Kuske, C. R. 1999. Levels of bacterial community diversity in four arid soils compared by cultivation and 16S rRNA gene cloning. *Applied and Environmental Microbiology* 65, 1662–1669.

Furlong, M. A., Singleton, D. R., Coleman, D. C., and Whitman, W. B. 2002. Molecular and culture-based analysis of prokaryotic communities from an agricultural soil and the burrows and casts of the earthworm *Lumbricus rubellus*. *Applied and Environmental Microbiology* 68, 1265–1279.

Glick, B. R. 1995. The enhancement of plant growth by free-living bacteria. *Canadian Journal of Microbiology* 41, 109–117.

Gremion, F., Chatzinotas, A., and Harms, H. 2003. Comparative 16S rDNA and 16S rRNA sequence analysis indicates that *Actinobacteria* might be a dominant part of the metabolically active bacteria in heavy metal-contaminated bulk and rhizosphere soil. *Environmental Microbiology* 5, 896–907.

Janssen, P. H., Yates, P. S., Grinton, B. E., Taylor, P. M., and Sait, M. 2002. Improved culturability of soil bacteria and isolation of pure culture of novel members of the divisions *Acidobacteria, Actinobacteria, Proteobacteria, and Verrucomicrobia*. *Applied and Environmental Microbiology* 68, 2391–2396.

Joseph, J. S., Hugenholtz, P., Sangwan, P., Osborne, C. A., and Janssen, P. H. 2003. Laboratory cultivation of widespread and previously uncultured soil bacteria. *Applied and Environmental Microbiology* 69, 7210–7215.

Kindler, R., Miltner, A., Thullner, M., Richnow, H.-H., and Kästner, M. 2009. Fate of bacterial biomass derived fatty acids in soil and their contribution to soil organic matter. *Organic Geochemistry* 40, 29–37.

Lane, D. J. 1991. 16/23S rRNA Sequencing. In: Stackcbrandt, E., and M. Goodfellow, M. (Eds.), *Nucleic acid techniques in bacterial systematics*. John Wiley & Sons, Chichester, United Kingdom, pp. 115–175.

Maidak, B. L., Cole, J. R., Lilburn, T. G., Parker, C. T., Saxman, Jr., P. R., Farris, R. J., Garrity, G. M., Olsen, G. J., Schmidt, T. M., and Tiedje, J. M. 2001. The RDP-II (Ribosomal Database Project). *Nucleic Acid Research* 29, 173–174.

Maidak, B. L., Olsen, G. J., Larsen, N., Overbeek, R., McCaughey, M. J., and Woese, C. W. 1997. The RDP (Ribosomal Database Project). *Nucleic Acid Research* 25, 109–110.

Makarov, M. I., Haumaier, L., and Zech, W. 2002. Nature of soil organic phosphorus: an assessment of peak assignments in the diester region of ^{31}P NMR spectra. *Soil Biology & Biochemistry* 34, 1467–1477.

Nannipieri, P., Ascher, J., Ceccherini, M. T., Landi, L., Pietramellara, G., and Renella, G. 2003. Microbial diversity and soil function. *European Journal of Soil Science* 54, 655–670.

Osborne, C. A., Galic, M., Sangwan, P., and Janssen, P. H. 2005. PCR-generated artefact from 16S rRNA gene-specific primers**.** *FEMS Microbiology Letters* 248, 183–187.

Page, R. D. 1996. TreeView: an application to display phylogenetic trees on personal computers. *Computer Applications in the Biosciences* 12, 357–358.

Palleroni, N. J. 1992. Introduction to the family pseudomonadaceae. In: Balows, W., Trüper, H. G., Drowkin, M., Harder, W., and Schleifer, K.-H. (Eds.), *The prokaryotes*. Springer-Verlag, New York, N.Y., pp. 3071–3085.

Pearson, W. R., and Lipman, D. J. 1988. Improved tools for biological sequence comparison. *Proceeding of the National Academy of Sciences of USA* 85, 2444–2448.

Peixoto, R. S., da Costa Coutinho, H. L., Rumjanek, N. G., Macrae, A., and Rosado, A. S. 2002. Use of *rpo*B and 16S rRNA genes to analyse bacterial diversity of a tropical soil using PCR and DGGE. *Letters in Applied Microbiology* 35, 316–320.

Rajalakshmi, S., and Shethna, Y. I. 1980. Spore and crystal formation in *Bacillus thuringiensis* var. *thuringiensis* during growth in cystine and cysteine. *Journal of Biosciences* 2, 321–328.

Simpson, A. J., Simpson, M. J., Smith, E., Kelleher, B. P. 2007. Microbially derived inputs to soil organic matter: are current estimates too low? *Environmental Science and Technology* 41, 8070–8076.

Swofford, D. L. 1998. PAUP*. Phylogenetic Analysis Using Parsimony (and Other Methods), Version 4. Sunderland, MA:Sinauer Associates.

Thakuria, D., Schmidt, O., Finan, D., Egan, D., and Doohan, F. M. 2010. Gut wall bacteria of earthworms: a natural selection process. *International Society of Microbial Ecology* 4, 357–366.

Thakuria, D., Schmidt, O., Mac Siúrtáin, M., Egan, D., and Doohan, F. M. 2008. Importance of DNA quality in comparative soil microbial community structure analysis. *Soil Biology & Biochemistry* 40, 1390–1403.

Vassey, J. K. 2003. Plant growth promoting rhizobacteria as biofertilizers. *Plant and Soil* 255, 571–586.

Chapter 3

Assessing the fate and Transformation of Microbial Residues in Soil

Assessing the fate and transformation of microbial residues in soil

3.1 Introduction

Soil organic matter represents the largest active C and N pools in the terrestrial environment (Trumbore et al., 1990) but its genesis is poorly understood (Kindler et al., 2009). It has been generally accepted that the C in SOM is predominantly plant derived (Kögel-Knabner, 2002). However, only a small fraction of the yearly litter and root input becomes part of the stable OM pool, with most of it integrated into microbial biomass after repeated processing (Dijkstra et al., 2006). It is believed that the structure, stability reactivity and other properties of SOM is significantly impacted by the nature of the precursor material, since the microbial and the plant derived biomass residues differ significantly in their molecular structures (Kindler et al., 2009). As the need to model C and N transformation in soils becomes more important, it is therefore essential to know the exact composition of input materials (Kögel-Knabner, 2002).

Soil microorganisms act as both a source and a sink for soil P (Bünemann et al., 2008). Microbial inputs in the form of C-P compounds (Quinn et al., 2007) are dominated by nucleic acids with 60% of total P and phospholipids, accounting for 5-30% of the microbial inputs to soils (Kögel-Knabner, 2006). In soils, the OM pool includes many compounds that contain both C and P and thus the cycling of P in soil should be considered in conjunction with that of C (Sannigrahi et al., 2006). Soil P exists in a multitude of chemical forms which differ widely in their behaviour in the soil environment (Turner et al., 2003b). Nonetheless, much of the chemical nature and dynamics of soil organic P remains unknown, despite constituting up to 90% of total P in some soils, providing a source of P for plant uptake (Turner et al., 2003a,b; Kögel-Knabner, 2006), and influencing biological processes, such as litter decomposition and microbial activity (Lair et al., 2009).

In recent decades, the amount of solar UV-B radiation reaching the Earth's surface has increased significantly, primarily due to increased stratospheric ozone depletion (Pancotto et al., 2005). This is of special importance as it has been demonstrated that photodegradation is competitive with microbial microbially mediated reactions in the decomposition of surface exposed litter and microbial biomass (Kovac

et al., 1998). Several studies have investigated the effects of UV-B radiation on litter decomposition (Pancotto et al., 2003, 2005); however, the effects of solar radiation on soil microbial biomass decomposition have been neglected (Johnson et al., 2002).

In this chapter, the High Resolution Magic Angle Spinning (HR-MAS) and ^{31}P solution state NMR analysis of $^{13}C/^{15}N$ isotopically enriched soil microbial biomass and microbial leachates degraded under ambient and elevated UV conditions are presented. The goals of this initial investigation were to: (i) monitor the degradation and transformation of major biochemical components (proteins, carbohydrates and lipids), and (ii) and delineate the contribution of labile and biochemically recalcitrant fractions of bulk microbial biomass to the SOM pool during a decomposition study. We reasoned that the results of this investigation will help us to address the knowledge gap regarding the fate of the major microbial components in soil by answering specific questions pertaining to the biochemical contribution of microbial biomass to the labile and recalcitrant SOM pools. Moreover, because the contribution of (both living and dead) microbial biomass to SOM has been underestimated it is important to understand how it degrades in soil and if it degrades in a similar way to plant materials.

3.2 Materials and Methods

3.2.1 Media and growth conditions

Microbes were cultured in minimal medium containing $(^{15}NH_4)_2SO_4$ (99 atom%; Isotec, Inc., Miamisburg, OH, USA) according to a modified version of the protocol described by Wyndham (1986). ^{13}C glucose and unlabelled acetate were added as carbon sources and were maintained at a concentration of 5 mM each during culturing. Starter cultures were prepared using approximately 100 mg of sieved, homogenized light clay-loam Oakpark soil to inoculate 100 ml of growth medium. The origin, management history and textural characteristics of the soil used to prepare the labelled biomass have been described in ***Section 2.2.1***. The starter cultures were incubated at room temperature for 1 week with reciprocal shaking at 125 strokes min^{-1}. A 1 mL aliquot was removed from the flask and used to inoculate new flasks containing a growth solution (100 mL) to prevent any possible carryover of soil particles from the initial culture. Cultures were incubated for an additional two weeks and amended with ^{13}C D-glucose (99 atom%; Isotec, Inc., Miamisburg, OH, USA) and acetate every 48 h.

Identical controls were prepared without the addition of soil. In these controls, no microbial growth was observed. The resulting biomass was harvested and washed with a large excess of distilled water by centrifugation at 6000 rpm for 30 min. The biomass was then freeze-dried and stored at -20°C for further analysis.

3.2.2 Decomposition experiment

Duplicate degradation experiments were conducted as outlined in ***Figure 3.2.2.1*** according to a modified version of the protocol described by Kelleher et al. (2006). The experimental design attempted to mimic *in situ* conditions and enable the collection of transformed and leached organic matter for further analysis. The cost of producing the labelled microbial biomass and its limited supply prohibited the burying of residues or even laying them directly on the soil surface. Alternatively, glass funnels (65 mm top diameter and 121 mm in length) with borosilicate sintered discs (20 mm in diameter) of grade 4 porosity were submerged until flush with soil in a 10" clay pot. The soil used was a native light clay-loam Oakpark soil (***Section 2.2.1***) from which the microbial biomass was propagated.

The cavity beneath the sintered disc was filled with ~0.3 g of the native soil and secured with glass wool and 0.4 g of the labelled biomass and clay-complexes (used in ***Chapters 3*** and ***4***, respectively), unlabelled biomass (used in ***Chapters 3***, ***5*** and ***6***), or unlabelled clay-complexes (used in ***Chapter 5***), evenly distributed (~ 2 mm thick) on the surface of the sintered disc. This set up enables microbes in the soil to access the microbial biomass. The biomass was sprinkled with water every second day to mimic rain and the runoff was collected in a vial attached to the end of the funnel. Moisture levels were kept constant throughout the experiment. Runoffs were collected at 6, 14 or 26 weeks post degradation and biomass and clay-complexes were randomly sampled over the same period, freeze-dried and stored at -80ºC for further analysis. Sampling protocols were the same for all experiments. The decomposition experiments were conducted under laboratory conditions due to the precious nature and limited availability of the enriched biomass. We fully acknowledge that glass filtered sunlight does not completely represent natural light, and results may have differed if the experiments were carried out *in situ*. One apparatus was placed in an unheated area with windows such that the temperature and sunlight exposure would roughly mimic that of the outside environment. It should be noted that the average annual temperature in Ireland is ~9ºC. A second apparatus was placed in a top only ultraviolet irradiating

chamber (LZC-1) operated at a frequency of 60 Hz (Luzchem Research Inc., Canada). The chamber was fitted with 8 UV lamps alternating between the near wavelength UV (UVB-300 nm with a peak at 313 nm) and the long-wavelength UV (UVA-350 nm). The chamber temperature was maintained at ~25ºC. Considering the relatively small amount of the starting material (0.4 g) and unaccountable contributions from living microbial biomass, it was not possible to obtain accurate dry mass for the samples at each point during the study. However, based on the mass of the material submitted for NMR analysis, back calculations indicated that >60% of all the starting materials had been degraded during the study.

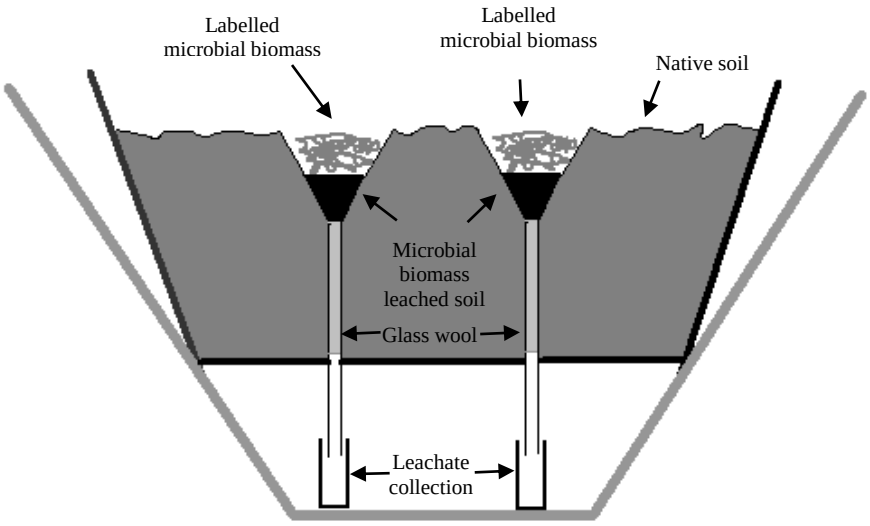

Figure 3.2.2.1: Experimental setup for degradation study of labelled and unlabelled soil microbial biomass.

3.2.3 High resolution magic angle spinning (HR-MAS) NMR

Thoroughly dried labelled samples (~20 mg) were placed in a 4 mm Zirconium Oxide Rotor and 60 µl of DMSO-d_6 was added as a swelling solvent in a dry atmosphere. It is essential to dry the samples thoroughly and use only ampules of DMSO-d_6 to prevent a large water peak often centred at ~3.3 ppm that can obscure many of the real microbial signals. After homogenization of the sample using a stainless steel mixing rod, the rotor was doubly sealed using a Kel-F sealing ring and a Kel-F rotor cap. ^{1}H HR-MAS NMR spectra were acquired using a Bruker 500 MHz Avance spectrometer fitted with a 4-mm triply tuned ^{1}H-^{13}C-^{15}N HR-MAS probe fitted with an actively shielded Z gradient at a spinning speed of 10 kHz. ^{1}H NMR was acquired while simultaneously decoupling both ^{13}C ^{15}N nuclei. Scans (256) were acquired with a 2 s delay between pulses, a sweep width of 20 ppm and 8 K time domain points. ^{1}H

Diffusion Gated Experiments were used with a bipolar pulse longitudinal encode-decode sequence (Wu et al., 1995). Scans (1024) were collected using 1.25 ms, 333 mT m^{-1} sine shaped gradient pulse, a diffusion time of 30 ms, 8192 domain time domain points and a sample temperature of 298 K. In essence the ‘‘gate’’ was optimized at the strongest diffusion filtering possible while minimizing signal loss through relaxation. As a result the more rigid components dominated the transform spectrum while mobile components were essentially gated.

^{13}C spectra were collected in different modes, including inverse gated ^{1}H and ^{15}N decoupling, and conventional decoupling during acquisition (both ^{1}H and ^{15}N). Due to the strong signal from the labelled carbon, both approaches yielded the same spectrum. The inverse gated spectra are shown here. Scans (16 K) were acquired with a delay of 5 times that of the measured *T*1 relaxation (commonly resulting in a delay of ~4s [note: ^{13}C relaxation was fast as a result of ^{13}C-^{13}C interactions]), a sweep width of 300 ppm and 16 K time domain points. The spectra were processed with a zero-filling factor of 2 and an exponential multiplication, which resulted in a line broadening of 1 Hz in the transformed spectrum. One-dimensional ^{15}N spectra were acquired with and without DEPT enhancement. Scans (128 K) were performed with a recycle delay of 5 s, 32 K time domain points, a sweep width of 1000 ppm, and decoupling of both 1H and ^{13}C during acquisition. The spectra were processed with a zero-filling factor of 2 and an exponential multiplication, which resulted in a line broadening of 10 Hz in the transformed spectrum.

^{1}H-^{13}C Heteronuclear Single Quantum Coherence (HSQC) spectra were collected in a phase sensitive mode using Echo/Antiecho-TPPI gradient selection and sensitivity enhancement. Scans (8) were collected for each of the 128 increments in the F1 dimension. Two Kelvin data points were collected in F2, a 1J ^{1}H-^{13}C (145 Hz) and a relaxation delay of 2s was employed, ^{15}N and ^{1}H were decoupled during acquisition. Similar conditions were employed for ^{1}H-^{15}N HSQC except 16 scans, 1J ^{1}H-^{15}N (90 Hz), were used with decoupling of both ^{13}C and ^{1}H during acquisition. For all HSQC spectra both dimensions were processed using sine-squared functions with phase shifts of 90º and a zero-filling factor of 2.

Numerous additional NMR experiments were acquired but have not been shown here, including ^{13}C-^{13}C HSQC-TOCSY (2-D and 3-D), ^{13}C-^{13}C INADEQUATE, ^{1}H-^{13}C

ADEQUATE, and ^{1}H-^{13}C long range HMQC. While their detailed interpretation will be the focus of future work, we would like to point out that the basic assignments are consistent with the full suite of multidimensional NMR experiments acquired (Kelleher et al., 2006).

3.2.4 Phosphorus extraction

Phosphorus was extracted by shaking 1 g of soil or approximately 0.1 g of freeze-dried unlabelled initial or degraded microbial biomass with 20 ml of a solution containing 0.25 M NaOH and 0.05 M EDTA for 16 h at 20°C. The extracts were centrifuged at 10,000 xg for 30 min, and the supernatant carefully decanted, frozen at -20°C, and subsequently freeze-dried over several days. Freeze-dried NaOH-EDTA extracts (~100 mg) were redissolved in 1 ml of 1M NaOH and 0.1 ml D_2O (for signal lock) and transferred to 5-mm NMR tubes. The addition of NaOH ensures consistent chemical shifts and optimum spectral resolution at solution pH >12 (Turner et al., 2003b).

3.2.5 Solution ^{31}P NMR spectroscopy

Solution ^{31}P NMR spectra were acquired using a Bruker DRX 400 spectrameter (Bruker, Germany) operating at 243 MHz with a 5-mm probe. Spectra were acquired using a 30° pulse width, a total acquisition time of 1.5 s (pulse delay 0.808 s, acquisition time 0.673) and broadband proton decoupling. The delay time used in this study allows sufficient spin-lattice relaxation between scans for P compounds in NaOH-EDTA, confirmed by detailed study of relaxation time for P compounds in various extracts (Cade-Menun et al., 2002). Temperature was regulated at 24°C. Between 80 and 400 scans or 1024 scans (soil extract) were collected to obtain acceptable signals. The spectra presented have a line broadening of 5 Hz. Spectra were collected soon after preparation (within 1 h) to circumvent the possible degradation. Spectral interpretation was based on literature assignment (Turner et al., 2003b). All NMR experiments were carried out in duplicate.

3.3 Results and Discussion

Before any discussion is carried out, it is important to note that soil microbial biomass samples are complex mixtures. Therefore, major assignments represent the predominant species (not all species) in a given region and overlap from components at lower concentrations may occur in many regions of the spectra (Simpson et al., 2007a). It is also important to note that in 2-D HSQC NMR, both the carbon and proton atoms are dispersed into two dimensions. Only protons attached to carbons are detected in HSQC experiment; thus, exchangeable protons (OH, NH, etc.) that are detected in ^{1}H spectrum will not be detected in the 2D version (Kelleher and Simpson, 2006).

3.3.1 ^{13}C NMR analysis of microbial biomass

In ***Figure 3.3.1.1*** the HR-MAS ^{13}C NMR spectra of initial microbial biomass (starting material) and microbial biomass degraded under ambient and UV conditions are presented. The region between 0 and 50 ppm is assigned to paraffinic carbons (Knicker et al., 1996). The broad spectral resonances indicate a predominantly heterogeneous structural composition of the samples (Kaiser et al., 2001). A strong distinct peak in the spectra near 30 ppm is characteristic of long-chained polymethylene-C. This was also confirmed by FT-IR spectra showing strong bands at 2929, and 2856 cm^{-1} and a characteristic shoulder at 2960 cm^{-1} (data not shown). Other signals originating in this region are attributed to short-chained or branched terminal methyl (CH_3), methylene (CH_2), and tertiary or quaternary (C) aliphatic-C structures such as those found in lipids (likely from bacterial membrane) and proteins (Karl et al., 2007; Solomon et al., 2007). The spectra show strong signals in the range 45–120 ppm (with a peak maximum near 73 ppm) which were assigned to carbon atoms in carbohydrates and lipids including the anomeric carbon and units adjacent to esters (Solomon et al., 2007). The resonances at 50–110 ppm could be also due to carbons bound to heteroatoms (Allard et al., 1997) most likely to oxygen. The resonances around 100 ppm can be assigned to anomeric C-1 carbon in carbohydrates (Guggenberger and Zech, 1994) and/or –O–C–O– functionalities. It should be noted that the signal intensity in the region between 60 and 45 originated from NH_2-substituted C, most probably from C_x in amino acid residues and proteins (Knicker et al., 1996; Kögel-Knabner, 1997). The signals resonating between 120 and 160 ppm are attributed to aromatic-C and olefinic-C which are not distinguishable. The signals at 140–160 ppm can be assigned to aromatic esters and amides (Gelin et al., 1996), and the aromatic region between 145 and 160

ppm contains signal from hetero-substituted (O, N) aromatic carbons. Strong to moderate signals resonating in the region between 160 and 200 ppm are indicative of carbonyl-C in carboxylic groups, amides and aliphatic esters (Mayer et al., 1999; Solomon et al., 2007).

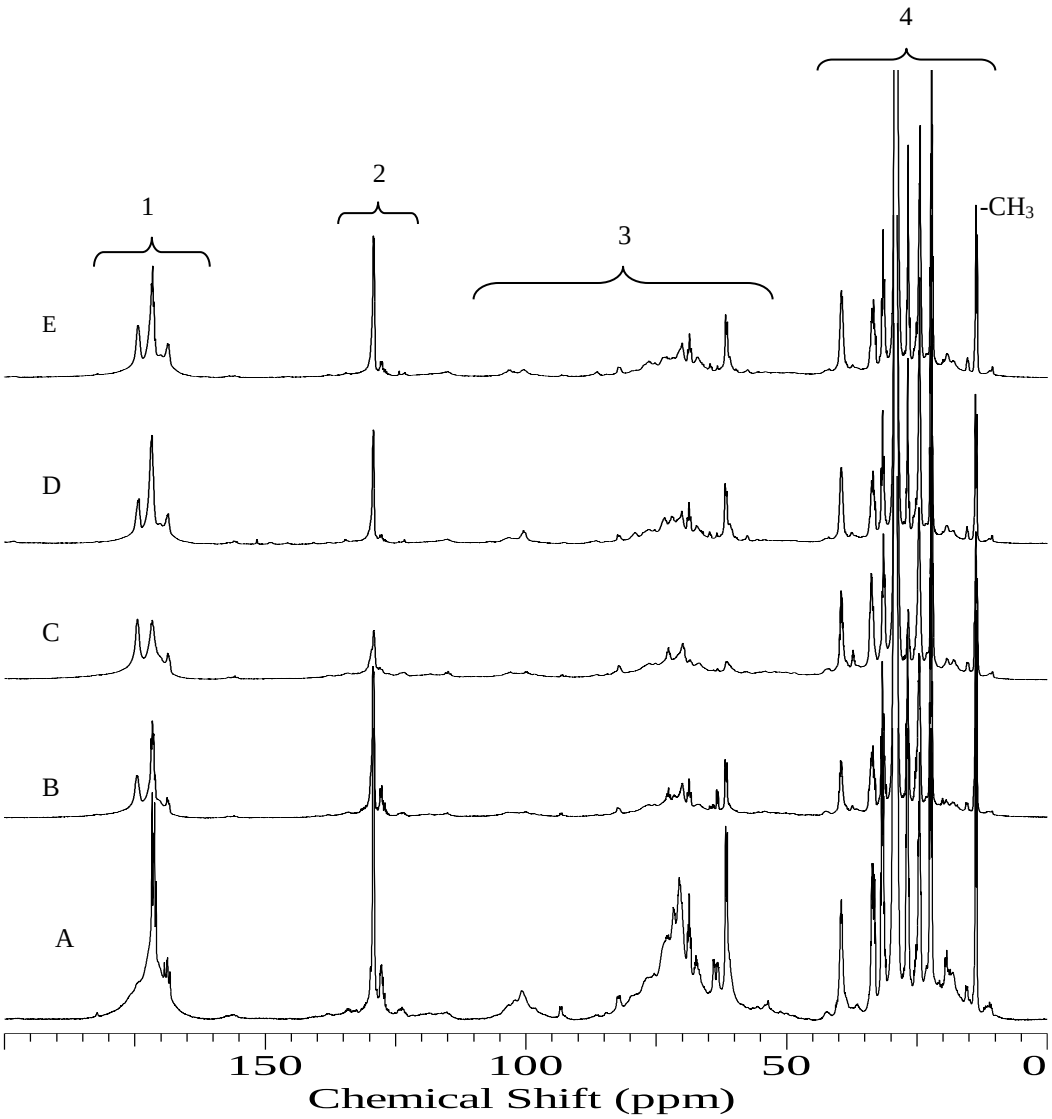

Figure 3.3.1.1: 1D ^{13}C NMR spectra of A) initial microbial biomass (0 h), biomass degraded under ambient conditions for B) 6 and C) 14 weeks, and that degraded under UV irradiation for D) 6 and E) 14 weeks. Numbers and brackets represent general assignments as follows: 1) C=O of esters, acids and/or amides, 2) olefinic and/or aromatic C=C, 3) C-O and/or C-N bonds and 4) CH_2 groups in polymethylenic chain. The regions highlighted should only be used as a reference as to the predominant species in each area. Similar contributions from other species are present in some regions.

3.3.2 ^{1}H and Diffusion Edited NMR analysis of microbial biomass

Figure 3.3.2.1 compares the HR-MAS ^{1}H NMR spectra of the initial and degraded microbial biomass, which are clearly dominated by the intense paraffinic proton signals in the region 0–2.5 ppm (Lundberg et al., 2001). The signal resonating near 0.8 ppm is attributed to resonances from methylic protons of alkyl groups. Peaks around 1.0–1.5 ppm with a dominant peak centred near 1.3 ppm can be attributed to methylene protons (Karl et al., 2007). Signals in the region 2–3 ppm are assigned to protons from various substituted methylenes and methines β to functionality in a hydrocarbon, as would be the case for a lipoprotein and lipid. However, carbonyl, esters and methyl groups of aliphatic ketones could also occur at 2.1 ppm (Kelleher et al., 2006; Karl et al., 2007). Peaks observed between 3.0 and 4.6 ppm are predominantly due to signals from protons in carbohydrates (Lundberg et al., 2001). Signals resonating in the range of 4.8–5.4 ppm are assigned to protons associated with double bonds and esters, possibly form lipids or phospholipids. In addition, the region between 6 and 9 ppm is addressed to signals from amides in peptides aromatic and olefinic structures (Kelleher et al., 2006).

To further emphasize signals from larger macromolecular/rigid species, diffusion edited NMR experiments were carried out on initial and degraded microbial biomass (Wu et al., 1995). In diffusion edited NMR experiments small molecules are essentially gated from the final spectrum while signals from more rigid macromolecules which display little transitional diffusion are preserved (Simpson, 2002). The diffusion edited spectra in ***Figure 3.3.2.2*** compared to that of the conventional ^{1}H NMR spectra in ***3.3.2.1***, shows a generally similar profile, suggesting that the structures present are macromolecular in nature and/or rigid and exhibit little, if any translational diffusion. All spectra were dominated by aliphatic signals (indicating they are still preserved in rigid domains), and are likely preserved because of their recalcitrant structure and hydrophobicity (Simpson et al., 2006).

Although slightly attenuated (suggesting a greater contribution from smaller units that have some translational diffusion), signals from carbohydrates that were not removed during diffusion editing would suggest the presence of a polymeric carbohydrate component that is likely to be associated with bacterial cell wall (Lam et al., 2007). Carbohydrate signals that were gated from experiments are likely to be susceptible to mineralization and rapid conversion to CO_2 (Kogel-Knabner, 2002).

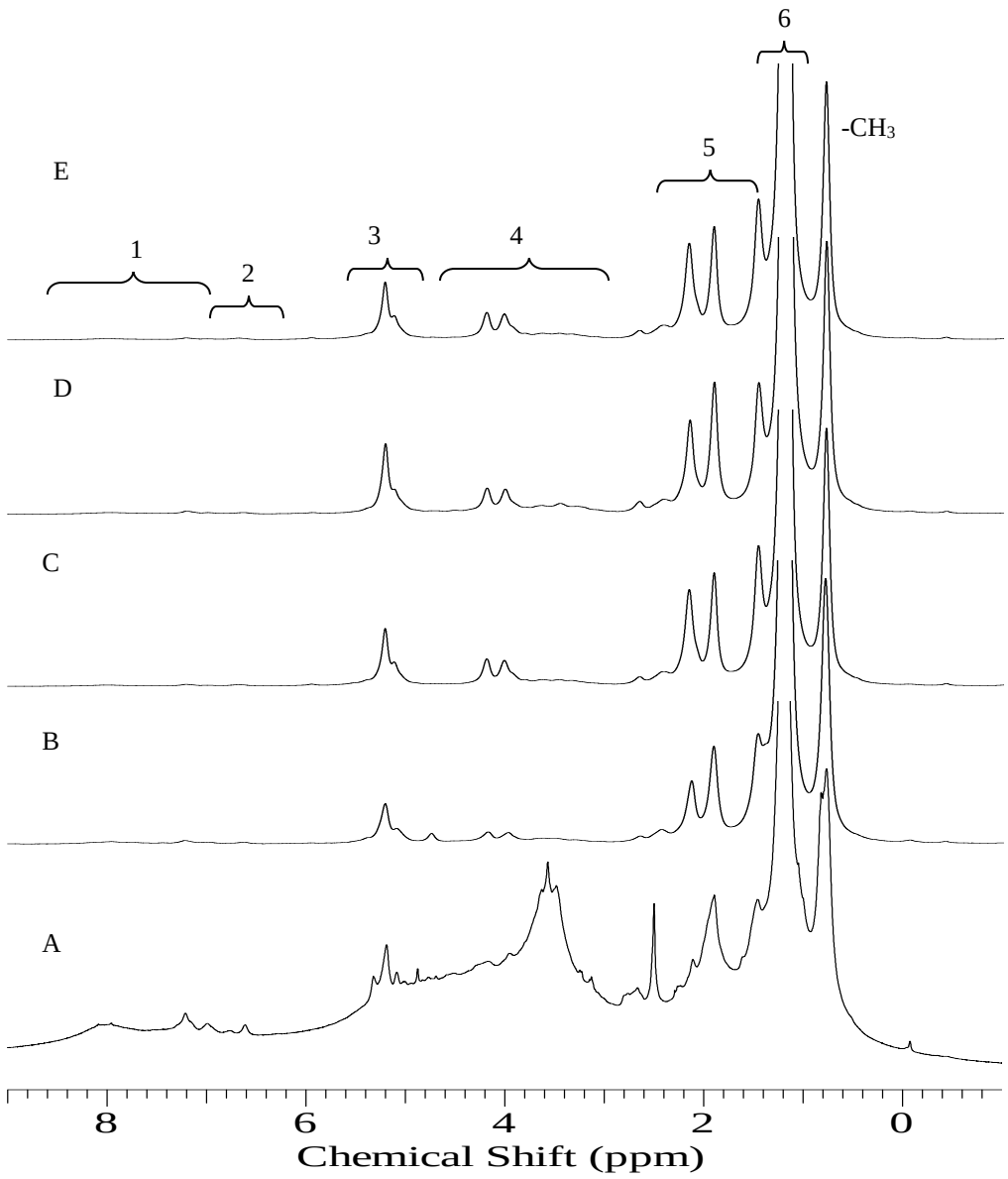

Figure 3.3.2.1: 1D ^{1}H NMR spectra of A) initial microbial biomass (0 h), biomass degraded under ambient conditions for B) 6 and C) 14 weeks, and that degraded under UV irradiation for D) 6 and E) 14 weeks. Numbers and brackets represent general assignments as follows: 1) amides in peptides 2) signals from aromatic rings including aromatic residues, some amide signals in peptides may also resonate in this area, 3) protons on α carbon in peptides, 4) protons in carbohydrates, protons α to an ester, ether, and hydroxyl in aliphatic chains will also resonate in this region, 5) signals from various substituted methylenes and methanes β to a functionality in hydrocarbons, signals from some amino acid side chains will also resonate here, and 6) CH_2, main chain methylene in lipids.

A characteristic resonance ascribed to CH_3 in methylated amino acid side chains is clearly distinguishable in the diffusion edited NMR suggesting the presence of intact protein/peptide. Furthermore, the resonances attributed to amide bonds and amino acid residues (~5.3 ppm) can be attributed to protein/peptide as it is also present in the ^{1}H

NMR spectra. Complementary evidence of the presence of protein/peptide in the degraded samples is provided by the emergence of α-protons from amino acids in ***Figure 3.3.3.1*** and discrete protein bands in ***Figure 6.3.1.2***.

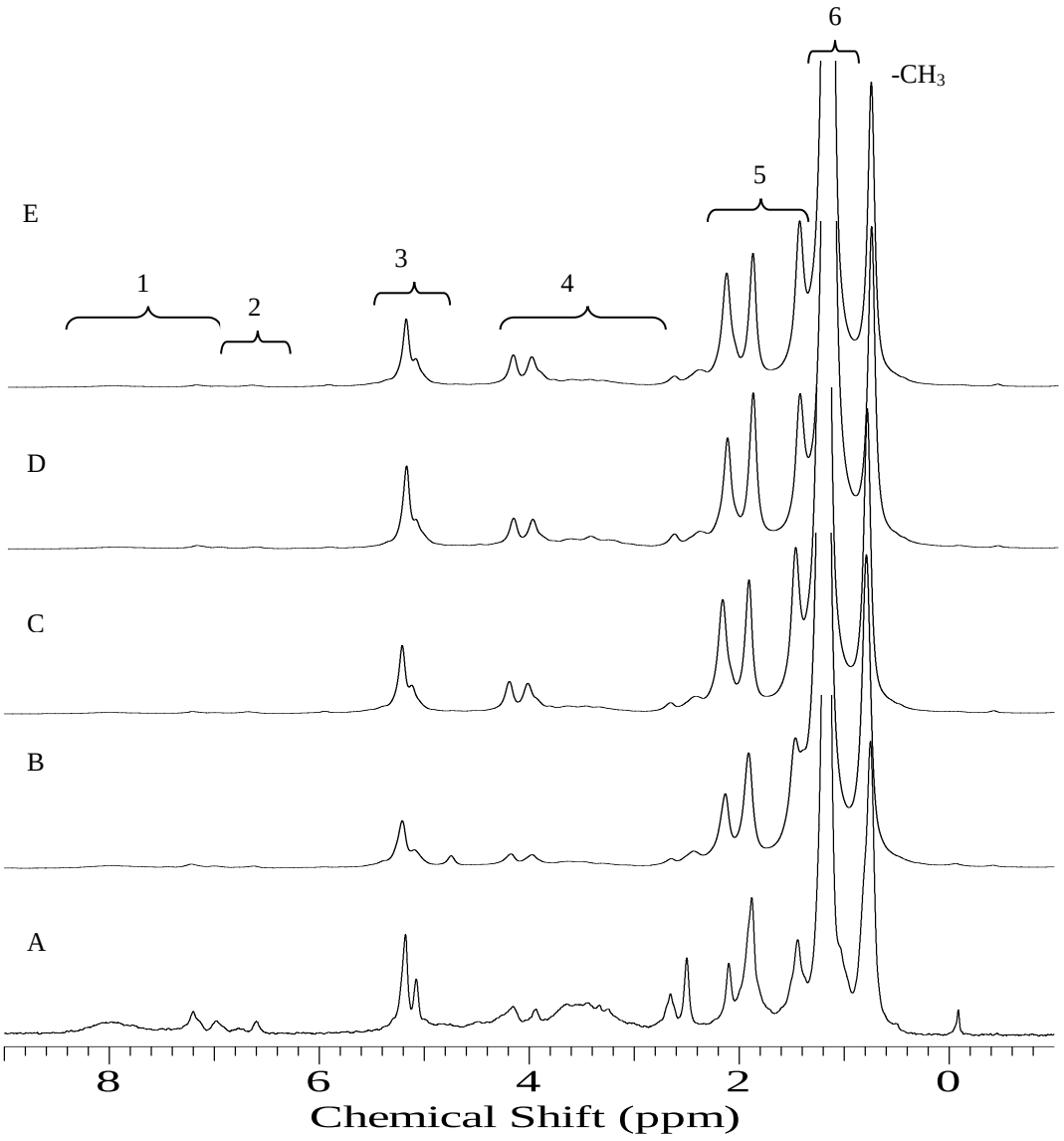

Figure 3.3.2.2: Diffusion edited NMR spectra of A) initial microbial biomass (0 h), biomass degraded under ambient conditions for B) 6 and C) 14 weeks, and that degraded under UV irradiation for D) 6 and E) 14 weeks.

3.3.3 ^{13}C HSQC NMR analysis of microbial biomass

The 1-D HR-MAS NMR provided substantial detail of the samples studied. However, spectral overlap from the multitude of compounds makes specific structural assignments difficult. To circumvent this problem, the application of 2-D HR-MAS NMR experiments were employed (Simpson et al., 2006). The superimposed HSQC NMR spectra in ***Figure 3.3.3.1*** support assignments made from 1-D spectra and identify

a range of chemical constituents present, including 1) aromatic fragments, with possible resonances from aromatic amino acids, 2) double bonds and esters, possibly from lipids or phospholipids, 3) anomeric protons, 4) C-H bonds in carbohydrates, 6) α-protons/carbons in protein/peptides and 7) C-H bonds from various aliphatic structures including fatty acids and amino acids. More specific assignments are; 5) CH_2 in carbohydrates, 8) aliphatic methyl $(CH_2)_n$ in lipids, and 9) terminal CH_3 or CH_3 in methylated amino acid side chain residues. Note, these assignments have been verified by investigation of the HSQC spectra of actual biopolymers representing the major structural classes, namely proteins, carbohydrates and lipids (***Figure 3.3.3.2***), and are also consistent with other 2-D experiments such as long range ^{1}H–^{1}H and ^{13}C–^{13}C couplings (data not shown) as well as literature assignments (Simpson et al., 2006). General assignments of the major structural classes are given in the Figure caption (see ***Figure 3.3.3.2***).

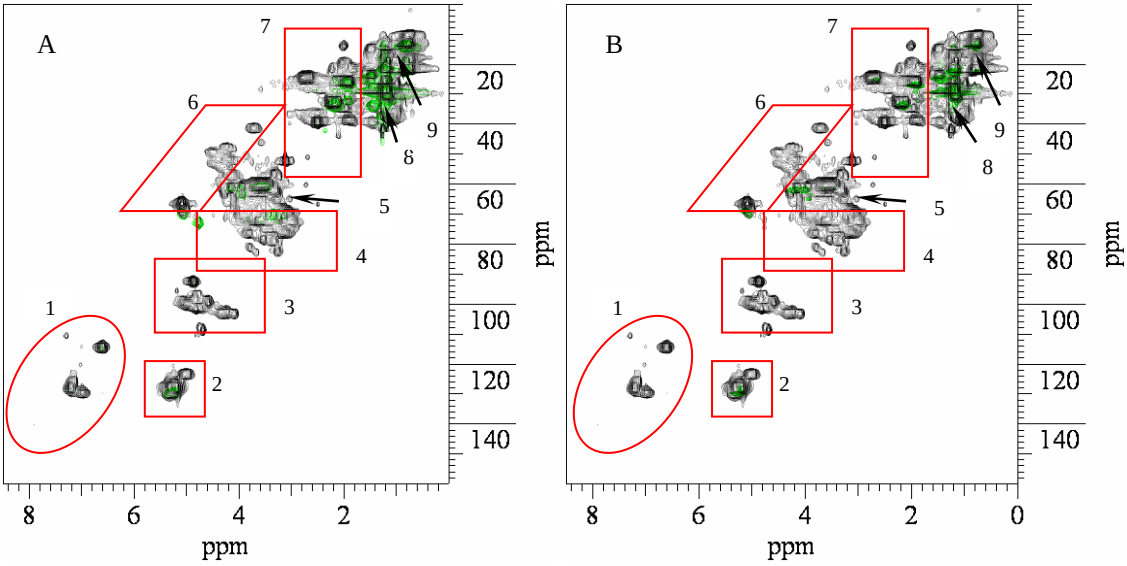

Figure 3.3.3.1: ^{1}H–^{13}C HR-MAS HSQC spectra of A) initial microbial biomass (black) and biomass degradation under ambient conditions for 14 weeks (green); B) initial microbial biomass (black) and biomass degradation under UV conditions for 14 weeks (green). General and specific assignments have been made using a full range of multidimensional NMR experiments and the use of standards as outlined in **Figure 3.3.3.2**.

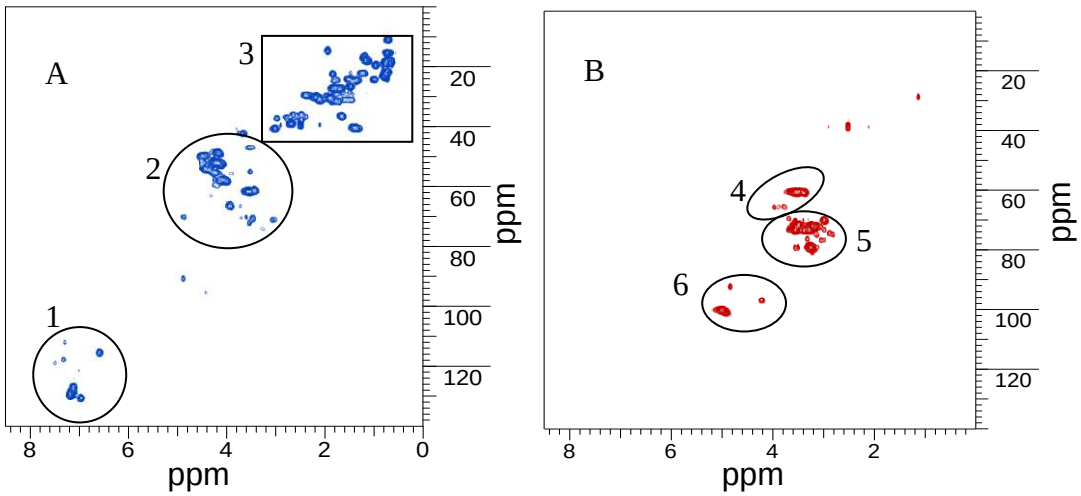

Figure 3.3.3.2: HSQC spectra of biopolymer representatives. A) Bovine Serum Albumen (protein) and B) Amylopectin (carbohydrate). The highlighted regions outlined in the two spectra represent general assignments of the major structural classes as follows; 1) aromatic side chain residue, 2) amino acid α-protons in peptide chains, 3) aliphatic side chain residues, 4) CH_2 in carbohydrate, 5) CH in carbohydrate and 6) anomeric units.

3.3.4 Quantitative analysis

The general assignments that can be reasonably resolved in the 1-D ^{13}C HR-MAS NMR spectrum are; 190–160 ppm – carbonyl carbon, 160–110 – aromatics/double bonds, 110–58 ppm – carbohydrates and 50–0 ppm – aliphatic (Kelleher et al., 2006). Since there are no clear spectral boundaries that define where one group of structures starts and another ends, the quantification offered here can best be described as a relative change in quantity between samples over the degradation period, rather than absolute quantification. ***Figure 3.3.4.1*** illustrates the proportional increase and decrease of major biochemical classes as a function of time for all samples. From these graphs, the most notable pattern throughout the degradation process is the consistent loss of carbohydrates. Carbohydrates accounted for approximately 30% of the biomass at time 0 h (initial biomass), decreasing by approximately 31% and 35% after 14 week degradation under ambient and UV conditions, respectively. The remaining carbohydrates are likely more chemically recalcitrant through their interactions with lipids in the form of lipopolysaccharides (Kögel-Knabner, 2002). The degradation of carbohydrates was associated with a simultaneous increase in the aliphatic content of the biomass. Aliphatics dominated the samples and accounted for approximately 51% of the initial biomass, increasing relatively by approximately 8.5% and 18% after 14 weeks degradation under ambient UV conditions, respectively. Carbonyl groups constituted

approximate 11% of the fresh biomass, increasing relatively by approximately 11% under both conditions over the 14 week period. This relative increase in carbonyl groups would suggest a greater contribution from smaller units, most likely from decarboxylation events active during the degradation of labile lipids (Rhead et al., 1971). The aromatics were the least significant of the biochemical classes, accounting for only 8% of the fresh biomass. However, there was no significant difference in the aromatic content of the degraded biomass when compared to the starting material.

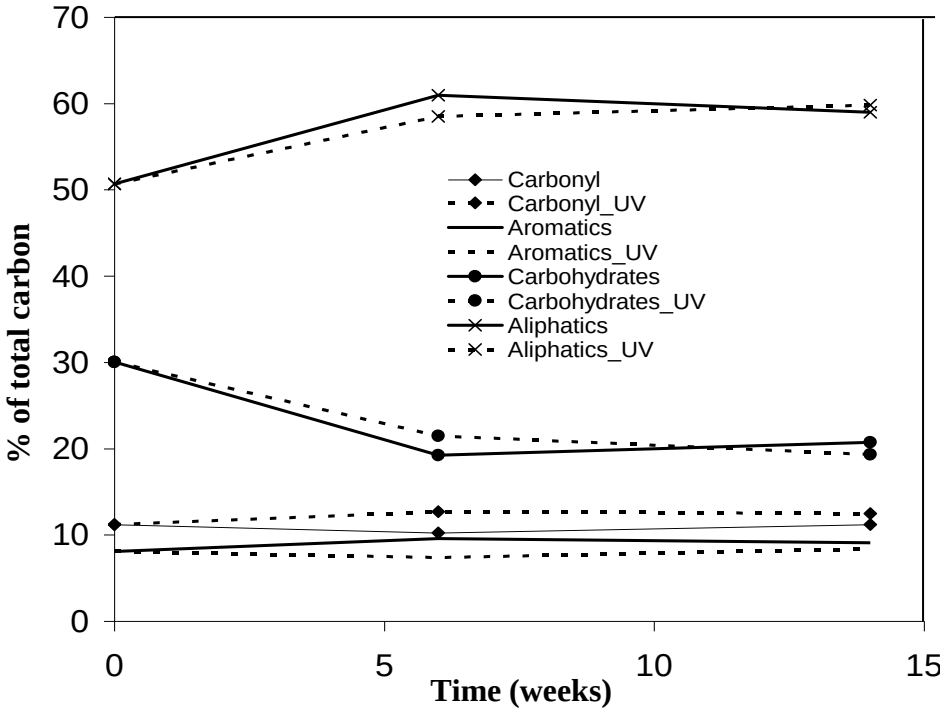

Figure 3.3.4.1: Percentage increases and decreases of major biochemical pools as a function of time for degraded soil microbial biomass.

It is clear that the ^{13}C NMR spectrum of the starting material was dominated by signals originating from aliphatic-C species (45–0 ppm), increasing relatively in the degraded samples and represent, according to integrals of our ^{13}C NMR spectra, more than half the C atoms in each sample (***Figure 3.3.4.1***; Kögel-Knabner, 1997, 2000, 2002). This would suggest that aliphatic structures were selectively preserved concomitant with the degradation of labile materials producing enrichment of the resistant aliphatic material throughout the degradation process (Grundy et al., 2009). This suggestion is in agreement with previous observations that alkly-C, such as those in polymethylenic structures is the most biologically stable form of organic carbon found in soil OM (Baldock et al., 1990, 1997, 2004). The synthesis of aliphatic-C structures from O-alkyl C by microbes has also been reported (Baldock et al., 1990), and should

not be ruled out as a likely contributor to the relative increase in aliphatic-C observed over the course of the degradation.

It further emerges (***Figure 3.3.1.1***) that polymethylenic [$(CH_2)_n$] C in long-chained aliphatic structures (~30 ppm) was the dominant aliphatic-C species in the samples. There is considerable complementary evidence showing that polymethylenic [$(CH_2)_n$] C (C_{16} and C_{18}) dominated the initial biomass typically increases transiently in the degraded biomass (***Chapter 5***). The detection of long-chained polymethylenic-C species in the HR-MAS ^{13}C NMR spectra (***Figure 3.3.1.1B-E***) and GC-MS chromatograms (***Figures 5.3.1.1B-D*** and ***5.3.2.1B-D***) of the degraded biomass supports the conclusion that the polymethylenic-C of paraffinic structures is primarily responsible for the increase in aliphatic-C in soils (Knicker et al., 1996). Such structures have been found in the resistant biopolymers of algae (Derenne et al., 1992). In contrast, a reduction in the relative intensity of aliphatic-C species resonating near 15 ppm (terminal methyl-C), 20 ppm (methylene-C) and 45 ppm (tertiary-C) was observed after 14 weeks of decomposition. These resonances are most probably attributed to the degradation of labile lipids and proteinaceous material resonating in this region. This hypothesis is favoured by supporting evidence in ***Chapters 5*** and ***6***, respectively. Moreover, assuming that every amide-C in peptides is accompanied by, an average, two C contributing to the signals in the chemical shift region between 45 and 0 ppm, approximately one third to one half of the signal intensity in this aliphatic region can also be attributed to proteinaceous material (Knicker et al., 1996; Kögel-Knabner, 2002). Therefore the loss of proteinaceous signals in this region may further explain the reduction in the relative intensity of some signals resonating here. This assumption is clearly supported by the presence of crosspeaks labelled 7, 8 and 9 in ***Figure 3.3.3.1***.

Comparison of the 1-D HR-MAS ^{13}C NMR spectrum of the initial biomass with those of the degraded biomass (***Figure 3.3.1.1A-E***) clearly shows a relative decrease in the signal intensity in the chemical shift region between 120 and 45 ppm, and is clearly supported by annotated crosspeaks in HSQC spectra of ***Figure 3.3.3.1***. These resonances are attributed to carbohydrates, esters and amino acid residues and they reflect the fact that the predominant reactions occurring during prolonged degradation of the biomass are degradation and removal of carbohydrates and proteinaceous materials. This concept is explored in greater detail in ***Chapters 5*** and ***6***, respectively. Similar observations were made in previous studies (Knicker et al., 1996; Kögel-Knabner, 2002;

Kelleher et al., 2006) investigating the molecular composition of plant and microbial residues as inputs in SOM. A moderate peak with a maximum near 102 ppm observed in the fresh biomass, most likely due to mainly anomeric carbon of carbohydrates was not observed in the degraded biomass. The absence of this band probably indicates that many of the carbohydrate groups had been oxidized to hydroxy acids such as aldonic acids (Wershaw et al., 1996). Note, the utilization of free carbohydrate may change the dynamics of the microbial community to one that is capable of degrading more recalcitrant components such as aliphatics (Berg and McClaugherty, 2003).

A diminution in the intensity of the aromatic and olefinic signals between 150 and 120 ppm indicates that these compounds have degraded in the microbial biomass. This is also clearly supported by annotated crosspeaks in HSQC spectra of ***Figure 3.3.3.1***. However, considering the relative amount of carbonyl-C (160-200 ppm) observed in the degraded samples, it is our interpritation that a significant proportion of these signals comprise carboxylic acids linked to polymethylene chains. Although it is possible that they are bound in other ways (amides and esters), this structure is favoured because it is commonly encountered in lipids (Knicker et al., 1996); moreover, proteins were significantly degraded in the biomass (***Chapter 6***). Several authors reported that these amides and esters could be an integral part of the polymethylenic network of refractory algaenan (Derenne et al., 1993; Knicker et al., 1996) and suggest that some of them could be proteinaceous or lipidic in nature (Knicker et al., 1996). The structures described are frequently found in the resistant biopolymer of algae (Simpson et al., 2003). The relatively large signal due to carboxyl C may also be indicative of strong oxidative transformation of organic material in the degraded samples (Kaiser et al., 2001).

Despite the labile nature of proteinaceous material in the environment, the concurrent observation that proteinaceous materials have survived degradation supports the concept of ‘encapsulation’ (Knicker and Hatcher, 1997). This concept argues that organic materials incorporated within sedimentary organic matrix are protected from bacterial hydrolysis. Such organic matrices are usually composed of highly aliphatic materials (Yamashita and Tanoue, 2004). Other mechanisms suggested for protein preservation or recycling include abiotic processes such as condensation reactions which result in reduced degradability (Hedges, 1978; Nagata and Kirchman, 1997). Additionally, several characteristics and processes may increase protein resistance to

degradation by altering their structure to occlude the peptide bond (Rillig et al., 2007). For example, chemical modifications of proteins by carbohydrate and lipid in the forms of glycoproteins and lipoproteins, respectively have been demonstrated to preserve proteins (Zang et al., 2001).

3.3.5 Nitrogen NMR analysis of microbial biomass

Direct 1-D ^{15}N HR-MAS NMR data were also collected on all samples. The resulting ^{15}N HR-MAS NMR spectra revealed the predominance of protonated amide-N in both fresh and degraded biomass (data not shown). This does not exclude the possibility of non-protonated nitrogen present in the materials below detection limits. However, it does indicate that amide-N was the principal form of nitrogen present in the biomass studied and this remained largely unchanged over the degradation process. To further study the protonated fraction, an inverse ^{1}H detection approach was applied where N is indirectly detected through its attached protons (Ernst et al., 1987).

Proteins are known to undergo rapid biodegradation in soils and at the same time are rapidly recycled through microbial activity (Kögel-Knabner, 2000). Here, semi solid ^{1}H–^{15}N HR-MAS NMR HSQC spectroscopy was employed to provide an insight into the nature of the refractory nitrogen in degrading soil microbial biomass. In ***Figure 3.3.5.1*** the ^{1}H–^{15}N HR-MAS NMR HSQC spectra of initial microbial biomass and microbial biomass degraded under ambient and UV conditions for 6 and 14 weeks is illustrated. In each case, the dominant resonance indicates that the major form of the organic ^{15}N is consistent with amide-N functional groups, most likely protein/peptides (Kögel-Knabner, 2000). Although the ^{15}N NMR spectra of fresh and degraded biomass is of a predominantly proteinaceous nature, we cannot conclusively exclude the contribution of signals from heterocyclic nitrogen, such as purines/pyrimidine, indoles, imidazoles (including heterocyclic-N in histidine) and substituted pyrroles to the intensity of the resonance from amide-N (Kincker et al., 1996; Zang et al., 2001). This hypothesis is favoured as variable quantities of purines, pyrimidines and amino sugars were detected in the acid hydrolysates of the initial and degraded microbial biomass (***Figures 5.3.3.1*** and ***5.3.6.1***; ***Tables 5.3.3.1*** and ***5.3.6.1***). Signals from nitrogen in acetylated amino sugars, lactams, and carbazoles may also contribute to the intensity of this resonance (Kincker et al., 1996). Studies of degraded algal residues using ^{15}N solid-state NMR have indicated that these signals resonate between –145 and –220 ppm, but may expand to –270 ppm, incorporating the dominant resonance (–259 ppm) of the

spectrum assigned to amide-N (Knicker et al., 1996; Kögel-Knabner, 1997). There was very little or no significant shift in the relative intensity of the resonance assigned to amide-N in the degraded biomass (***Figure 3.3.5.1B-E***) when compared with the ^{15}N NMR spectrum of the initial biomass (***Figure 3.3.5.1A***). Based on this fact it follows that few, if any, major qualitative changes in the composition of amide-N functionality occurred during the degradation period.

Considering that more than 80% (Kögel-Knabner, 2000) of the ^{15}N-signal intensity in the microbial ^{1}H–^{15}N HSQC NMR spectra can be assigned to amide-like structures, more than half the signal intensity in the ^{13}C chemical shift region between 200 and 160 ppm in the ^{13}C NMR spectra of the fresh and degraded biomass can be assigned to amide-C (Knicker et al., 1996). The comparable intensities of the signals between 200–160 ppm and 65–45 ppm (***Figure 3.3.1.1***) indicate that almost all the nitrogen in amide bonds is additionally bound to alkyl carbon, as would be expected from peptides (Knicker, 2000; Zang et al., 2001). These results are strongly indicative of the highly refractory nature of amide-N, and are in agreement with observations that amide-N survives chemical and microbial degradation and is even resistant to acid hydrolysis, commonly applied to convert proteins to free amino acids (Knicker et al., 1996; Knicker, 2000). The identification of proteinaceous material in 1-D ^{1}H, 1-D ^{13}C, DE, 2-D ^{13}C and 2-D ^{15}N NMR spectra of microbial biomass degraded in a clay-free environment suggests that processes other than mineral adsorption/protection is responsible for the survival of peptide structures. A possible explanation for this recalcitrance is that such amides may be an integral part of the paraffinic network of refractory alkyl compounds (alkyl-amide; Knicker et al., 1996).

The possibility also exists that such amide functionalities are chemically (for example through the association with carbohydrates) protected (Kelleher et al., 2006) or simply “labelled” microbial species consuming the isotopically enriched food source. Studies have demonstrated that the preservation of organic nitrogen in algal sediments is a result of abiotic reactions of amino groups with carbohydrates (Millard, 1917; Hedges, 1978). Despite the labile nature of proteins, a relatively significant quantity of proteinaceous persisted in the degraded biomass. In addition, new cross-peaks appeared in the degraded samples. Exact assignments are impossible with the current data but questions regarding their appearance arise. For example, are they specific products of decomposition or are they species selectively preserved from the original proteinaceous

materials? Or, alternatively could they be specific species synthesized from the labelled biomass by soil microbes (Kelleher et al., 2006). Undoubtedly, significant analytical work is required in this area to answer these questions.

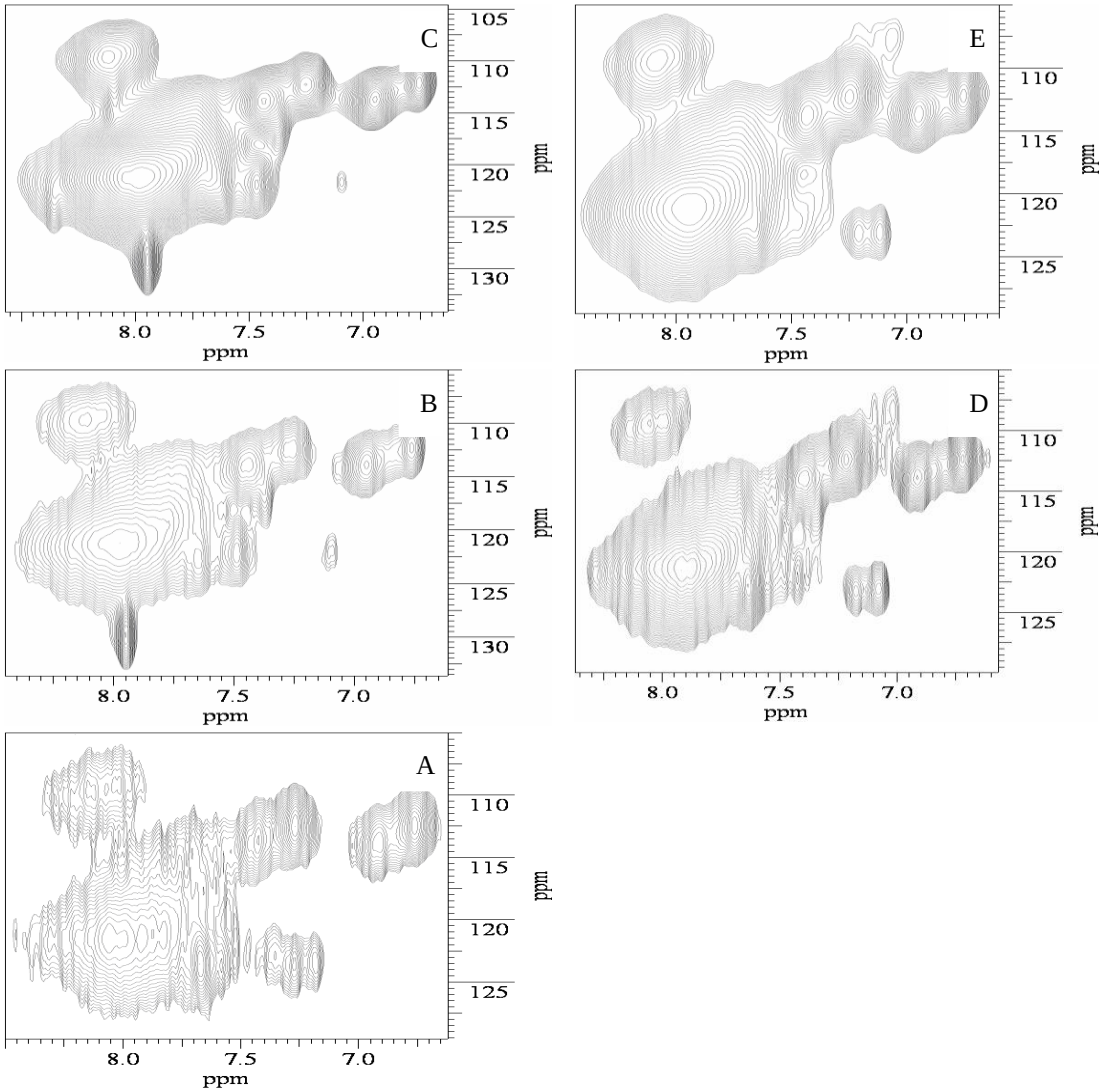

Figure 3.3.5.1: $^{1}H–^{15}N$ HR-MAS NMR HSQC spectra of A) initial microbial biomass (0 h), biomass degraded under ambient conditions for B) 6 and C) 14 weeks, and that degraded under UV irradiation for D) 6 and E) 14 weeks.

3.3.6 ^{13}C NMR analysis of microbial leachate

Figure 3.3.6.1 shows the 1-D ^{13}C HR-MS NMR spectra of microbial leachates degraded under ambient and UV conditions. General assignments, consistent with those reported in the literature, can be made as to the major components present (Karl et al., 2007; Solomon et al., 2007). Major components are applicable to all ^{13}C NMR spectra and include, 1) carbonyl-C in carboxylic acid, amide groups and ester bonds, 2) aromatic-C and olefinic-C possibly from unsaturated lipids, phospholipids or aromatic

amino acids, 3) a mixture of carbohydrates, amino acids and lipids including the anomeric carbon and units adjacent to esters, and may be associated with bacterial cell wall, and 4) aliphatic components, primarily medium- to short-chained or branched terminal CH_3, CH_2, and tertiary- or quaternary-C.

After 6 weeks degradation under ambient conditions, the microbial leachate was dominated by aliphatic-C species (region 4; ~38% of total carbon integral of major biochemical pools), decreasing relatively by approximately 19% after 14 weeks. Simultaneously, there a relative increase (~18%) in carbohydrates (region 3) which was the dominant C species (34.22%) in the spectrum after 14 weeks degradation (***Figure 3.3.6.1***). These results are somewhat surprising and contradict previous findings (Knicker et al., 1996) which suggest that the predominant reactions occurring during prolonged degradation are degradation and removal of carbohydrates. However, considering that up to one half of the signals resonating in region 4 may be proteinaceous in origin, the loss of aliphatic-C is likely due to the degradation of labile proteinaceous material resonating in this region (Kögel-Knabner, 2002). Moreover, it is likely that lipids were lost to consumption by bacteria as a source of energy and/or hydrolysis by lipases contained in bacterial cells growing in the leachate (Yoshimura et al., 2009). The quantitative differences between the lipid composition of the degraded microbial biomass and microbial leachates are clearly observed in ***Chapter 5***.

In contrast, under UV-induced decomposition, the microbial leachate was dominated by signals from carbohydrate species (36.5%) after 6 weeks degradation (***Figure 3.3.6.1 C***), increasing relatively to other components by approximately 18% after 14 weeks. The ^{13}C HSQC NMR spectra in ***Figure 3.3.7.1*** provided complementary and conclusive evidence to support the conclusion that the UV degraded samples were dominated by carbohydrates (cross-peaks in regions 4 and 5). We postulate that the relative concentration of polysaccharide in the degraded sample is due to the accumulation of water soluble material leached from the degraded biomass. It should also be noted that a moderate peak ***Figure 3.3.6.1*** near 102 ppm was not attenuated, and would suggest that no carbohydrate was lost through oxidation as is usually the case (Wershaw et al., 1996). Qualitatively, it is difficult to distinguish a pattern of degradation within the aliphatic chemical shift region (region 4) of the 1-D HR-MAS ^{13}C NMR spectra of the UV irradiated microbial leachates ***Figure 3.3.6.1 C*** and ***D***. However, according to integrals of our ^{13}C NMR spectra, aliphatic-C was largely

unchanged over the course of the degradation process and accounted for approximately 31% of the total C atoms in each UV irradiated sample. These results have significant implications for C sequestration and stabilization in the subsoil and should be the focus of more detailed investigations.

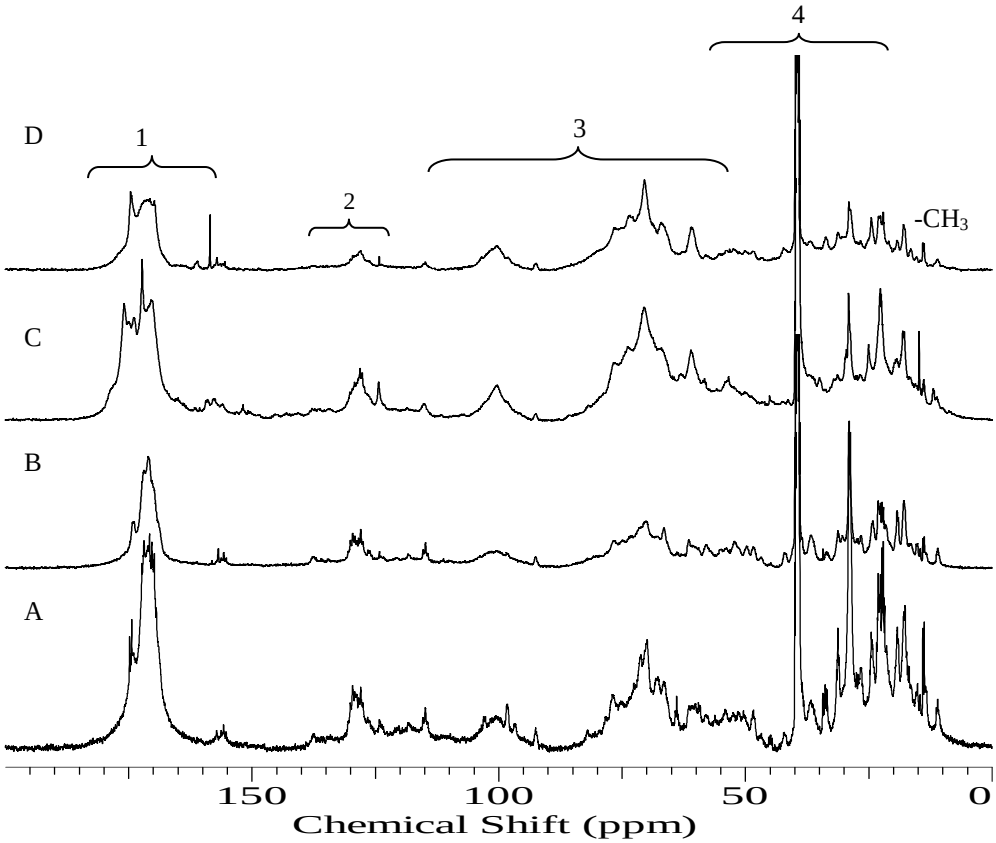

Figure 3.3.6.1: 1D ^{13}C NMR spectra of microbial leachates degraded under ambient conditions for A) 6 and B) 14 weeks, and that degraded under UV irradiation for C) 6 and D) 14 weeks. Numbers and brackets represent general assignments as follows: 1) C=O of esters, acids and/or amides, 2) olefinic and/or aromatic C=C, 3) C-O and/or C-N bonds and 4) CH_2 groups in polymethylenic chain. The regions highlighted should only be used as a reference as to the predominant species in each area. Similar contributions from other species are present in some regions. More details of the general regions are given in the text.

An interesting observation is that a dominant peak characteristic of polymethylenic [$(CH_2)_n$] C in long-chained aliphatic structures (Kögel-Knabner, 1997, 2002) that was observed (near 32 ppm) in the ^{13}C NMR spectra of the ambient and UV degraded biomass (***Figure 3.3.1.1***) was significantly attenuated in the ^{13}C NMR spectra of all microbial leachates, as were other aliphatic signals. The relative reduction in concentration of aliphatic-C species observed in the leachates may be interpreted as the preferential adsorption of aliphatic components to soil minerals as they leached through the soil (***Figure 3.3.6.1***). Convincing evidence of the preferential adsorption of

aliphatic-C to clay minerals is presented in ***Chapter 4***. Moreover, this suggestion is strongly supported by the findings of Kaal et al. (2005) who attributed the limited detection of tannins in soil leachates to their adsorption to soil minerals. Additionally, the hydrophobic nature of lipids may have influenced the amounts of aliphatic material leached and accumulated.

Signal 2 (aromatic and olefinic-C) in ***Figure 3.3.6.1*** showed little variation in concentration in of the ambient and the UV degraded microbial leachates accounting for roughly 21% of the total C in all samples over the degradation period. However, signal 1 (carboxyl/amide-C) was slightly more variable, accounting for 14 and 11% of the total C in the ^{13}C NMR spectra of leachates degraded under ambient conditions for 6 and 14 weeks, respectively, and approximately 12 and 6% of the total C in UV degraded samples over the same period. The relative reduction in concentration of carboxyl/amide-C is most likely do to biological and photochemical degradation of proteinaceous materials and labile fatty acids in the samples. ***Figure 3.3.7.1*** also serves to complement these data by spreading the signals over two dimensions to circumvent overlapping signals.

3.3.7 ^{13}C HSQC NMR analysis of microbial leachate

The HSQC NMR spectra in ***Figure 3.3.7.1*** support assignments made from the 1-D ^{13}C NMR spectra and identifies a range of chemical constituents present, including 1) aromatic fragments, with possible resonances from aromatic amino acids, 2) double bonds and esters, possibly from lipids or phospholipids, 3) anomeric protons, 4) C-H bonds in carbohydrates, 6) α-protons/carbons in protein/peptides and 7) C-H bonds from various aliphatic structures including fatty acids and amino acids. More specific assignments are; 5) CH_2 in carbohydrates, 8) aliphatic methyl $(CH_2)_n$ in lipids, and 9) terminal CH_3 or CH_3 in methylated amino acid side chain residues. General and specific assignments have also been made using a full range of multidimensional NMR experiments as well as literature assignments (Simpson et al., 2007a).

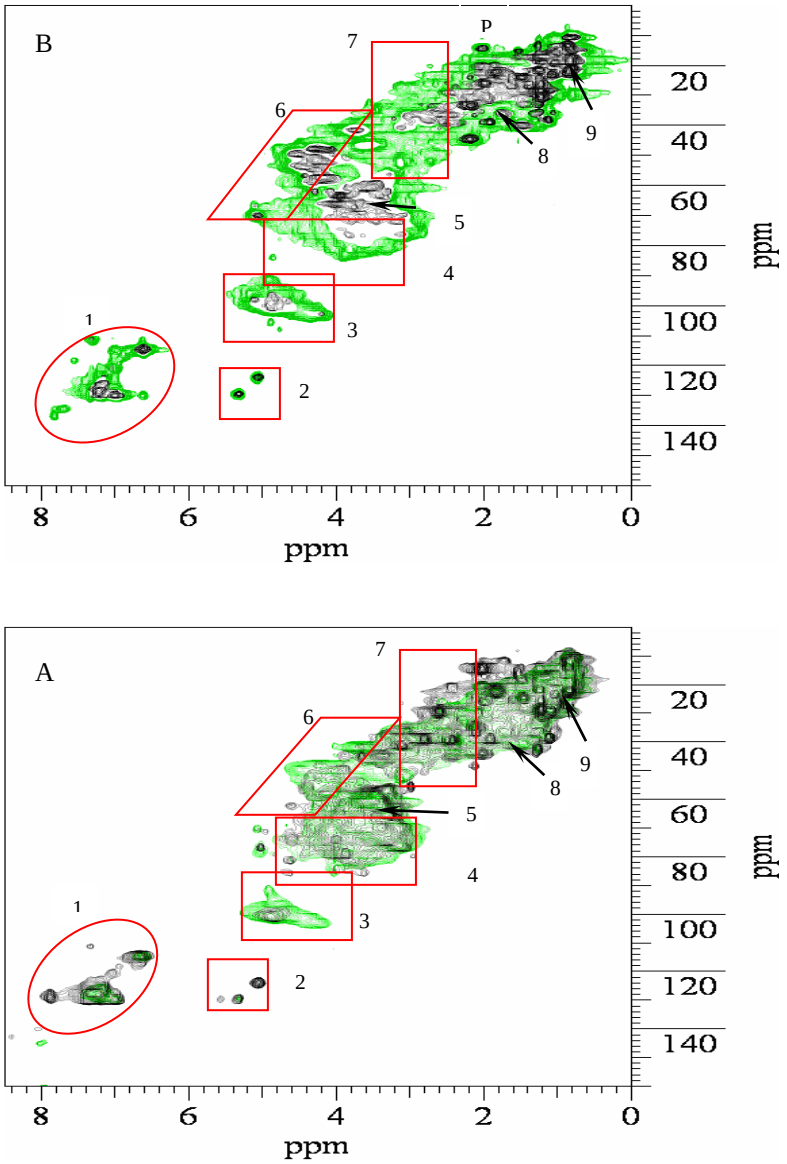

Figure 3.3.7.1: $^{1}H–^{13}C$ HR-MAS HSQC spectra of A) microbial leachates degraded under ambient conditions for 6 weeks (black) and 14 weeks (green) and B) that degraded under UV irradiation for 6 (black) and 14 weeks (green). Basic assignments for the major structural groups are as follows: 1) aromatic fragments, 2) double bonds, 3) anomeric protons, 4) C-H bonds in carbohydrates, 6) α-protons/carbons in protein/peptides and 7) C-H bonds from various aliphatic structures including fatty acids and amino acids. More specific assignments are; 5) CH_2 in carbohydrates, 8) aliphatic methyl $(CH_2)_n$ in lipids, and 9) terminal CH_3 or CH_3 in methylated amino acid side chain residues and P; N-acetyl peptidoglycan.

It has been demonstrated that compounds containing double bonds are highly reactive (Goni and Hedges, 1990) and are known to degrade readily due to the presence of these labile allylic centres (Rontani et al., 2009). However, signals resonating from double bonds (region 2) showed no obvious pattern of decomposition under ambient

degradation ***Figure 3.3.7.1A***. These results are not surprising, as it has also been demonstrated that potentially labile bonds (Largeau et al., 1986) and double bonds in algenan (Simpson et al., 2003) persist in the environment for long periods of time (Deshmukh et al., 2003), and may be protected by biopolymers that shield the labile linkers in an aliphatic chain (Kelleher et al., 2006). This stabilization suggests that these double bonds may be present in aliphatic chains as indicated in ***Chapter 5*** (***Section 5.3.3***). In contrast, signals assigned to double bonds were depleted in the UV degraded microbial leachate after 14 weeks (***Section 5.3.4***). The significant loss of these structures from the UV irradiated samples may be due to photochemical degradation of protective biopolymer into biologically oxidizable or volatile structures, as has been shown for marine DOM (Kieber et al., 1989; Mopper et al., 1991).

3.3.8 ^{1}H and Diffusion Edited NMR analysis of microbial leachate

Figures 3.3.8.1 and ***3.3.8.2*** illustrate the conventional 1-D ^{1}H HR-MS and the diffusion edited ^{1}H NMR spectra of degraded microbial leachates dissolved in DMSO-d_6, while the 1-D ^{1}H spectrum of a standatd protein, bovine serum albumin is represented for comparison in ***Figure 3.3.8.2A***. General peak designations represent the predominant species present and are consistent with those previously reported. The assignments can be defined as; contribution from amide signals in peptides and aromatic amino acid residues (regions 1 and 2) consistent with the presence of intact proteinaceous material. 3) Protons associated with double bonds (mono- and di-unsaturated acyl chains) and esters, possibly form lipids or phospholipids 4) predominantly signals from carbohydrates. Some signals from amino acids and proteins may also resonate in this region. 5) Signals from various substituted methylenes and methines β to a functionality in a hydrocarbon, as would be the case for a lipoprotein and lipid. Region 6) is consistent with aliphatic methylene $(CH_2)_n$ carbons (likely from bacterial membrane) including that in aliphatic rings and chains and methyl groups bound to carbon (Lundberg et al., 2001: Kelleher et al., 2006; Karl et al., 2007). More specific assignments refer to i); terminal CH_3 in methylated amino acid side chain residues, and are consistent with a side chain residue in the ^{1}H NMR spectrum of bovine serum albumen (BSA), ii) contributions from N-acetyl group in peptidoglycans, and iii) novel peptides.

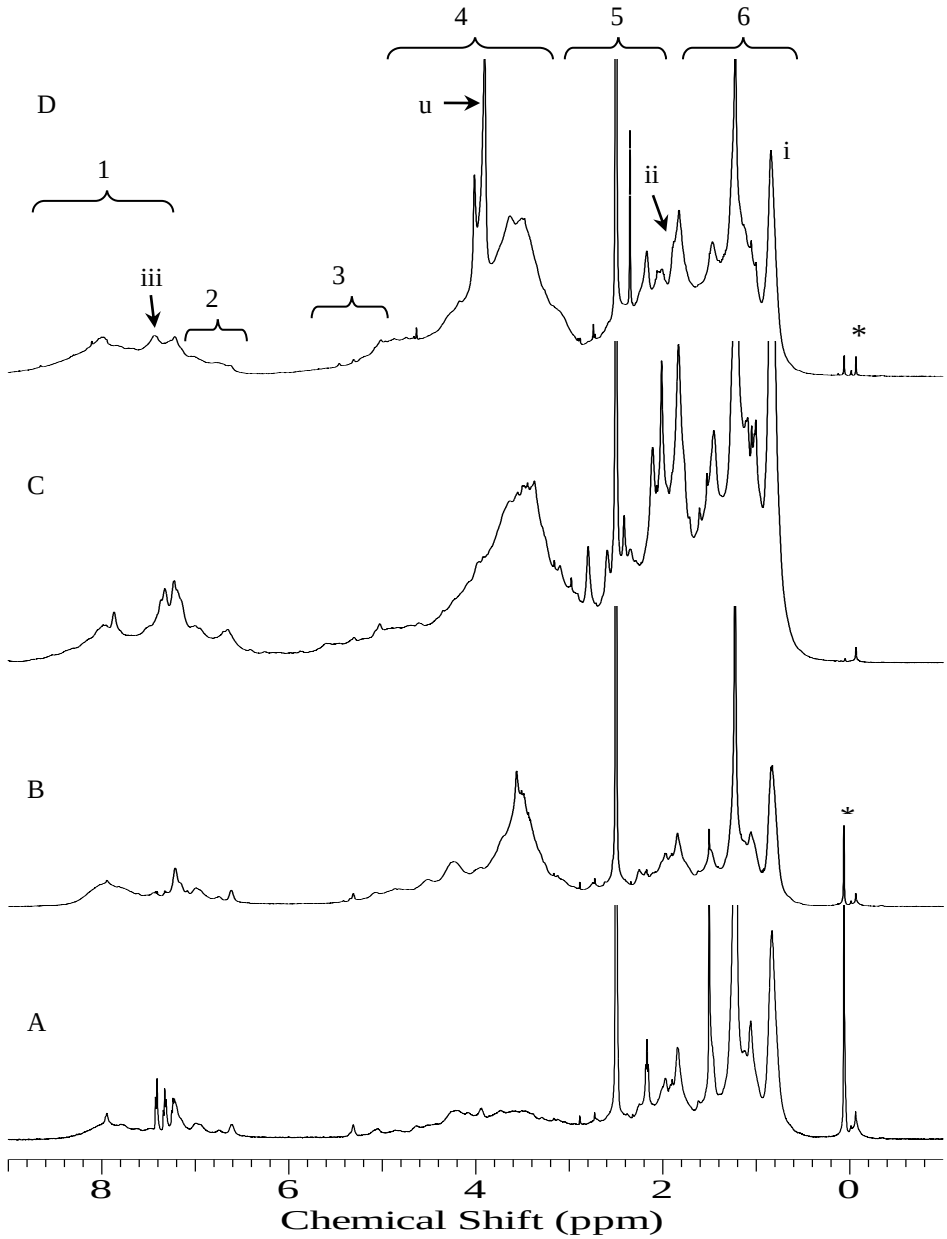

Figure 3.3.8.1: 1D ^{1}H NMR spectra of microbial leachates degraded under ambient conditions for A) 6 and B) 14 weeks, and that degraded under UV irradiation for C) 6 and D) 14 weeks. Numbers and brackets represent general assignments as follows: 1) amides and amide signals in peptides 2) signals from aromatic rings including aromatic residues, some amide signals in peptides may also resonate in this area, 3) protons on α carbon in peptides, 4) protons in carbohydrates, protons α to an ester, ether, and hydroxyl in aliphatic chains will also resonate in this region, 5) signals from various substituted methylenes and methanes β to a functionality in hydrocarbons, signals from some amino acid side chains will also resonate here, 6) protons in aliphatic species. (i) CH3 in methylated amino acid side chain; (ii); peptidoglycan, (iii); novel peptides; u; unknown compound and *; resonance from natural silicate species.

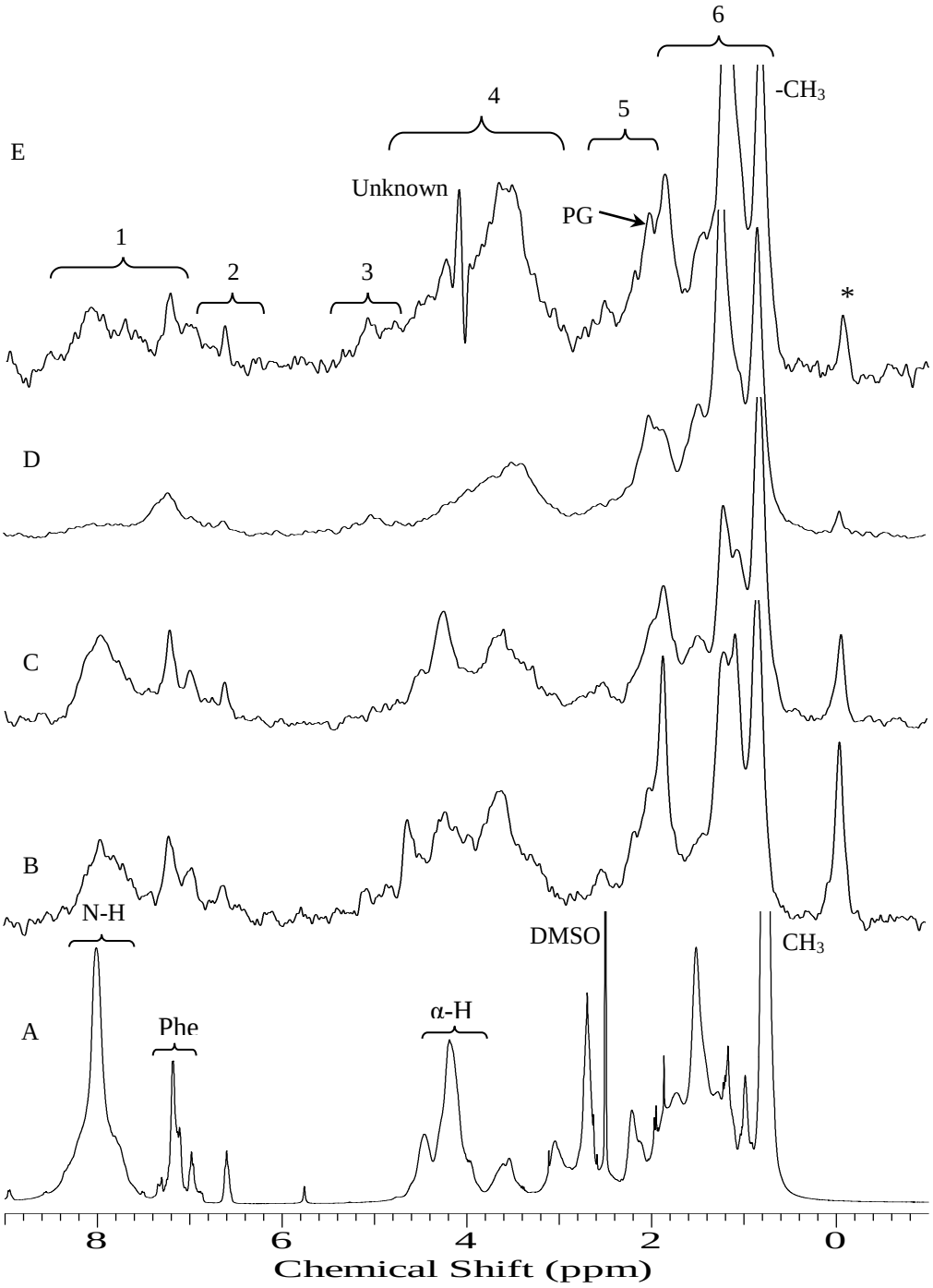

Figure 3.3.8.2: 1-D ^{1}H spectrum of a standatd protein, bovine serum albumin (A); diffusion edited NMR spectra of microbial leachates degraded under ambient conditions for B) 6 and C) 14 weeks, and that degraded under UV irradiation for D) 6 and E) 14 weeks. PG, peptidoglycan; Phe, phenylalanine and *; resonance from natural silicate species.

The samples investigated display largely similar spectral profiles and ratios of major biochemical components with a characteristic dominance from signals assigned to polymethylene [$(CH_2)n$] C (~1.29 ppm) in aliphatic compounds indicating they are still preserved in rigid domains. Signals from carbohydrates also represent one of the dominant species indicating that they are preserved as large polymeric structures that

could potentially be associated to bacterial cell wall (Lam et al., 2007). Resonances attributed to amide signals in protein/peptide and aromatic amino acids (regions 1 and 2) are partially unchanged by the diffusion gate, strongly suggesting that this material is of significant size and is likely to be intact polymeric protein structures that have survived the degradation process. These data are consistent with the findings of Kelleher et al. (2007) who reported the presence of intact polymeric protein structures in marine sediments using diffusion edited NMR.

This interpretation is further supported by the spectral similarity to the 1D ^{1}H NMR spectrum of protein standard BSA, a characteristic resonance ascribed to CH_3 in methylated amino acid side chains and the presence of α-protons from amino acids in ***Figure 3.3.7.1***. Furthermore, substantial amounts of intact proteins were subsequently isolated from the samples investigated and separated on 1-D SDS-PAGE (***Figure 6.3.1.3***). Other signals previously identified in the conventional ^{1}H NMR spectra of degraded microbial leachates (see annotation for ***Figure 3.3.8.1***) also appear to be preserved in the rigid domain. We speculate that proteins were preserved as intact polymeric structures in the form of long-term protein-dissolved organic matter interactions or protein-mineral interactions that render them unavailable to bacterial and photolytic degradation (Aluwihare et al., 2005). Hydrophobic and hydrogen-bond interactions between proteinaceous material and non-protein components have been proposed as major forces of N stabilization (Nguyen and Harvey, 2003). Other possible mechanisms involved in the preservation of the major biochemical components in the degraded leachates were previously discussed.

Contributions from microbial cell wall components (signal ii) observed in microbial leachates can be assigned to N-acetyl peptidoglycan (***Figure 3.3.8.1***) that is confirmed by cross-peaks also observed in HSQC spectra in ***Figure 3.3.7.1***. Cross-peaks were identified by a comparative analysis with Advanced Chemistry Development (ACD) software and literature data on the basis of their characteristic chemical shifts. N-acetyl peptidoglycan comprises up to 90% by weight of gram-positive bacteria and is a key structural component in all microbial cell walls (Simpson et al., 2007a). Structurally, it comprises roughly equal amounts of amino sugars strands with peptide bridges (Hedges et al., 2001). However, it must be noted that it is not possible to accurately quantify contributions of peptide in the form of peptidoglycan in the sample due to spectral overlap. Using rough estimates based on deconvolution of

spectral profiles, Simpson et al. (2007a) determined that the peptide contribution of peptidoglycan in humin was relatively small. The presence of peptidoglycan in the diffusion edited NMR spectra is of no surprise as it is resistant to many chemical and biological processes and has been found as a constituent of the most refractory components of SOM (Simpson et al., 2007b). It is likely that peptidoglycan also contributed to the intensity of the carbohydrate signals observed in the proton spectra of the samples investigated.

Another key observation is the presence of trace amounts of natural silicate species (Si) in the 1-D ^{1}H HR-MS and the diffusion edited ^{1}H NMR spectra of the degraded microbial leachates (***Figures 3.3.8.1*** and ***3.3.8.2***). This is particularly important since carbon sequestration in the ocean has been linked with the global cycling of silicon (Tréguer et al., 1995; Ragueneau et al., 2000). The conventional thought is that the primary source of continental silicon flux into the ocean is due to weathering in terrestrial biogeosystems (van Breemen and Buurman, 2002). However, silicon dynamics in terrestrial biogeosystems cannot be understood solely on the basis of mineral weathering (Sommer et al., 2006). The presence of silicate species in microbial leachates would therefore suggest that soil microorganisms are capable of accumulating stable amounts of silicon and may play a more vital role in silicon cycling than currently thought. If this is the case, then soil microbial biomass (or at least the heterothophic fraction) may play an even more significant role in the removal and sequestration of atmospheric CO_2 in soil as inorganic bicarbonates. In addition, microbially accumulated silicon may further influence the hydrologic properties of soils and improve their capacity to stabilize the labile C pool and reduce atmospheric CO_2 levels through the dissolution of CO_2 in soil solution, ultimately producing carbonate which is then sequestered as inorganic C in soils. These findings further demonstrate shortfalls in our knowledge of microbial contributions to SOM and carbon sequestration and raise important new questions and highlight the need for greater research into the qualitative significance of silicon and its impact on the carbon biogeochemical cycle.

An even more significant discovery is the appearance of novel peptides (iii; ~7.4 ppm) in the 1D ^{1}H HRMS NMR spectrum of the microbial leachate incubated under UV irradiation for 14 weeks (***Figure 3.3.8.1D***) that is confirmed by cross-peaks appearing in the ^{15}N HSQC NMR spectrum in ***Figure 3.3.9.1*** that cannot be found in any other sample. Also of interest is the appearance of an unknown compound in the same sample

which appears to be preserved in the rigid domain (***Figure 3.3.8.2E***), indicating that it is macromolecular in nature. These findings demonstrate the potential for the photochemical transformation of organic material into novel photoproducts. The formation of novel photoproducts from DOM was previously reported (Kieber et al., 1989). It is also possible that these structures were formed after random condensation and polymerization reactions of degrading proteinaceous material (Nguyen and Harvey, 2003).

3.3.9 Nitrogen NMR analysis of microbial leachate

Figure 3.3.9.1 illustrates the $^{1}H–^{15}N$ HR-MAS NMR HSQC spectra of microbial leachates degraded under ambient and UV conditions for a period of 14 weeks. Considering the spectroscopic evidence, it emerges that amide-N functionalities, most likely protein/peptides represent the major form of the organic ^{15}N in all samples. This would suggest that microbially derived amide-N is an integral part of the stable N pool of SOM. Although the major form of organic N in the ^{15}N NMR spectra of the degraded samples is of a predominantly proteinaceous nature, the contribution of signals from heterocyclic nitrogen, such as purines/pyrimidine, indoles, imidazoles (including heterocyclic-N in histidine) and substituted pyrroles to the intensity of the resonance from amide-N (Knicker et al., 1996; Zang et al., 2001) cannot be discounted. Several studies of degraded algal residues have reported that signals from nitrogen in acetylated amino sugars, lactams, and carbazoles resonate between –145 and –220 ppm, but may expand to –270 ppm, incorporating the dominant resonance (–259 ppm) of the spectrum assigned to amide-N (Knicker et al., 1996; Kögel-Knabner, 1997). It is also noteworthy that the $^{1}H–^{15}N$ HR-MAS NMR HSQC spectra of the UV irradiated microbial varied slightly from that of the samples degraded under ambient conditions with the emergence of novel peptides in ***Figure 3.3.9.1D*** and new cross-peaks, possibly photoproducts unknown to us at this time. Or, alternatively they could be specific species synthesized from the labelled biomass due to UV-induced changes in the initial microbial community.

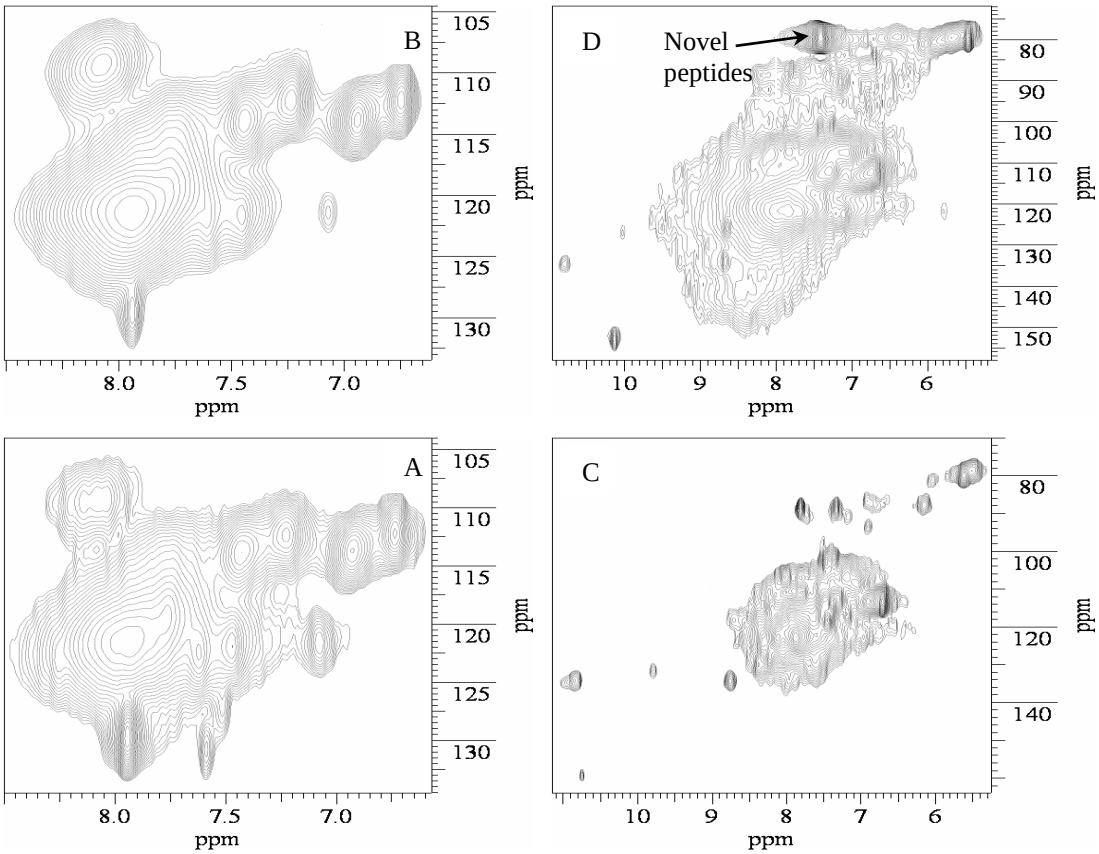

Figure 3.3.9.1: $^{1}H–^{15}N$ HR-MAS NMR HSQC spectra of microbial leachate degraded under ambient conditions for A) 6 and B) 14 weeks, and that degraded under UV irradiation for C) 6 and D) 14 weeks.

The refractory nature of amide-N in ambient and UV degraded microbial biomass was previously discussed in ***Section 3.3.5***. This can thus be assumed for the amide-N detected in the ambient and UV degraded microbial leachates. Although microbial biomass degradation was carried out in clay-free environment, the leachates were allowed to percolate through the initial soil [(a light clay-loam soil) as depicted in ***Figure 3.2.2.1***] from which the microbes were propagated. Therefore, considering the amount of protein/peptide detected in the 1-D ^{1}H, 1-D ^{13}C, diffusion, 2-D ^{13}C and 2-D ^{15}N NMR spectra of the degraded microbial leachates, it would be plausible to suggest that clays with their sorptive and protective characteristic were probably important in protecting proteins from biological and photochemical degradation as clay-protein complexes (Knicker et al., 1996; Zang et al., 2001). In addition, it is likely that amides were an integral part of the paraffinic network of refractory alkyl compounds (alkyl-amide; Knicker et al., 1996). Other chemical modifications such as those involving carbohydrates were probably important in the protecting proteinaceous material from degradation (Millard, 1917; Hedges, 1978; Kelleher et al., 2006). Refractory organic or

inorganic matrices are also known to protect intrinsically labile organic substances allowing them to persist much longer than their chemistries would suggest (Joyce et al., 1984).

3.3.10 Solution ^{31}P NMR analysis of microbial biomass

The Solution ^{31}P-NMR signals of P compounds (both organic and inorganic) of interest in environmental studies generally fall between 25 and –25 ppm (Cade-Menun, 2005). These include: phosphonates with a C-P bond, at 20 ppm; orthophosphate at 5–7 ppm; orthophosphate monoesters, with one C moiety per P, at 3–6 ppm; orthophosphate diesters (two C moieties per P), including phospholipids and deoxyribonucleic acid (DNA), at 2.0 to –1 ppm; pyrophosphate at –4 to –5 ppm; and polyphosphate at –20 ppm. Although rarely reported for environmental samples, a peak for the terminal P group in the polyphosphate chain should also be present at –4 to –5 ppm (Cade-Menun, 2005).

Figure 3.3.10.1 illustrates the solution ^{31}P NMR spectra of initial microbial biomass extracted with NaOH-EDTA, and reveals a high variability of types of P compounds present in the sample. It is clear that the spectrum was dominated by a strong narrow signal attributed to orthophosphate resonating near 5.9 ppm, Signals assigned to phosphonates (around 20 ppm) and orthophosphate diesters (two C moieties per P), including phospholipids and deoxyribonucleic acid (DNA), at 2.5 to –1 ppm were only detected in trace amounts. Resonances in the phosphonate region of the spectrum (20 ppm) may also be derived from cyclophosphate end groups in phosphodiester-containing bacterial polysaccharides (Egan et al., 1982). It is likely that the teichoic acids of *Bacillus subtilis* contain such end groups (Makarov et al., 2002). A weak signal corresponding to the positions of P atoms in inorganic polyphosphate chains (containing P-O-P bonds) was observed near –22 ppm. Other signals detected in the initial microbial biomass extract are: 1) orthophosphate monoesters, with one C moiety per P, at 3–6 ppm, 2) orthophosphate diesters (two C moieties per P), including phospholipids and deoxyribonucleic acid (DNA), at 2.5 to –1 ppm and 3) pyrophosphate, a specific inorganic polyphosphate with chain length n = 2 which produced a signal at –4 to –5 ppm. Signals from terminal P groups in the polyphosphate chain may also resonate in this region (Makarov et al., 2002; Cade-Menun, 2005).

The orthophosphate monoester, *myo*-inositol hexakisphosphate (phytic acid) is a relatively stable form of soil P and P atoms on the inositol ring may contribute significantly to the intensity of signals in the chemical shift region between 4 and 5 ppm (Turner et al., 2003b). Possible contributions from other orthophosphate monoesters resonating in this region, including sugar phosphates (glucose phosphates at 3.39 ppm and 5.36 ppm), mononucleotides (4.32 to 4.78 ppm) and the monoester breakdown products of phospholipids (choline phosphate at 4.05 ppm, ethanolphosphate at 4.71 ppm). It should be noted that possible artifacts (β-glycerophosphate and phosphatidic acid) resulting from the chemical breakdown of phosphatidyl choline in NaOH-EDTA, may contribute to the resonances in the chemical shift region attributed to monoesters (Turner et al., 2003a).

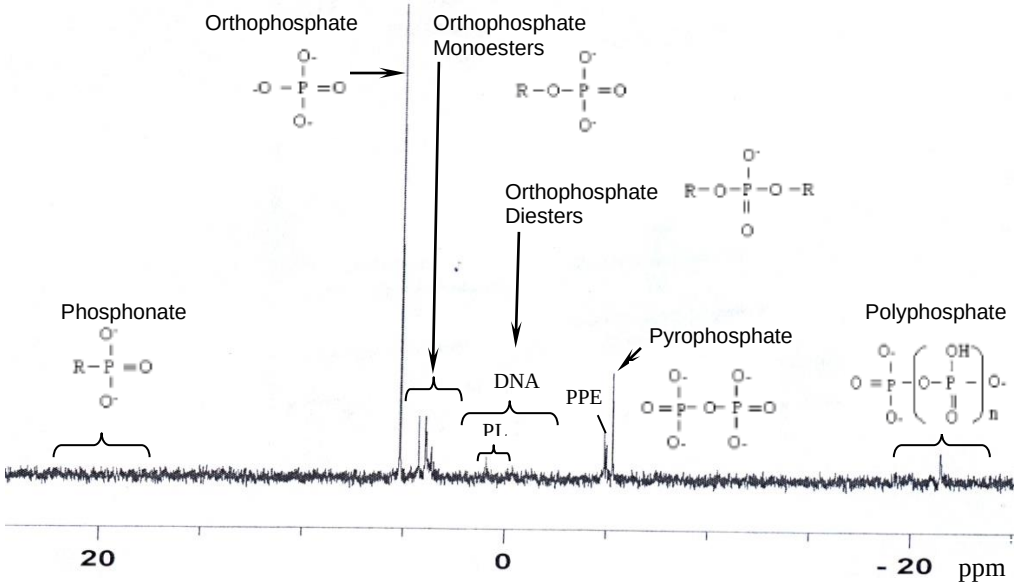

Figure 3.3.10.1: A solution ^{31}P-nuclear magnetic resonance (NMR) spectrum of a freeze-dried microbial biomass ('fresh') sample extracted with NaOH-EDTA. The spectrum illustrates the diversity of P species in microbial sample, including phosphonates, orthophosphates, orthophosphate monoesters, orthophosphate diesters such as phospholipids (PL) and deoxyribonucleic acid (DNA), pyrophosphate and polyphosphate, with the terminal P in the polyphosphate chain indicated by PPE.

Orthophosphate diesters are a heterogeneous group of P containing compounds, comprising of: 1) phospholipids, 2) teichoic acids which are known to accumulate in microbially active soils (Makarov et al., 2002) and 3) DNA which accumulates in soils with low microbial activity (Cade-Menun, 2005). Signals between 0 and 1 ppm were previously assigned to teichoic acids (e.g., Condron et al., 1990), which are present in the cell walls of gram-positive bacteria and some actinomycetes (Turner et al., 2003b).

However, teichoic acids were recently measured at 1.9 ppm in delippidized extracts of the gram-positive bacteria *Bacillus subtelis* (Makarov et al., 2002), suggesting that they do not contribute greatly to the observed signals in the orthophosphate diester region of the alkaline microbial extract. This is possible, because bacterial cell walls are assembled from P-free teichuronic acid units in P limited environments (Turner et al., 2003b). Further support comes from the fact that teichoic acids are the main constituents (>50%) of some bacterial cell walls (e.g., *B. subtilis* previously identified from our mixed cultures; ***Chapter 2***), and are soluble in acids as well as in alkali (Makarov et al., 2002). Therefore, the lack of a pronounced effect on the intensity of the resonances in the low field of the diester region associated with teichoic acids would strongly suggest they do not contribute significantly to the signals in the orthophosphate diester region of the sample.

The main signal from DNA was at –0.63 ppm, with a shoulder at approximately –0.40. While DNA was stable in NaOH-EDTA extracts, it would appear that RNA degraded almost immediately in the extracts. Although some DNA may have been degraded, it has been shown that a sample of degraded DNA containing polynucleotides gives similar signals to intact DNA, plus groups of poorly resolved peaks between 0 and 1 ppm (Turner et al., 2003b). Signals from organic polyphosphate may also contribute to the resonances in the regions of the spectrum assigned to inorganic polyphosphates. Signals from adenosine diphosphate (ADP) corresponding to β phosphates may resonate near –4.71 ppm, similarly, adenosine triphosphate (ATP) may have produced signals at –19.68 ppm corresponding to β phosphates (Turner et al., 2003b). Turner et al. (2003a) attributed weak signals from ADP in soil extracts to a large microbial biomass concentration.

The ^{31}P-NMR spectra of NaOH-EDTA extracts of microbial biomass degraded under ambient conditions and UV irradiation (6, 14 and 26 weeks) were dominanted by a peak resonating near 5.9 ppm (***Figure 3.3.10.2***). This peak can be attributed to inorganic orthophosphate (as PO^{3-}_4 in the alkaline solution; Turner et. al., 2003b). Two weak signals attributed to signals from monoesters and diesters were also observed between 3 and 5 ppm and 2 to –1 ppm, respectively after 6 weeks degradation. An additional band arising from pyrophosphate resonances was detected in depleted amounts for the samples degraded at 6 weeks under both conditions (***Figure 3.3.10.2***).

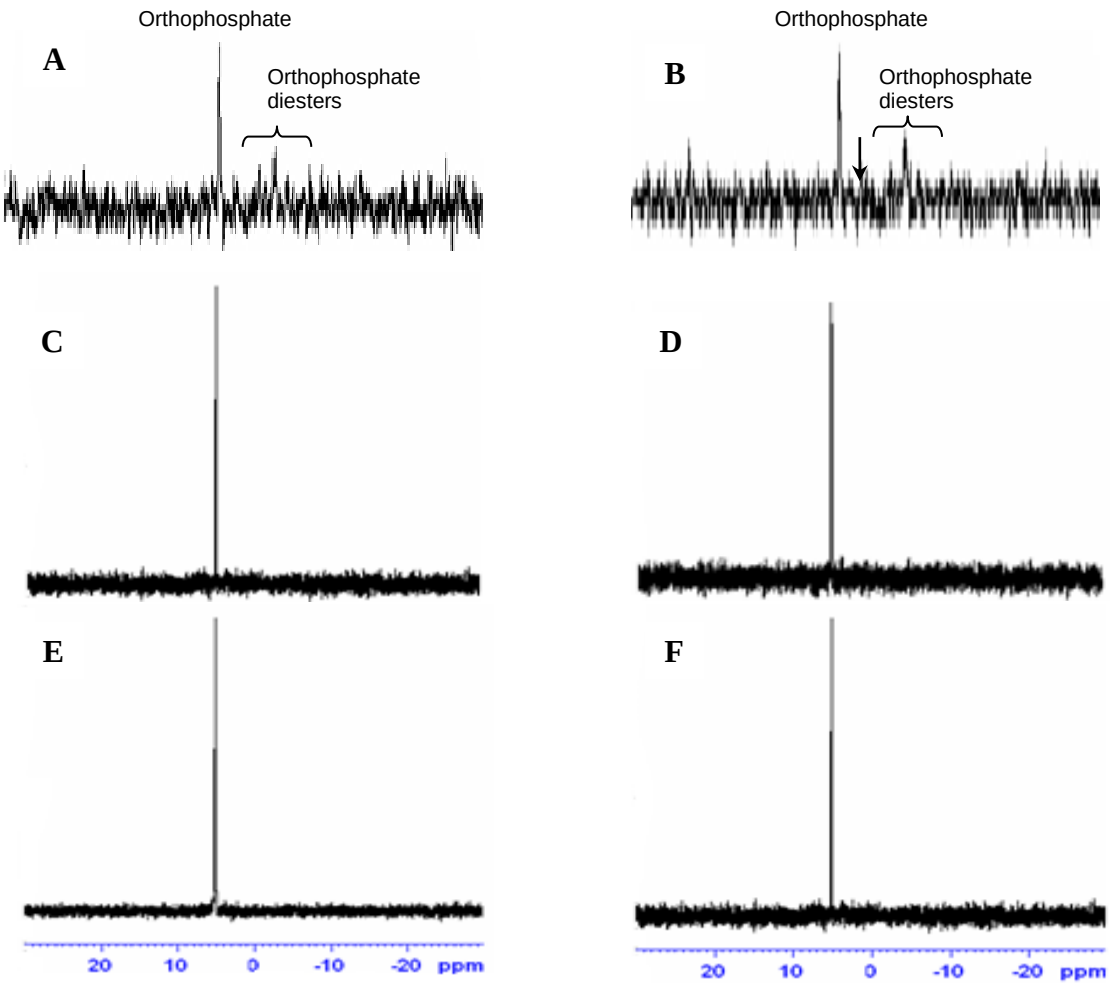

Figure 3.3.10.2: ^{31}P-NMR spectra of microbial biomass degraded under ambient conditions for A) 6 weeks; C) 14 weeks; and E) 26 weeks; and microbial biomass degraded under UV irradiation for B) 6 weeks; D) 14 weeks; and 26 weeks. The samples were extracted with NaOH-EDTA.

Differences were observed in the solution ^{31}P-NMR spectra of the initial and degraded microbial biomass. Except for the samples degraded at 6 weeks (***Figure 3.3.10.2A*** and ***B***) with relatively moderate signals, all spectra were dominated by a well resolved peak attributed to inorganic orthophosphate resonating near 5.9 ppm. This would suggest that these compounds ressisted both microbial and photodegradation for at least 6 weeks, and could be consistent with the observation of orthophosphate in humic substances (Guggenberger et al., 1996). After six weeks degradation, signals from phosphonates (~20 ppm), orthophosphate diesters (2.5 to –1 ppm), pyrophosphate (–4 to –5 ppm) and polyphosphate (–20 ppm) were not detected in the degraded samples. This would suggest that these P compounds are labile or water soluble and were possibly mineralized under biological and photolytic conditions. This hypothesis

is supported by the findings of Nziguheba and Bünemann (2005) who demonstrated the preferential mineralisation of phosphate diesters in tropical soils. Signals resonating from phospholipids (1 to –1 ppm) constituted one of the major diester components in the initial biomass (***Figure 3.3.10.1***). However, phospholipids are labile microbial-cell-wall components of living microorganisms, and are rapidly degraded by phospholipases soon after cell death (Glaser, 2005; Pelz et al., 2005). Therefore, it is not surprising that orthophosphate diesters were very much attenuated in the NaOH-EDTA extracts of the degraded microbial samples.

Further to the possible loss of P containing compounds from the microbial biomass as a result of degradation, it should be noted that bacterial organic P compounds degrade rapidly in alkaline solution (Turner et al., 2003b). This is also supported by the findings of Hinedi et al. (1988) who reported a decrease in orthophosphate diesters when sewage sludge was incubated with acid and alkaline soil. Although signals attributed to various organic P compounds were clearly observed in the alkaline extract of the initial biomass, this was probably due in part to the high natural abundances of these compounds resisting alkaline degradation. However, it is tempting to speculate that even if trace amounts of these compounds were present in the samples after degradation, it is most likely that they were rapidly lost to alkaline hydrolysis during sample preparation and acquisition.

It would appear that trace amounts of orthophosphate monoesters survived the conditions of degradation and alkaline hydrolysis after 26 weeks of dgeradation, suggesting some degree of selective preservation to these compounds. This is not surprising because recalcitrant soil P is known to contain orthophosphate monoesters dominated by inositol phosphates, explaining why they are the major functional class of organic P in most soils (Turner et al., 2002). In a study investigating P composition in temperate pasture soils, Turner et al. (2003a) also reported that orthophosphate monoesters were the major P fraction in all soils. However, the results presented here should be interpreted with caution as it is likely that the concentrations of orthophosphate monoesters can be overestimated in studies involving alkaline extraction. This is due mainly to the degradation of some orthophosphate diesters, specifically RNA and phosphatidyl choline, during extraction and acquisition (Makarov et al., 2002; Turner et al., 2003b). Orthophosphate diesters dominate organic P inputs to the soil from plants and microbes, but are rapidly degraded upon release and typically

represent only a small proportion of the soil organic P (Turner et al., 2003a). Furthermore, some orthophosphate diester compounds, for example phospholipids, including phosphatidyl serine and phosphatidyl choline usually observed at 1.56 ppm and 0.78 ppm, respectively are known to degrade rapidly in alkaline solution (Turner et al., 2003b). A combination of these factors may account for the loss of orthophosphate diester compounds over the degradation process. In contrast, Koukol et al. (2006) suggest that a loss of monoesters with simultaneous increases in diphosphates, polyphosphates and phosphonates in an alkaline extract of spruce needle litter was attributed to microbial decomposition of the litter.

The extent of the susceptibility of orthophosphate diesters to alkaline degradation varies among the different P compounds (Turner et al., 2003b). For example, Makarov et al. (2002) and Turner et al. (2003a) demonstrated that a considerable proportion of monoesters can be represented by mononucleotides derived from the complete alkaline hydrolysis of RNA within a few hours, so are unlikely to contribute significantly to the measured concentration of orthophosphate diesters. This represents the complete reverse of the stability of DNA-P. This would suggest that the signal close to 0 in the fresh biomass is most probably dominated by DNA-P. It is not known whether some part of RNA can be protected from alkaline hydrolysis being incorporated in biological structures (Makarov et al., 2002). It has been suggested that phosphatidyl choline has the fastest rate of degradation, for any phospholipid, under alkaline conditions, with almost complete conversion to orthophosphate monoesters within 24 h. Phosphatidyl choline appeared to degrade to glycerophosphate (4.81 ppm) and phosphatidic acid (5.15 ppm). Phosphatidyl serine degraded much slower (Brannon and Sommers, 1985 in Turner et al., 2003b). These findings may further explain the selective preservation of signals from orthophosphate monoesters relative to their diester counterparts, observed over the course of the degradation. Based on the lability of orthophosphate diesters, it is clear that these compounds are intimately linked with biological nutrient turnover in soils (Condron et al., 1990; Frossard et al., 2000).

The rapid degradation of some orthophosphate diesters in alkaline solution is an unavoidable limitation on the characterization of organic P compounds from soils, plants and microbes, because alkaline solutions are required to extract organic P (Turner et al., 2003b). Indeed, degradation of orthophosphate may have been significant in the current study. Strong acid extractions may be employed to extract large proportions of

organic P from some soils; however, these extracts are unusable for subsequent ^{31}P NMR spectroscopy without additional treatment. Therefore, the degradation of some organic P compounds must be accepted as an artifact of organic P analysis by current procedures (Turner et al., 2003b). Given the rapid nature of the degradation of RNA and phosphatidyl choline, it seems probable that most degradation will occur during extraction and lyophilization. Therefore, the possibilities to reduce this are limited, although the rehydration of freeze-dried extracts immediately before NMR analysis is advisable (Turner et al., 2003b).

In natural conditions, polyphosphate accumulation is highly important for the phosphorus cycle. Polyphosphates have many important functions in organisms; above all, they serve as a phosphorus source for biosynthesis of nucleic acids and phospholipids. Moreover, they can function as an energy source or buffer against pH stress (Koukol et al., 2006). The lack of polyphosphates in the alkaline extracts of the degraded samples, particularly those degraded under ambient conditions may be a result of complete utilization by microbes grazing on the biomass. We can only hypothesize that in each case, the harvesting of the samples coincided with the exponential growth phase of microbes decomposing the biomass, and this may explain the lack of polyphosphate signals in the NaOH extracts of the degrading sample. Similarly, Novák et al. (2005) detected a low amount of diphosphate and no polyphosphates in NaOH extracts of spruce needle intensively colonized by *Penicillium* cf *chrysogenum*. Katchmann and Fetty (1955) attributed the low polyphosphate content of yeast to their exponential growth phase. Koukol et al. (2006) also suggested that the absence of polyphosphate does not imply missing microbial activity.

Another form of phosphorus, the phosphonates (phosphonolipids), are of great interest, as their nature in soils in poorly understood. Phosphonates occur widely among biogenic and anthropogenic compounds in the form of phosphonolipids and as side groups on polysaccharides and glycoproteins (Sannigrahi et al., 2006). Phosphonates in soils are most probably produced by bacteria, fungi, amoeba and snails because they are all capable of producing 2-aminoethyl phosphonic acid (Koukol et al., 2006). However, phosphonates are reasonably labile to microbial degradation, restricting their detection to wet, cold or acidic soils where the activity of microbes capable of synthesizing phosphonatase enzymes and utilizing phosphonates is inhibited (Tate and Newman, 1982). Considering the relative natural abundance of phosphonates, its lability to

microbial degradation and alkaline hydrolysis, it is no surprise that phosphonates were not detected in the initial biomass the extracts of the degraded samples (Turner et al., 2003a). These findings seem conflicting with suggestions by other authors who suggest that the strong covalent C-P bonds in phosphonates make them resistant to chemical, thermal and photolytic degradation (Ternan et al., 1998), opening possibilities for further investigations.

Phosphorus-esters (in the initial and degraded biomass) and phosphonates (not detected) are the two organic functional groups identified. These functional groups are of particular importance as they play key roles in the coupled C and P geochemical cycles. Sannigrahi et al. (2006) demonstrated a strong association between P in DMO with carbohydrates and amino acids. The association of P with carbohydrates is not surprising given that they constitute a major fraction in C in DOM. P-esters are known to associate strongly with carbohydrates in a variety of biomolecules such as nucleic acids (DNA and RNA), nucleotides (e.g., ATP) and sugar phosphates. The association of P with amino acids may be in the form of phosphoamino acids (Sannigrahi et al., 2006). In bacteria, the amino acids histidine, aspartic acid and glutamic acid, are preferentially phosphorylated (Yan et al., 1998).

Phosphonates, the second organic-P functional group which we failed to identify is also known to associate strongly with carbohydrates and amino acids in the form of side groups on glycoproteins and polysaccharides (White and Metcalf, 2004). We hypothesized that these associations are most probably exhibited in soils containing quantifiable levels of carbohydrate C, amino acids, glycolproteins, phospholipids and lipopolysaccharides. Therefore, an understanding of the chemistry of these associations is fundamental to our understanding of C and P biogeochemical cycles. Another potentially significant association is the relationship between lipid-C and P content of microbial biomass. Probably the most important association of P with lipids is in the form of phospholipids. P-esters can also be associated with lipopolysaccharides, which are composed of amino sugars and fatty acids, and are components of the cell walls of Gram-negative bacteria (Sannigrahi et al., 2006).

Pyrophosphate and polyphosphate detected in soils are linked to soil microbial activity. However, unlike long-chain polyphosphates, which are readily degraded, pyrophosphate can be stabilised by adsorption in the soil and remain for many months.

Thus, in soils, it is highly likely that pyrophosphate concentrations probably reflect both microbial turnover and the potential for stabilisation in the soil (Turner et al., 2003a). It tempting to suggest, that although some compounds were detected in relatively small quantities, this does not preclude them from involvement in soil P turnover.

By investigating the degradation and transformation of major microbial components from a mixed culture (***Chapter 2***) of ^{13}C-labelled microbial biomass and microbial leachates in a model degradation study, we have gained critical insights into the fate of microbially derived OM in soil. The biochemically recalcitrant microbial fraction was enriched with alkyl-C structures and resist decomposition due to intrinsic structural properties, whereas other biochemical components (e.g. proteins and carbohydrates) appeared to have a higher turnover (at least in the top horizon). This would suggest that the biochemical recalcitrance of microbially derived aliphatic biomacromolecules may significantly enhance the sequestration and storage of atmospheric CO_2. Few studied reported higher contributions of alkyl-C to subsoil OM than to surface SOM (Baldock et al., 1997; Skjemstad et al., 2001). However, there is considerable evidence to suggest that this may not always be the case as microbially derived lipids have been shown to adsorb strongly to clays (***Chapters 4*** and ***5***), even as they leach through soil (***Sections 3.3.6-8***).

During decomposition of microbial biomass and microbial leachates, the loss of OM under ambient degradation may have resulted from a variety of processes. These include the mineralization of OM, microbial reworking of OM resulting in the utilization and transformation of various biomolecules, or simply as a source of energy. Although UV radiation was the dominant variable in the UV degraded biomass, the influence of biotic involvement cannot be unequivocally ruled out. Moreover, the loss of organic components observed in the degraded samples (relative to the starting material) could be a result of abiotic processes other than photodegradation, such as physical fragmentation or leaching. UV irradiation may exert influence on the decomposition process by two major mechanisms: (i) a biotic effect, manifested through changes in the community of decomposer organisms and their activity (Robson et al., 2004) and (ii) an abiotic effect caused by difference in the direct photodegradation (Pancotto et al., 2005) of the biomass and microbial leachates. It is most likely that direct photochemical mineralization was the main mechanism involved in the UV irradiated samples with a lesser contribution from indirect photodegradation resulting in changes in the lability of

organic compounds (Austin and Vivanco, 2006). Microbially derived OM was typically more degraded under UV conditions than ambient conditions, suggesting that photochemical transformation of biorefractory compounds into biologically oxidizable or volatile compounds had occurred. This phenomenon was previously demonstrated in marine DOM (Kieber et al., 1989; Mopper et al., 1991). These results demonstrate that photochemical degradation has an important role in the cycling of biologically refractory soil microbial components. This role is likely to become even more important in the future as depletion of the ozone increases the solar UV-B flux (Mopper et al., 1991).

The decomposition of major microbial components in the UV degraded biomass demonstrates that UV irradiation is likely to function as a stress on the soil surface community. This disagrees with the results obtained by Rinnan et al. (2005) who, through the use of chloroform fumigation and analysis of lipid biomarkers, found that differing levels of UV in arctic systems had no significant effect on microbial biomass carbon. Although the effects of UV radiation on soil microbial biomass is only effective to soil depths of approximately 2 mm (Jeffery et al., 2007, 2009), this effect is likely to be significant in arable soils considering that microbial biomass concentrations are greater in the uppermost surface layer (1 mm) compared to deeper layers. We further hypothesize that the effects of UV radiation on soil microbial biomass in arable soils is likely to be magnified by: i) anthropogenic perturbation such as tillage; ii) physical perturbation such as that caused by erosion; chemical perturbation caused by the application of farm chemicals; and iv) bioturbation through the actions of soil fauna (Jeffery et al., 2007).

3.4 Conclusions

We found that the major biochemical components of soil microbial biomass and microbial leachates were relatively stable under ambient and UV degradation, suggesting that a significant fraction of these biomolecules contribute to the stable SOM pool. We further conclude that the major biochemical components of soil microbial biomass are intrinsically stabilized; whereas, the biochemical components of microbial leachates are stabilized through a combination of chemical recalcitrance and physical protection provided by soil minerals and encapsulation in dissolved OM. The

biochemical signatures of the ambient and UV degraded samples did not vary significantly; however, greater losses of OM occurred under UV conditions and novel photoproducts were detected in the UV degraded leachates. This would suggest that UV degradation was more effective against the recalcitrant microbial fraction and is capable of producing new photoproducts during degradation and transformation of microbially derived OM.

According to our C integrals, approximately 51% of the initial biomass consisted of aliphatic-C (with a strong contribution from polymethylenic [$(CH_2)_n$] C structures), increasing relatively after 14 weeks decomposition. This was accompanied by a simultaneous decrease in the relative concentrations of proteins and carbohydrates, suggesting that these compounds were preferentially degraded. Conversely, carbohydrates were the dominant components in the microbial leachates and the polymethylenic-C structures observed in the degraded biomass were not detected in the leachates. Moreover, large amounts of proteins were detected in the leachates. These findings lead us to conclude that proteins and carbohydrates were preferentially leached form the microbial biomass due to their soluble nature and that polymethylenic-C structures were preferentially adsorbed to soil minerals during leaching.

In addition, solution ^{31}P NMR indicated that inorganic orthophosphate was the dominant form of phosphorus in the initial and degraded biomass and was the only form of phosphorus surviving beyond 6 weeks of the decomposition process. Trace amounts of organic P containing compounds (monoesters and diesters) were stabilized for up to 6 weeks of decomposition; however, these compounds were not detected as degradation progressed. We attributed these observations to a combination of degradation (microbial and UV) and the inherent shortfalls of the methods of extraction and data acquisition. However, it is evident that microbial biomass is an important source of the refractory OM pool.

3.5 References

Allard, B., Templier, J., and Largeau, C. 1997. Artifactual origin of mycobacterial bacteran. Formation of mela- noidin-like artifact macromolecular material during the usual isolation process. *Organic Geochemistry* 26, 691–703.

Aluwihare, L. I., Repeta, D. J., Pantoja, S., and Johnson C. G. 2005. Two chemically distinct pools of organic nitrogen accumulate in the ocean. *Science* 308, 1007–1010.

Austin, A. T., and Vivanco, L. 2006. Plant litter decomposition in a semi-arid ecosystem controlled by photodegradation. *Nature* 422, 555–558.

Baldock, J. A., Massiello, C. A., Gelinas, Y., and Hedges, J. L. 2004. Cycling and composition of organic matter in terrestrial and marine ecosystems. *Marine Chemistry* 92, 39–64.

Baldock, J. A., Oades, J. M., Nelson, P. N., Skene, T. M., Golchin, A., and Clarke, P. 1997. Assessing the extent of decomposition of natural organic materials using solid state ^{13}C NMR. *Australian Journal of Agricultural Research* 35, 1061–1083.

Baldock, J. A., Oades, J. M., Vassallo, A. M., and Wilson, M. A. 1990. Significance of microbial activity in soils as demonstrated by solid-state ^{13}C NMR. *Environmental Science and Technology* 24, 527–530.

Berg, B., and McClaugherty, C. 2003. *Plant litter, decomposition, humus formation, carbon sequestration*. Springer, Berlin.

Browman, M. G., and Tabatabai, M. A. 1978. Phosphodiesterase activity of soils. *Soil Science Society of Ameriaca Journal* 42, 284–290.

Bünemann, E. K., Marschner, P., Smernik, R. J., Conyers, M., and McNeill, A. M. 2008. Soil organic phosphorus and microbial community composition as affected by 26 years of different management strategies. *Biology and Fertilty of Soils* 44, 717–726.

Cade-Menun, B. J. 2005. Characterizing phosphorus in environmental and agricultural samples by ^{31}P nuclear magnetic resonance spectroscopy. *Talanta* 66, 359–371.

Cade-Menun, B. J., Liu, C. W., Nunlist, R., and McColl, J. G. 2002. Soil and litter phosphorus-31 nuclear magnetic resonance spectroscopy: extractants, metals, and phosphorus relaxation times. *Journal of Environmental Quality* 31, 457–465.

Condron, L. M., Frossard, E., Tiessen, H., Newman, R. H., and Stewart, J. W. B. 1990. Chemical nature of organic phosphorus in cultivated and uncultivated soils under different environmental conditions. *European Journal of Soil Science* 41, 41–50.

Derenne, S., Largeau, C., and Taulelle, F. 1993. Occurrence of non-hydrolysable amides in the macromolecular constituent of *Scenedesmus quadricauda* cell wall as revealed by

^{15}N NMR: origin of N-alkylnitriles in pyrolysates of ultralaminae-containing kerogens. *Geochimica et Cosmochimica Acta* 57, 851–857.

Derenne, S., Le Berre, F., Largeau, C., Hatcher, P. G., Connan, J., and Raynaud, J. F. 1992. Formation of ultralaminae in marine kerogens via selective of thin resistant outer walls of microalgae. *Organic Goechemistry* 19, 345–350.

Deshmukh, A. P., Simpson, A. J., and Hatcher, P. G. 2003. Evidence of cross-linking in tomato cutin using HR-MAS NMR spectroscopy. *Phytochemistry* 64, 1163–1170.

Dijkstra, P., Ishizu, A., Doucett, R., Hart, S. C., Schwartz, E., Menyailo, O. V., and Hungate, B. A. 2006. ^{13}C and ^{15}N natural abundance of soil microbial biomass. *Soil Biology & Biochemistry* 38, 3257–3266.

Egan, W., Schneerson, R., Werner, K. E., and Zon, G. 1982. Structural studies and chemistry of bacterial capsular polysaccharides. Investigations of phosphodiester-linked capsular polysaccharides isolated from *Haemophilus influenzae* types a, b, c, and f: NMR spectroscopic identification and chemical modification of end groups and the nature of basecatalyzed hydrolytic depolymerization. *Journal of the American Chemical Society* 104, 2898–2910.

Ernst, R. R. Bodenhausen, G., and Wokaun, A. 1987. *Principles of nuclear magnetic resonance in one and two dimensions*. Clarendon Press, Oxford.

Frossard, E., Condron, L. M., Oberson, A., Sinaj, S., and Fardeau, J. C. 2000. Processes governing phosphorus availability in temperate soils. *Journal of Environmental Quality* 29, 15–23.

Gelin, F., Boogers, A. A. M., Sinninghe Damasté , J. S., Hatcher, P. G. and de Leeuw, J. 1996. Novel, resistant microalgal polyethers: an important sink of organic carbon in the marine environment? *Geochimica et Cosmochimica Acta* 60, 1275–1280.

Glaser, B. 2005. Compound-specific stable-isotope (δ^{13}C) analysis in soil science. *Journal of Plant Nutrition and Soil Science* 168, 633–648.

Goni, M. A., and Hedges, J. I. 1990. The diagenetic behaviour of cutin aids in buried conifer needles and sediments from a coastal marine environment. *Geochimica et Cosmochimica Acta Acta* 54, 3083–3093.

Grundy, A. S., Strickland, M. S., Lauber, C. L., Bradford, M. A., and Fierer, N. 2009. The influence of microbial communities, management, and soil texture on soil organic matter chemistry. *Geoderma* 150, 278–286.

Guggenberger, G., and Zech, W. 1994. Composition and dynamics of carbohydrates and lignin-degradation products in two coniferous forests. N.E. Bavaria, Germany. *Soil Biology & Biochemistry* 26, 19–27.

Guggenberger, G., Haumaire, L., Thomas, R. J., and Zech, W. 1996. Assessing the organic phosphorus status of an Oxisol under tropical pastures following initial savanna using ^{31}P NMR spectroscopy. *Biology and Fertility of Soils* 23, 332–339.

Hedges, J. I. 1978. The formation and clay mineral reactions of melanoidins. *Geochimica et Cosmochimica Acta* 42, 69–76.

Hedges, J. I., Baldock, J. A., Gélinas, Y., Lee, C., Peterson, M., and Wakeham, S. G. 2001. Evidence of non-selective preservation of organic matter in sinking marine particles. *Nature* 409, 801–804.

Hinedi, Z. R., Chang, A. C., and Lee, R. W. K. 1988. Mineralization of phosphorus in sludge-amended soils monitored by phosphorus-31-nuclear magnetic resonance spectroscopy. *Soil Science Society of America Journal* 52, 153–1596.

Jeffery, S., Harris, J. A., Rickson, R. J., and Ritz, K. 2007. Microbial community phenotypic profiles changed markedly with depth within the first centimetre of the arable soil surface. *Soil Biology & Biochemistry* 39, 1226–1229.

Jeffery, S., Harris, J. A., Rickson, R. J., and Ritz, K. 2009. The spatial quality of light influences the temporal development of microbial phenotype at the arable soil surface. *Soil Biology & Biochemistry* 41, 553–560.

Johnson, D., Campbell, C. D., Lee, J. A., Callaghan, T. V., and Gwynn-Jones, D. 2002. Arctic microorganisms respond more to elevated UV-B radiation than CO_2. *Nature* 416, 82–83.

Joyce, G. F., Visser, G. M., van Boeckel, C. A. A., van Boom, J. H., Orgel, L. E., and van Westrenen, J. 1984. Chiral selection in poly(C)-directed synthesis of oligo(G). *Nature* 310, 602–604.

Kaal, J., Nierop, K. G. J., and Verstraten, J. M. 2005. Retention of tannic acid and condensed tannin by Fe-oxide-coated quartz sand. *Journal of Colloid and Interface Science* 287, 72–79.

Kaiser, K., Guggenberger, G., Haumaier, L., and Zech, W. 2001. Seasonal variation in the chemical composition of dissolved organic matter in organic forest floor layer leachates of old-growth Scots pine (*Pinus sylvestris* L.) and European beech (*Fagus sylvatica* L.) stands in northeastern Bavaria, Germany. *Biochemistry* 55, 103–143.

Karl, J., Nieman, C., Holz, R. C., and Sims, R. C. 2007. ^{13}C NMR analysis of biologically produced pyrene residues by *Mycobacterium* sp. KMS in the presence of humic acid. *Environmental Science and Technology* 41, 242–249.

Katchmann, B. W., and Fetty, W. O. 1955. Phosphorus metabolism in growing cultures of *Saccharomyces cerevisiae*. *Journal of Bacteriology* 69, 607–615.

Kelleher, B. P., and Simpson, A. J. 2006. Humic substances in soils: are they really chemically distinct? *Environmental Science and Technology* 40, 4605–4611.

Kelleher, B. P., Simpson, A. J., Rogers, R. E., Dearman, J., and Kingery, W. L. 2007. Effects of organic matter from sediments on the growth of marine gas hydrates. *Marine Chemistry* 103, 237–249.

Kelleher, B. P., Simpson, M. J., and Simpson, A. J. 2006. Assessing the fate and transformation of plant residues in the terrestrial environment using HR-MAS NMR spectroscopy. *Geochimica et Cosmochimica Acta* 70, 4080–4094.

Kieber, D. J., McDaniel, J., and Mopper, K. 1989. Photochemical source of biological substrates in sea water: implications for carbon cycling. *Nature* 341, 637–639.

Kindler, R., Miltner, A., Thullner, M., Richnow, H.-H., and Kästner, M. 2009. Fate of bacterial biomass derived fatty acids in soil and their contribution to soil organic matter. *Organic Geochemistry* 40, 29–37.

Knicker, H. 2000. Solid-state 2-D double cross polarization magic angle spinning ^{15}N ^{13}C NMR spectroscopy on degraded algal residues. *Organic Geochemistry* 31, 337–340.

Knicker, H., and Hatcher, P. G. 1997. Survival of protein in an organic-rich sediment. Possible protection by encapsulation in organic matter. *Naturwissenschaften* 84, 231–234.

Knicker, H., Scaroni, A. W., and Hatcher, P. G. 1996. ^{13}C and ^{15}N NMR spectroscopic investigation on the formation of fossil algal residues. *Organic Geochemistry* 24, 661–669.

Köbel-Knabner, I. 2000. Analytical approaches for characterizing soil organic matter. *Organic Geochemistry* 31, 609–625.

Kögel-Knabner, I. 1997. ^{13}C and ^{15}N NMR spectroscopy as a tool in soil organic matter studies. *Geoderma* 80, 243–270.

Kögel-Knabner, I. 2002. The molecular organic composition of plant and microbial residues as inputs in soil organic matter. *Soil Biology & Biochemistry* 34, 139–162.

Kögel-Knabner, I. 2006. Chemical structure of organic N and organic P in soil. In: Nannipieri, P., and Smalla, K. (Eds), *Nucleic acids and proteins in soil*. Springer-Verlag Berlin Heidelberg, pp. 23–48.

Koukol, O., Novák, F., Hrabal, R., and Vosátka, M. 2006. Saprotrophic fungi transform organic phosphorus from spruce needle litter. *Soil Biology & Biochemistry* 38, 3372–3379.

Kovac, N., Faganeli, J., Sket, B., and Bajt, O. 1998. Characterization of macroaggregates and photodegradatoin of their water soluble fraction. *Organic Geochemistry* 29, 1623–1634.

Lair, G. J., Zehetner, F., Khan, Z. H., and Gerzabek, M. H. 2009. Phosphorus sorption-desorption in alluvial soils of a young weathering sequence at the Danube River. *Geoderma* 149, 39–44.

Lam, B., Baer, A., and Alaee, M. 2007. Major structural components in freshwater dissolved organic matter. *Environmental Science and Technology* 41, 8240–8247.

Largeau, C., Derenne, S., Casadevall, E., Kadouri, A., and Sellier, N. 1986. Pyrolysis of immature torbanite and of the resistant bio-polymer (Prb a) isolated from extant alga Botryococcus-Braunii-mechanism of formation and structure of torbanite. *Organic Geochemistry* 10, 1023–1032.

Lundberg, P., Ekbald, A., and Nilsson, M. 2001. ^{13}C NMR spectroscopy studies of forest soil microbial activity: glucose uptake and fatty acid biosynthesis. *Soil Biology & Biochemistry* 33, 621–632.

Makarov, M. I., Haumaier, L., and Zech, W. 2002. Nature of soil organic phosphorus: an assessment of peak assignments in the diester region of ^{31}P NMR spectra. *Soil Biology & Biochemistry* 34, 1467–1477.

Mayer, C., Moritz, R., Kirschner, C., Borchard, W., Maibbaum, R., Wingender, J., and Flemming, H.-C. 1999. The role of intermolecular interactions: studies on model systems for bacterial biofilms. *International Journal of Biological Macromolecules* 26, 3–16.

Millard, L. C. 1917. General reaction between amino acids and sugars: the biological consequences. *CR Soc Biology* 72, 599–601.

Mopper, K., Zhou, X., Kieber, R. J., Kieber, D. I., Sikorski, R. J., and Jones, R. D. 1991. Photochemical degradation of dissolved organic carbon and its impact on oceanic carbon cycle. *Nature* 353, 60–62.

Nagata, T., and Kirchman, D. L. 1997. Roles of submicron particles and colloids in microbial food webs and biogeochemical cycles within marine environments. In: Jones, T. (Ed.), *Advances in microbial ecology*. Plenum, New York, pp. 81–103.

Nguyen, R. T., and Harvey, H. R. 2003. Preservation via macromolecular associations during *Botryococcus braunii* decay: proteins in the Pula Kerogen. *Organic Geochemistry* 34, 1391–1403.

Novák, F., Hrabal, R., Koukol, O., and Bartošová, I., Kalčík, J. 2005. Transformation of organic phosphorus during Picea abies needle litter decomposition. In: Zaujec, A.,

Bielek, P., Gonet, S.S., Debska, B., Cieslewicz, J. (Eds.), *Humic substances in ecosystems 6*, Proceedings of the Sixth International Conference, Račkova Dolina, June 19–22, pp. 122–125.

Nziguheba, G., and Bünemann, E. K. 2005. Organic phosphorus dynamics in tropical agroecosystems. In: Turner, B. L., Frossard, E., and Baldwin, D. (Eds), *Organic phosphorus in the environment*. CABI, Wallingford, UK, pp 243-268.

Pancotto, V. A., Sala, O. E., and Cabello, M. 2003. Solar UV-B decreases decomposition in herbaceous plant litter in Tierra del Fuego, Argentina: potential role of an altered decomposer community. *Global Change Biology* 9, 1465–1474.

Pancotto, V. A., Sala, O. E., Robson, M., Caldwell, M. M., and Scopel, A. L. 2005. Direct and indirect effects of solar ultraviolet-B radiation on long-term decomposition. *Global Change Biology* 11, 1982–1989.

Pelz, O., Abraham, W. R., Saurer, M., Siegwolf, R., and Zeyer, J. 2005. Microbial assimilation of plant-derived carbon in soil traced by isotope analysis. *Biology and Fertility of Soils* 41, 153–162.

Quinn, J. P., Kulakova, A, N., Cooley, N, A., and McGrath, J. W. 2007. New ways to break an old bond: the bacterial carbon-phosphorus hydrolases and their role in the biogeochemical phosphorus cycling. *Environmental Microbiology* 9, 2392–2400.

Ragueneau, O., Tréguer, P., and Leynaert, A. 2000. A review of the Si cycle in the modern ocean: recent progress and missing gaps in the application of biogenic opal as a paleoproductivity proxy. *Global and Planetary Change* 26, 317–365.

Rhead, M. M., Eglinton, G., and Draffan, G. H. 1971. Conversion of oleic acid to saturated fatty acids in seven estuary sediments. *Nature* 232, 327–330.

Rillig, M. C., Caldwell, B. A., Wösten, H. A. B., and Sollins, P. 2007. Role of proteins in soil carbon and nitrogen storage: controls of persistence. *Biogeochemistry* 85, 25–44.

Rinnan, R., Keinanen, M. M., Kasurinen, A., Askikainen, J., Kekki, T. K., Holopainen, T., Ro-Poulson, H. M. T. N., and Michelsen, A. 2005. Ambient ultraviolet radiation in the artic reduces root biomass and alters microbial microbial community composition but has no effects on microbial biomass. *Global Change Biology* 11, 564–574.

Robson, T. M., Pancotto, V. A., Ballaré, C. L. 2004. Reduction of solar UV-B mediates changes in the Sphagnum capitulum microenvironment and the peatland microfungal community. *Oecologia* 140, 480–490.

Rontani, J.-F., Zabeti, N., and Wakeham, S. G. 2009. The fate of marine lipids: biotic vs. abiotic degradation of particulate sterols and alkenones in the Northwestern Mediterranean Sea. *Marine Chemistry* 113, 9–18.

Sannigrahi, P., Ingall, E. D., and Benner, R. 2006. Nature and dynamics of phosphorus-containing components of marine dissolved and particulate organic matter. *Geochimica et Cosmochimica Acta* 70, 5868–5882.

Simpson, A. J. 2002. Determining the molecular weight, aggregation structures, and interactions of natural organic matter using diffusion ordered spectroscopy. *Magnetic Resonance in Chemistry* 40, S72–S82.

Simpson, A. J., Simpson, M. J., Kingery, W. L., Lefebvre, B. A., Moser, A., Williams, A. J., Kvasha, M., and Kelleher, B. P. 2006. The application of ^{1}H high-resolution magic-sngle spinning NMR for the study of clay-rrganic associations in natural and synthetic complexes. *Langmuir* 22, 4498–4503.

Simpson, A. J., Simpson, M. J., Smith, E., and Kelleher, B. P. 2007a. Microbially derived inputs to soil organic matter: are current estimates too low. *Environmental Science and Technology* 41, 8070–8076.

Simpson, A. J., Song, G., Smith, E., Lam, B., Novotny, E. H., and Hayes, M. H. B. 2007b. Unraveling the structural components of soil humin by use of solution-state nuclear magnetic resonance spectroscopy. *Environmental Science and Technology* 41, 876–883.

Simpson, A. J., Zang, X., Kramer, R., and Hatcher, P. G. 2003. New insights on the structure of algaenan from *Botryoccocus braunii* race A and its hexane insoluble botryals based on multidimensional NMR spectroscopy and electrspray-mass spectrometry techniques. *Phytochemistry* 62, 783–796.

Skjemstad, J. O., Dalal, R. C., Janik, L. J., and McGowan, J. A. 2001. Changes in chemical nature of soil organic carbon in Vertisols under wheat in southeastern Queensland. *Australian Journal of Soil Research* 39, 343–359.

Solomon, D., Lehmann, J., Thies, J., Schäfer, T., Liang, B., Kinyangi, J., Neves, E., Petersen, J., Luizão, F., and Skjemstad, J. 2007. Molecular signature and sources of biochemical recalcitrance of organic C in Amazonian Dark Earths. *Geochimica et Cosmochimica Acta* 71, 2285–2298.

Sommer, M., Kaczorek, D., Kuzyakov, Y., and Breuer, J. 2006. Silicon pools and fluxes in soils and landscape-a review. *Journal of Plant Nutrition and Soil Science* 169, 310–329.

Stevenson, F. 1994. *Humus chemistry, genesis, composition, reaction*. Wiley & Sons, New York.

Tate, K. R., and Newman, R. H. 1982. Phosphorus fractions of a climosequence of soils in a New Zealand tussock grassland. *Soil Biology & Biochemistry* 14, 191–196.

Ternan, N. G., McGrath, J. W., McMullan, G., and Quinn, J. P. 1998. Organophosphonates: occurrence, synthesis and biodegradation by microorganisms. *World Journal of Microbiology and Biotechnology* 14, 635–647.

Tréguer, P., Nelson, D. M., and Van Bennekom, A. J. 1995. The silica balance in the world ocean: a reestimate. *Science* 268, 375–379.

Trumbore, S. E., Bonani, G., and Wolfli, W. 1990. The rates of carbon cycling in several soils from AMS ^{14}C measurements of fractionated soil organic matter. In: Bouwman, A.F. (Ed.), *Soils and the greenhouse effect*. John Wiley, New York, NY, pp. 405–414.

Turner, B. L., Mahieu, N., and Condron, L. M. 2003a. The phosphorus composition of temperate pasture soils determined by NaOH-EDTA extraction and solution state ^{31}P NMR spectroscopy. *Organic Geochemistry* 34, 1199–1210.

Turner, B. L., Mahieu, N., and Condron, L. M. 2003b. Phosphorus-31 nuclear magnetic resonance spectral assignments of phosphorus compounds in soil NaOH-EDTA extracts. *Soil Science Society of America Journal* 67, 497–510.

Turner, B. L., Paphazy, M. J., Haygarth, P. M., and McKelvie, I. A. 2002. Inositol phosphates in the environment. *Phylosophical Transactions of the Royal Society of London B* 357, 449–469.

Van Breemen, N., and Buurman, P. 2002. *Soil formation*. Kluwer Academic Publishers.

Wershaw, R. L., Llaguno, E. C., and Leenheer, J. A. 1996. Mechanism of formation of humus coatings on mineral surfaces 3. Composition of adsorbed organic acids from compost leachate on alumina by solid-state ^{13}C NMR. *Colloide and Surfaces A: Physicochemical and Engineering Aspects* 108, 213–223.

White, A. K., and Metcalf, W. W. 2004. Two C-P Lyase operons in *Pseudomonas stutzeri* and the oxidation of phosphonates, phosphate and hypophosphite. *Journal of Bacteriology* 186, 4730–4739.

Wu, D., Chen, A., and Johnson Jr., C. S. 1995. An improved diffusion-ordered spectroscopy experiment incorporating bipolar-gradient pulses. *Journal of Magnetic Resonance, Series A* 115, 260–264.

Wyndham, R. C. 1986. Evolved aniline catabolism in *Acinatobacter calcoaceticus* during continuous culture of river water. *Applied and Environmental Microbiology* 51, 781–789.

Yamashita, Y., and Tanoue, E. 2004. Chemical characteristics of amino acid-containing dissolved organic matter in seawater. *Organic Geochemistry* 35, 679–692.

Yan, J. X., Packer, N. H., Gooley, A. A., and William, K. L. 1998. Protein phosphorylation: technologies for the identification if phosphoamino acids. *Journal of Chromatography A* 80, 23–41.

Yoshimura, K., Ogawa, T., and Hama, T. 2009. Degradation and dissolution properties of photosynthetically-produced phytoplankton lipid materials in early diagenesis. *Marine Chemistry* 114, 11–18.

Zang, X., Nguyen, R. T., Harvey, H. R., Knicker, H., and Hatcher, P. G. 2001. Preservation of proteinaceous material during the degradation of green alga *Botryococcus braunii*: a solid-state 2D ^{15}N ^{13}C NMR spectroscopy study. *Geochimica et Cosmochimica Acta* 65, 3299–3305.

Chapter 4

Clay-organo Interactions

Clay-organo interactions

4.1 Introduction

The sorption of OM to clay minerals is an important process in the natural environment (Feng et al., 2005), with significant geochemical implications (Hedges and Keil, 1999). This association stabilizes soil organic carbon in the global C cycle (Ladd et al., 1985; Spain, 1990) and influences transport and bioavailability of nutrients and contaminants in soils and waters (Hedges and Keil, 1999). It is therefore widely assumed that the inhibiting effect of soil minerals on decomposition can strongly influence the turnover of SOM and soil respiration rates (Hsieh, 1996; Parfitt et al., 1997). Several studies have provided insights into the relationship between OM and mineral surfaces (Sollins et al., 1996; Kothawala et al., 2008); however, the precise mode or combination of mechanisms for organic matter sorption is still uncertain (Simpson et al., 2006). In order to improve our knowledge of soil and sediment biogeochemistry and environmental reactivity, it is therefore necessary to understand the fundamental interactions and mechanisms of stabilization and preservation of organic compounds through physical protection from biodegradation or selective preservation (Simpson et al., 2006).

Given the lack of molecular-level understanding of the mechanisms associated with the sorption and stabilization of OM by clay minerals, a study was undertaken to address this knowledge gap and expand the current understanding of clay-organo complexes. In this study, the interactions of microbes and microbial proteins with montmorillonite and kaolinite clay minerals were investigated. Here, scanning electron microscopy (SEM), elemental X-ray analysis of SEM images, X-ray diffraction patterns and advanced NMR approaches were employed to obtain molecular-level information about clay-microbial complexes, clay-protein complexes and acid hydrolyzed residues of clay-microbial complexes. Montmorillonite and kaolinite clay minerals were selected for use as representatives of clays because they are ubiquitous in nature and have been well characterized. Furthermore, montmorillonite and kaolinite have very different characteristics and together will provide a more ‘soil-like’ representation of organo-mineral associations (Wattel-Koekkoek et al., 2001). Acid hydrolysis was used to provide very harsh conditions to further determine the nature of the association between

microbial biomass and clay surfaces. This work helps to elucidate which organic species bind preferentially to clay mineral surfaces and assesses if these are any different from other complexes, it also provides critical insights about the physical protection of microbially derived OM (the same could be true for plant derived OM) by clay minerals.

4.2 Materials and Methods

4.2.1 Microbial propagation and bacterial growth on clay

Microbes were cultured from a light clay-loam Oakpark soil (***Chapter 2***) according to a modified version of the protocol described by Wyndham (1986). The medium was a minimal medium and contained: 100 ml of 10 mM phosphate buffer (7.5 mM $K_2HPO_4 \cdot 3H_2O$; 2.5 mM $NaH_2PO_4 \cdot H_2O$) pH 7.0; 10 ml of 1x ammonium/magnesium solution [2.5 mM $(NH_4)_2SO_4$; 1.0 mM $MgSO_4 \cdot 7H_2O$]; and 1 ml of 1x trace element solution (32.2 µM $EDTANa_2 \cdot H_2O$; 50 µM NaOH; 1.4 µM $ZnSO_4 \cdot 7H_2O$; 2.4 µM $MnSO_4 \cdot 4H_2O$; 0.4 µM $CuSO_4 \cdot 5H_20$; 10.8 µM $FeSO_4 \cdot 7H_2O$; 36.6 µM Na_2SO_4; 0.4 µM $NaMoO_4 \cdot 2H_2O$) pH 7.0. Each component was prepared separately and the pH adjusted before being combined to obtain the respective final concentrations. The medium was supplemented with 5 mg yeast extract (Sigma) and sterilized. Alternatively, duplicate cultures were amended with montmorillonite or kaolinite clay mineral (1 mg mL^{-1}) and incubated for a further two weeks at RT. The resulting complexes were harvested and washed with a large excess of distilled water by centrifugation at 6000 rpm for 30 min (see ***Section 4.2.4*** for further details of clay-organo complexes). The complex was then freeze-dried and stored at -20°C for further analysis.

4.2.2 Protein extraction

Soluble proteins were extracted from microbial biomass (~4.1 x 10^{10} cells) according to a modified version of the methods described by Ogunseitan (1993) and Singleton et al. (2003). Microbial biomass (5 ml culture A_{600} = 1.5-3.0) was harvested as previously described and the pellet washed in 1 ml of cold 50 mM Tris-HCl, pH 7.4, and suspended in 500 µl of a solution containing 50 mM Tris-HCl (pH 7.5), 10% sucrose, 1 mM dithiothreitol. The suspensions were gently mixed and 500 µl of a solution containing Lysozyme (600 µg mL^{-1}), 4 mM EDTA, and 0.2% polyoxyethelene

20 cetyl ether (Brij-58) was added and the suspensions incubated on ice for 1 h with gentle mixing every 15 min. The lid of each sample was pierced with a dissection needle before the suspensions were subjected to four freeze-thaw cycles from a dry-ice acetone bath to 37°C for efficient cell lysis. The lysates were centrifuged at 18,000 xg for 30 min at 4°C and the supernatants recovered from the cell debris and other particulates for protein determination and clay-protein interactions.

Prior to conducting any further analysis, the extracted proteins were purified using acetone precipitation. The mixture of proteins was precipitated by adding four volumes of cold 80% (v/v) acetone to the sample and incubation on dry ice for 3 h. The sample was then centrifuged at 14,000 x g at 4ºC for 10 min and the supernatant carefully removed. The pellet was washed twice with cold acetone (100%), and allowed to air dry. The sample was resuspended in equal volume of molecular grade water (Sigma) at 4ºC overnight.

4.2.3 Determination of protein concentration

The concentration of extracted proteins was evaluated using the Bradford Dye protein determination reagent according to the manufacturer's protocol (Sigma). Reaction mixtures (triplicates) were prepared to a final volume of 3.1 ml and contained 100 µl of each protein extract and 3.0 ml of the Bradford reagent. The reaction were gently mixed using a vortex and allowed to incubate at RT for between 5 and 45 min. The light absorbance of the protein extract-dye complex was determined with a UV-Visible spectrophotometer at 595 nm (Cary 50 Scan UV-Visible Spectrophotometer, Varian). The concentration of proteins in the extracts was determined by interpolating the absorbance readings at 595 nm against a standard curve generated with bovine serum albumin (Sigma). All samples (including the standard proteins) were duplicated.

4.2.4 Sorption experiments

Sorption was carried out on montmorillonite (SWy-2) and kaolinite (KGa-1) clay minerals using previously published methods (Koskella and Stotzky, 1997; Fu et. al., 2007) with the below modifications. The minerals used in this study were obtained from the Clay Mineral Society (CMS) Repository Source. Stock suspensions of the < 2 µm-particle-size of montmorillonite was prepared in deionized water or 10 mM Tris-HCl buffer (pH 7.0) at a concentration of 5 mg ml^{-1}. A 1:10 dilution (0.5 mg mineral ml^{-l}) was prepared using quantified microbes or microbial proteins suspended in Tris-

HCL buffer (pH 7.0). Sterile 50 ml polyethylene containing 10 ml aliquots of the reaction mixture were incubated on an end-over-end shaker at 200 rpm and 25±1°C for 3 h (Stuart® Roller Mixer SRT1, UK), and centrifuged at 16,000 xg for 15 min. The equilibrium adsorption (initial concentration – equilibrium supernatant) was determined as the number of cells and/or milligram of protein per gram of mineral. Control experiments were performed with minerals in the absence of microbes or microbial proteins. The clay-organo complexes were washed with deionized water and centrifugation, until protein detection in the supernatant was negligible (Three washes). The total amount of microbes or protein recovered in the equilibrium supernatant and in all washes was subtracted from the amount initially added to determine the amount of protein bound. There was negligible adsorption of microbial proteins to the walls of the polyethylene tubes as determined by the controlled assays. Samples were done in duplicates. In this study, the content of the bacterial protein was used to represent the titre of bacteria cells.

4.2.5 Direct microscopy and elemental analysis

The nature of microbial and microbial proteins association with montmorillonite clay mineral was determined using an Hitachi S-3000N VP scanning electron microscope equipped with an energy dispersive X-ray spectrometer (EDS). Scans were carried out at an accelerated voltage of 15-20 kV. The elemental content of pure clay minerals and clay mineral complexes, expressed as intensity of the characteristic radiation for an atom, was monitored by EDS equipped with a Sapphire Si(Li) detector.

4.2.6 X-ray diffraction analysis

Powdered X-ray diffraction analysis of un-reacted clays and montmorillonite-organo complexes was performed on a Bruker AXS D8 Advanced diffractometer with collimated nickel-filtered Cu-K_α radiation (0.1543 nm), at 40 kV and 40 mA. A DEFRAC Evaluation Data Collector software package was employed to capture and process raw data. A Bruker EVA Graphics and Identification software package was used for qualitative identification of the minerals form the patterns obtained by scanning at a scan speed of 1°2θ/min and increments of 0.02([°2θ]; Ekosse, 2005).

4.2.7 Acid hydrolysis

Acid hydrolysis was performed on clay-organo complexes using previously published procedures (Otto and Simpson, 2007) modified as described below. Briefly,

complexes (<0.1 g) were hydrolyzed under reflux with 5 ml of 12 M HCl at 105ºC for 8 h. After cooling, the hydrolysates were vacuum filtered through glass fibre filters (Whatman GF/A) and the residues collected and air dried for NMR analysis.

4.2.8 High resolution magic angle spinning (HR-MAS) NMR

Thoroughly dried samples (~20 mg) were placed in a 4 mm Zirconium Oxide Rotor and 60 µl of DMSO-d_6 or D_2O was added as a swelling solvent in a dry atmosphere. It is essential to dry the samples thoroughly and use only ampules of DMSO-d_6 or D_2O to prevent a large water peak often centred at ~3.3 ppm that can obscure many of the real microbial signals. After homogenization of the sample using a stainless steel mixing rod, the rotor was doubly sealed using a Kel-F sealing ring and a Kel-F rotor cap. ^{1}H HR-MS NMR spectra were acquired using a Bruker 500 MHz Avance spectrometer fitted with a 4-mm triply tuned ^{1}H-^{13}C-^{15}N HR-MS probe fitted with an actively shielded Z gradient at a spinning speed of 10 kHz. ^{1}H NMR was acquired while simultaneously decoupling both ^{13}C ^{15}N nuclei. Scans (256) were acquired with a 2 s delay between pulses, a sweep width of 20 ppm and 8 K time domain points. ^{1}H Diffusion Gated Experiments were used with a bipolar pulse longitudinal encode-decode sequence (Wu et al., 1995). Scans (1024) were collected using 1.25 ms, 333 mT m^{-1} sine shaped gradient pulse, a diffusion time of 30 ms, 8192 domain time domain points and a sample temperature of 298 K. In essence the ‘‘gate’’ was optimized at the strongest diffusion filtering possible while minimizing signal loss through relaxation. As a result the more rigid components dominate the transform spectrum while mobile components are essentially gated.

4.3 Results and Discussion

4.3.1 Equilibrium adsorption

Montmorillonite adsorbed greater quantities of soil microbes and soil microbial proteins when compared with kaolinite (***Table 4.3.1.1***) indicating that it has a greated equilibrium adsorption for microbes and microbial proteins when compared with kaolinite. This difference in the equilibrium adsorption of both minerals is most likely due to the 2:1 expanding capacity of montmorillonite (Lee et al., 2003), its high CEC (0.8-1.2mol_c kg^{-1}), high specific surface area and high absorbance potential for bio-organics (Lünsdorf et al., 2000). Franchi et al. (1999) have demonstrated that a higher

amount of exchangeable cations on the mineral surface can favour the adsorption process of a polyanion (such as proteins) to a clay surface.

Table 4.3.1.1: Equilibrium adsorption of montmorillonite and kaolinite clay minerals complexed with soil microbes and soil microbial proteins.

Clay mineral	Equilibrium adsorption	
	Microbial biomass (cells g^{-1})	Microbial protein (mg g^{-1})
Montmorillonite	$3.70 \times 10^{10} \pm 1.0^{8}$	919±1
Kaolinite	$3.33 \times 10^{10} \pm 5.0^{7}$	726.5±1.5

4.3.2 Scanning electron microscopy and elemental analysis

The scanning electron micrograph of pure montmorillonite revealed a petal-like structure which is known to be the main microstructural feature characterizing smectite clay minerals (***Figure 4.3.2.1A***; Rhouta et al., 2006). In contrast, the scanning electron micrograph of kaolinite revealed a book-type structure, in which coherent plates are separated by cleavage planes in the views along the *b* or *a* axes (***Figure 4.3.2.1C***; Shoval et al., 2002). However, the microstructural features of the mineral were obscured in the resulting clay-complexes (***Figure 4.3.2.1B*** and ***D***).

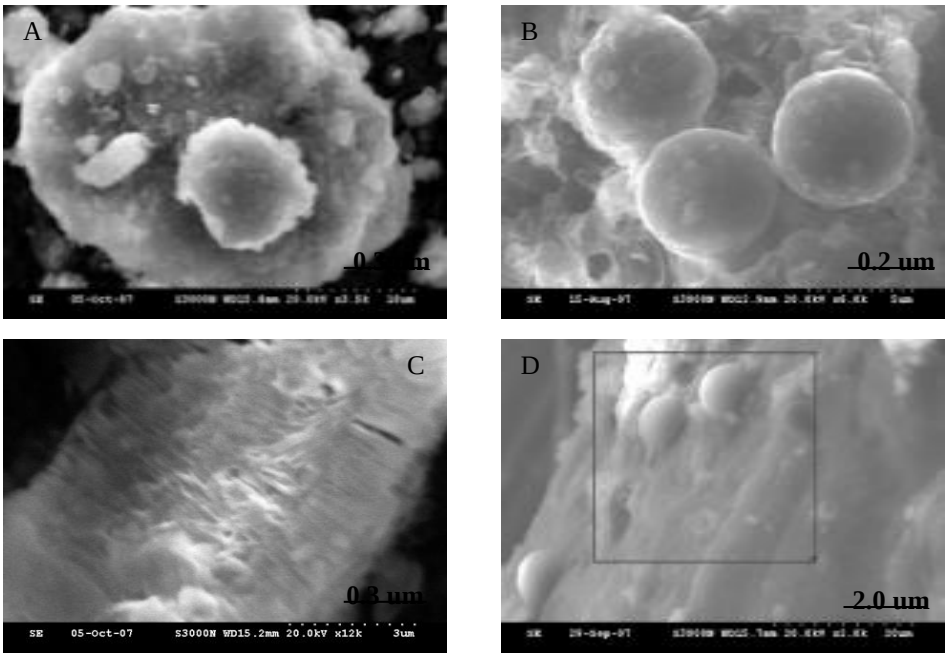

Figure 4.3.2.1: Scanning electron micrographs of A) pure montmorillonite, B) montmorillonite-microbial complex, C) pure kaolinite and D) kaolinite-microbial complex.

The interactions of cocci and rod-shaped microbes a few µm in size, with the planar surfaces of the mineral is evident (***Figure 4.3.2.1B*** and ***D***). Microbial attachment

occurred as single and multi cells, and in some cases appeared to be encased in an extracellular exudate. Furthermore, cells were distributed randomly and densely over the clay surfaces, suggesting that adsorption and binding sites for the cells were probably distributed over the clay surfaces (Chaerun et al., 2005). Scanning electron micrographs also revealed that organic materials were not evenly distributed on clay surfaces, and in some cases not in direct contact with the mineral surfaces. Similar trends of SOM accumulations on mineral surfaces have been previously reported (Mayer and Xing, 2001).

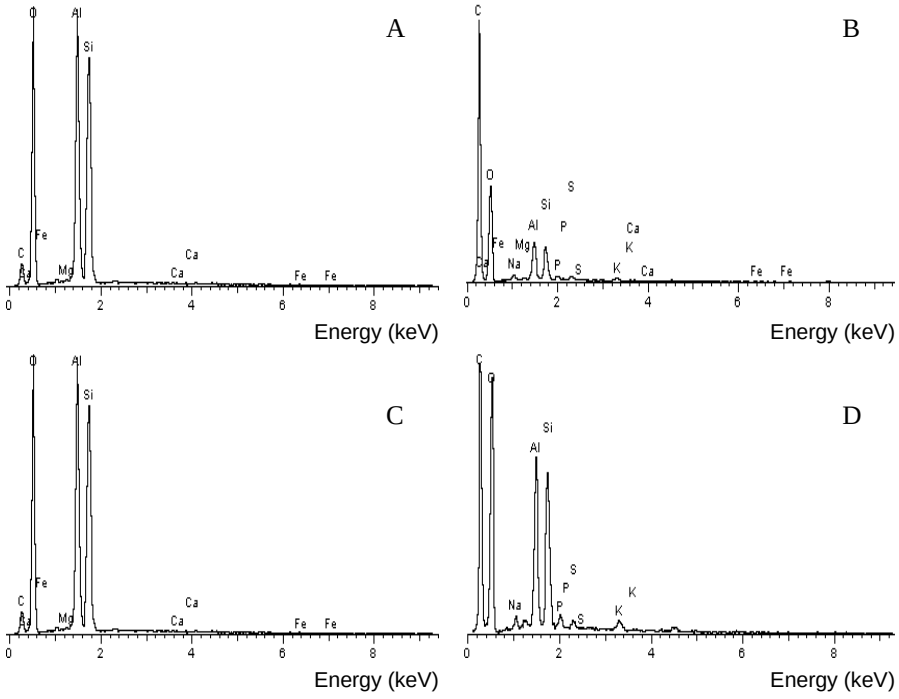

Figure 4.3.2.2: EDS spectra of A) pure montmorillonite, B) montmorillonite-microbial complex, C) pure kaolinite and D) kaolinite-microbial complex.

Elemental X-ray analysis of pure montmorillonite and kaolinite showed large quantities of O, Al and Si, small amounts of C, and traces of Mg, Ca and Fe (***Figure 4.3.2.2A*** and ***C***). However, clay-organo complexes showed significant increases in the relative concentration of C and a reduction in the amounts of O, Al and Si (***Figure 4.3.2.2B*** and ***D***). The relative increase in the C content and reductions in the O, Al and Si contents of clay complexes suggest the presence of an abundance of organic C most likely derived from microbal cells, microbial exudates and proteins inundating the clay surfaces (Tazaki, 2005). Trace amounts of P and S were also observed in montmorillonite and kaolinite complexes. The source of the P observed may be derived

from bacterial cell wall phosphates, capsular lipids containing polysaccharides, phosphate esters and/or nucleic acids, while S was probably derived from S containing amino acids, cysteine, homocysteine and methionine present in protein/peptide (Tazaki, 2005). Except for relatively higher abundances of elemental O, Al and Si in the EDS spectrum of kaolinite clay-complexe (***Figure 4.3.2.2D***) suggesting that kaolinite adsorbed fewer microbial cells than montmorillonite, no significant differences were observed between the EDS spectra of the clay-complexes (***Figure 4.3.2.2***). This interpretation is consistent with the results presented in ***Table 4.3.1.1***.

4.3.3 X-ray diffraction analysis

To clarify whether the silicate layers of montmorillonite and kaolinite were intercalated in the microbial and protein complexes, powdered XRD analysis was performed on the pure and organo-clay complexes. ***Figure 4.3.3.1*** illustrates the diffraction patterns of pure montmorillonite, the montmorillonite-microbial complex and the montmorillonite-protein complex. Pure montmorillonite showed a characteristic sharp narrow peak at $2\theta = 6.72^{o}$ with a d-spacing of 13.3 Å (***Figure 4.3.3.1A***). Clay-complexes resulting from microbes grown on montmorillonite and microbes sorbed to montmorillonite each showed a strong sharp peak at $2\theta = 5.8^{o}$, which is a basal reflection $d_{(001)}$ value of 15.5 Å (***Figure 4.3.3.1C*** and ***D***). A strong sharp peak at $2\theta = 5.7^{o}$, corresponding to a basal reflection $d_{(001)}$ value of 15.6 Å is shown for the montmorillonite-protein complex (***Figure 4.3.3.1B***). This represents an increase in the basal reflection $d_{(001)}$ values of 2.2 and 2.3 Å, respectively when compared with pure montmorillonite. The increases in the $d_{(001)}$ crystal lattice X-ray spacings of montmorillonite-organic complexes suggest the intercalation of the interlamellar region of montmorillonite. The slightly broader and more irregular peaks of montmorillonite-complexes provide complementatry evidence of the intercalation of the inner regions of montmorillonite (Chaerun et al., 2005).

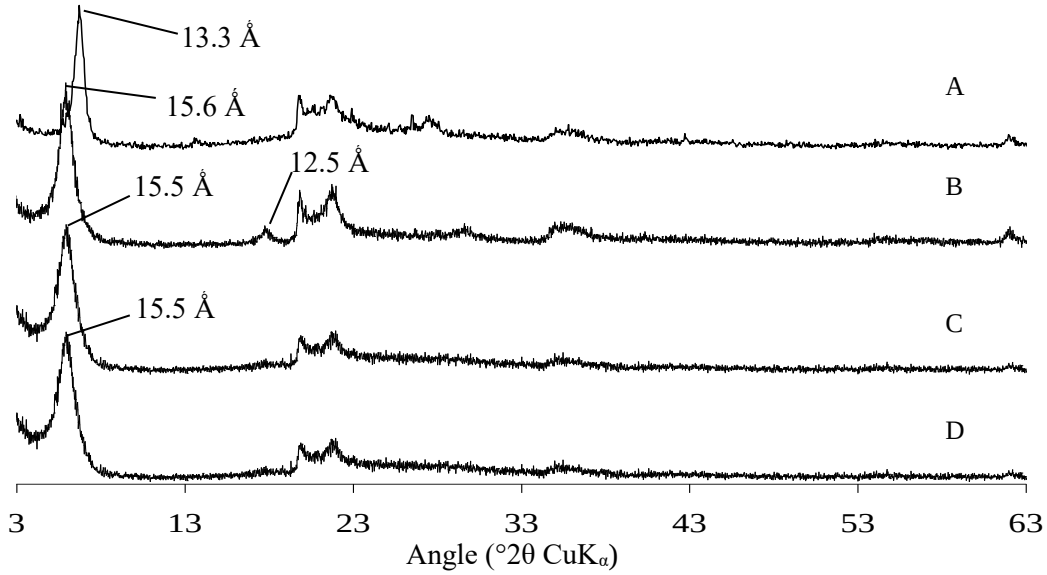

Figure 4.3.3.1: Powdered X-ray diffraction patterns of (A) pure montmorillonite, (B) microbial proteins sorbed to montmorillonite, (C) microbes sorbed to montmorillonite and (D) microbes grown on montmorillonite.

The $d_{(001)}$ crystal lattice increases of montmorillonite suggest that intact microbes or microbial proteins did not intercalate when the average minimum size of bacterial cells and microbial proteins are taken into account (Angioi et al., 2005). Intercalation of the interlamellar region of montmorillonite by intact cells and polymeric protein molecules is likely to be limited by steric hindrances and electrostatic repulsions between the negative charges of the clay surface and polyanionic nature of bacterial cell walls and proteins (Franchi et al., 1999). We hypothesize that extracellular polymeric substances (EPS) produced by bacteria and used to anchor cells to clay surfaces may be responsible for the interlayer expansion observed for montmorillonite-microbial complexes (Chaerun et al., 2005). Microbially secreted EPS frequently carry a negative charge due to the presence of uronic acids that adsorb strongly to negatively charged clay surfaces through polyvalent cation bridging (Chenu, 1995). The relatively small increases in the $d_{(001)}$ basal reflection of the intercalated montmorillonite may be accounted for by two possible mechanisms: i) either intercalated organic materials migrated during thermal treatment (to remove interlamellar water), to the external surfaces of the mineral, or ii) they migrate to the inner vacant sites of the octahedral layer of the mineral. However, the latter mechanism was not observed as there was no increase in the d_{060} reflection (one sixth of the *b* unit cell parameter) of the 2:1 aluminosilicate complexes (Bakandritsos et al., 2006).

Further evidence of the intercalation of montmorillonite was provided by a noticeable diffraction peak positioned at 2θ = 17.0º (12.5 Å) for all montmorillonite complexes (***Figure 4.3.3.1***; Yu et al., 2000). It should also be noted that microbes and proteins were exposed to a range of physico-chemical conditions that may have influenced changes to their initial structures. These changes could be in the form of cellular fragments or monomeric units of proteins and other biomolecules and may also account for the relatively small increases in the $d_{(001)}$ crystal lattice of montmorillonite-complexes. Powdered X-ray diffractograms of unreacted kaolinite, kaolinite-microbial and -protein complexes collected at 2θ range 5-65º showed a strong sharp narrow peak at 2θ = 12.2º, which is a basal reflection d_{001} of 7.1 Å (***Figure 4.3.3.2***). This suggests that microbes and microbial proteins did not penetrate kaolinite, indicating that sequestration occurred primarily on external surfaces. This is as expected as kaolinite is a non-expanding mineral (Franchi et al., 1999).

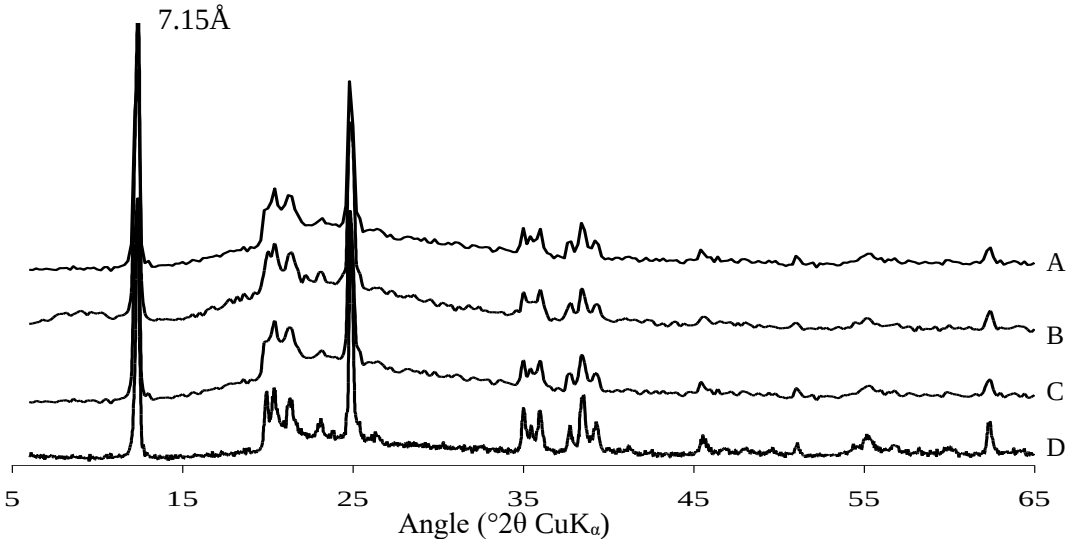

Figure 4.3.3.2: Powdered X-ray diffraction patterns of (A) pure kaolinite, (B) microbial proteins sorbed to kaolinite, (C) microbes sorbed to kaolinite and (D) microbes grown on kaolinite.

4.3.4 NMR analysis of clay-organo complexes

Several studies have investigated the sorption of soluble OM to mineral surfaces (Vermeer and Koopal, 1998; Vermeer et al., 1998). However, these reports have focused on quantitative descriptors, such as thermodynamic values and isotherm shape, to yield empirical relationships from which mechanistic information is extrapolated. Here, we apply an advanced NMR approach that employs high-resolution magic-angle spinning (HR-MAS) to provide direct evidence as to which "soil-like" organic

structures preferentially associate with clay mineral surfaces. HR-MAS NMR spectroscopy allows for the analysis of semisolid and swellable materials with resolution close to that afforded by true solution-state NMR (Simpson et al., 2006). In HR-MAS NMR, deuterated solvents are used to swell the sample. Dipolar interactions that are predominant in solid materials are decreased by the addition of solvent and are averaged by MAS, allowing solution-state experiments to be carried out on samples that are not fully soluble. In this study, HR-MAS NMR was applied to study microbes and microbial proteins sorbed to montmorillonite clay mineral. In addition to HR-MAS NMR, solution-state NMR techniques were applied in tandem to identify the organic species that are not associated with the clay surface (data not shown).

Figure 4.3.4.1 displays the ^{1}H HR-MAS NMR spectra of microbes and montmorillonite-microbial complexes dissolved in D_2O. The spectral regions have been assigned and confirmed using a range of multidimensional HR-MAS NMR experiments (data not shown) and data from published literature (Simpson et al., 2006). General peak designations can be defined as; amide signals in peptides and aromatic amino acid residues (regions 1 and 2) consistent with the presence of intact proteinaceous material, 3) protons associated with double bonds and esters, possibly form lipids or phospholipids 4) predominantly signals from carbohydrates, 5) signals from various substituted methylenes and methenes β to a functionality in hydrocarbons, signals from some amino acid side chains will also resonate here and 6) protons in aliphatic species. More specific assignments include i) signals from various substituted methylenes, and methines β to a functionality in a hydrocarbon, as would be the case for a lipoprotein and lipid, and ii) peptidoglycan.

The ^{1}H HR-MAS NMR spectrum of un-reacted microbes is dominated by aliphatic structures (***Figure 4.3.4.1A***), increasing relatively in the clay-microbial complexes (***Figure 4.3.4.1A***). This would suggest that aliphatic groups (especially long-chained polymethylene [$(CH_2)n$] structures; ~1.29 ppm) preferentially sorbed to montmorillonite surfaces in the presence of carbohydrates and proteins (Feng et al., 2005, 2006). This was further emphasized by the presence of aliphatic species (region 6) which retained its relative dominance in the diffusion edited NMR spectra of clay-complexes, indicating that they are preserved in the rigid domains (***Figure 4.3.4.2***). In the free form, protons β to the carbonyl in ester groups resonate at ~2.2 ppm and are well defined (***Figure 4.3.4.1A***); however, in the complexes, they are slightly perturbed

and less defined (***Figure 4.3.4.1B*** and ***C***), providing complementary evidence that aliphatic moieties are preferentially sorbed (Simpson et al., 2006). Reported adsorption of aliphatic components to mineral surfaces have been consistent and have been characterized by the highly aliphatic nature of OM associated with clay fraction in soils (Schnitzer et al., 1988; Ulrich et al., 1988; Wershaw et. al., 1996a,b). Simpson et al. (2006) concurred that aliphatic species in organic mixtures preferentially bind to clay surfaces in the presence of simple carbohydrates and amino acids.

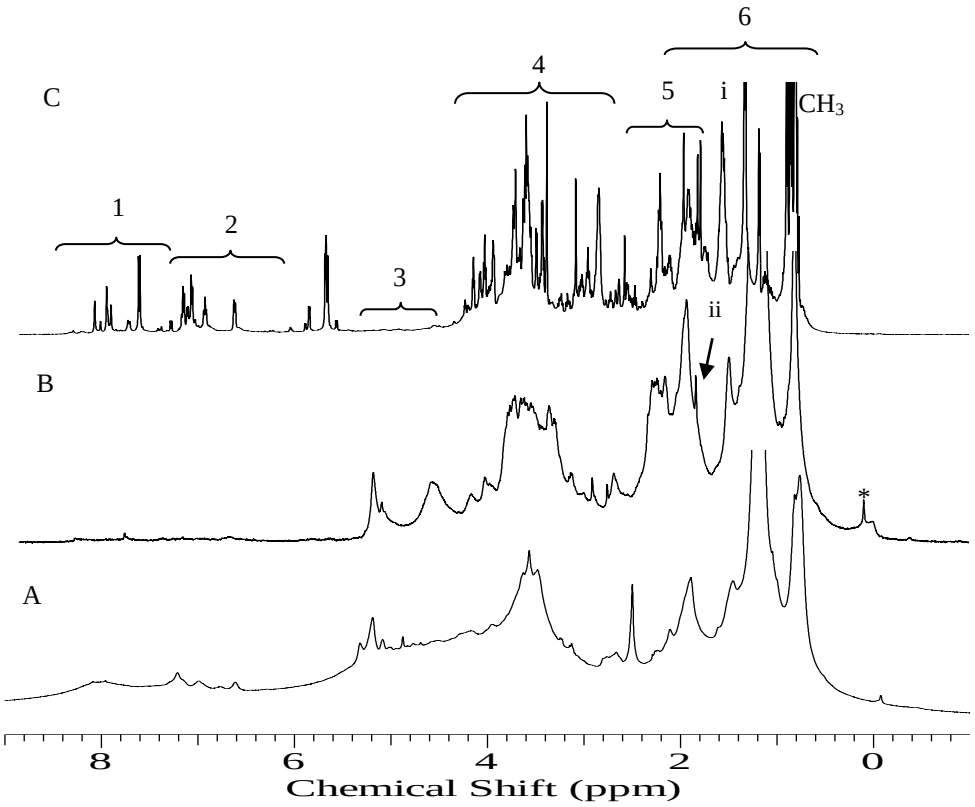

Figure 4.3.4.1: ^{1}H HR-MAS NMR spectra of (A) microbes dissolved in D_2O; B) microbes grown on montmorillonite dissolved in D_2O; and (C) microbes sorbed to montmorillonite dissolved in D_2O. Numbers and brackets represent general assignments as follows: (1) amides signals in peptides; (2) signals from aromatic rings including aromatic residues, some amide signals in peptides may also resonate in this area; (3) protons on α carbon in peptides; (4) protons in carbohydrates, protons α to an ester, ether, and hydroxyl in aliphatic chains will also resonate in this region; (5) signals from various substituted methylenes and methenes β to a functionality in hydrocarbons, signals from some amino acid side chains will also resonate here; and (6) aliphatic protons. More specific assignments include i), CH_2, main chain methylene in lipids; (ii) peptidoglycan. *Resonance from TMS.

Hydrophobic interactions between the $RCOO^-$ groups of aliphatic-C with Al ions in montmorillonite, at least initially, appears to be the primary mechanism involved in the formation of clay-organo complexes (Skjemstad, 1992; Parfitt et al., 1997, 1999; Simpson et al., 2006). This mechanism is favoured since most aliphatic components in

soil extracts contain polar functionalities, it is likely that these groups are responsible for initiating the surface interaction, probably through cation binding (Skipper et al., 1989). Subsequently, hydrophobic interactions may become more pronounced as the remainder of the molecule replaces water from the clay surface, producing a hydrophobic clay surface to which the tail can efficiently associate. Moreover, if clay microbial associations had resulted from the interactions of polar groups (OH, C=O, etc.) alone, then sugars and proteinaceous materials would have a stronger preference for montmorillonite surfaces (Simpson et al., 2006).

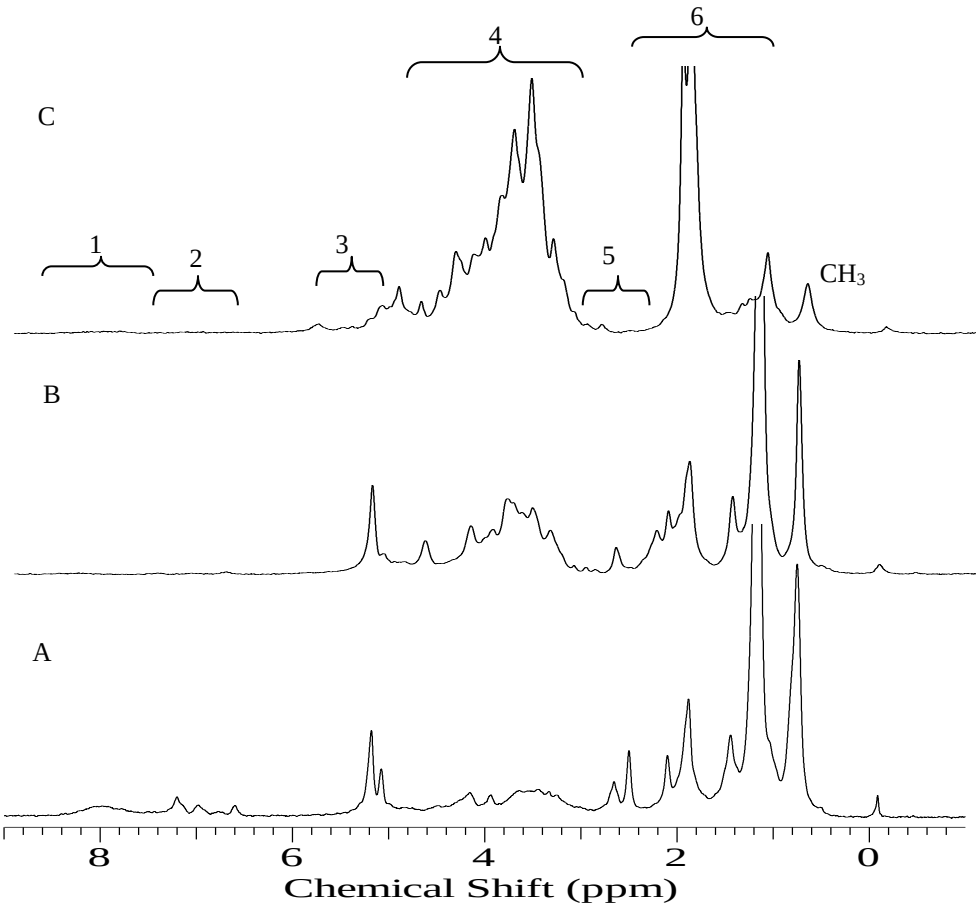

Figure 4.3.4.2: Diffusion NMR spectra of (A) microbes dissolved in D_2O; (B) microbes grown on montmorillonite dissolved in D_2O; and (C) microbes sorbed to montmorillonite dissolved in D_2O. Numbers and brackets represent general assignments as follows: (1) amides signals in peptides; (2) signals from aromatic rings including aromatic residues, some amide signals in peptides may also resonate in this area; (3) protons on α carbon in peptides; (4) protons in carbohydrates, protons α to an ester, ether, and hydroxyl in aliphatic chains will also resonate in this region; (5) signals from various substituted methylenes and methenes β to a functionality in hydrocarbons, signals from some amino acid side chains will also resonate here; and (6) aliphatic protons.

Although hydrophobic interactions may be a major sorption mechanism, no single sorption can adequately explain the formation of clay-organo complexes. The

formation of particularly strong organo-mineral associations could be favoured by polar organic functional groups of amphiphiles interacting via ligand exchange (Kleber et al., 2007) with singly coordinated mineral hydroxyls, forming stable complexes (Wershaw et al., 1996b). Spectral evidence of the relative abundance of aliphatic species adsorbed to montmorillonite is consistent with multilayer sorption of fatty acids, hydrogen bonding between the carboxylic groups of free fatty acids and by van der Waals attraction between the hydrocarbon chains (Ulrich et al., 1988; Kindler et al., 2009).

The ^{1}H HR-MAS NMR spectra of the clay-microbial complexes indicate a contribution from carbohydrates (***Figure 4.3.4.1A*** and ***B, region 4***). While not as significant as that of aliphatic acids, it is clear that carbohydrates also sorbed strongly onto montmorillonite. Similarly, these compounds were not removed during diffusion editing (***Figure 4.3.4.2 A*** and ***B***) indicating the involvement and significance of large polymeric carbohydrate components in the adsorption process. Wattel-Koekkoek et al. (2001) reported that kaolinite-associated SOM was rich in polysaccharide products. It should also be noted that the relative concentration of carbohydrates is higher in complexes of microbes sorbed to clay than in complexes of microbes grown on clay. This may be due in part to the difference in the amounts of microbially produced EPS during microbial propagation on montmorillonite and sorption of microbes to montmorillonite. Typical constituents of EPS are polysaccharides and proteins, often accompanied by nucleic acid and lipids (Mayer et al., 1999). It is likely that the main interaction between montmorillonite and carbohydrates is a result of hydrogen bonding mainly active between hydroxyl groups (Mayer et al., 1999).

Proteins also played a key role in the formation and structure of organo-mineral complexes. This may be due in part to their ability to associate irreversibly to mineral surfaces (Soil Survey Staff, 1999; Kleber et al., 2007). A number of aromatic signals (most likely form the aromatic amino acids; region 2) and signals from amide-N in peptide/protein (region 1) of comparable intensities were observed in the ^{1}H HR-MAS NMR spectrum of microbes sorbed to clay (***Figure 4.3.4.1***). Complementary evidence of the role of protein/peptide in the association is provided by peptidic CH_3 resonances in the ^{1}H HR-MAS NMR spectra (***Figure 4.3.4.1***) and diffusion edited NMR spectra (***Figure 4.3.4.2***) of clay-microbial complexes. Taken together, this would suggest that proteins/peptides exhibit a strong association with montmorillonite surfaces, and is consistent with the findings of similar studies (Wattel-Koekkoek et al., 2001; Feng et

al., 2005, 2006). Other studies also suggest that aromatic (Ulrich et al., 1988) and peptidic compounds are preferentially adsorbed to clays, with strength of bonding varying over several orders of magnitude depending on the protein (Hedges and Hare, 1987; Hedges and Oades, 1997; Rillig et al., 2007). Note, other signals previously identified in the conventional ^{1}H NMR spectra (see annotation for ***Figure 4.3.4.1***) are attenuated.

Given the diversity of functional groups making up proteins, it is difficult to discern the processes that dominated adsorption of proteins to montmorillonite. However, it can be argued here that several proposed mechanisms including electrostatic interactions, ligand exchange and physisorption (Rillig et al., 2007) may be involved. Furthermore, it has been demonstrated that conformational changes in proteins increase their adhesive strength through a combination of hydrophobic interactions and electrostatic binding (Kleber et al., 2007). Considering the ^{1}H HR-MAS NMR evidence, it is apparent that large amounts of proteinaceous material were adsorbed to montmorillonite. This observation is consistent with the concept of 'zonal effect', which argues that the sorption of proteins creates a basal layer to prime the adsorption of other amphiphilic molecular fragments more strongly than they would to clean clay surfaces, creating a N-rich zone near the mineral surfaces (Sollins et al., 2006). In addition, we surmise that a similar but complementary concept, 'support preconditioning', played a significant role in the adsorption of microbial proteins to montmorillonite surfaces. This concept explains that the adsorption of proteins to a mineral may increase the number of adsorption sites (polar function groups) on the newly coated surface. This effect is also considered a routine step preceding the adhesion of microorganisms to mineral surfaces (Bakker et al., 2004). Therefore, on the basis of the ^{1}H HR-MAS NMR data, it is our interpretation that 'zonal effect' and 'support preconditioning' were the major mechanisms involved in the adsorption of proteins to montmorillonite surfaces.

Peptidoglycan (previously observed in ***Chapter 3***), a bacterial cell wall biomarker was also observed in the proton NMR of the clay-microbial complexes (***Figure 4.3.4.1***), suggesting that it was strongly sorbed to the clay surfaces. These findings are consistent with those of Simpson et al. (2007) who attributed the detection of peptidoglycan in clay-rich humin fractions to the strong association of microbes with clay components in soils. Peptidoglycan comprises up to 90% by weight of gram-

positive bacteria and is a key structural component in all microbial cell walls (Simpson et al., 2007). Structurally, it comprises roughly equal amounts of amino sugars strands with peptide bridges (Hedges et al., 2001). Although it is not possible to accurately quantify contributions of each component in peptidoglycan due to spectral overlap, it has been determined that the peptide contribution of peptidoglycan in humin was relatively small (Simpson et al., 2007). Therefore, while it is likely that the spectral contribution of peptidoglycan to carbohydrates and proteins was minimal, it is our interpretation that peptidoglycan played a more important role in the formation of clay-organo complexes.

4.3.5 NMR analysis of acid hydrolyzed clay-microbial complexes

Acid hydrolysis is a commonly used technique to isolate and quantify labile and recalcitrant fractions of SOM (Knicker et al., 1996; Knicker, 2000). Here, acid hydrolysis was employed to provide very harsh conditions to determine the nature of the association between microbial biomass and montmorillonite surfaces (***Section 4.2.7***). The conventional ^{1}H NMR spectra and diffusion edited NMR spectra of acid hydrolyzed clay-microbial complexes dissolved in D_2O are presented in ***Figure 4.3.5.1***. General assignments are consistent with those reported in the literature (see annotation for ***Figure 4.3.5.1***). The conventional ^{1}H NMR spectra and diffusion edited NMR spectra of acid hydrolyzed clay-microbial complexes show a largely similar profile with a characteristic dominance from signals assigned to aliphatic compounds (regions 3 and 4). The fact that these lipids remained unchanged even after acid hydrolysis, unequivocally demonstrates a strong and preferential interaction of these species with montmorillonite. These results also have important implications for the stabilization of OM on clay surfaces and are discussed in more details below. The stabilization of microbially derived fatty acids is also discussed in ***Chapter 5***.

Considerable contributions from peptidic CH_3 resonances and protons on α carbon in peptides (region 1) were observed in the ^{1}H NMR spectra of acid treated clay complexes (***Figure 4.3.5.1A*** and ***C***). These signals remained unchanged during diffusion gating (***Figure 4.3.5.1B*** and ***D***) but not as dominant as aliphatic species. Furthermore, the peptidic CH_3 resonance was also present in the ^{1}H NMR spectrum of bovine serum albumen (Simpson, 2002). These findings clearly demonstrate that proteins were also strongly adsorbed to montmorillonite surfaces and have survived acid hydrolysis probably as intact polymeric substances. The stabilization of microbially derived

proteins by clay minerals (montmorillonite and kaolinite) is further explored in ***Chapter 6***. It would appear that signals designated to carbohydrates were probably less well adsorbed and protected by montmorillonite, making them more susceptible to acid hydrolysis. This is supported by the fact that signals resonating from carbohydrates were gated from the spectra during diffusion editing, suggesting a greater contribution from smaller units that have some translational diffusion (***Figure 4.3.5.1B*** and ***D***). It should also be noted that a relatively higher concentration of carbohydrates survived acid hydrolysis as microbes grown on montmorillonite (***Figure 4.3.5.1A***) compared with microbes sorbed to montmorillonite (***Figure 4.3.5.1C***), a reflection, perhaps, of the difference in the strengths of the association.

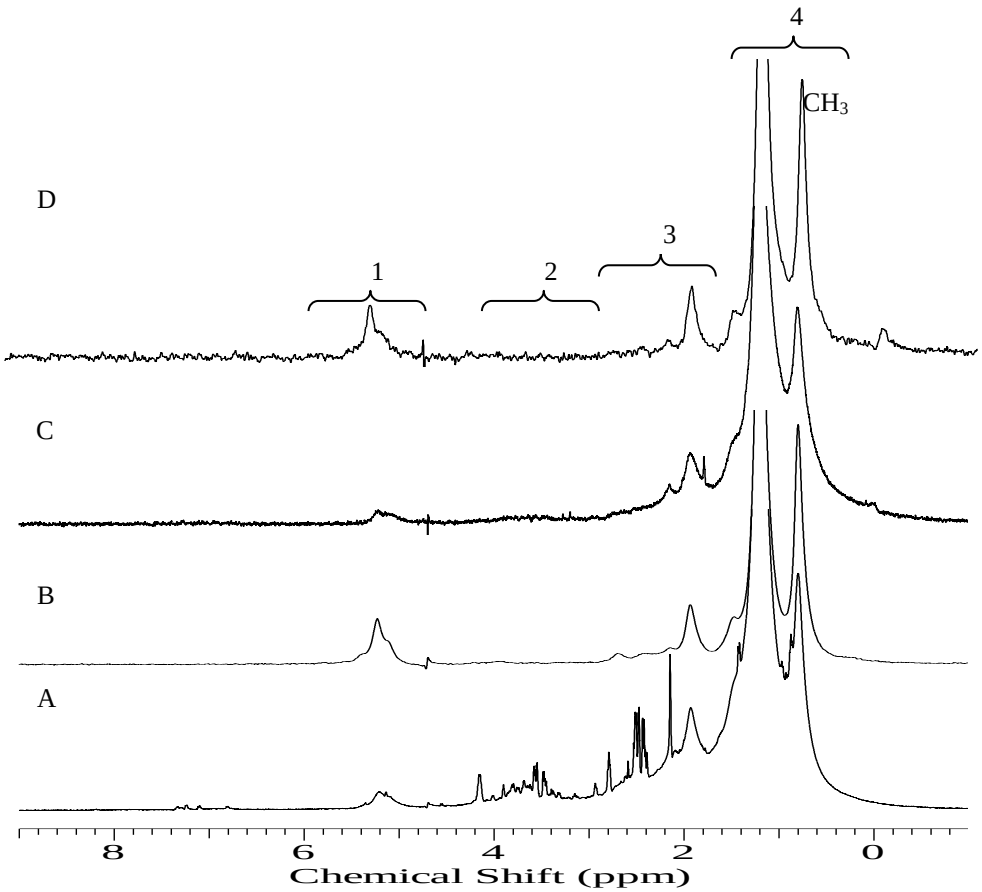

Figure 4.3.5.1: ^{1}H NMR spectra of acid hydrolyzed residues of (A) microbes grown on montmorillonite; and (C) microbes sorbed to montmorillonite; diffusion NMR spectra of (B) microbes grown on montmorillonite; and (D) microbes sorbed to montmorillonite. Numbers and brackets represent general assignments as follows: (1) protons on α carbon in peptides; (2) protons in carbohydrates, protons α to an ester, ether, and hydroxyl in aliphatic chains will also resonate in this region; (3) signals from various substituted methylenes and methenes β to a functionality in hydrocarbons, signals from some amino acid side chains will also resonate here; and (4) aliphatic protons.

4.3.6 NMR analysis of microbial protein and clay-protein complexes

Several studies have pointed to the significance of proteins in the formation of clay-organo complexes and the stabilization of SOM (e.g. Kleber et al., 2007; Miltner et al., 2009). Despite these and other reports, not much is understood about the mechanistic aspects of these processes. However, we anticipate that the data presented here, coupled with current and future investigations, will advance our understanding of the processes involved in the stabilization of plant and microbially derived proteins in soils.

In ***Figure 4.3.6.1*** the ^{1}H HR-MAS NMR spectra of microbial proteins (***Section 4.2.2***) and montmorillonite-protein complex dissolved in DMSO-d_6 are illustrated. General peak designations can be defined as; contribution from amide signals in peptides and aromatic amino acid residues (regions 1 and 2) consistent with phenylalanine; 3, signals from aromatic amino acids; 4, protons and α-carbons in peptides; 5, α-protons (peptides); 6, α-carbons in Arg, Asp and Val; 7, aliphatic side chains; and 8, anomeric sugars. i) Indicates the side chain protons in Arg, Asp and Val (Simpson et al., 2006).

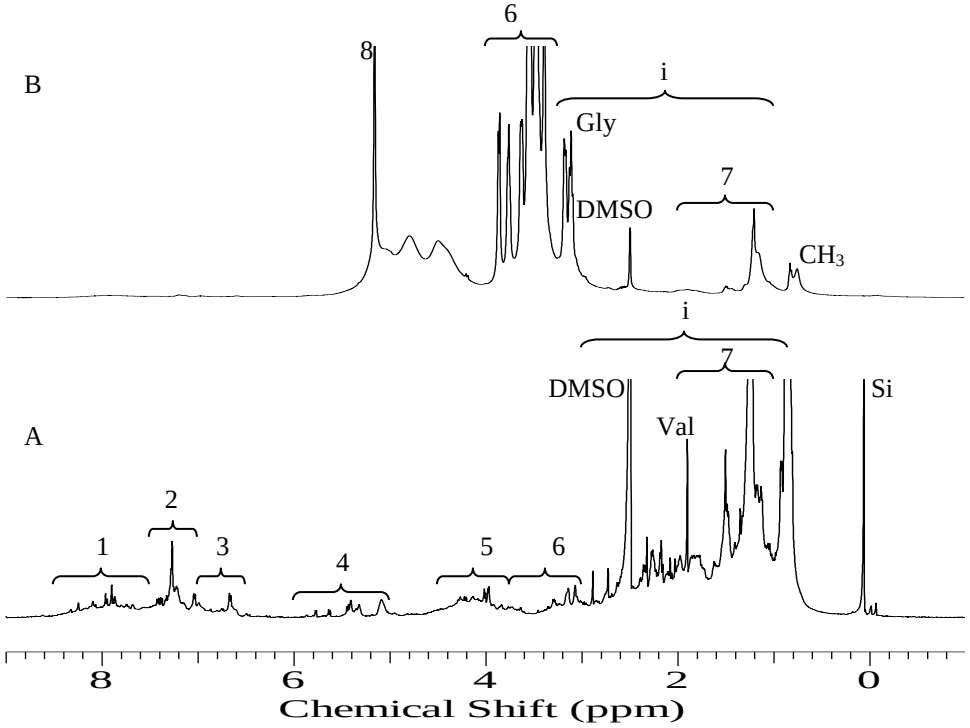

Figure 4.3.6.1: ^{1}H NMR spectra of (A) microbial proteins sorbed to montmorillonite dissolved in DMSO-d_6, and (B) microbial proteins dissolved in DMSO-d_6. The assignments provided for spectra B and C refer to 1, amide; 2, phenylalanine; 3, signals from aromatic amino acids; 4, protons and α-carbons in peptides; 5, α-protons (peptides); 6, α-carbons in Arg, Asp and Val; 7, aliphatic side chains; and 8, anomeric sugars; i, indicates the side chain protons in Arg, Asp and Val.

The ^{1}H NMR spectrum of the protein extract was dominated by signals resonating from α-carbons in amino acid residues (region 6). There was also substantial contribution from the amino acid residue glycine. A considerable resonance attributed to anomeric sugars was also clearly visible at ~5.2 ppm (***Figure 4.3.6.1B***). It must be acknowledged here that despite our best efforts, other macromolecular components may have been co-extracted with proteins. The contribution from aliphatic side chains and terminal CH_3 in amino acid side chains was less significant. In contrast, the ^{1}H NMR spectrum of the montmorillonite-complex was dominated by a characteristic signal from CH_3 resonance in methylated amino acid side chains and other aliphatic side chains (region 7). There were also significant contributions from α-protons (region 5) and the aromatic amino acid residue, phenylalanine (peak 2). This would suggest that aromatic amino acid residues are probably most responsible for the interactions of proteins with clay mineral surfaces. These findings are in agreement with Kaiser and Guggenberger (2003) who suggested that carbonyl groups bonded to aromatic structures are preferentially sorbed to hydrous Al and Fe compounds in soils, and Feng et al. (2005, 2006) who demonstrated the preferential adsorption of terminal CH_3 groups to clay surfaces. Signals from α-carbons in Arg, Asp and Val appear attenuated in the clay-protein complex and may be a result of intercalation of these residues in the interlamellar region of montmorillonite. The intercalation of montmorillonite by the amino acid glycine was previously demonstrated by Kelleher et al. (2003). Spence and Kelleher (2008) also demonstrated the intercalation of montmorillonite using total protein extract. Note that some peaks in ***Figure 4.3.6.1B*** (especially between 1.5 and 3 ppm, and 5.5 and 8.5 ppm) do not appear to be present in microbes in the free form. In fact, this is not the case; the signals are from protons in amino acid side chains, which are at very low concentrations in the uncomplexed biomass and are not visible at the expansion shown.

The diffusion edited NMR spectra of proteins and montmorillonite-protein complex are shown in ***Figure 4.3.6.2***. The diffusion edited NMR spectrum of montmorillonite-protein complex was dominated by signals assigned to aliphatic side chains in amino acids (***Figure 4.3.6.2B***). The resonance attributed to double bonds in aromatic amino acid residues (region 2) also appeared to be preserved in the rigid domain, supporting the earlier suggestion that these functionalities are probably the most important in the association of proteins to clay surfaces. Signals from α-carbons in Arg, Asp and Val (region 3) appear as macromolecular species in the diffusion spectrum

of proteins (***Figure 4.3.6.2A***), but are attenuated in the clay-complex ***Figure 4.3.6.2B***). This would suggest a greater contribution from smaller units that have some translational diffusion, and may suggest a less significant role in the association of proteins with clay curfaces.

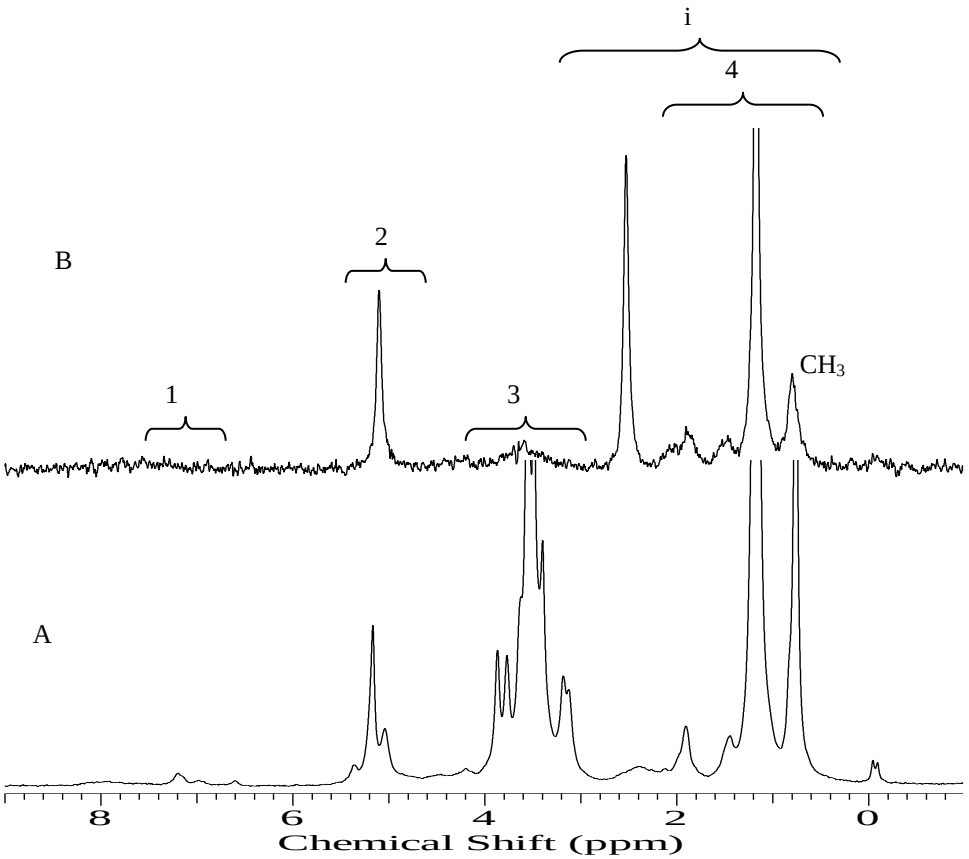

Figure 4.3.6.2: DE NMR spectra of (A) microbial proteins dissolved in DMSO-d_6 and (B) microbial proteins sorbed to montmorillonite dissolved in DMSO-d_6. The assignments provided refer to 1, phenylalanine; 2, double bonds in aromatic amino acid residues. Signals from protons and α-carbons in peptides may resonate here too; 3, is assigned to α-carbons in Arg, Asp and Val and 4, aliphatic side chains; i, indicates the side chain protons in Arg, Asp and Val.

4.4 Conclusions

We have demonstrated that montmorillonite adsorbes greater quantities of microbes and microbially proteins under ambient laboratory conditions when compared with kaolinite. This is due mainly to the the higer CEC and 2:1 expanding capacity of montmorillonite. Furthermore, our results indicated the intercalation of the inner regions of montmorillonite, while adsorption of organic materials was limited to the external surfaces of kaolinite. Except for minor variability in the relative abundance of major microbial biomolecules, there were no significant differences in the NMR spectra of the

microbes grown on montmorillonite and microbes sorbed to montmorillonite. Our results also revealed that aliphatic components were preferentially associated with the mineral, while there were strong associations from proteins and carbohydrates using a variety of mechanisms. This interpretation is unequivocally supported by the NMR spectra of acid hydrolyzed clay-microbial residues. Moreover, acid hydrolysis results would suggest that clay minerals play a critical role in the stabilization of microbial-derived OM. Further experiments are underway that will supplement these findings. It would appear that aromatic amino acid residues and aliphatic side chains in some amino acids are probably the most important structures in the association of proteins to clay surfaces.

4.5 References

Angioi, S., Polati, S., Roz, M., Rinaudo, C., Gianotti, V., and Gennaro, M.C. 2005. Sorption studies of chloroanilines on kaolinite and montmorillonite. *Environmental Pollution* 134, 35–43.

Bakandritsos, A., Simopoulos, A., and Petridis, D. 2006. Iron changes in natural and Fe(III) loaded montmorillonite during carbon nanotube growth. *Nanotechnology* 17, 1112–1117.

Bakker, D. P., Busscher, H. J., van Zanten, J., de Vries, J., Klijnstra, J. W., and van der Mei, H. C. 2004. Multiple linear regression analysis of bacterial deposition to polyurethane coatings after conditioning film formation in the marine environment. *Microbiology* 150, 1779–1784.

Chaerun, S.K., Tazaki, K., Asada, R., and Kogure, K. 2005. Interaction between clay minerals and hydrocarbon-utilizing indigenous microorganisms in high concentrations of heavy oil: implications for bioremediation. *Clay Minerals* 40, 105–114.

Chenu, C. 1995. Extracellular polysaccharides: an interface between microorganisms and soil constituents. In: Huang, P. M., Berthelin, P. M., Bollag, J.-M., McGill, W. B., and Page, A. L. (Eds.), *Environmental impact of soil component interactions. Natural and anthropogenic organics*. CRC Press, Boca Raton, FL., pp. 217–233.

Ekosse, G-I. E. 2005. Fourier transform infrared spectrometry and X-ray powder diffraction and complementary techniques in characterizing clay size fraction of kaolin. *Journal of Applied Science & Environmental Management* 9, 43–48.

Feng, X., Simpson, A. J., and Simpson, M. J. 2005. Chemical and mineralogical controls on humic acid sorption to clay mineral surfaces. *Organic Geochemistry* 36, 1553–1566.

Feng, X., Simpson, A. J., and Simpson, M. J. 2006. Investigating the role of mineral-bound humic acid in phenanthrene sorption. *Environmental Science and Technology* 40, 3260–3266.

Franchi, M., Bramanti, E., Morassi Bonzi, L., Luigi Orioli, P., Vettori, C., and Gallori, E. 1999. Clay-nucleic acid complexes: characterization and implications for the preservation of genetic materials in primeval habitats. *Origins of Life and Evolution of the Biosphere* 29, 279–315.

Fu, Q., Dong, Y., Hu, H., and Huang, Q. 2007. Adsorption of the insecticidal protein of *Bacillus thuringiensis* subsp. *Kurstaki* by soil minerals: effects of organic acid ligands. *Applied Clay Sciences* 37, 201–206.

Hedges, J. I., and Hare, P. 1987. Amino acid adsorption by clay minerals in distilled water. *Geochimica et Cosmochimica Acta* 51, 255–259.

Hedges, J. I., and Keil, R. G. 1999. Organic geochemical perspectives on estuarine processes: sorption reactions and consequences. *Marine Chemistry* 65, 55–65.

Hedges, J. I., and Oades, J. M. 1997. Comparative organic geochemistries of soils and marine sediments. *Organic Geochemistry* 27, 319–361.

Hedges, J. I., Baldock, J. A., Gélinas, Y., Lee, C., Peterson, M., and Wakeham, S. G. 2001. Evidence of non-selective preservation of organic matter in sinking marine particles. *Nature* 409, 801–804.

Hsieh, Y. P. 1996. Soil organic carbon pools of two tropical soils inferred by carbon signatures. *Soil Science Scociety of America Journal* 60, 117–1121.

Kaiser, K., and Guggenberger, G. 2003. Mineral surfaces and soil organic matter. *European Journal of Soil Science* 54, 219–236.

Kelleher, B. P., Oppenheimer, S. F., Han, F. X., Willeford, K. O., Simpson, M. J., Simpson A. J. and Kingery, W. L. 2003. Dynamic systems and phase plane analysis of protease-clay interactions. *Langmuir* 19, 9411–9417.

Khalil, H., Mahajan, D., Rafailovich, M. 2005. Polymer-montmorillonite clay nanocomposites. Part 1: complexation of montmorillonite clay with a vinyl monomer. *Polymer International* 54, 423–427.

Kindler, R., Miltner, A., Thullner, M., Richnow, H.-H., and Kästner, M. 2009. Fate of bacterial biomass derived fatty acids in soil and their contribution to soil organic matter. *Organic Geochemistry* 40, 29–37.

Kleber, M., Sollins, P., and Sutton, R. 2007. A conceptual model of organo-mineral interactions in soils: self-assembly of organic molecular fragments into zonal structures on mineral surfaces. *Biogeochemistry* 85, 9–24.

Knicker, H. 2000. Solid-state 2-D double cross polarization magic angle spinning ^{15}N ^{13}C NMR spectroscopy on degraded algal residues. *Organic Geochemistry* 31, 337–340.

Knicker., H., Scaroni, A. W., and Hatcher, P. G. 1996. ^{13}C and ^{15}N NMR spectroscopic investigation on the formation of fossil algal residues. *Organic Geochemistry* 24, 661–669.

Koskella, J., and Stotzky, G. 1997. Microbial utilization of free and clay-bound insecticidal toxins from *Bacillus thuringiensis* and their retention of insecticidal activity after incubation with microbes. *Applied and Environmental Microbiology* 63, 3561–3568.

Kothawala, D. N., Mooe, T. R., and Hendershot, W. H. 2008. Adsorption of dissolved organic carbon to mineral soils: a comparison of four isotherm approaches. *Geoderma* 148, 43–50.

Ladd, J. N., Amato, M., and Oades, J. M. 1985. Decomposition of plant materials in Australian soils: III. Residual organic and microbial biomass C and N from isotope-labelled legume materials and soil organic matter decomposing under field conditions. *Australian Journal of Soil Research* 23, 603–611.

Lee, L., Saxena, D., and Stotzky, G. 2003. Activity of free and clay-bound insecticidal proteins from *Bacillus thuringiensis* subsp. israelensis against the mosquito *Culex pipien*s. *Applied and Environmental Microbiology* 69, 4111–4115.

Lünsdorf, H., Abraham, W.-R., and Timmis, K. N. 2000. 'Clay hutches': a novel interaction between bacteria and clay minerals. *Environmental Microbiology* 2, 161–168.

Mayer, C., Moritz, R., Kirschner, C., Borchard, W., Maibaum, R., Wingender, J., and Flemming, H.-C. 1999. The role of intermolecular interactions: studies on model systems for bacterial biofilms. *International Journal of Biological Macromolecules* 26, 3–16.

Mayer, L. M., Xing, B. 2001. Organic matter-surface area relationships in acid soils. *Soil Science Society of America Journal* 65, 250–258.

Miltner, A., Kindler, R., Knicker, K., Richnow, H-H, and Kästner, M. 2009. Fate of microbial biomass-derived amino acids in soil and their contribution to soil organic matter. *Organic Geochemistry* 40, 978–985.

Ogunseitan, O. A. 1993. Direct extraction of proteins from environmental samples. *Journal of Microbial Methods* 17, 273–281.

Otto, A., and Simpson, M. J. 2007. Analysis of soil organic matter biomarker by sequential chemical degradation and gas chromatography-mass spectrometry. *Journal of Separation Science* 30, 272–282.

Parfitt, R. L., Theng, B. K. G., Whitton, J. S., and Shepherd, T. G. 1997. Effects of clay minerals and land use on organic matter pools. *Geoderma* 75, 1–12.

Parfitt, R. L., Yuan, G., and Theng, B. K. G. 1999. A ^{13}C-NMR study of the interactions of soil organic matter with aluminium and allophane in podzols. *European Journal of Soil Science* 50, 695–700.

Rhouta, B., Amjoud, M., Mezzane, D., and Alimoussa, A. 2006. Proton conductivity in Al-stevensite pillared clays. *Moraccan Journal of Condensed Matter* 7, 77–81.

Rillig, M. C., Caldwell, B. A., Wösten, H. A. B., and Sollins, P. 2007. Role of proteins in soil carbon and nitrogen storage: controls of persistence. *Biogeochemistry* 85, 25–44.

Schnitzer, M., Ripmeester, J. A., and Kodama, H. 1988. Characterization of the organic matter associated with soil clay. *Soil Science* 145, 448–454.

Shoval, S., Yariv, S., Michaelian, K. H., and Boudeulle Panczer, G. 2002. Hydroxyl-stretching bands in polarized micro-raman spectra of oriented single-crystal Keokuk kaolinite. *Clays and Clay Minerals* 50, 56–62.

Simpson, A. J. 2002. Determining the molecular weight, aggregation structures, and interactions of natural organic matter using diffusion ordered spectroscopy. *Magnetic Resonance in Chemistry* 40, S72–S82.

Simpson, A. J., Simpson, M. J., Kingery, W, L., Lefebvre, B. A., Moser, A., Williams, A. J., Kvasha, M., and Kelleher, B. P. 2006. The application of ^{1}H high-resolution magic-angle spinning NMR for the study of clay–organic associations in natural and synthetic complexes. *Langmuir* 22, 4498–4508.

Simpson, A. J., Song, G., Smith, E., Lam, B., Novotny, E. H., and Hayes, M. H. B. 2007. Unraveling the structural components of soil humin by use of solution-state nuclear magnetic resonance spectroscopy. *Environmental Science and Technology* 41, 876–883.

Singleton, I., Merrington, G., Colvan, S., and Delahunty, J. S. 2003. The potential of soil protein-based methods to indicate metal contamination. *Applied Soil Ecology* 23, 25–32.

Skipper, N. T., Refson, K., and McConnell, J. D. C. 1989. Computer calculations of water-clay interactions using atomic pair potentials. *Clay Minerals* 24, 411–425.

Skjemstad, J. O. 1992. Genesis of podzols on coastal dunes in southern Queensland .III. The role of aluminum organic complexes in profile development. *Australian Journal of Soil Research* 30, 645–665.

Soil Survey Staff. 1999. *Soil taxonomy: a basic system of soil classification for making and interpreting soil surveys*, 2nd Ed. U. S. Government Printing Press, Washington, DC.

Sollins, P., Swanston, C., Kleber, M., Filley, T., Kramer, M., Crow, S., Caldwell, B. A., Lajtha, K., and Bowden, R. 2006. Organic C and N stabilization in a forest soil: evidence from sequential density fractionation. *Soil Biology & Biochemistry* 38, 3313–3324.

Spain, A. 1990. Influence of environmental conditions and some soil chemical properties on the carbon and nitrogen contents of some Australian rainforest soils. *Australian Journal of Soil Research* 28, 825–839.

Spence, A., and Kelleher, B. P. 2008. Soil microbes and soil microbial proteins: interactions with clay minerals. *FEBS Journal* 275, Suppl. 1, 281.

Tazaki, K. 2005. Microbial formation of halloysite-like mineral. *Clays and Clay Minerals* 53, 224–233.

Ulrich, H. J., Stumm, W., and Cosovic, B. 1988. Adsorption of aliphatic fatty acids on aquatic interfaces. Comparison between two model surfaces: the mercury electrode and δ-Al_2O_3, colloids. *Environmental Science and Technology* 22, 37–41.

Vermeer, A. W. P., and Koopal, L. K. 1998. Adsorption of humic acids to mineral particles. 2. Polydispersity effects with polyelectrolyte adsorption. *Langmuir* 14, 4210–4216.

Vermeer, A. W. P., van Riemsdijk, W. H., and Koopal, L. K. 1998. Adsorption of humic acid to mineral particles. 1. Specific and electrostatic interactions. *Langmuir* 14, 2810–2819.

Wagai, R., Mayer, L. M., and Kitayama, K. 2009. Extent and nature of organic coverage of soil mineral surfaces assessed by gas sorption approach. *Geoderma* 149, 152–160.

Wattel-Koekkoek, E. J. W., van Genuchten, P. P. L., Buurman, P., and van Lagen, B. 2001. Amount and composition of clay-associated soil organic matter in a range of kaolinitic and smectitic soils. *Geoderma* 99, 27–49.

Wershaw, R. L., Llaguno, E. C., and Leenheer, J. A. 1996b. Mechanism of formation of humus coatings on mineral surfaces 3. Composition of adsorbed organic acids from compost leachate on alumina by solid-state ^{13}C NMR. *Colloids and Surfaces A: Physicochemical and Engineering Aspects* 108, 213–223.

Wershaw, R. L., Llaguno, E. C., Leenheer, J. A., Sperline, R. P., and Song, Y. 1996a. Mechanism of formation of humus coatings on mineral surfaces 2. Attenuated total reflectance spectra of hydrophobic and hydrophilic fractions of organic acids from compost leachate on alumina. *Colloids and Surfaces A: Physicochemical and Engineering Aspects* 108, 199–211.

Wu, D., Chen, A., and Johnson Jr., C. S. 1995. An improved diffusion-ordered spectroscopy experiment incorporating bipolar-gradient pulses. *Journal of Magnetic Resonance, Series A* 115, 260–264.

Wyndham, R. C. 1986. Evolved aniline catabolism in *Acinatobacter calcoaceticus* during continuous culture of river water. *Applied and Environmental Microbiology* 51, 781–789.

Yu, C. H., Norman, M. A., Newton, S. Q., Miller, D. M., Teppen, B .J., Schäfer, L. 2000. Molecular dynamics simulations of the adsorption of proteins on clay mineral surfaces. *Journal of Molecular Structure* 556, 95–103.

Chapter 5

Degradation of Microbial Lipids and Amino Acids

Degradation of microbial lipids and amino acids

5.1 Introduction

OM entering natural ecosystems can be divided into several classes of biomolecules including polysaccharides (e.g. cellulose, chitin, and peptidoglycan), proteins, lipid/aliphatic materials and lignin (Kögel-Knabner, 2002). Lipids constitute an important biochemical class in living organisms, and although not as abundant as amino acids and carbohydrates, they are a major carbon pool in microbial biomass, making up 5 to 20% of the total carbon (Wakeham et al., 1997; Oursel et al., 2007). Soil lipids consist of a wide variety of organic compounds such as fatty acids, *n*-alkyl hydrocarbons (alkenes and alkanes), *n*-alkyl alcohols, sterols, terpenoids, chlorophyll, fats, waxes and resins, as well as phospholipids (Jandl et al., 2002) and are an important component of natural OM in soils (Sun et al., 2000).

These compounds originate from both plants and animals as products of decomposition and exudation, as well as from various other pedogenic sources, including fungi, bacteria and mesofauna (Bull et al., 2000a). Of the classes of lipids, fatty acids are the most abundant and probably the most investigated (Jandl et al., 2002). The composition of accumulated lipids in soils is influenced by a wide range of processes, including bioturbation, oxidation, microbial degradation and hydrolysis (Naafs et al., 2004). Many lipids are reactive and subject to readily discernable modifications to their original molecular structure as a consequence of degradation reactions, thus allowing biogeochemical reaction sequences to be studied (Colombini et al., 2005b).

It has been demonstrated that, unlike plant materials, soil microbial biomass is highly sensitive to elevated UV-B radiation (Johnson et al., 2002). In the present work, we used GC-MS to investigate the occurrence of biodegradation and photooxidation products of microbial lipids and amino acids from a mixed culture of microbial biomass, microbial leachates, montmorillonite-microbial complexes and leachates of montmorillonite-microbial complexes degraded under ambient laboratory conditions and intense UV-A/UV-B radiation. More specifically, we would like to determine: (i) whether the biodegradation and photodegradation processes participate efficiently in the

degradation process of microbial-derived fatty acids and amino acids; (ii) whether there are any differences between biodegradation and photooxidation products of microbial lipids and amino acids; (iii) whether microbially-derived lipids and amino acids are protected by clay minerals and if they degrade differently in a clay-free environment; and (iv) whether some of these degradation products are sufficiently stable and specific to serve as markers of biodegradation and photooxidation processes.

5.2 Materials and Methods

5.2.1 Microbial propagation and bacterial growth on clay

Microbial biomass was cultured from a light clay-loam Oakpark soil (***Chapter 2***) and clay-microbial complexes were prepared using montmorillonite as previously described in ***Section 4.2.1***. The medium was a minimal medium containing unlabelled $(NH_4)_2SO_4$ as a source of nitrogen, and all cultures were amended with unlabelled glucose and acetate as sources of carbon. All other parameters and growth conditions were previously described (See ***3.2.1***).

5.2.2 Decomposition experiment

The degradation of microbial biomass and montmorillonite-complexes for lipid and amino acid analysis was conducted as previously outlined in ***Section 3.2.2***.

5.2.3 Solvent extraction

Total solvent extraction was performed on initial and degraded microbial biomass, initial and degraded montmorillonite-complexes, degraded microbial leachates and leachates of montmorillonite-microbial complexes according to a modified version of the protocol described by Otto et al. (2005). Lyophilized samples (0.05 - 0.1 g) were sonicated twice for 15 min, each time with 2 ml Milli-Q water to remove highly polar water soluble compounds. The combined water extracts were centrifuged at 2500 rpm for 30 min, decanted, freeze-dried and stored at -20°C for subsequent analyses. The water extracted residues were freeze-dried to remove excess water and then extracted with solvents as follows: samples were sonicated twice for 15 min with 2 ml methanol, then dichloromethane:methanol (1:1; v/v), followed by dichloromethane. The combined total solvent extracts (‘‘free lipids’’) were filtered through glass fiber filters (Whatman GF/A) using a Buckner apparatus, concentrated by rotary evaporation, and dried

completely in 2 ml glass vials under a constant stream of nitrogen gas. The extract yields were determined by weighing the dried residue, and were stored at room temperature for subsequent analyses.

5.2.4 Acid hydrolysis (AHY)

Acid hydrolysis was performed on the solvent extracted residues of the initial and degraded microbial biomass and the initial and degraded complexes using previously published procedures (Otto and Simpson, 2007) modified as described below. Briefly, the microbial residues (<0.1 g) were hydrolyzed under reflux with 10 ml of 6 M HCl at 105ºC for 8 h. After cooling, the hydrolysates were vacuum filtered through glass fiber filters (Whatman GF/A) and the extracts were evaporated to dryness by rotary evaporation at 40 ºC under vacuum. The dried extracts were resuspended in 20 ml Milli-Q water and the pH adjusted to 6.7 with 0.4 M potassium hydroxide. The samples were centrifuged at 4000 rpm for 10 min to remove all precipitate and the supernatants were freeze-dried. The freeze-dried extracts were then dissolved in 3 ml of methanol and centrifuged at 4000 rpm for 10 min to remove any excess salts that were produced during the neutralization step. The acid hydrolized products were then transferred into 4 ml vials and evaporated to dryness by a stream of nitrogen for further analysis.

5.2.5 Derivatization

Derivatization of total solvent and AHY extracts was performed according to a modified version of the protocols described by Otto et al. (2005). Total solvent and acid hydrolyzed extracts were each redissolved in 500 µl of dichloromethane:methanol (1:1; v/v). Aliquots of the extracts (50 µl) were dried in a stream of nitrogen and then converted to trimethylsilyl (TMS) derivatives by reaction with 45 µl *N,O-bis*-(trimethylsilyl)trifluoroacetamide (BSTFA) and 5 µl pyridine for 2 h at 70 ºC. After cooling, 50 µl of hexane was added to dilute the extracts.

5.2.6 ***GC-MS analysis***

Gas chromatography-mass spectrometry (GC-MS) analyses of the derivatized extracts were performed on an Agilent model 6890N gas chromatograph coupled to an Agilent 5975C InertXL mass selective detector (MSD) with Triple-Axis Detector. Separation was achieved on a HP-5MS chemically bonded fused-silica capillary column (Hewlett Packard), with stationary phase 5% phenyl-95% methylpolysiloxane, and of

dimensions 0.25 mm i.d., 0.25 µm film thickness and 30 m length. The GC operating conditions were as follows: initial temperature 65 ºC, 2 min isothermal, then ramped at 6ºC min^{-1} up to 300ºC, 20 min isothermal. The carrier gas was helium (purity of 99.9995%) at a constant flow of 1.0 mL min^{-1}. The samples (1 µ) were autoinjected (Agilent 7683B autosampler) into the front inlet port with a 1:2 split and the injector temperature set at 280 ºC. The mass spectrometer was operated in the electron impact mode (EI) at 70 eV ionization energy, ion source temperature 230ºC, scan range *m/z* 50-650 and interface temperature 280ºC. Data were acquired and processed with the Agilent Chemstation G1701DA software. Individual compounds were identified by comparison of mass spectrometric fragmentation patterns with literature (Otto et. al., 2005; Otto and Simpson, 2007), NIST and Wiley MS data libraries.

5.3 Results

5.3.1 Lipid analysis of ambient degraded microbial biomass

Fatty acid methyl esters are an established tool to study the dynamics of soil microbial communities in response to environmental changes (Schulze, 2005), and are being applied here to study the degradation dynamics of soil microbial biomass and microbial leachates. The GC-MS chromatograms of silylated total solvent extracts of initial and ambient degraded biomass are presented in (***Figure 5.3.1.1*****)** and contain a series of aliphatic lipids, glycerol and polysaccharides, and show minor variation among the samples. The detection of polysaccharides in the ‘‘lipid’’ fraction of the total lipid extract is due to the use of methanol as one of the medium polar-to-polar solvents (Otto and Simpson, 2007). At the molecular level, all fatty acid extracts were dominated by even-numbered, medium- to long-chain saturated fatty acids hexadecanoic acid [palmitic acid; ($C_{16:0}$)] and octadecanoic acid [stearic acid; ($C_{18:0}$), ***Figure 5.3.1.1B-D***]. Monoenoic fatty acids represented by two isomers of hexadecenoic acid and octadecenoic acid were also dominant compounds in the extracts. The isomers detected were *cis*-9, *trans*-11 isomers [*cis*-9(*Z*), *trans*-11(*E*)] of hexadecenoic and octadecenoic acids. The major isomer of hexadecenoic acid was found to be (*Z*)-9-hexadecenoic acid [palmitoleic acid; ($C_{16:1}$)], while *cis*-9(*Z*) oleic acid ($C_{18:1}$), as enumerated from the carboxyl terminus of the molecule, was the major isomer of octadecenoic acid. Polyenoic fatty acids were represented by dienoic C_{18} (18:2ω9) acids.

Other short- and medium- to long-chain homologues of *n*-alkanoic acids in the range of C_8-C_{24} with a preference of even numbered molecules were detected up to 14 weeks, reducing to C_8-C_{18} acids after 26 weeks of decomposition. A series of naturally occurring methyl esters ($C_{16:1}$, $C_{16:2}$, $C_{16:3}$, $C_{18:1}$and $C_{18:1}$) were also detected in variable amounts in the starting material only. Other *n*-alkenoic acids detected include a C_4 acid common to all samples, tetradecenoic acid in the starting material, octenoic acid at 14 and 26 weeks degradation and hexenoic acid at 26 weeks degradation. We were unable to detect polyenoic acids after 14 weeks degradation. *α,ω*-Alkanedioic acids were detected in the initial biomass and the sample degraded for 14 weeks and comprised of C_4-C_7 and C_4 acids, respectively. *n*-Alkanes in the range of C_{15}-C_{27} with a distribution profile showing an odd-over-even predominance (detected at 14 weeks), C_{15}-C_{20} (detected at 6 weeks) and C_{16}-C_{18}, C_{22} and C_{29} (detected in the starting material, were only present as minor components. We failed to detect *n*-alkanes after 14 weeks degradation (***Table 5.3.1.1***).

Relatively low concentrations of branched-chain [*iso*- (C_4) and *anteiso*- (C_5)] fatty acids were detected in only the initial sample and that degraded for 26 weeks (***Table 5.3.1.1***). α/β/ω-Hydroxyalkanoic acids (C_2-C_8) with both normal-and *iso*-branched structures were present in the starting material, while normal α/β-hydroxyalkanoic acids (C_2-C_4 and C_{10}) were identified in the degraded samples. Glyceric acid, glycerol and a series of $C_{16:1}$, C_{16}, $C_{18:1}$ and C_{18} monoacylglycerides were detected at varying concentrations. Except for the sample degraded for 26 weeks, a variety of carbohydrates (pentoses and hexose) consisting of the monosaccharides arabinoic acid galactose, xylitol, and fructose were also detected in variable amounts.

The total solvent extracts of the degraded biomass also contained neutral lipids, with the sterol, C_{27}-cholest-5-en-3β-ol (cholesterol) being the most abundant, followed by other C_{28} and C_{29}-sterols; ergosta-5-en-3β-ol (campesterol), stigmasta-5,22-dien-3β-ol (stigmasterol), and stigmast-5-en-3β-ol (β-sitosterol). The isoprenoid alcohol, 3,7,11,15-tetramethylhexadec-2(*E*)-en-1-ol, [(*E*)-phytol; a bacteriochlorophyll derivative] and the saturated terprenoid alkane, pristane were present in trace amounts in the samples degraded for 6 and 14 weeks, respectively. Glycerol, a series of $C_{16:1}$, C_{16}, $C_{18:1}$ and C_{18} monoacylglycerides Variable amounts of phosphoric acid was also present in the degraded samples, while the *cis*-configured alkylamides, 9-octadecenamide, (*Z*) was present in only the sample degraded for 14 weeks (***Table 5.3.1.1***). A homologous

series of unknown compounds, the mass spectra of which show various characteristic fragment ions, were also identified in the samples (***Figure 5.3.1.1***). Fatty acids having chains of less than 12 carbon atoms constitute only a small proportion of the total fatty acid extracts.

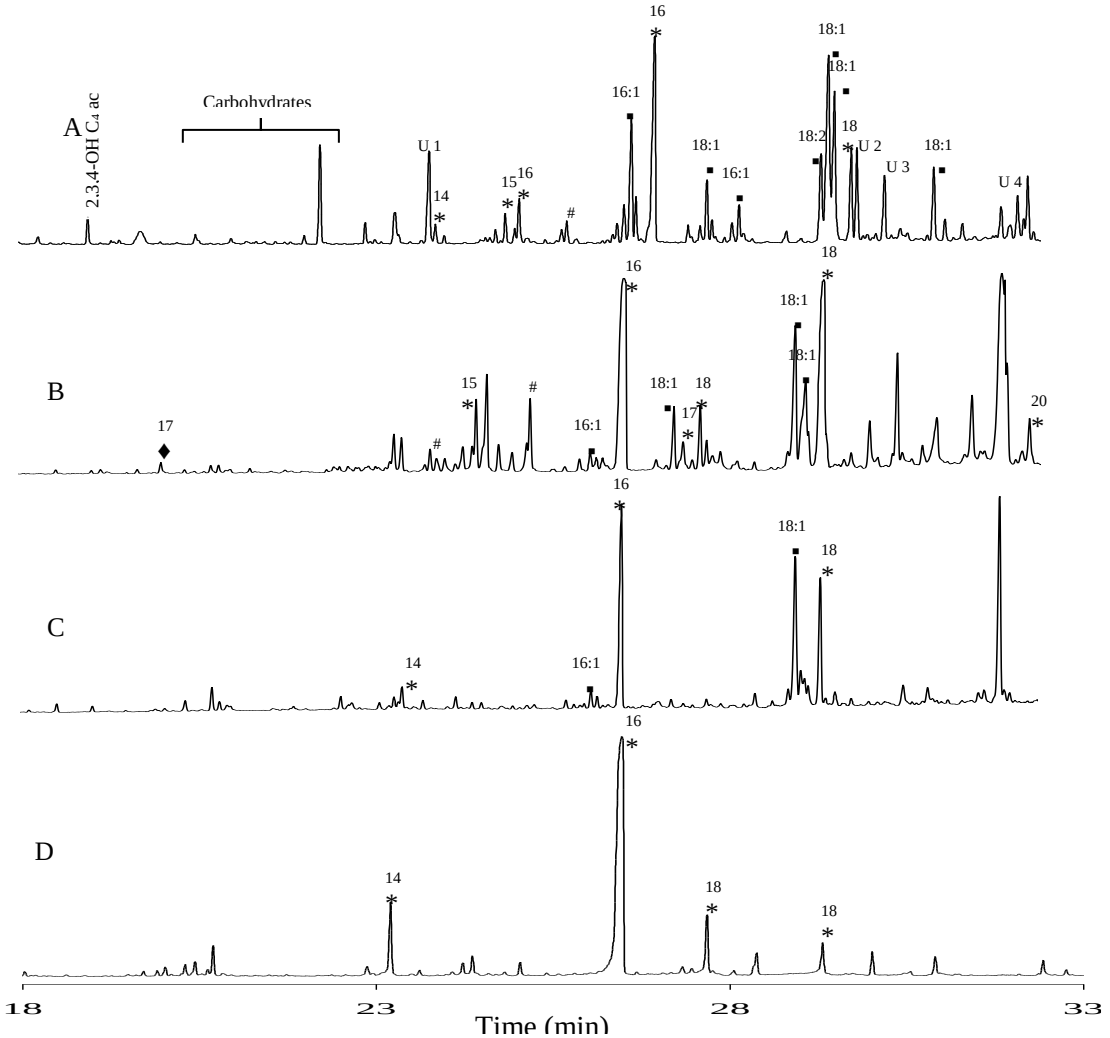

Figure 5.3.1.1: GC-MS chromatograms (TIC) of silylated total lipid extracts of (A) initial microbial biomass and microbial biomass degraded under ambient conditions for (B) 6, (C) 14 and (D) 26 weeks. Numbers refer to total carbon numbers in aliphatic series. ♦ = *n*-alkanes, * = *n*-alkanoic acid, ▪ = *n*-alkenoic acid, # = carbohydrates, u = unknown and ac = acid.

Table 5.3.1.1: Occurrence of identified compounds from the total solvent extracts of initial microbial biomass and microbial biomass degraded under ambient conditions.

Compound	MW	Composition	Degradation period			
			0^{WD}	6^{WD}	14^{WD}	26^{WD}
n-Alkanes						
n-Pentadecane	212	$C_{15}H_{32}$	–	+	+	–
n-Hexadecane	226	$C_{16}H_{34}$	+	+	+	–
n-Heptadecane	240	$C_{17}H_{36}$	+	+	+	–
n-Octadecane	254	$C_{18}H_{38}$	+	+	+	–
n-Nonadecane	268	$C_{19}H_{40}$	–	+	+	–
n-Eicosane	282	$C_{20}H_{42}$	–	+	+	–
n-Heneicosane	296	$C_{21}H_{44}$	–	–	+	–
n-Docosane	310	$C_{22}H_{46}$	+	–	+	–
n-Tricosane	324	$C_{23}H_{48}$	–	–	+	–
n-Heptacosane (C_{27})	380	$C_{27}H_{56}$	–	–	+	–
n-Nonacosane	408	$C_{29}H_{60}$	+	–	–	–
n-Alkanoic acids						
2-Methylpropanoic acid	88	$C_4H_8O_2$	–	–	–	+
2-Methylbutanoic acid	102	$C_5H_{10}O_2$	–	–	–	+
Hexanoic acid	116	$C_6H_{12}O_2$	–	+	–	–
Octanoic acid	144	$C_8H_{16}O_2$	+	+	–	–
Nonanoic acid (C_9)	158	$C_9H_{18}O_2$	–	+	+	–
Decanoic acid	172	$C_{10}H_{20}O_2$	–	+	+	–
Dodecanoic acid	200	$C_{12}H_{24}O_2$	–	–	+	+
n-Tetradecanoic acid (C_{14})	228	$C_{14}H_{28}O_2$	+	+	+	+
n-Pentadecanoic acid	242	$C_{15}H_{30}O_2$	+	+	+	+
n-Hexadecanoic acid (C_{16})	256	$C_{16}H_{32}O_2$	+	+	+	+
Pentadecanoic acid, 14-methyl-, methyl ester	270	$C_{17}H_{34}O_2$	–	+	–	–
Heptadecanoic acid	270	$C_{17}H_{34}O_2$	+	+	+	+
n-Octadecanoic acid (C_{18})	284	$C_{18}H_{36}O_2$	+	+	+	+
Octadecanoic acid methyl ester	298	$C_{19}H_{38}O_2$	+	+	–	–
Nonadecanoic acid	298	$C_{19}H_{38}O_2$	+	–	–	–
n-Eicosanoic acid (C_{20})	312	$C_{20}H_{40}O_2$	–	+	+	–
n-Docosanoic acid (C_{22})	340	$C_{22}H_{44}O_2$	+	+	+	–
n-Tetracosanoic acid (C_{24})	368	$C_{24}H_{48}O_2$	+	+	+	–
n-Alkenoic acids						
2-Butenoic acid	86	$C_4H_6O_2$	+	+	+	+
2-Hexenoic acid	114	$C_6H_{10}O_2$	–	–	–	+
2-Octenoic acid	142	$C_8H_{14}O_2$	–	–	+	+
9-Tetradecenoic acid	226	$C_{14}H_{26}O_2$	+	–	–	–
cis-n-hexadec-9-enoic acid	254	$C_{16}H_{30}O_2$	+	+	+	–
7,10,13-Hexadecatrienoic acid, methyl ester	264	$C_{17}H_{28}O_2$	+	–	–	–
7,10-Hexadecadienoic acid, methyl ester	266	$C_{17}H_{30}O_2$	+	–	–	–
9-Hexadecenoic acid, methyl ester, (Z)-	268	$C_{17}H_{32}O_2$	+	–	–	–
n-Octadeca-9,12-dienoic acid ($C_{18:2}$)	280	$C_{18}H_{32}O_2$	+	–	+	–
n-Octadec-9-enoic acid ($C_{18:1}$)	282	$C_{18}H_{34}O_2$	+	+	+	–
11-cis or trans-Octadecenoic acid	282	$C_{18}H_{34}O_2$	+	+	–	–
11,14-Octadecadienoic acid, methyl ester	294	$C_{19}H_{34}O_2$	+	–	–	–

(*continued on next page*

Table 5.3.1.1 (*continued*)

Compound	MW	Composition	Degradation period			
			0^{WPD}	6^{WPD}	14^{WPD}	26^{WPD}
8 or 9-Octadecenoic acid (Z)-, methyl ester	296	$C_{19}H_{36}O_2$	+	+	–	–
11-Octadecenoic acid, methyl ester	296	$C_{19}H_{36}O_2$	+	–	–	–
n-Alkanedioic acids						
Butanedioic acid	118	$C_4H_6O_4$	+	–	+	–
Heptanedioic acid	160	$C_7H_{12}O_4$	+	–	–	–
hydroxyalkanoic aicds						
α-Hydroxyacetic acid	76	$C_2H_4O_3$	+	+	–	–
α-Hydroxypropanoic acid	90	$C_3H_6O_3$	+	–	+	–
β-hydroxybutanoic acid	104	$C_4H_8O_3$	+	+	+	+
2-Ethyl-3-hydroxypropionic acid	118	$C_5H_{10}O_3$	+	–	–	–
3-Hydroxydecanoic acid	188	$C_{10}H_{20}O_3$	–	–	–	+
Isoprenoid derivatives						
Pristane	268	$C_{19}H_{40}$	–	–	+	–
Phytol	296	$C_{20}H_{40}O$	–	+	–	–
Saccharides						
Arabinoic acid	150	$C_5H_{10}O_5$	+	+	–	–
Xylitol	152	$C_5H_{12}O_5$	+	–	–	–
D-Fructose	180	$C_6H_{12}O_6$	+	+	+	–
D-Galactose	180	$C_6H_{12}O_6$	–	+	–	–
Monoacylglycerols						
Glyceric acid	106	$C_3H_6O_4$	+	–	–	–
Glycerol	92	$C_3H_8O_3$	+	+	+	+
$C_{16:1}$ Monoacylglyceride	328	$C_{19}H_{36}O_4$	+	+	–	–
C_{16} Monoacylglyceride	330	$C_{19}H_{38}O_4$	+	+	–	–
$C_{18:1}$ Monoacylglyceride	356	$C_{21}H_{40}O_4$	+	+	–	–
C_{18} Monoacylglyceride (Stearin)	358	$C_{21}H_{42}O_4$	+	+	–	–
Other compounds						
Phosphoric acid triethyl ester	182	$C_6H_{15}O_4P$	–	+	+	+
9-Octadecenamide, (Z)-	281	$C_{18}H_{35}NO$	–	–	+	–
Cholest-5-en-3 β-ol	386	$C_{27}H_{46}O$	–	–	–	+
Ergost-5-en-3-ol, (3 β,24R)-	400	$C_{28}H_{48}O$	–	–	–	+
Stigmasta-5,22-dien -3β-ol	412	$C_{29}H_{48}O$	–	–	+	+
Stigmasta-5,24(28)-dien-3á-ol	412	$C_{29}H_{48}O$	–	+	–	–
Stigmast-5-en-3β-ol	414	$C_{29}H_{50}O$	–	–	–	+
Unknowns						
Unknown 1 *m/z*						
Unknown 2 *m/z*						
Unknown 3 *m/z*						
Unknown 4 *m/z*						

^{WD} Represents the degradation period in weeks.

+ Represents the occurrence of compounds identified as methyl esters or TMS derivatives in the initial or ambient degraded microbial biomass.

– Signifies the absence of compounds in the initial or ambient degraded microbial biomass.

5.3.2 Lipid analysis of UV degraded microbial biomass

The total ion chromatograms (TICs) of the organic solvent extracts of the UV degraded microbial biomass are illustrated in ***Figure 5.3.2.1***, and the occurrences of individual compounds are given in ***Table 5.3.2.1***. It is interesting to note, that except for the occurrence of C_{22} and C_{24} *n*-alkanoic acids and *cis*-9(*Z*) oleic acid at 26 weeks; $C_{18:1}$ methyl ester at 14 weeks; and a C_9 di-acid and pristine at 6 weeks (***Table 5.3.2.1***), the composition and relative abundances of free lipid classes are similar to the organic solvent extracts of the ambient degraded microbial biomass (***Figure 5.3.1.1*** and ***Table 5.3.1.1***). We also failed to identify glycerol in the extracts of the UV degraded biomass.

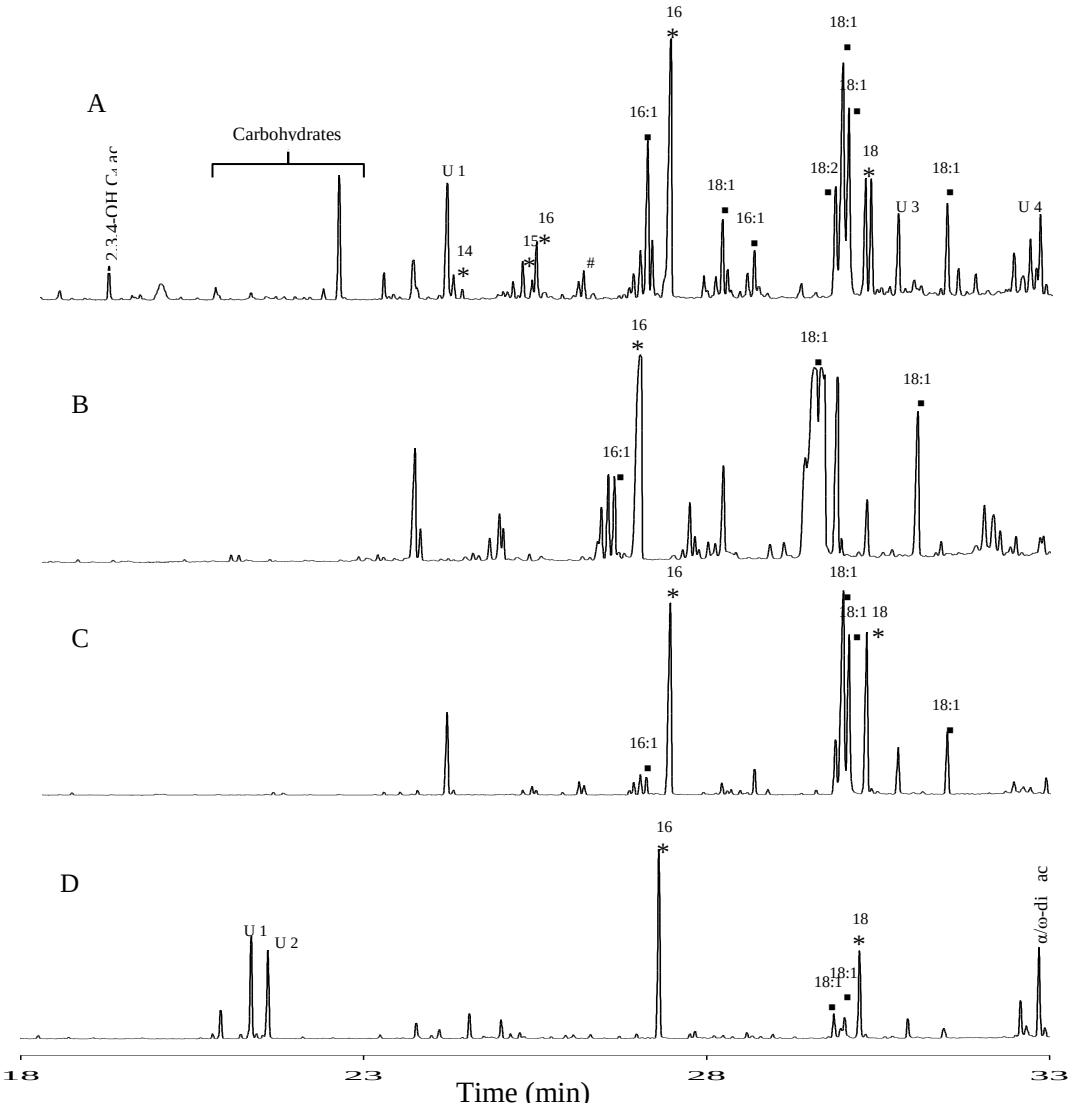

Figure 5.3.2.1: GC-MS chromatograms (TIC) of silylated total lipid extracts of (A) initial microbial biomass and microbial biomass degraded under UV conditions for (B) 6, (C) 14 and (D) 26 weeks. Numbers refer to total carbon numbers in aliphatic series. ♦ = *n*-alkanes, * = *n*-alkanoic acid, ▪ = *n*-alkenoic acid, # = carbohydrates, u = unknown and ac = acid.

Table 5.3.2.1: Occurrence of identified compounds from the total solvent extracts of initial and UV degraded microbial biomass.

Compound	MW	Composition	Degradation period			
			0^{WPD}	6^{WPD}	14^{WPD}	26^{WPD}
n-Alkanes						
n-Pentadecane	212	$C_{15}H_{32}$	–	–	+	–
n-Hexadecane	226	$C_{16}H_{34}$	+	+	+	–
n-Heptadecane	240	$C_{17}H_{36}$	+	+	+	–
n-Octadecane	254	$C_{18}H_{38}$	+	+	+	–
n-Nonadecane	268	$C_{19}H_{40}$	–	+	+	–
n-Eicosane	282	$C_{20}H_{42}$	–	–	+	–
n-Docosane	310	$C_{22}H_{46}$	+	–	+	–
n-Tricosane	324	$C_{23}H_{48}$	–	–	+	–
n-Hexacosane	366	$C_{26}H_{54}$	–	+	+	–
n-Heptacosane (C_{27})	380	$C_{27}H_{56}$	–	–	+	–
n-Nonacosane	408	$C_{29}H_{60}$	+	–	–	–
n-Alkanoic acids						
2-Methylpropanoic acid	88	$C_4H_8O_2$	+	–	–	+
2-Methylbutanoic acid	102	$C_5H_{10}O_2$	+	–	–	+
Hexanoic acid	116	$C_6H_{12}O_2$	–	+	–	–
Octanoic acid	144	$C_8H_{16}O_2$	+	+	+	–
Nonanoic acid (C_9)	158	$C_9H_{18}O_2$	–	+	+	–
Decanoic acid	172	$C_{10}H_{20}O_2$	–	+	+	–
Dodecanoic acid	200	$C_{12}H_{24}O_2$	–	–	+	+
n-Tetradecanoic acid (C_{14})	228	$C_{14}H_{28}O_2$	+	+	+	+
n-Pentadecanoic acid	242	$C_{15}H_{30}O_2$	+	+	+	–
n-Hexadecanoic acid (C_{16})	256	$C_{16}H_{32}O_2$	+	+	+	+
Heptadecanoic acid	270	$C_{17}H_{34}O_2$	+	+	+	+
n-Octadecanoic acid (C_{18})	284	$C_{18}H_{36}O_2$	+	+	+	+
Octadecanoic acid methyl ester	298	$C_{19}H_{38}O_2$	+	+	+	–
Nonadecanoic acid	298	$C_{19}H_{38}O_2$	+	–	–	–
n-Eicosanoic acid (C_{20})	312	$C_{20}H_{40}O_2$	–	+	+	+
n-Docosanoic acid (C_{22})	340	$C_{22}H_{44}O_2$	+	+	+	+
n-Tetracosanoic acid (C_{24})	368	$C_{24}H_{48}O_2$	+	+	–	–
n-Alkenoic acids						
2-Butenoic acid	86	$C_4H_6O_2$	+	+	+	–
2-Octenoic acid	142	$C_8H_{14}O_2$	–	–	–	+
9-Tetradecenoic acid	226	$C_{14}H_{26}O_2$	+	–	–	–
cis-n-hexadec-9-enoic acid	254	$C_{16}H_{30}O_2$	+	+	+	–
7,10,13-Hexadecatrienoic acid, methyl ester	264	$C_{17}H_{28}O_2$	+	+	–	–
7,10-Hexadecadienoic acid, methyl ester	266	$C_{17}H_{30}O_2$	+	–	–	–
9-Hexadecenoic acid, methyl ester, (Z)-	268	$C_{17}H_{32}O_2$	+	+	–	–
n-Octadeca-9,12-dienoic acid ($C_{18:2}$)	280	$C_{18}H_{32}O_2$	+	+	–	–
n-Octadec-9-enoic acid ($C_{18:1}$)	282	$C_{18}H_{34}O_2$	+	+	+	+
11-cis or trans-Octadecenoic acid	282	$C_{18}H_{34}O_2$	+	+	–	–
11,14-Octadecadienoic acid, methyl ester	294	$C_{19}H_{34}O_2$	+	–	–	–
8 or 9-Octadecenoic acid (Z)-, methyl ester	296	$C_{19}H_{36}O_2$	+	+	+	–
11-Octadecenoic acid, methyl ester	296	$C_{19}H_{36}O_2$	+	–	–	–

(*continued on next page*)

Table 5.3.2.1 (*continued*)

Compound	MW	Composition	Degradation period			
			0^{WPD}	6^{WPD}	14^{WPD}	26^{WPD}
n-Alkanedioic acids						
Butanedioic acid	118	$C_4H_6O_4$	+	–	+	–
Heptanedioic acid	160	$C_7H_{12}O_4$	+	–	–	–
Nonanedioic acid	188	$C_9H_{16}O_4$	–	+	–	–
hydroxyalkanoic aicds						
α-Hydroxyacetic acid	76	$C_2H_4O_3$	+	+	–	–
α-Hydroxypropanoic acid	90	$C_3H_6O_3$	+	+	+	–
β-hydroxybutanoic acid	104	$C_4H_8O_3$	+	+	+	+
2-Ethyl-β-hydroxypropionic acid	118	$C_5H_{10}O_3$	+	–	–	–
β-Hydroxydecanoic acid	188	$C_{10}H_{20}O_3$	–	–	–	+
2,3,4-Trihydroxybutanoic acid	136	$C_4H_8O_5$	+	–	–	–
Isoprenoid derivatives						
Pristane	268	$C_{19}H_{40}$	–	+	+	–
Phytol	296	$C_{20}H_{40}O$	–	+	–	+
Saccharides						
Arabinoic acid	150	$C_5H_{10}O_5$	+	–	–	–
Xylitol	152	$C_5H_{12}O_5$	+	–	–	–
D-Fructose	180	$C_6H_{12}O_6$	+	+	+	–
D-Galactose	180	$C_6H_{12}O_6$	–	+	–	–
Monoacylglycerols						
Glyceric acid	106	$C_3H_6O_4$	+	–	–	–
Glycerol	92	$C_3H_8O_3$	+	–	–	–
$C_{16:1}$ Monoacylglyceride	328	$C_{19}H_{36}O_4$	+	+	–	–
C_{16} Monoacylglyceride	330	$C_{19}H_{38}O_4$	+	+	–	–
$C_{18:1}$ Monoacylglyceride	356	$C_{21}H_{40}O_4$	+	+	+	–
C_{18} Monoacylglyceride (Stearin)	358	$C_{21}H_{42}O_4$	+	+	–	–
Other compounds						
Phosphoric acid triethyl ester	182	$C_6H_{15}O_4P$	–	+	+	+
9-Octadecenamide, (Z)-	281	$C_{18}H_{35}NO$	–	–	+	–
Cholest-5-en-3 β-ol	386	$C_{27}H_{46}O$	–	–	–	+
Ergost-5-en-3-ol, (3 β,24R)-	400	$C_{28}H_{48}O$	–	–	–	+
Stigmasta-5,22-dien -3β-ol	412	$C_{29}H_{48}O$	–	–	+	+
Stigmasta-5,24(28)-dien-3α-ol	412	$C_{29}H_{48}O$	–	+	–	–
Stigmast-5-en-3β-ol	414	$C_{29}H_{50}O$	–	–	–	+

^{WD} Represents the degradation period in weeks.

+ Represents the occurrence of compounds identified as methyl esters or TMS derivatives in the initial or UV degraded microbial biomass.

– Signifies the absence of compounds in the initial or UV degraded microbial biomass.

5.3.3 Lipid analysis of ambient degraded microbial leachates

Figure 5.3.3.1 shows the TICs of silylated total lipid extracts of microbial leachates degraded under ambient conditions, and clearly demonstrates that all samples were dominated *n*-16:0 and *n*-18:0 saturated fatty acids. Additionally, a homologous series of *n*-alkanoic acids ranging from C_6-$C_{20,}$ $C1_6$-C_{20} and C_9-C_{24} with an even-over-odd predominance were detected in different amounts in the extracts of samples degraded for 6, 14 and 26 weeks, respectively (***Table 5.3.3.1***). Monoenoic fatty acids

were represented by $C_{4:1}$ (ω-2), $C_{8:1}$ (Δ2), $C_{16:1}$ (Δ9) and two isomers of oleic acid [$C_{18:1}$; *cis*-9(*Z*) and *trans*-11(*E*)], the *trans*-11(*E*) configured $C_{18:1}$ was not detected after 6 weeks decomposition. A single C_4 α,ω-di-acid was detected in the sample degraded for 26 weeks, while the isoprenoid derivative phytane was detected at 6 and 14 weeks.

Normal and mono-unsaturated α/β/ω-hydroxy acids (C_2-C_5 and C_{18}) were present in the degraded samples in less significant amounts. *n*-alkanes (C_{16}-C_{26}) with a slight even-over-odd predominance were also detected in relatively low concentrations in the extracts of microbial leachates degraded for 6 and 14 weeks, but were undetected in extract of the sample degraded for 26 weeks. The *n*-alkene, 1-Octadecene was detected in the extracts of the samples degraded for 6 and 14 weeks. Other compounds present in the extracts include benzoic acid which was detected as a minor component in all samples; benzene acetic acid detected only at 6 weeks; the stearic alcohol, octadecan-1-ol and the aromatic ketone, acetophenone which were identified only at 26 weeks. Triethyl phosphate was detected in trace quantities at 6 and 26 weeks (***Table 5.3.3.1***).

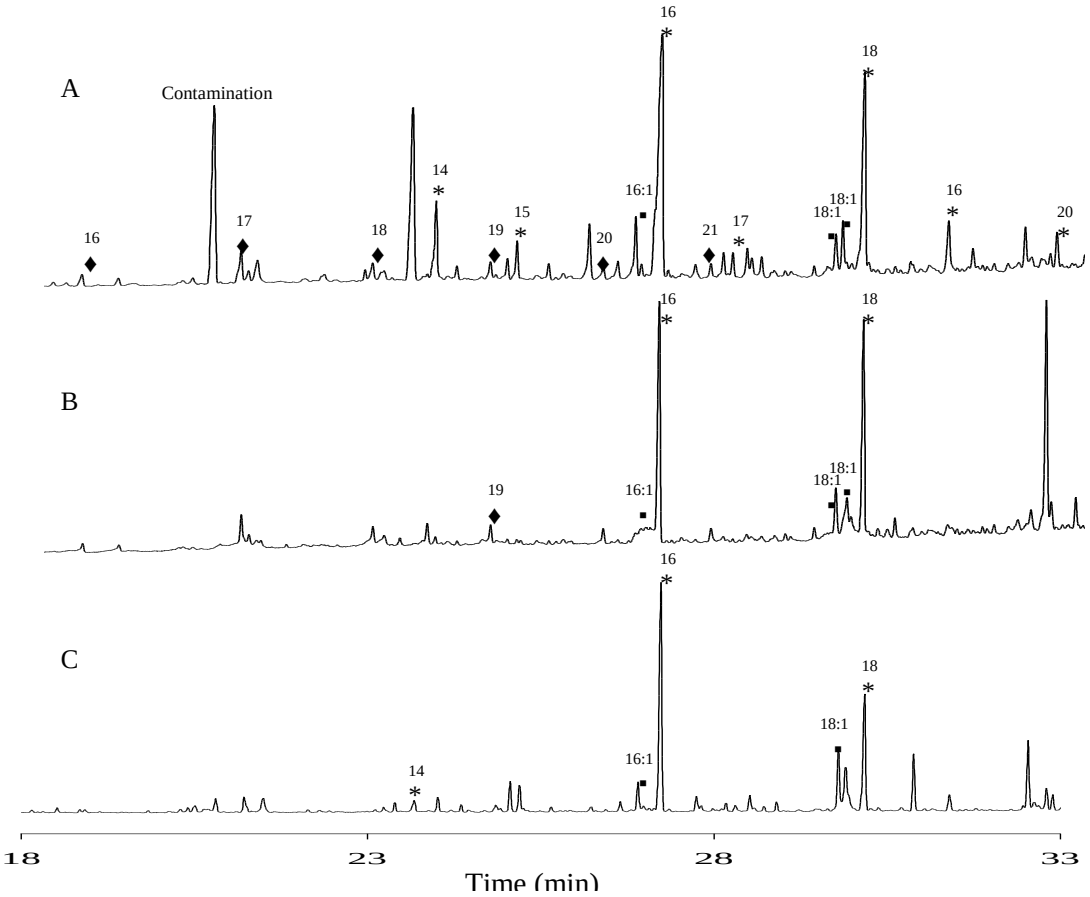

Figure 5.3.3.1: GC-MS chromatograms (TIC) of silylated total lipid extracts of microbial leachates degraded under ambient conditions for (A) 6, (B) 14 and (C) 26 weeks. Numbers refer to total carbon numbers in aliphatic series. ♦ = *n*-alkanes, * = *n*-alkanoic acid, ▪ = *n*-alkenoic acid.

Table 5.3.3.1: Occurrence of identified compounds from the total solvent extracts of microbial leachates degraded under ambient conditions.

Compound	MW	Composition	Degradation period		
			6^{WPD}	14^{WPD}	26^{WPD}
n-Alkanes					
n-Hexadecane	226	$C_{16}H_{34}$	+	–	–
n-Heptadecane	240	$C_{17}H_{36}$	+	+	–
n-Octadecane	254	$C_{18}H_{38}$	+	+	–
n-Nonadecane	268	$C_{19}H_{40}$	+	+	–
n-Eicosane	282	$C_{20}H_{42}$	+	+	–
n-Heneicosane	296	$C_{21}H_{44}$	+	+	–
n-Docosane	310	$C_{22}H_{46}$	+	+	–
n-Pentacosane	352	$C_{25}H_{52}$	–	+	–
n- Hexacosane	366	$C_{26}H_{54}$	+	–	–
n-Alkenes					
1-Octadecene	252	$C_{18}H_{36}$	+	+	–
n-Alkanoic acids					
Hexanoic acid	116	$C_6H_{12}O_2$	+	–	–
Nonanoic acid	158	$C_9H_{18}O_2$	+	–	+
Decanoic acid	172	$C_{10}H_{20}O_2$	+	–	+
Dodecanoic acid	200	$C_{12}H_{24}O_2$	+	–	+
n-Tetradecanoic acid (C_{14})	228	$C_{14}H_{28}O_2$	+	–	+
n-Pentadecanoic acid	242	$C_{15}H_{30}O_2$	+	–	+
n-Hexadecanoic acid (C_{16})	256	$C_{16}H_{32}O_2$	+	+	+
Heptadecanoic acid	270	$C_{17}H_{34}O_2$	+	–	–
n-Octadecanoic acid (C_{18})	284	$C_{18}H_{36}O_2$	+	+	+
n-Eicosanoic acid (C_{20})	312	$C_{20}H_{40}O_2$	+	+	+
n-Docosanoic acid (C_{22})	340	$C_{22}H_{44}O_2$	–	+	+
n-Tetracosanoic acid (C_{24})	368	$C_{24}H_{48}O_2$	–	+	+
n-Alkenoic acids					
2-Butenoic acid	86	$C_4H_6O_2$	+	–	–
2-Octenoic acid	142	$C_8H_{14}O_2$	+	–	+
cis-n-hexadec-9-enoic acid	254	$C_{16}H_{30}O_2$	+	+	+
n-Octadec-9-enoic acid ($C_{18:1}$)	282	$C_{18}H_{34}O_2$	+	+	+
11-cis or trans-Octadecenoic acid	282	$C_{18}H_{34}O_2$	+	–	–
n-Alkanedioic acids					
Butanedioic acid	118	$C_4H_6O_4$	–	–	+
hydroxyalkanoic aicds					
α-Hydroxyacetic acid	76	$C_2H_4O_3$	+	+	–
α-Hydroxypropanoic acid	90	$C_3H_6O_3$	+	+	+
β-hydroxybutanoic acid	104	$C_4H_8O_3$	+	–	–
α-Hydroxy-2-pentenoic acid	116	$C_5H_8O_3$	+	–	–
α-Hydroxypentanedioic acid	148	$C_5H_8O_5$	+	–	–
ω-Hydroxyoctadecanoic acid	300	$C_{18}H_{36}O_3$	+	–	–
Isoprenoid derivatives					
Phytane	282	$C_{20}H_{42}$	+	+	–

(*continued on next page*)

Table 5.3.3.1 (*continued*)

Compound	MW	Composition	Degradation period		
			6^{WPD}	14^{WPD}	26^{WPD}
Other compounds					
α-Acetophenone	120	C_8H_8O	–	–	+
Benzoic acid	122	$C_7H_6O_2$	+	+	+
Benzeneacetic acid	136	$C_8H_8O_2$	+	–	–
Phosphoric acid triethyl ester	182	$C_6H_{15}O_4P$	+	–	+
Octadecan-1-ol	270	$C_{18}H_{38}O$	–	–	+

^{WD} Represents the degradation period in weeks.
+ Represents the occurrence of compounds identified as methyl esters or TMS derivatives in the ambient degraded microbial leachates.
– Signifies the absence of compounds in the ambient degraded microbial leachates.

5.3.4 Lipid analysis of UV degraded microbial leachates

Figure 5.3.4.1 and ***Table 5.3.4.1*** show the occurrences of individual compounds of the organic solvent extracts of the UV degraded microbial leachates. The composition and relative abundances of free lipid classes are largely similar to the organic solvent extracts of the ambient degraded microbial leachates (***Figure 5.3.3.1*** and ***Table 5.3.3.1***) with the exception of a few notable differences. The *n*-alkenes, 1-octadecene and 1-nanodecene were only detected in the extracts of the samples degraded for 6 and 26 weeks, respectively. *n*-Alkanoic acids were found to be less variable in the extracts of the leachates degraded for 14 and 26 weeks, and ranged from C_{14}-C_{18} and C_9-C_{18}, respectively, with a reference of even numbered molecules.

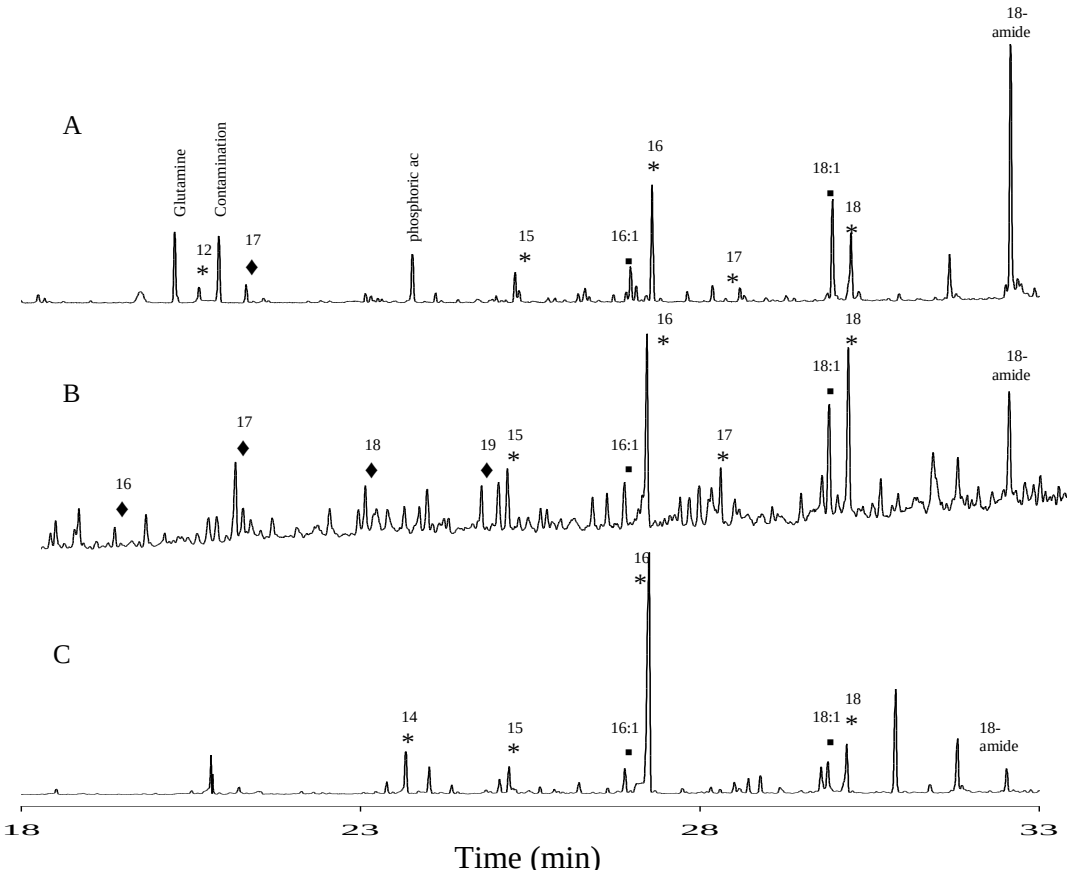

Figure 5.3.4.1: GC-MS chromatograms (TIC) of silylated total lipid extracts of microbial leachates degraded under UV conditions for (A) 6, (B) 14 and (C) 26 weeks. Numbers refer to total carbon numbers in aliphatic series. ♦ = *n*-alkanes, * = *n*-alkanoic acid, ▪ = *n*-alkenoic acid.

Table 5.3.4.1: Occurrence of identified compounds from the total solvent extracts of microbial leachates degraded under UV conditions.

Compound	MW	Composition	Degradation period		
			6^{WPD}	14^{WPD}	26^{WPD}
n-Alkanes					
n-Hexadecane	226	$C_{16}H_{34}$	+	–	–
n-Heptadecane	240	$C_{17}H_{36}$	+	+	–
n-Octadecane	254	$C_{18}H_{38}$	+	+	–
n-Nonadecane	268	$C_{19}H_{40}$	+	+	–
n-Eicosane	282	$C_{20}H_{42}$	+	+	–
n-Heneicosane	296	$C_{21}H_{44}$	+	+	–
n-Docosane	310	$C_{22}H_{46}$	+	+	–
n-Pentacosane	352	$C_{25}H_{52}$	–	+	–
n- Hexacosane	366	$C_{26}H_{54}$	+	–	–
n-Alkenes					
1-Octadecene	252	$C_{18}H_{36}$	+	+	–
n-Alkanoic acids					
Hexanoic acid	116	$C_6H_{12}O_2$	+	–	–
Nonanoic acid	158	$C_9H_{18}O_2$	+	–	+
Decanoic acid	172	$C_{10}H_{20}O_2$	+	–	+
Dodecanoic acid	200	$C_{12}H_{24}O_2$	+	–	+
n-Tetradecanoic acid (C_{14})	228	$C_{14}H_{28}O_2$	+	–	+
n-Pentadecanoic acid	242	$C_{15}H_{30}O_2$	+	–	+
n-Hexadecanoic acid (C_{16})	256	$C_{16}H_{32}O_2$	+	+	+
Heptadecanoic acid	270	$C_{17}H_{34}O_2$	+	–	–
n-Octadecanoic acid (C_{18})	284	$C_{18}H_{36}O_2$	+	+	+
n-Eicosanoic acid (C_{20})	312	$C_{20}H_{40}O_2$	+	+	+
n-Docosanoic acid (C_{22})	340	$C_{22}H_{44}O_2$	–	+	+
n-Tetracosanoic acid (C_{24})	368	$C_{24}H_{48}O_2$	–	+	+
n-Alkenoic acids					
2-Butenoic acid	86	$C_4H_6O_2$	+	–	–
2-Octenoic acid	142	$C_8H_{14}O_2$	+	–	+
cis-n-hexadec-9-enoic acid	254	$C_{16}H_{30}O_2$	+	+	+
n-Octadec-9-enoic acid ($C_{18:1}$)	282	$C_{18}H_{34}O_2$	+	+	+
11-cis or trans-Octadecenoic acid	282	$C_{18}H_{34}O_2$	+	–	–
n-Alkanedioic acids					
Butanedioic acid	118	$C_4H_6O_4$	–	–	+
hydroxyalkanoic aicds					
α-Hydroxyacetic acid	76	$C_2H_4O_3$	+	+	–
α-Hydroxypropanoic acid	90	$C_3H_6O_3$	+	+	+
β-hydroxybutanoic acid	104	$C_4H_8O_3$	+	–	–
α-Hydroxy-2-pentenoic acid	116	$C_5H_8O_3$	+	–	–
α-Hydroxypentanedioic acid	148	$C_5H_8O_5$	+	–	–
ω-Hydroxyoctadecanoic acid	300	$C_{18}H_{36}O_3$	+	–	–
Isoprenoid derivatives					
Phytane	282	$C_{20}H_{42}$	+	+	–

(*continued on next page*)

Table 5.3.4.1 (*continued*)

Compound	MW	Composition	Degradation period		
			6^{WPD}	14^{WPD}	26^{WPD}
Other compounds					
α-Acetophenone	120	C_8H_8O	–	–	+
Benzoic acid	122	$C_7H_6O_2$	+	+	+
Benzeneacetic acid	136	$C_8H_8O_2$	+	–	–
Phosphoric acid triethyl ester	182	$C_6H_{15}O_4P$	+	–	+
Octadecan-1-ol	270	$C_{18}H_{38}O$	–	–	+

^{WD} Represents the degradation period in weeks.
+ Represents the occurrence of compounds identified as methyl esters or TMS derivatives in the UV degraded microbial leachates.
– Signifies the absence of compounds in the UV degraded microbial leachates.

5.3.5 Amino acid analysis of ambient degraded microbial biomass

The acid hydrolysates of the initial and ambient degraded soil microbial biomass yielded a series of proteinogenic and non-proteinogenic amino acids (predominantly L-enantiomers), amino sugars, carbohydrates, amides, purines and pyrimidines (***Figure 5.3.5.1*** and ***Table 5.3.5.1***). Several TMS derivatives of low molecular weight (LMW) hydroxy acids, fatty acid esters of the class *n*-alkanoic acids (C_5-C_{18}), and *n*-alkenoic acids (C_3-C_{18}), were also detected in variable quantities (data not shown). A total of 18 hydrolysable amino acids including the non-proteinogenic amino acid, aminomalonic acid and two uncommon amino acids (L-pyroglutamic acid and hydroxyproline) were detected in the acid hydrolysate of the starting material (***Figure 5.3.5.1A*** and ***Table 5.3.5.1***). Amino acids with neutral, hydrophobic side chains comprised the bulk (53.3%) of the hydrolysable proteinogenic amino acids in the sample. This was followed by amino acids with polar uncharged side chains (20%), and contributions from polar acidic and polar basic residues of 13.3% each. The composition and distribution of hydrolysable proteinogenic amino acids from the biomass degraded for 6 and 26 weeks were identical to that of the starting material, while the non-protein amino acid, aminomalonic acid was detected in the sample degraded for 26 weeks (***Table 5.3.5.1***).

A total of 18 proteinogenic amino acids including homologues of cysteine and serine (DL-homocysteine and L-homoserine, respectively) and isomers of valine and leucine/isoleucine (norvaline and norleucine, respectively) were detected in the biomass degraded for 14 weeks. Two non-protein amino acids, DL-ornithine and hydroproline were also identified. Neutral, hydrophobic residues, polar uncharged, polar acidic and polar basic residues comprised 50, 21.4, 14.3 and 14.3%, respectively of the hydrolysable protein amino acids in the sample degraded for 14 weeks (***Table 5.3.5.1***).

Several amino acids from each group were dominant in the chromatograms, while non-proteinogenic amino acids comprised only a small fraction of the total hydrolysable amino acids in the samples (***Figure 5.3.5.1***). The amino sugars galactosamine and the carbohydrate galactose were identified in variable only in the starting material and at 6 weeks degradation, while myo-inositol and glucose were only detected in the starting material and at 14 weeks, respectively. Glucosamine was present in variable concentrations in all samples. Other nitrogenous based compounds including nucleic acid components, purines and pyrimidines; and the primary amine/primary alcohol ethanolamine were also present in the hydrolysates of all samples, while urea was only identified in the samples degraded for 6 and 14 weeks.

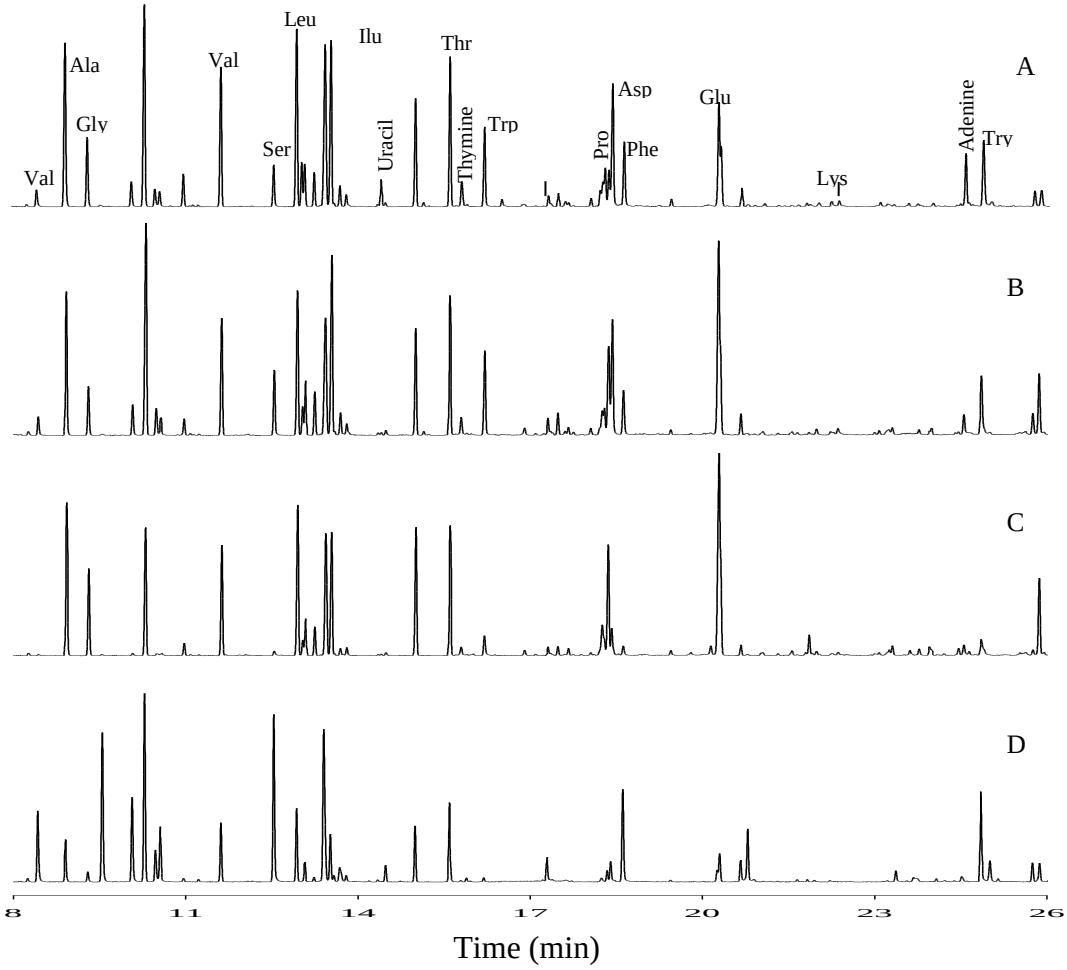

Figure 5.3.5.1: GC-MS chromatograms (TIC) of silylated acid hydrolysates of (A) initial microbial biomass and microbial biomass degraded under ambient conditions for (B) 6, (C) 14 and (D) 26 weeks. Amino acids are designated by the three letter code.

Table 5.3.5.1: Occurrence of identified compounds from the acid hydrolysates of initial microbial biomass and microbial biomass degraded under ambient conditions.

Compound	MW	Composition	Degradation period			
			0 WPD	6WPD	14WPD	26 WPD
Amino acids						
Glycine	72	$C_2H_5NO_2$	+	+	+	+
L-Alanine	89	$C_3H_7NO_2$	+	+	+	+
Serine	105	$C_3H_7NO_3$	+	+	+	+
L-Aspartic	133	$C_4H_7NO_4$	+	+	+	+
DL-Homocysteine	135	$C_4H_9NO_2S$	–	–	+	–
L-Homoserine derivative	119	$C_4H_9NO_3$	–	–	+	–
L-Threonine	119	$C_4H_9NO_3$	+	+	+	+
L-Pyroglutamic acid	129	$C_5H_7NO_3$	+	–	–	–
L-Proline	115	$C_5H_9NO_2$	+	+	+	+
L-Glutamic acid	147	$C_5H_9NO_4$	+	+	+	+
L-Valine	117	$C_5H_{11}NO_2$	+	+	+	+
DL-Norvaline	117	$C_5H_{11}NO_2$	–	–	+	–
DL-Ornithine	132	$C_5H_{12}N_2O_2$	–	–	+	–
L-Histidine	155	$C_6H_9N_3O_2$	+	+	+	+
L-Leucine	131	$C_6H_{13}NO_2$	+	+	–	+
L-Norleucine	131	$C_6H_{13}NO_2$	–	–	+	–
DL-Isoleucine	131	$C_6H_{13}NO_2$	+	+	+	+
L-Lysine	146	$C_6H_{14}N_2O_2$	+	+	+	+
Hydroxyproline	131	$C_9H_9NO_3$	+	–	+	–
L-phenylalanine	165	$C_9H_{11}NO_2$	+	+	+	+
Tyrosine	181	$C_9H_{11}NO_3$	+	+	+	+
DL-Tryptophan	204	$C_{11}H_{12}N_2O_2$	+	+	+	+
Aminomalonic acid	119	$C_3H_5NO_4$	+	–	–	+
Amino sugars						
Galactosamine	179	$C_6H_{13}NO_5$	+	+	–	–
D-Glucosamine, N-acetyl	221	$C_{18}H_{15}NO_6$	+	+	+	+
Carbohydrates						
Glucose	180	$C_6H_{12}O_6$	–	–	+	–
Galactose	180	$C_6H_{12}O_6$	+	+	–	–
Myo-Inositol	180	$C_6H_{12}O_6$	+	–	–	–
Purines						
Adenine	135	$C_5H_5N_5$	+	+	+	+
Guanine	151	$C_5H_5N_5O$	+	+	–	–
Pyrimidines						
Uracil	112	$C_4H_4N_2O_2$	+	+	+	+
Cytosine	111	$C_4H_5N_3O$	+	+	+	+
Thymine	126	$C_5H_6N_2O_2$	+	+	+	+
Amino alcohols						
Ethanolamine	61	C_2H_7NO	+	+	+	+
Other compounds						
Urea	60	CH_4N_2O	–	+	+	–

WD Represents the degradation period in weeks. + Represents the occurrence of compounds identified from silylated hydrolysates of initial or degraded microbial biomass. – Signifies the absence of compounds in the hydrolysates of initial or degraded microbial biomass.

5.3.6 Amino acid analysis of UV degraded microbial biomass

The occurrences of individual compounds of acid hydrolysates of the initial and UV degraded microbial biomass are presented in ***Figure 5.3.6.1*** and ***Table 5.3.6.1*** and are almost identical to those of the ambient degraded biomass (***Figure 5.3.5.1*** and ***Table 5.3.5.1***). The most notable differences include the detection of trace amounts of pyroglutamic acid in the UV degraded samples and urea in the extract of the sample degraded for 26 weeks. We also failed to detect homocysteine, homoserine and norvaline in the UV degraded biomass (***Table 5.3.6.1***).

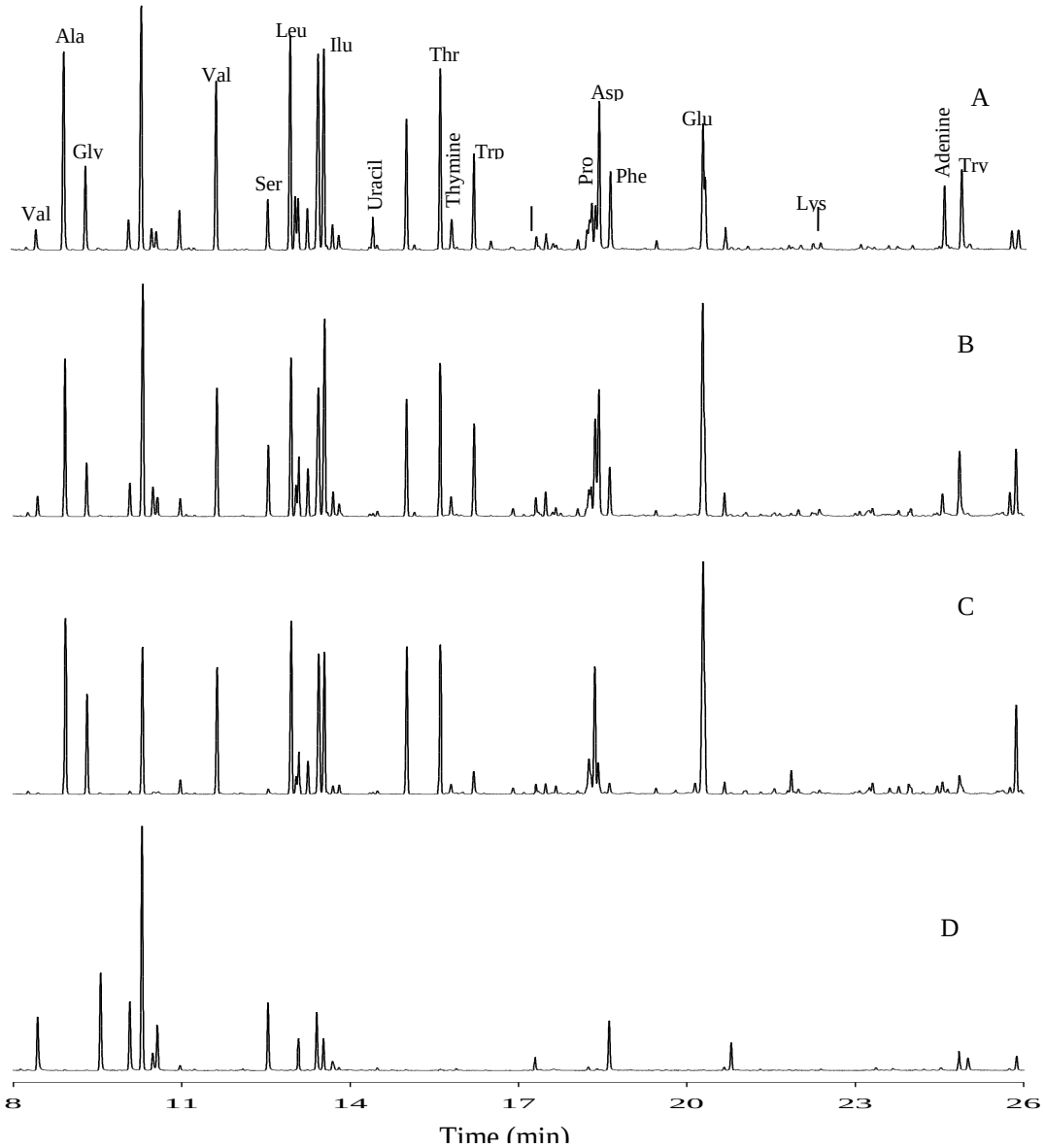

Figure 5.3.6.1: GC-MS chromatograms (TIC) of silylated acid hydrolysates of (A) initial microbial biomass and microbial biomass degraded under UV conditions for (B) 6, (c) 14 and (D) 26 weeks. Amino acids are designated by the three letter code.

Table 5.3.6.1: Occurrence of identified compounds from the acid hydrolysates of initial microbial biomass and microbial biomass degraded under UV conditions.

Compound	MW	Composition	Degradation period			
			0^{WPD}	6^{WPD}	14^{WPD}	26^{WPD}
Amino acids						
Glycine	72	$C_2H_5NO_2$	+	+	+	+
L-Alanine	89	$C_3H_7NO_2$	+	+	+	+
Serine	105	$C_3H_7NO_3$	+	+	+	+
L-Aspartic	133	$C_4H_7NO_4$	+	+	+	+
L-Threonine	119	$C_4H_9NO_3$	+	+	+	+
L-Pyroglutamic acid	129	$C_5H_7NO_3$	+	+	+	+
L-Proline	115	$C_5H_9NO_2$	+	+	+	+
L-Glutamic acid	147	$C_5H_9NO_4$	+	+	+	+
L-Valine	117	$C_5H_{11}NO_2$	+	+	+	+
DL-Ornithine	132	$C_5H_{12}N_2O_2$	–	–	+	–
L-Histidine	155	$C_6H_9N_3O_2$	+	+	+	+
L-Leucine	131	$C_6H_{13}NO_2$	+	+	+	+
L-Norleucine	131	$C_6H_{13}NO_2$	–	–	+	–
DL-Isoleucine	131	$C_6H_{13}NO_2$	+	+	+	+
L-Lysine	146	$C_6H_{14}N_2O_2$	+	+	–	+
Hydroxyproline	131	$C_9H_9NO_3$	+	–	–	–
L-phenylalanine	165	$C_9H_{11}NO_2$	+	+	+	+
Tyrosine	181	$C_9H_{11}NO_3$	+	+	+	+
DL-Tryptophan	204	$C_{11}H_{12}N_2O_2$	+	+	+	+
Aminomalonic acid	119	$C_3H_5NO_4$	+	+	+	+
Amino sugars						
Galactosamine	179	$C_6H_{13}NO_5$	+	–	–	–
D-Glucosamine, N-acetyl	221	$C_{18}H_{15}NO_6$	+	+	+	+
Carbohydrates						
Galactose	180	$C_6H_{12}O_6$	+	+	+	+
Myo-Inositol	180	$C_6H_{12}O_6$	+	+	–	+
Purines						
Adenine	135	$C_5H_5N_5$	+	+	+	+
Guanine	151	$C_5H_5N_5O$	+	+	–	–
Pyrimidines						
Uracil	112	$C_4H_4N_2O_2$	+	+	+	+
Cytosine	111	$C_4H_5N_3O$	+	+	+	+
Thymine	126	$C_5H_6N_2O_2$	+	+	+	+
Amino alcohols						
Ethanolamine	61	C_2H_7NO	+	+	+	+
Other compounds						
Urea	60	CH_4N_2O	–	+	+	+

^{WD} Represents the UV degradation period in weeks. + Represents the occurrence of compounds identified from silylated hydrolysates of initial or UV degraded microbial biomass. – Signifies the absence of compounds in the hydrolysates of initial or UV degraded microbial biomass.

5.3.7 Lipid analysis of ambient degraded montmorillonite-complexes

The TICs of the organic solvent extracts of initial (starting material) and degraded momtmorillonite-microbial complexes are presented in ***Figure 5.3.7.1*** and contain a series of aliphatic lipids [*n*-alkanes (C_{17}, C_{18} and C_{26} detected only in the starting material), *n*-alkanoic acids, *n*-alkenoic acids, normal α/β/ω-hydroxy acids, and di-acid], steroids, glycerol, monoacylglyciredes, and carbohydrates. Occurrences of individual compounds are given in ***Table 5.3.7.1***. The *n*-alkanoic acids (C_6-C_{22}), including C_{16} and C_{18} methyl esters are the major components of the starting material with a preference of even numbered molecules and the highest relative abundances (C_{max}) at C_{16} and C_{18} are predominant lipids in the extract. These compounds ranged from C_{16}; C_{22} in after 6 weeks; C_{14}–C_{18} after 14 weeks and C_{15}–C_{24} after 26 weeks decomposition. Mono- and polyenoic fatty acids (including *cis*-configurated $C_{16:1}$ methyl ester) ranged from C_4–C_{18} with a strong even-over-odd dominance were detected in variable amounts in the starting material. Methyl interrupted polyeonic fatty acids were represented by $C_{18:3}$ and $C_{18:2}$ (*n*9) molecules were only detected in the starting material. Normal-alkenoic acids C_6-C_{18} including *cis*-configured C_{18} methyl esters were less variable in the degraded complexes (C_6; C_8 and C_{14}–C_{18}; ***Table 5.3.7.1***). Mono-saturated C_{18} acid was represented by 9(*Z*) and 11(*E*) isomers

The *n*-alkanedioic acids, butanidioic acid and *n*-octadeca-9,12-dienoic acid-methyl ester were identified only the starting material, while 1,10-decanedioic acid were detected as major components at 6 and 14 weeks. Normal α/β/ω-hydroxy acids were detected only in the solvent extract of the starting material and ranged from C_3–C_{14}, while 9, 10-epoxy-18-hydroxyoctadecanoic acid was detected in the complex degraded for 14 weeks and was the only hydroxyacid detected in the degraded samples. The free carbohydrates detected in the initial complex were arabinoic acid, fructose, galactose, xylitol and galactitol, while the disaccharide sucrose was the only free carbohydrate detected in the solvent extracts of the degraded complexes. Glyceric acid was present only in the starting material, variable amounts of glycerol and C_{16} monoacylglyceride were detected in all samples, while $C_{18:1}$ monoacylglyceride was identified only in the degraded complexes and C_{18} monoacylglyceride (stearin) detected in the starting material and the complex degraded for 26 weeks. The mono-saturated alkyl amide, 9-octadecenamide was detected in all degraded complexes and oleanitrile detected only at 26 weeks. Two steroids, C_{27}-cholest-5-en-3β-ol and C_{29}-stigmasta-5,22-dien-3β-ol (stigmasterol) were also detected as major components in all sample. A mixture of

other sterols including ergosta-5-en-3β-ol and ergost-5,7,22-trien-3α-ol (detected only at 26 weeks); cholesta-5,24-diene, 3α- and stigmast-5-en-3β-ol (detected only at 14 and 26 weeks); and ergosta-5,22-dien-3α-ol acetate (identified at 6 and 14 weeks) were also major components of the degraded complexes.

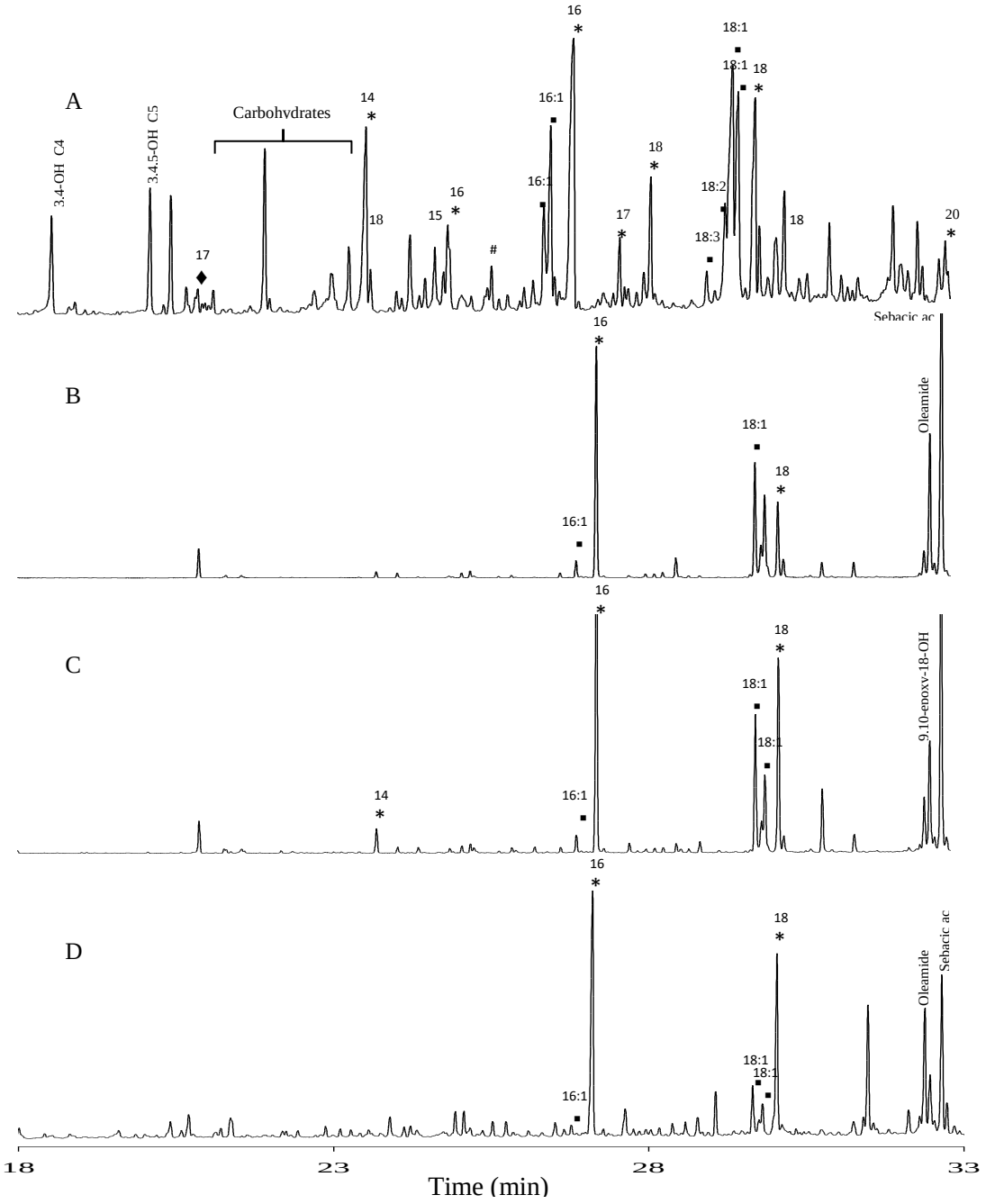

Figure 5.3.7.1: GC-MS chromatograms (TIC) of silylated total lipid extracts of (A) initial montmorillonite-microbial complex and montmorillonite-microbial complexes degraded under ambient conditions for (B) 6, (C) 14 and (D) 26 weeks. Numbers refer to total carbon numbers in aliphatic series. ♦ = *n*-alkanes, * = *n*-alkanoic acid, ▪ = *n*-alkenoic acid, # = carbohydrates and ac = acid.

Table 5.3.7.1: Occurrence of identified compounds from the total solvent extracts of initial montmorillonite-microbial complex and montmorillonite-microbial complexes degraded under ambient conditions.

Compound	MW	Composition	Degradation period			
			0^{WPD}	6^{WPD}	14^{WPD}	26^{WPD}
n-Alkanes						
n-Heptadecane	240	$C_{17}H_{36}$	+	–	–	–
n-Eicosane	282	$C_{20}H_{42}$	+	–	–	–
n-Octadecane	254	$C_{18}H_{38}$	+	–	–	–
n- Hexacosane	366	$C_{26}H_{54}$	+	–	–	–
n-Alkanoic acids						
Hexanoic acid	116	$C_6H_{12}O_2$	+	–	–	–
n-Tetradecanoic acid (C_{14})	228	$C_{14}H_{28}O_2$	+	–	+	–
n-Pentadecanoic acid	242	$C_{15}H_{30}O_2$	+	–	+	+
n-Hexadecanoic acid (C_{16})	256	$C_{16}H_{32}O_2$	+	+	+	+
n-Hexadecanoic acid methyl ester	270	$C_{17}H_{34}O_2$	+	–	–	–
Heptadecanoic acid	270	$C_{17}H_{34}O_2$	+	–	+	–
n-Octadecanoic acid (C_{18})	284	$C_{18}H_{36}O_2$	+	+	+	+
Octadecanoic acid, methyl ester	298	$C_{19}H_{38}O_2$	+	–	–	–
n-Eicosanoic acid (C_{20})	312	$C_{20}H_{40}O_2$	+	–	–	+
n-Docosanoic acid (C_{22})	340	$C_{22}H_{44}O_2$	+	–	–	+
n-Tetracosanoic acid (C_{24})	368	$C_{24}H_{48}O_2$	–	–	–	+
n-Alkenoic acids						
2-Butenoic acid	86	$C_4H_6O_2$	+	–	–	–
2-Pentenoic acid	100	$C_5H_8O_2$	+	–	–	–
2-Hexenoic acid	114	$C_6H_{10}O_2$	–	–	–	+
2-Octenoic acid	142	$C_8H_{14}O_2$	+	–	+	+
cis-n-hexadec-9-enoic acid	254	$C_{16}H_{30}O_2$	+	+	+	+
9-Hexadecenoic acid, methyl ester, (Z)-	268	$C_{17}H_{32}O_2$	+	–	–	–
n-Octadeca-3,6,9-trienoic acid ($C_{18:3}$)	278	$C_{18}H_{30}O_2$	+	–	–	–
n-Octadeca-9,12-dienoic acid ($C_{18:2}$)	280	$C_{18}H_{32}O_2$	+	–	–	–
n-Octadec-9-enoic acid ($C_{18:1}$)	282	$C_{18}H_{34}O_2$	+	+	+	–
11-cis or trans-Octadecenoic acid	282	$C_{18}H_{34}O_2$	–	+	+	+
8 or 9-Octadecenoic acid (Z)-, methyl ester	296	$C_{19}H_{36}O_2$	–	–	+	–
n-Alkanedioic acids (di-acids)						
Butanedioic acid	118	$C_4H_6O_4$	+	–	–	–
1,10-Decanedioic acid	202	$C_{10}H_{18}O_4$	–	+	+	–
n-Octadeca-9,12-dienoic acid-methyl ester	294	$C_{19}H_{34}O_2$	+	–	–	–
hydroxyalkanoic aicds						
α-Hydroxypropanoic acid	90	$C_3H_6O_3$	+	–	–	–
β-hydroxybutanoic acid	104	$C_4H_8O_3$	+	–	–	–
(R*,S*)-3,4-Dihydroxybutanoic acid	120	$C_4H_8O_4$	+	–	–	–
2,3,4-Trihydroxybutanoic acid	136	$C_4H_8O_5$	+	–	–	–
3,4,5-Trihydroxypentanoic acid	150	$C_5H_{10}O_5$	+	–	–	–
3-Hydroxyoctanoic acid	160	$C_8H_{16}O_3$	+	–	–	–
3-Hydroxytetradecanoic acid	244	$C_{14}H_{28}O_3$	+	–	–	–
9,10-epoxy-18- hydroxyoctadecanoic acid	314	$C_{18}H_{34}O_4$	–	–	+	–

(*continued on next page*)

Table 5.3.7.1 (*continued*)

Compound	MW	Composition	Degradation period			
			0^{WPD}	6^{WPD}	14^{WPD}	26^{WPD}
Saccharides						
Arabinoic acid	150	$C_5H_{10}O_5$	+	–	–	–
Xylitol	152	$C_5H_{12}O_5$	+	–	–	–
D-Fructose	180	$C_6H_{12}O_6$	+	–	–	–
D-Galactose	180	$C_6H_{12}O_6$	+	–	–	–
Galactitol	182	$C_6H_{14}O_6$	+	–	–	–
Sucrose	342	$C_{12}H_{22}O_{11}$	–	+	+	+
Monoacylglycerols						
Glyceric acid	106	$C_3H_6O_4$	+	–	–	–
Glycerol	92	$C_3H_8O_3$	+	+	+	+
C_{16} Monoacylglyceride	330	$C_{19}H_{38}O_4$	+	+	+	+
$C_{18:1}$ Monoacylglyceride	356	$C_{21}H_{40}O_4$	–	+	+	+
C_{18} Monoacylglyceride (Stearin)	358	$C_{21}H_{42}O_4$	+	–	–	+
Other compounds						
Oleanitrile	263	$C_{18}H_{33}N$	–	–	–	+
9-Octadecenamide	281	$C_{18}H_{35}NO$	–	+	+	+
Cholesta-5,24-diene, 3 α -	384	$C_{27}H_{44}O$	–	–	+	+
Cholest-5-en-3 β-ol	386	$C_{27}H_{46}O$	+	+	+	+
Ergosta-5,7,22-trien-3-α-ol	396	$C_{28}H_{44}O$	–	–	–	+
Ergost-5-en-3-ol, (3 β,24R)-	400	$C_{28}H_{48}O$	–	–	–	+
Stigmasta-5,22-dien -3β-ol	412	$C_{29}H_{48}O$	+	+	+	+
Stigmast-5-en-3β-ol	414	$C_{29}H_{50}O$	–	–	+	+
Ergosta-5,22-dien-3-ol, acetate	440	$C_{30}H_{48}O_2$	–	+	+	–

^{WD} Represents the degradation period in weeks.

+ Represents the occurrence of compounds identified as methyl esters or TMS derivatives in the initial or ambient degraded montmorillonite-microbial complexes.

– Signifies the absence of compounds in the initial or ambient degraded montmorillonite-microbial complexes.

5.3.8 Lipid analysis of UV degraded montmorillonite-complexes

The compositions of the organic solvent extracts of the UV degraded montmorillonite-complexes are illustrated in ***Figure 5.3.8.1*** and ***Table 5.3.8.1*** and are identical in all respects to those of the ambient degraded montmorillonite-complexes (***Figure 5.3.7.1*** and ***Table 5.3.7.1***).

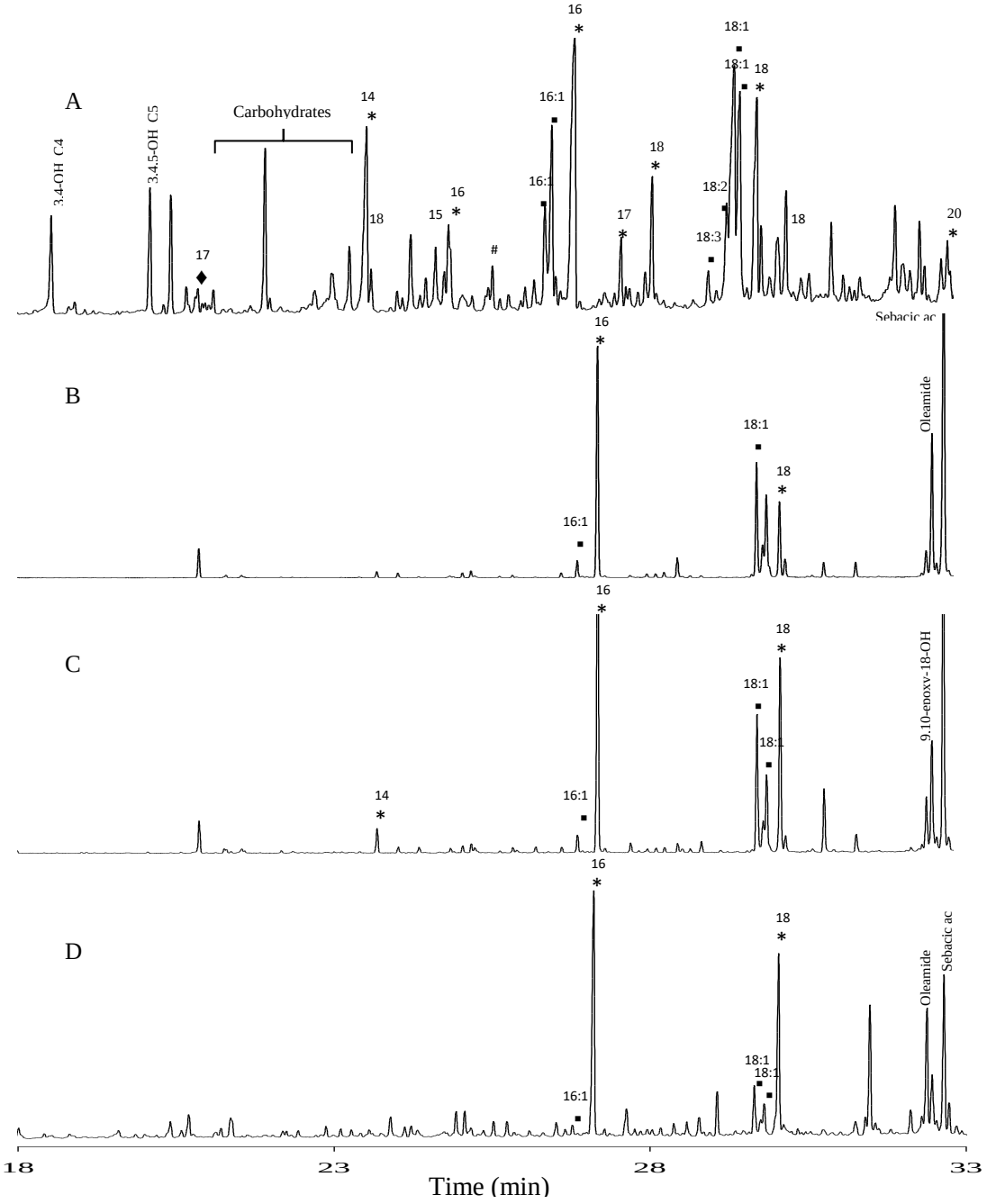

Figure 5.3.8.1: GC-MS chromatograms (TIC) of silylated total lipid extracts of (A) initial montmorillonite-microbial complex and montmorillonite-microbial complexes degraded under UV conditions for (B) 6, (C) 14 and (D) 26 weeks. Numbers refer to total carbon numbers in aliphatic series. ♦ = *n*-alkanes, * = *n*-alkanoic acid, ▪ = *n*-alkenoic acid, # = carbohydrates and ac = acid.

Table 5.3.8.1: Occurrence of identified compounds from the total solvent extracts of initial montmorillonite-microbial complex and montmorillonite-microbial complexes degraded under UV conditions.

Compound	MW	Composition	Degradation period			
			0^{WPD}	6^{WPD}	14^{WPD}	26^{WPD}
n-Alkanes						
n-Heptadecane	240	$C_{17}H_{36}$	+	–	–	–
n-Octadecane	254	$C_{18}H_{38}$	+	–	–	–
n- Hexacosane	366	$C_{26}H_{54}$	+	–	–	–
n-Alkanoic acids						
Hexanoic acid	116	$C_6H_{12}O_2$	+	–	–	–
n-Tetradecanoic acid (C_{14})	228	$C_{14}H_{28}O_2$	+	–	+	–
n-Pentadecanoic acid	242	$C_{15}H_{30}O_2$	+	–	+	+
n-Hexadecanoic acid (C_{16})	256	$C_{16}H_{32}O_2$	+	+	+	+
n-Hexadecanoic acid methyl ester	270	$C_{17}H_{34}O_2$	+	–	–	–
Heptadecanoic acid	270	$C_{17}H_{34}O_2$	+	–	+	–
n-Octadecanoic acid (C_{18})	284	$C_{18}H_{36}O_2$	+	+	+	+
Octadecanoic acid, methyl ester	298	$C_{19}H_{38}O_2$	+	–	–	–
n-Eicosanoic acid (C_{20})	312	$C_{20}H_{40}O_2$	+	–	–	+
n-Docosanoic acid (C_{22})	340	$C_{22}H_{44}O_2$	+	–	–	+
n-Tetracosanoic acid (C_{24})	368	$C_{24}H_{48}O_2$	–	–	–	+
n-Alkenoic acids						
2-Butenoic acid	86	$C_4H_6O_2$	+	–	–	–
2-Pentenoic acid	100	$C_5H_8O_2$	+	–	–	–
2-Hexenoic acid	114	$C_6H_{10}O_2$	–	–	–	+
2-Octenoic acid	142	$C_8H_{14}O_2$	+	–	+	+
cis-n-hexadec-9-enoic acid	254	$C_{16}H_{30}O_2$	+	+	+	+
9-Hexadecenoic acid, methyl ester, (Z)-	268	$C_{17}H_{32}O_2$	+	–	–	–
n-Octadeca-3,6,9-trienoic acid ($C_{18:3}$)	278	$C_{18}H_{30}O_2$	+	–	–	–
n-Octadeca-9,12-dienoic acid ($C_{18:2}$)	280	$C_{18}H_{32}O_2$	+	–	–	–
n-Octadec-9-enoic acid ($C_{18:1}$)	282	$C_{18}H_{34}O_2$	+	+	+	–
11-cis or trans-Octadecenoic acid	282	$C_{18}H_{34}O_2$	–	+	+	+
8 or 9-Octadecenoic acid (Z)-, methyl ester	296	$C_{19}H_{36}O_2$	–	–	+	–
n-Alkanedioic acids (di-acids)						
Butanedioic acid	118	$C_4H_6O_4$	+	–	–	–
1,10-Decanedioic acid	202	$C_{10}H_{18}O_4$	–	+	+	–
n-Octadeca-9,12-dienoic acid-methyl ester	294	$C_{19}H_{34}O_2$	+	–	–	–
hydroxyalkanoic aicds						
α-Hydroxypropanoic acid	90	$C_3H_6O_3$	+	–	–	–
β-hydroxybutanoic acid	104	$C_4H_8O_3$	+	–	–	–
(R*,S*)-3,4-Dihydroxybutanoic acid	120	$C_4H_8O_4$	+	–	–	–
2,3,4-Trihydroxybutanoic acid	136	$C_4H_8O_5$	+	–	–	–
3,4,5-Trihydroxypentanoic acid	150	$C_5H_{10}O_5$	+	–	–	–
β-Hydroxyoctanoic acid	160	$C_8H_{16}O_3$	+	–	–	–
β-Hydroxytetradecanoic acid	244	$C_{14}H_{28}O_3$	+	–	–	–
9,10-epoxy-18- hydroxyoctadecanoic acid	314	$C_{18}H_{34}O_4$	–	–	+	–

(*continued on next page*)

Table 5.3.8.1 (*continued*)

Compound	MW	Composition	Degradation period			
			0^{WPD}	6^{WPD}	14^{WPD}	26^{WPD}
Saccharides						
Arabinoic acid	150	$C_5H_{10}O_5$	+	–	–	–
Xylitol	152	$C_5H_{12}O_5$	+	–	–	–
D-Fructose	180	$C_6H_{12}O_6$	+	–	–	–
D-Galactose	180	$C_6H_{12}O_6$	+	–	–	–
Galactitol	182	$C_6H_{14}O_6$	+	–	–	–
Sucrose	342	$C_{12}H_{22}O_{11}$	–	+	+	+
Monoacylglycerols						
Glyceric acid	106	$C_3H_6O_4$	+	–	–	–
Glycerol	92	$C_3H_8O_3$	+	+	+	+
C_{16} Monoacylglyceride	330	$C_{19}H_{38}O_4$	+	+	+	+
$C_{18:1}$ Monoacylglyceride	356	$C_{21}H_{40}O_4$	–	+	+	+
C_{18} Monoacylglyceride (Stearin)	358	$C_{21}H_{42}O_4$	+	–	–	+
Other compounds						
Oleanitrile	263	$C_{18}H_{33}N$	–	–	–	+
9-Octadecenamide	281	$C_{18}H_{35}NO$	–	+	+	+
Cholesta-5,24-diene, 3 α -ol	384	$C_{27}H_{44}O$	–	–	+	+
Cholest-5-en-3 β-ol	386	$C_{27}H_{46}O$	+	+	+	+
Ergosta-5,7,22-trien-3-α-ol	396	$C_{28}H_{44}O$	–	–	–	+
Ergost-5-en-3-ol, (3 β,24R)-	400	$C_{28}H_{48}O$	–	–	–	+
Stigmasta-5,22-dien -3β-ol	412	$C_{29}H_{48}O$	+	+	+	+
Stigmast-5-en-3β-ol	414	$C_{29}H_{50}O$	–	–	+	+
Ergosta-5,22-dien-3-ol, acetate	440	$C_{30}H_{48}O_2$	–	+	+	–

^{WD} Represents the degradation period in weeks.

+ Represents the occurrence of compounds identified as methyl esters or TMS derivatives in the initial or UV degraded montmorillonite-microbial complexes.

– Signifies the absence of compounds in the initial or UV degraded montmorillonite-microbial complexes.

5.3.9 Lipid analysis of ambient degraded montmorillonite-microbial leachates

The chemical composition of solvent extractable lipids in montmorillonite-microbial leachates degraded under ambient conditions varied significantly from that of the clay-complexes (***Figure 5.3.7.1*** and ***Table 5.3.7.1***). Occurrences of individual compounds identified in the solvent extracts of degraded montmorillonite-microbial leachates are presented in ***Figure 5.3.9.1*** and ***Table 5.3.9.1***. Major compounds in the solvent extracts were a series of *n*-alkanoic acids (C_6-C_{18}) and comprised the predominant components of the solvent extracts with a strong preference of even numbered molecules and C_{max} at C_{16} and C_{18}. Compounds of the class *n*-alkenoic acids (C_4, C_5, C_{16}, C_{18}) and one hydroxy acid (α-Hydroxyacetic acid) were detected in significant proportions in the samples. Glycerol was detected only at 26 weeks, while C_{16} monoacylglyceride was detected in the extracts of the samples degraded for 6 and 14 weeks. Other compounds detected in considerable quantities were the N-containing

compounds; urea and oleanitrile (present only in the solvent extract of montmorillonite-complex leachate degraded for 26 weeks) and oleamide.

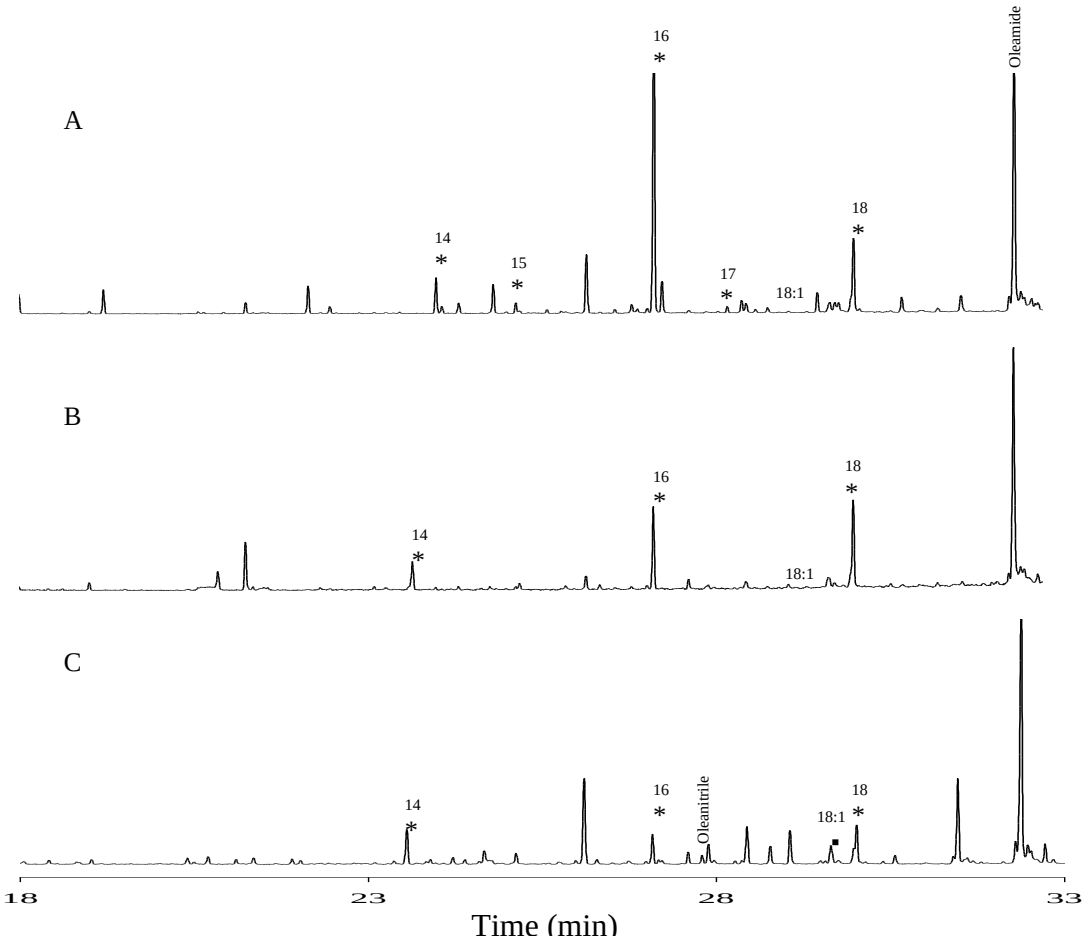

Figure 5.3.9.1: GC-MS chromatograms (TIC) of silylated lipids from the total solvent extracts of the leachates of montmorillonite-microbial complexes degraded under ambient conditions for (A) 6, (B) 14 and (C) 26 weeks. Numbers refer to total carbon numbers in aliphatic series. * = *n*-alkanoic acid and ▪ = *n*-alkenoic acid.

Table 5.3.9.1: Occurrence of identified compounds from the total solvent extracts of the leachates of montmorillonite-microbial complexes degraded under ambient conditions.

Compound	MW	Composition	Degradation period		
			6^{WPD}	14^{WPD}	26^{WPD}
n-Alkanoic acids					
Hexanoic acid	116	$C_6H_{12}O_2$	–	–	+
Octanoic acid	144	$C_8H_{16}O_2$	–	–	+
Nonanoic acid	158	$C_9H_{18}O_2$	–	–	+
Decanoic acid	172	$C_{10}H_{20}O_2$	–	–	+
Dodecanoic acid	200	$C_{12}H_{24}O_2$	–	–	+
n-Tetradecanoic acid (C_{14})	228	$C_{14}H_{28}O_2$	+	–	–
n-Pentadecanoic acid	242	$C_{15}H_{30}O_2$	+	–	–
n-Hexadecanoic acid (C_{16})	256	$C_{16}H_{32}O_2$	+	+	+
Heptadecanoic acid	270	$C_{17}H_{34}O_2$	+	–	–
n-Octadecanoic acid (C_{18})	284	$C_{18}H_{36}O_2$	+	+	+
n-Alkenoic acids					
2-Butenoic acid	86	$C_4H_6O_2$	+	–	–
2-Pentenoic acid	100	$C_5H_8O_2$	+	–	–
Hexadecenoic acid	254	$C_{16}H_{30}O_2$	+	+	–
11-cis or trans-Octadecenoic acid	282	$C_{18}H_{34}O_2$	+	+	+
hydroxyalkanoic aicds					
α-Hydroxyacetic acid	76	$C_2H_4O_3$	+	+	+
Monoacylglycerols					
Glycerol	92	$C_3H_8O_3$	–	+	+
C_{16} Monoacylglyceride	330	$C_{19}H_{38}O_4$	+	+	–
Other compounds					
Urea	60	CH_4N_2O	–	–	+
Oleanitrile	263	$C_{18}H_{33}N$	–	–	+
Oleamide	281	$C_{18}H_{35}NO$	+	+	+

^{WD} Represents the degradation period in weeks.

+ Represents the occurrence of compounds identified as methyl esters or TMS derivatives in ambient degraded montmorillonite-microbial leachates.

– Signifies the absence of compounds in ambient degraded montmorillonite-microbial leachates.

5.3.10 Lipid analysis of UV degraded montmorillonite-microbial leachates

In ***Figure 5.3.10.1*** and ***Table 5.3.10.1*** the occurrences of individual compounds of the organic solvent extracts of the UV degraded montmorillonite-microbial leachates are shown. Except for C_8 and C_9 di-acids and β-hydroxybutanoic acid detected 26 weeks after degradation, the composition and relative abundances of free lipid classes are largely similar to the organic solvent extracts of the ambient degraded leachates (***Figure 5.3.9.1*** and ***Table 5.3.9.1***).

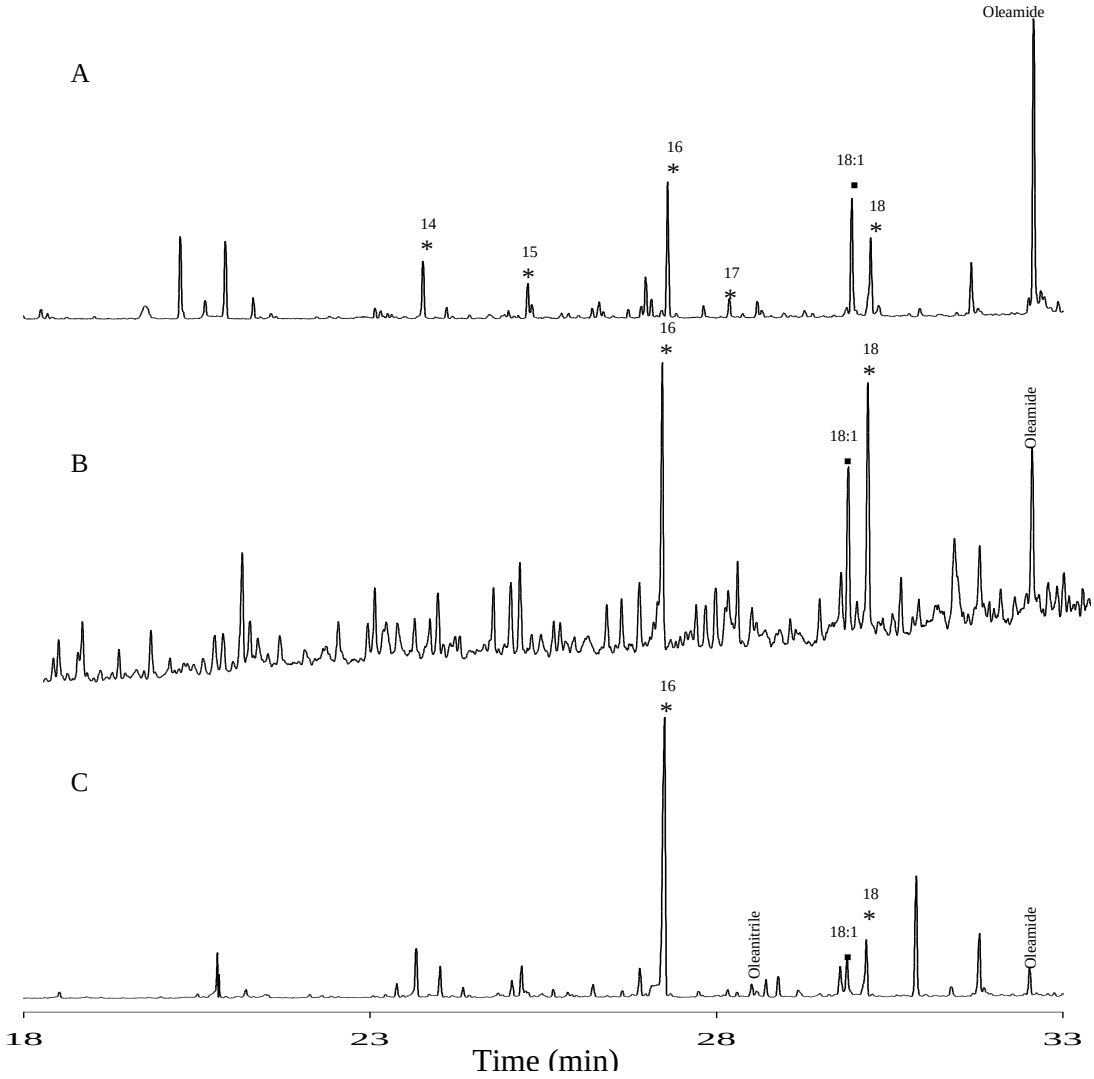

Figure 5.3.10.1: GC-MS chromatograms (TIC) of silylated lipids from the total solvent extracts of the leachates of montmorillonite-microbial complexes degraded under UV conditions for (A) 6, (B) 14 and (C) 26 weeks. Numbers refer to total carbon numbers in aliphatic series. * = *n*-alkanoic acid and ▪ = *n*-alkenoic acid.

Table 5.3.10.1: Occurrence of identified compounds from the total solvent extracts of the leachates of montmorillonite-microbial complexes degraded under UV conditions.

Compound	MW	Composition	Degradation period		
			6^{WPD}	14^{WPD}	26^{WPD}
n-Alkanoic acids					
Hexanoic acid	116	$C_6H_{12}O_2$	–	–	+
Octanoic acid	144	$C_8H_{16}O_2$	–	–	+
Nonanoic acid	158	$C_9H_{18}O_2$	–	–	+
Decanoic acid	172	$C_{10}H_{20}O_2$	–	–	+
Dodecanoic acid	200	$C_{12}H_{24}O_2$	–	–	+
n-Tetradecanoic acid (C_{14})	228	$C_{14}H_{28}O_2$	+	–	–
n-Pentadecanoic acid	242	$C_{15}H_{30}O_2$	+	–	–
n-Hexadecanoic acid (C_{16})	256	$C_{16}H_{32}O_2$	+	+	+
Heptadecanoic acid	270	$C_{17}H_{34}O_2$	+	–	–
n-Octadecanoic acid (C_{18})	284	$C_{18}H_{36}O_2$	+	+	+
n-Alkenoic acids					
2-Butenoic acid	86	$C_4H_6O_2$	+	–	–
2-Pentenoic acid	100	$C_5H_8O_2$	+	–	–
Hexadecenoic acid	254	$C_{16}H_{30}O_2$	+	+	–
11-cis or trans-Octadecenoic acid	282	$C_{18}H_{34}O_2$	+	+	+
n-Alkanedioic acids					
Octanedioic acid	174	$C_8H_{14}O_4$	–	–	+
Nonanedioic acid	188	$C_9H_{16}O_4$	–	–	+
hydroxyalkanoic aicds					
α-Hydroxyacetic acid	76	$C_2H_4O_3$	+	+	+
β-hydroxybutanoic acid	104	$C_4H_8O_3$	–	–	+
Monoacylglycerols					
Glycerol	92	$C_3H_8O_3$	–	+	+
C_{16} Monoacylglyceride	330	$C_{19}H_{38}O_4$	+	+	–
Other compounds					
Urea	60	CH_4N_2O	–	–	+
Oleanitrile	263	$C_{18}H_{33}N$	–	–	+
Oleamide	281	$C_{18}H_{35}NO$	+	+	+

^{WD} Represents the degradation period in weeks.

+ Represents the occurrence of compounds identified as methyl esters and/or TMS derivatives in UV degraded montmorillonite-microbial leachates.

– Signifies the absence of compounds in UV degraded montmorillonite-microbial leachates.

5.3.11 Amino acid analysis of ambient degraded montmorillonite-complexes

The chemical compositions of acid hydrolysates of initial and degraded montmorillonite-microbial complexes are presented in ***Figure 5.3.11.1*** and ***Table 5.3.11.1***. The starting material contained five (62.5%) neutral, nonpolar amino acids and three (37.5%) neutral nonpolar acid residues, respectively. Acid hydrolysis of the complex degraded for 6 weeks yielded six (60%) neutral, three nonpolar amino acids (30%) polar residues and the rare proteinogenic amino acid, DL-α-amino isobutyric acid. The acid hydrolysate of montmorillonite-microbial complex degraded for 26 weeks yielded twice the number of hydrolyzable amino acids (16) as the starting material, and

included L-pyroglutamic acid and aminomalonic acid. The protein amino acids consisted of seven (50%) neutral, four nonpolar residues including norvale (28.6%), two polar residues including homoserine (14.3%), and 1 acidic and basic amino acid residues, respectively. Myo-inositol, adenine and cytosine were detected only in the starting material. Uracil, thymine and glucosamine were present in all extracts.

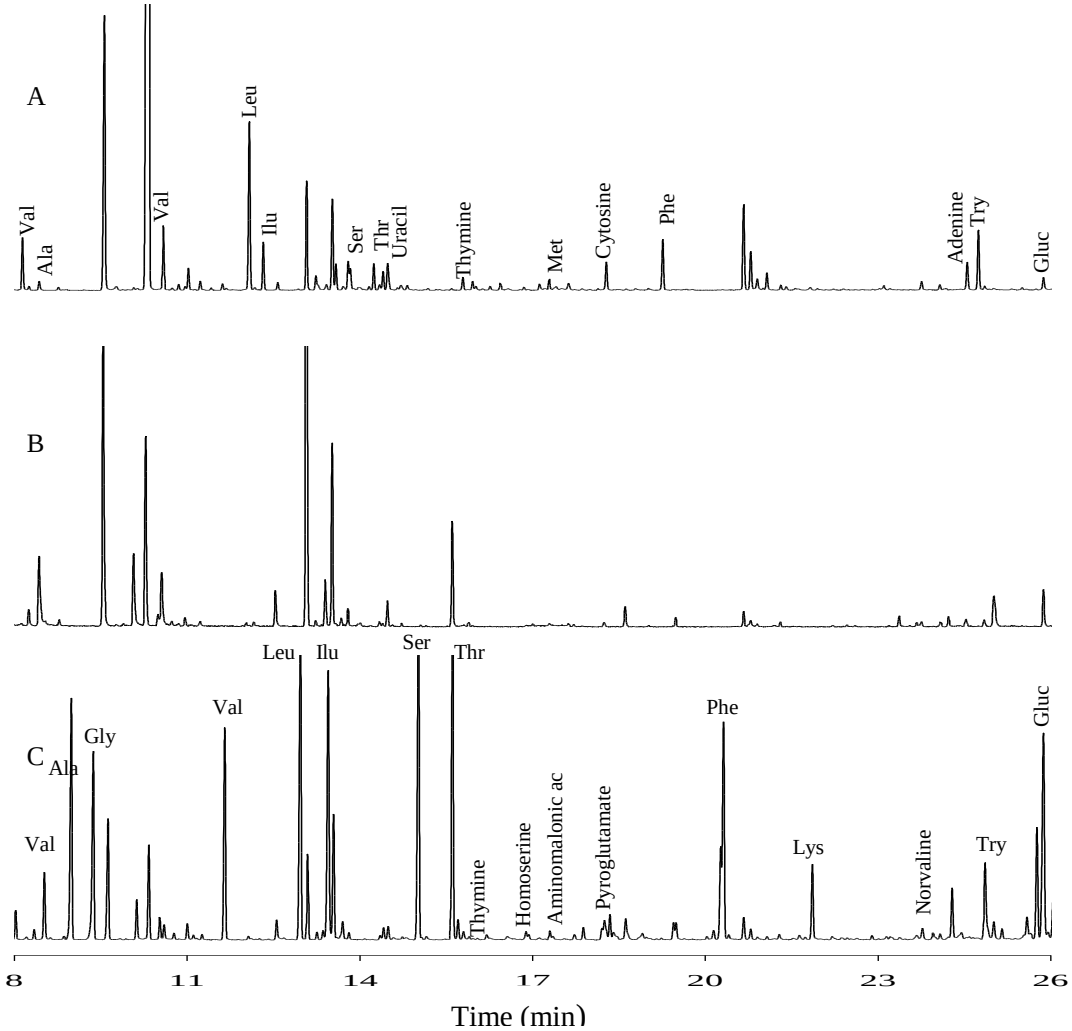

Figure 5.3.11.1: GC-MS chromatograms (TIC) of the acid hydrolysates of (A) initial montmorillonite-microbial complex and montmorillonite-microbial complexes degraded under ambient conditions for (B) 6, (C) 14 and (D) 26 weeks. Amino acids are represented by their three letter code.

Table 5.3.11.1: Occurrence of identified compounds from the acid hydrolysates of initial montmorillonite-microbial complex and montmorillonite-microbial complexes degraded under ambient conditions.

Compound	MW	Composition	Degradation period		
			0 WPD	6WPD	14WPD
Amino acids					
Glycine	72	$C_2H_5NO_2$	+	+	+
L-Alanine	89	$C_3H_7NO_2$	+	+	+
Serine	105	$C_3H_7NO_3$	+	+	+
L-Aspartic	133	$C_4H_7NO_4$	–	–	+
DL-β-Amino isobutyric acid	103	$C_4H_9NO_2$	–	+	–
L-Homoserine derivative	119	$C_4H_9NO_3$	–	–	+
L-Threonine	119	$C_4H_9NO_3$	+	+	+
L-Pyroglutamic acid	129	$C_5H_7NO_3$	–	–	+
L-Glutamic acid	147	$C_5H_9NO_4$	–	–	+
L-Valine	117	$C_5H_{11}NO_2$	+	+	+
DL-Norvaline	117	$C_5H_{11}NO_2$	–	–	+
L-Methionine	149	$C_5H_{11}NO_2S$	–	+	–
L-Leucine	131	$C_6H_{13}NO_2$	+	+	+
DL-Isoleucine	131	$C_6H_{13}NO_2$	–	–	+
L-Lysine	146	$C_6H_{14}N_2O_2$	–	–	+
L-phenylalanine	165	$C_9H_{11}NO_2$	+	+	+
Tyrosine	181	$C_9H_{11}NO_3$	+	+	+
Aminomalonic acid	119	$C_3H_5NO_4$	–	–	+
Amino sugars					
Myo-Inositol	180	$C_6H_{12}O_6$	+	–	–
D-Glucosamine, N-acetyl	221	$C_{18}H_{15}NO_6$	+	+	+
Carbohydrates					
Purines					
Adenine	135	$C_5H_5N_5$	+	–	–
Pyrimidines					
Uracil	112	$C_4H_4N_2O_2$	+	–	+
Cytosine	111	$C_4H_5N_3O$	+	–	–
Thymine	126	$C_5H_6N_2O_2$	+	–	+

WD Represents the degradation period in weeks.

+ Represents the occurrence of compounds identified from silylated hydrolysates of initial or ambient degraded montmorillonite-microbial complexes.

– Signifies the absence of compounds in the hydrolysates of initial or ambient degraded montmorillonite-microbial complexes.

5.3.12 Amino acid analysis of UV degraded montmorillonite-complexes

Figure 5.3.12.1 and ***Table 5.3.12.1*** represent the compositions of the acid hydrolysates of the un-degraded and UV degraded montmorillonite-microbial complexes and are virtually identical to their ambient degraded counterparts (***Figure 5.3.11.1*** and ***Table 5.3.11.1*****)**.

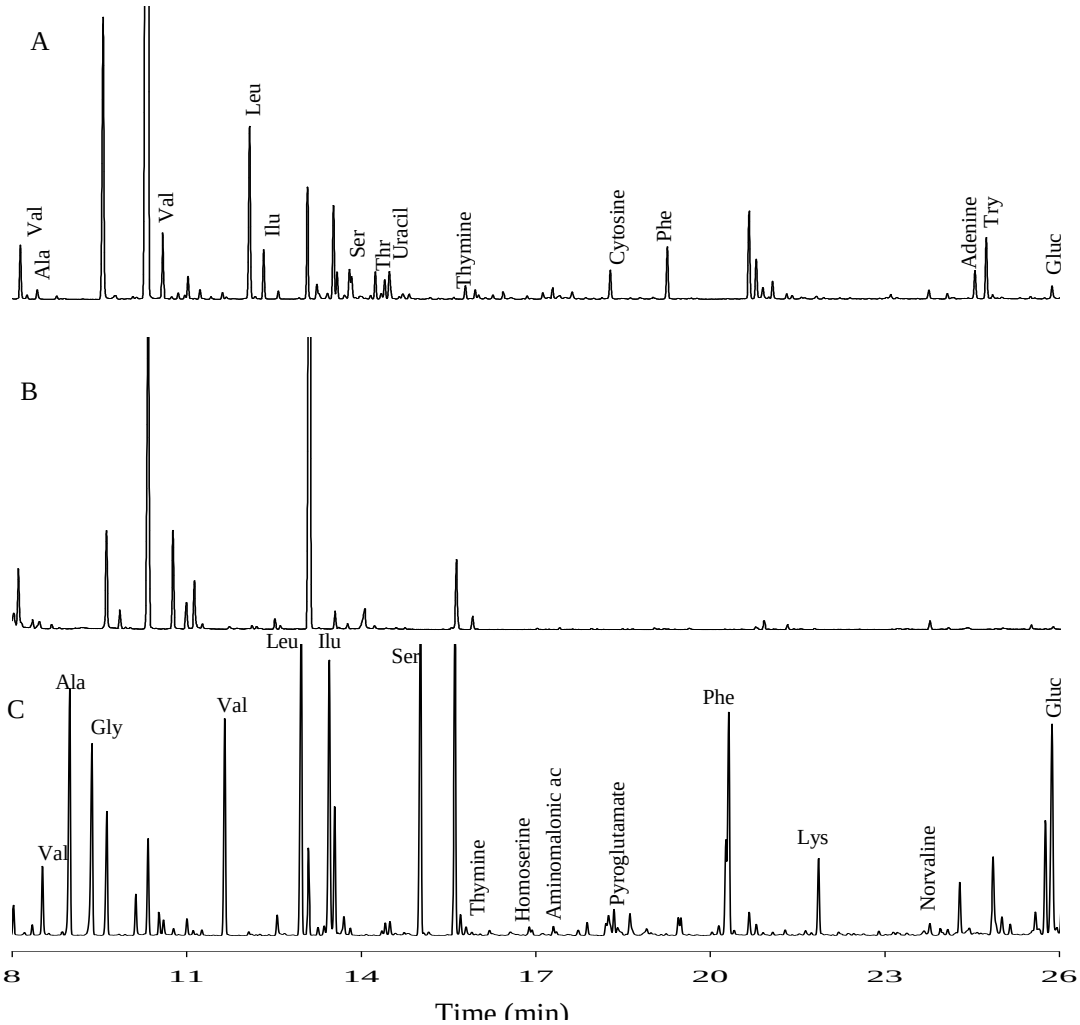

Figure 5.3.12.1: GC-MS chromatograms (TIC) of the acid hydrolysates of (A) initial montmorillonite-microbial complex and montmorillonite-microbial complexes degraded under UV conditions for (B) 6, (C) 14 and (D) 26 weeks. Amino acids are represented by their three letter code.

Table 5.3.12.1: Occurrence of identified compounds from the acid hydrolysates of initial montmorillonite-microbial complex and montmorillonite-microbial complexes degraded under UV conditions.

Compound	MW	Composition	Degradation period		
			0 WPD	6WPD	14WPD
Amino acids					
Glycine	72	$C_2H_5NO_2$	+	+	+
L-Alanine	89	$C_3H_7NO_2$	+	+	+
Serine	105	$C_3H_7NO_3$	+	+	+
L-Aspartic acid	133	$C_4H_7NO_4$	–	–	+
DL-β-Amino isobutyric acid	103	$C_4H_9NO_2$	–	+	–
L-Homoserine derivative	119	$C_4H_9NO_3$	–	–	+
L-Threonine	119	$C_4H_9NO_3$	+	+	+
L-Pyroglutamic acid	129	$C_5H_7NO_3$	–	–	+
L-Glutamic acid	147	$C_5H_9NO_4$	–	–	+
L-Valine	117	$C_5H_{11}NO_2$	+	+	+
DL-Norvaline	117	$C_5H_{11}NO_2$	–	+	+
L-Methionine	149	$C_5H_{11}NO_2S$	–	+	–
DL-Leucine	131	$C_6H_{13}NO_2$	+	+	+
DL-Isoleucine	131	$C_6H_{13}NO_2$	–	–	+
L-Lysine	146	$C_6H_{14}N_2O_2$	–	–	+
L-phenylalanine	165	$C_9H_{11}NO_2$	+	+	+
Tyrosine	181	$C_9H_{11}NO_3$	+	+	+
Aminomalonic acid	119	$C_3H_5NO_4$	–	–	+
Amino sugars					
Myo-Inositol	180	$C_6H_{12}O_6$	+	–	–
D-Glucosamine, N-acetyl	221	$C_{18}H_{15}NO_6$	+	+	+
Carbohydrates					
Purines					
Adenine	135	$C_5H_5N_5$	+	–	–
Pyrimidines					
Uracil	112	$C_4H_4N_2O_2$	+	–	+
Cytosine	111	$C_4H_5N_3O$	+	–	–
Thymine	126	$C_5H_6N_2O_2$	+	–	+

WD Represents the degradation period in weeks.

+ Represents the occurrence of compounds identified from silylated hydrolysates of initial or UV degraded montmorillonite-microbial complexes.

– Signifies the absence of compounds in the hydrolysates of initial or UV degraded montmorillonite-microbial complexes.

5.4 Discussion

5.4.1 Lipid analysis

Strong compositional differences were evident between the initial samples and the degraded samples as well as between the degraded biomass and microbial leachates. It is also evident that *n*-C_{16} and *n*-C_{18} silylated saturated fatty acid methyl esters were the dominant fatty acids detected in all the samples and underscore the bio- and photo-

refractory nature of these compounds and their contribution to the stable SOM pool. The compositional differences between the degraded biomass ans microbial leachates and the dominance of polymethylenic-C structures in the microbial biomass were first observed in ***Chapter 3***. Moreover, this is in agreement with Jandl et al. (2002) who demonstrated that *n*-C_{16} maximum at lower chain lengths (*n*-C_4 to *n*-C_{24}) of microbial origin were the dominant bio-refractory fatty acids in DOM and soils. The significant abundance of hexadecanoic acid may be further explained by the fact that it is a key intermediate of oleic acid degradation (Abraham et. al., 1998; Pereira et al., 2002). Several studies have shown that high amounts of oleic acid have degraded to form long-chained dihydroxylated acids such as, 9,10-dihydroxyoctadecanoic acid via the hydroxylation of unsaturated fatty acid chain (Colombini et al., 2005a, b). However, since such compounds were not detected as degradation products, this may further justify the contribution of oleic acid degradation to the intensity of palmitic acid in the degraded samples.

Considering the chromatographic data, it emerges that chain length was an important factor controlling fatty acid lability, and the preferential degradation of fatty acids with chain lengths 12 C or less represents a labile pool of organic matter. Moreover, it has been demonstrated that the degradation rate constant of 14:0 fatty acid was twice that of 24:0 (Sun and Wakeham, 1994). Haddad et al. (1992) also provided evidence to support the rapid degradation (oxidation) of short-chained fatty acids relative to their long-chained counterparts in shallow coastal sediments. Conversely, there is also evidence to suggest that shorter-chain aliphatic compounds did not always degrade at a faster rate than their longer-chain homologues. It is likely that the selective preservation of some shorter chain fatty acids was a result of chemical modification by polar cellular components, including amino acids and carbohydrates. Such compounds (glycoproteins and lipoproteins) were previously detected in degraded bulk microbial biomass using advanced NMR approaches (***Chapters 3*** and ***4***). The oxidation of *n*-alkanes to *n*-alkanols and ultimately to their *n*-alkanoic acids have been demonstrated (Amblés et al., 1994) and may explain the decomposition of some *n*-alkanes over the course of the degradation process. Moreover, the *n*-alkanol intermediate, octadecan-1-ol was detected in the microbial leachates of the ambient and UV degraded biomass. Considering that *n*-alkanes are a likely substrate for *in situ* microbial β-oxidation (Naafs et al., 2004), it is not surprising that these compounds are among the first to degrade.

It would appear that decarboxylation and demethylation were important mechanisms in the degradation of longer-chain fatty acids to shorter-chain homologues. Additionally, we would like to suggest that rapid microbial β-oxidation of longer-chain homologues coupled with microbial- or photooxidation of labile double bonds were active in the degradation process. For example, Bull et al. (2000b) demonstrated rapid degradation *n*-alkanoic acids leading to shorter-chain compounds of the same class, and the production of shorter-chain (C_{12}-C_{16}) saturated fatty acids from ^{14}C labeled oleic acid has been demonstrated (Rhead et al., 1971). Two biochemical pathways for this alteration have been postulated: (1) progressive chain shortening via loss of C2 units and double bonds reduction, and (2) β-oxidation to acetyl-CoA units followed by resynthesis of elongated or shorter chain fatty acids (Sun et al., 1997). It should be noted that since the degradation of *n*-alkanes and *n*-alkanoic acids results in the formation of the same lipid classes, in some instances, the products of degradation cannot be distinguished from the original biosynthesized homologues and degradation may only truly be discerned by compound specific stable isotope ratio analysis. However, a shift to shorter carbon chain-lengths as the predominant homologues of aliphatic acid series was observed from the starting materials to the degraded samples.

The main monounsaturated fatty acids present in the starting materials (un-reacted and clay-complexes), and the degraded samples were $C_{16:1}$ Δ9, $C_{18:1}$ Δ9, and $C_{18:1}$ Δ11 fatty acids. However, these compounds were detected in relatively smaller proportions as degradation progressed. Comparatively, we failed to detect *cis*-9(*Z*) octadecenoic acid in the microbial leachates after 6 weeks of degradation. This is especially true for the leachates of montmorillonite-microbial complexes where $C_{18:1}$ Δ9 was undetected over the course of the degradation. However, this is not surprising as we previously demonstrated the preferential adsorption of polymethylenic-C compounds and structures containing double bonds to montmorillonite (***Chapter 4***). The detection of *trans*-$C_{18:1}$ Δ11 fatty acid as the dominant enoic acid in the ambient and UV degraded samples over the degradation period may be attributed to the fact that the *trans* configuration is known to be seven-folds less reactive toward $^1O_2$ than the *cis*-geometry (Hurst et al., 1985). In addition, we reasoned that the occurrence of some enoic acids in the degraded sample was due to progressive chain lengthening, two carbons at a time, of already unsaturated short chain precursor resulted in the formation of longer-chain unsaturated fatty acid. This mechanism was first suggested by O'Leary (1962).

There is also evidence to suggest that molecular structure, particularly unsaturation (presence of double bonds) was an important factor controlling the lability of microbial fatty acids. This suggestion is in agreement with Sun et al. (1997) who demonstrated that unsaturated 16:1 and 18:1 degraded faster than saturated 16:0 and 18:0, respectively. Similarly, Nguyen et al. (2003) reported a rapid decrease of unsaturated 18:1 fatty acids, with only 16:0 fatty acids detected in a 201-day detritus after oxic degradation of *Botryococcus braunii*. Although the conventional view is that unsaturation is a key parameter in regulating the lability of lipids, this does not hold true for all unsaturated fatty acids, whose reactivity seemed independent of their degree of saturation (Grossi et al., 2003; Doménech-Carbó et al., 2006). For example, in some cases monounsaturated fatty acids were not found to be systematically more reactive than their saturated homologues, and the diunsaturated C_{29} sterols were degraded more slowly than the monounsaturated C_{29} sterol, suggesting that unsaturated structures may be an important part of the stable SOM pool. Moreover, the intrinsic stability of olefinic and/or aromatic C=C compounds was clearly demonstrated in ***Chapter 3***. These differences may be attributed to differences in the chemical structure (for example, the position and geometry of the double bonds) of the compounds (Grossi et al., 2003). It would also appear that physical by montmorillonite was important in the stabilization of labile double bonds.

5.4.2 Photooxidation and autoxidation of microbial lipids

The reactivity of unsaturated fatty acids relative to auto- and photooxidative processes logically and quickly increases with their degree of unsaturation (Frankel, 1998; Rontani, 1998). Although the loss of PUFA could also be due to grazing by microbes feeding on the biomass, evidence of degradation products of monounsaturated fatty acids and other aliphatic lipids allowed us to link the degradation of PUFA to the involvement of abiotic processes and may explain the loss of polyunsaturated (primarily $C_{18:2}$ and $C_{18:3}$) in the degraded samples. However, despite the expected production of oxidative products of these PUFA, such compounds were not detected in the degraded samples. This may be due to: (i) the involvement of cross-linked reactions leading to the formation of macromolecular structures non-amenable to analysis by gas chromatography, or (ii) the instability or volatility of these compounds (Christodoulou et al., 2009).

The oxidation products of PUFA are considered to be very sensitive tracers for these processes (Christodoulou et al., 2009); however, they were not sufficiently stable to be detected and used for this purpose. In contrast, autoxidation and photooxidation of monounsaturated fatty acids [such as oleic ($C_{18:1\Delta9}$), *cis*-vaccenic ($C_{18:1\Delta11}$) or palmitoleic ($C_{16:1\Delta9}$) acids] leads to the formation of oxidation products sufficiently stable to act as markers for these processes (Rontani et al., 2003; Christodoulou et al., 2009). Free radical oxidation of monounsaturated fatty acids produces a mixture of six *cis* and *trans* isomeric allylic hydroperoxides: 8-*trans*, 8-*cis*, 9-*trans*, 10-*trans*, 11-*trans*, and 11-*cis*, hydroperoxides (Christodoulou et al., 2009). Conversely, singlet oxygen-mediated photooxidation of monounsaturated fatty acids yields a mixture of 9- and 10-hydroperoxides with an allylic *trans*-double bong (Rontani, 1998), which can undergo high stereoselective radical allylic rearrangement respectively to 11-*trans* and 8-*trans* hydroperoxides. Given that *cis*-isoforms are specific indicators of autoxidative processes, the relative importance of photooxidation and autoxidation should be easily distinguished by quantifying these compounds (Marchand and Rontani, 2001).

Several classes of hydroxyacids (α-, β- and ω-) were observed throughout the total lipid extracts of the initial and degraded samples. The persistence and relative abundance of these compounds, particularly the α- and β-hydroxyacids in the degraded samples would suggest that these are slow cycling compounds, and their relative stability have been demonstrated in DOM (Wakeham et al., 2003). It has been hypothesized that the relative stability of bacterial hydroxyacids is linked to a macromolecular matrix (lipopolysaccharides), membrane and cell wall fragments (Wakeham et al., 2003). Previously (***Chapter 3***) we provided convincing evidence of the stabilization of microbial lipids linked to macromolecular structures (proteins and carbohydrates). A consequence of this protection is that membrane-bound amino acids and lipids, such as fatty acids and hydroxyacids, present in the biomass may survive degradation to a greater extent, when compared to "free" or uncomplexed molecules.

The occurrence of hydroxyacids (dominated by C_2-C_{10} acids) in the starting materials and the degraded samples resulted from the biological and/or photooxidation of the of their respective monounsaturated fatty acids (Marchand and Rontani, 2001). It is known that the production of hydroxyacids results mainly (>80%) from the reduction of the corresponding hydroperoxides and to a lesser extent (<20%) from reduction of the corresponding ketoacids (Marchand and Rontani, 2001; Rontani et al., 2003). However,

we failed to detect any hydroperoxides and ketoacids and attributed this to their labile nature. Moreover, we were unable to detect any allylic hydroxyacids which are products of type II photooxidation (i.e. involving singlet oxgen; Marchand and Rontani, 2001). Radical autoxidation was probably an important mechanism in the production of *cis*-hydroxyacids (Rontani et al., 2003). Other mechanisms implicated in the formation of hydroxyacids in degraded samples include hydroxylation of unsaturated fatty acids and a variety of mechanisms involving the possible migration of a radical nearer to the carboxylic group and the related cleavage closest to the carboxylic groups (Colombini et al., 2005b).

An additional oxidation product arising from $C_{18:1}$ Δ9, or Δ11 was 9,10-epoxy-18-hydroxyoctadecanoic acid detected only in the montmorillonite complexes degraded for 14 weeks. 9,10-Epoxydecanoic acids produced by the oxidation hydroperoxide have been previously reported in marine (Stephanou, 1992) and urban (Stephanou and Stratigakis, 1993) aerosols and were found to be labile. It is also well know that some bacteria may carry out enzymatic epoxidation of *cis* Δ9- fatty acids to 9,10-epoxyacids (Ruettinger and Fulco, 1981), these bacteria can further hydrolyse these epoxides to produce 9,10-dihydroxyacids (Michaels et al., 1980). In view of such evidence, we cannot conclusively rule out the involvement of biological activity in the UV irradiated samples. Epoxyacids can also be formed by cyclization of alkoxyl radicals derived from allylic hydroperoxides (Frankel, 1998). However, in this case, other epoxyacid isomers (e.g. 8,9- and 10,11-epoxyoctadecanoic acids) should be formed but we failed to detect these compounds in the degraded samples. Nevertheless, epoxy acids may be considered as important biochemical/molecular markers in the degradation of unsaturated microbial lipids in SOM.

C_{18} ω-hydroxycarboxylic acids were detected primarily in the starting materials. These compounds have been shown to result from the reduction of the corresponding ω-oxocarboxylic acids (Marchand and Rontani, 2001). Such compounds were initially discovered in remote marine aerosols from the North Pacific (Kawamura and Gagosian, 1987) and then detected in different sediment traps (Kawamura et al., 1990). They have been considered to originate in the atmosphere by photochemically-induced oxidative degradation of biogenic unsaturated fatty acids, which contain double bonds primarily at the C-9 position (Kawamura and Gagosian, 1987). Subsequently, it was demonstrated that heterolytic cleavage of allylic hydroperoxides resulting from the photodegradation

of phytoplanktonic monounsaturated fatty acids in the euphotic layer could represent another source of these compounds (Rontani, 1998). The production of some hydroxycarboxylic acids, primarily C_7-C_{11} ω-hydroxycarboxylic acids have been attributed to heterolytiic cleavage of saturated hydroperoxyacids (Rontani, 1998) and subsequent oxidation of the ω-oxocarboxylic acids thus formed (Rontani et al., 2003). This is a result of the considerably weaker migratory aptitude of alkyl groups (relative to the vinyl group), a much slower process than in the case of allylic hydroperoxides.

The production of some saturated hydroxyacids in the degraded samples may have resulted from the reduction of epoxyacids (Marchand and Rontani, 2001). However, no ω-hydroxycarboxylic acids were detected in our degraded samples. Equally, we failed to detect any allylic hydroperoxyacids, and this is probably due to the fact that heterolytic cleavage was strongly favoured in the degraded samples (Marchand and Rontani, 2001). 2-Hydroxy and 3-hydroxy fatty acids are common components of polar bacterial lipids (Rontani et al., 2003), and their increasing presence in dark controls is attributed to enzymatic release of polar lipids during the senescence of *Erythrobacter* sp. strain NAP1 and not of photochemical processes (Rontani et al., 2003). However, we have provided conflicting evidence as these compounds were detected in both ambient and UV degraded samples throughout the course of the degradation. It should also be noted that we failed to identify corresponding hydroxyacids resulting from the autoxidation and photooxidation of some monounsaturated fatty acids and the polyunsaturated fatty acids.

The saturated hydroxyacids were dominant (relative to allylic hydroxyacids) in the degraded samples as only one isomeric allylic monohydroxypentenoic acid was detected in the degraded samples (***Tables 5.3.3.1*** and ***5.3.4.1***). These results may be attributed to: (i) the reduction of the double bond in allylic hydoperoxyacids, (ii) the relative recalcitrance of saturated hydroperoxyacids towards degradation, (iii) the production of these saturated species in the degraded samples or (iv), the presence of an epoxyacid in the case of degraded clay-microbial complexes (Marchand and Rontani, 2001).

The detection of a homologous series of α,ω-dicarboxylic acids in the initial and degraded samples may be interpreted as a combination of autochthonous formation coupled with auto- and photooxidation products of unsaturated fatty acids (Kawamura et

al., 1990; Stephanou and Stratigakis, 1993). Grasset and Amblés (1998) identified C_9 alkanedioc acid as a microbial oxidation product of unsaturated *n*-alkanoic acids, and Rontani et al. (2003) detected small amounts of α,ω-dicarboxylic acids after irradiation of *Erythrobacter* sp. strain NAP1. The production of similar compounds was observed during the irradiation of senescent phytoplanktonic cells and ascribed to heterolytic cleavage of allylic hydroperoxides resulting from the photodegradation of phytoplanktonic unsaturated fatty acids (Rontani, 1998). Marchand and Rontani (2001) have also demonstrated that heterolytic cleavage of allylic hydroperoxides produced by autoxidation of Δ9 unsaturated fatty acids results in the formation of α,ω-dicarboxylic acids.

5.4.3 Degradation of polysaccharides and diterpenes

Compounds such as polysaccharides exhibited similar lability as the short- to medium-chain fatty acids, degrading rapidly after 6 or 14 weeks degradation. These results are also supported by the observation that carbohydrates, possible of a microbial origin degrade rapidly in soil horizons (Otto and Simpson, 2005). The lability of polysaccharides in the biomass is consistent with the preferential loss of storage polysaccharides, and was previously discussed in ***Chapter 3***.

The detection of phytol in the biomass after 6 weeks of decomposition may be linked to the growth of bacteriochlorophyll containing bacteria and/or algae on the decomposing biomass, since no phytol was detected in the starting material. Subsequent loss of the isoprenoid alcohol is most probably due to enzymatic- and/or photohydrolysis (van Bergen et al., 1997) and alternating β-decarboxymethylation and β-oxidation reaction sequences via (*Z*)-phytenic acid leading to mineralization (Hylemon and Harder, 1999). Several studies have provided evidence of a C_{18} isoprenoid methyl-ketone (Gillan et al., 1983; Bull et al., 2000a), (*E*)-phytenic acid and 4,8,12-trimethyltridecan-1-ol which can be metabolized via β-oxidation reaction sequences (Rontani et al., 1999) as degradation products of phytol. However we failed to identify any hydrolysis and/or oxidation products of phytol in the degraded samples. Interestingly, the diterpenoid alkane, phytane, a known reduction product of phytol (Hartgers et al., 2000) was detected in microbial leachates after 6 and 14 weeks degradation and confirms the involvement of reduction as one of the mechanisms involved in the degradation of phytol. In future work, samples will be treated with a fungicide to eliminate the presence of any fungal contaminants.

5.4.4 Degradation of sterols

Cholesterol is a major plant and animal sterol, but it has also been less frequently linked to fungi and algae and even less frequently to bacterial membrane constituents (Otto et al., 2005). All other sterols detected in the total lipid extracts of the degraded samples are commonly derived from fungal and plant sources (Otto and Simpson, 2005). Therefore, it is somewhat surprising to observe these compounds in the total lipid extracts of degraded soil microbial biomass, and their presence may be explained by the growth of algal and/or fungal contamination on the biomass during the decomposition process. This hypothesis is favoured given that no sterols were detected in the starting materials and the high moisture levels (irrigation water) of the samples throughout the course of the degradation. The degradation of sterols was variable, and the loss of some compounds may be attributed to the oxidation of unsaturated centres (Naafs et al., 2004). Various ketosteroids have been reported as bacterial oxidation products of sterols (Otto and Simpson, 2005); however, we were unable to identify such compounds in the lipid extract of the degraded samples. It would appear that due to the preferential degradation of aliphatic lipids which are predominant in the source biomass, some steroids appear to be relatively enriched in the degraded samples. These results would suggest that sterols can be at least partly preserved as free molecules in the biomass.

Due to the relative stability of and diverse functional groups that may be attached to the tetracyclic carbon skeleton of Δ^5-sterols, they may be useful for estimating relative effects of biotic and abiotic (photooxidation and autoxidation) degradation (Christodoulou et al., 2009). Free radical oxidation of Δ^5-sterols yields mainly 7α- and 7β-hydroperoxides and, to a lesser extent 5α/β,6α/β-epoxysterols and 3β,5α,6β-trihydroxysterols (Rontani et al., 2009). Conversely, singlet-oxygen mediated photooxidation produces mainly Δ^6-5α-hydroperoxides and low amounts of Δ^4-6α/6β-hydroperoxides (Rontani et al., 2009). A few bacteria are also known to produce Δ^5-3,7-dihydroxysterols from the corresponding sterols (Christodoulou et al., 2009). It is possible that we failed to detect these degradation products due to (i) allylic rearrangement and (ii) homolytic cleavage resulting in ring cleavage (Christodoulou et al., 2009). It is intriguing to propose that the loss of sterols may also be due to aerobic bacterial mineralization involving an initial terminal degradation attack of the side-chain. The lability of diunsaturated sterols can be attributed to the autoxidation of the cyclic double bond followed by an additional autoxidation of the side-chain (Rontani et

al., 2009). Variable amounts of monoacylglycerol, a major constituent of microbial membranes and a storage lipid was detected in the initial and degraded samples.

5.4.5 Analysis of acid hydrolysable compounds

The acid hydrolysates of the initial and degraded microbial biomass and clay-microbial complexes contained a series of proteinogenic and non-proteinogenic amino acids. The amino acid patterns of the samples did not vary significantly over the decomposition period, suggesting that proteins were degraded as whole macromolecules rather than as free amino acids. This suggestion is strongly supported by the electrophoretic patterns of protein extracts in ***Chapter 6***. As expected, the proteinogenic amino acids were dominated by L-enantiomers with less significant contributions from the DL-isoforms. It is most likely that the presence of DL-enantiomers is a result of acid hydrolysis-induced racemization of their L-enantiomers at terminal positions (Bremner, 1950; Amelung et al., 2006). Neutral, nonpolar amino acids were the most common residues in the samples, while glycine, alanine, valine, isoleucine, luecine, threonine, tyrosine, glutamic acid and phenylalanine were the most abundant residues.

However, it should be noted that under conditions of acid hydrolysis, it is likely that the occurrence of certain amino acids was overestimated, underestimated or undetected due to chemical modification or complete degradation during the hydrolysis process (Bremner, 1950; Shevchenko et al., 2000). For example, acid-induced decomposition of purines may give rise to elevated levels of glycine and simultaneous diminution of purines in the degraded samples. It should also be noted that the amino acids asparagine and glutamine may either be completely destroyed or desamidated to variable extents, with complete desamidation producing aspartic acid and glutamic acid, respectively during hydrolysis (Wilson and Walker, 2000). In addition, the partial destruction of tryptophan in strong mineral acids has been reported (Shevchenko et al., 2000). This lability is due to its indole side chain (Yamashita and Tanoue, 2004) and is significantly enhanced in the presence of carbohydrate leading to complete destruction of the molecule (Bremner, 1950). Therefore, it is not surprising that this amino acid was not detectable in the acid hydrolysates of the fresh and degraded samples.

Alanine and glutamic acid are predominant amino acids in bacterial peptideglycan (Yamashita and Tanoue, 2004). Therefore, the occurrence of relatively high abundances of these residues in the degraded samples is of no surprise considering

that peptidoglycan is resistant to many chemical and biological processes and has been found as a constituent of the most refractory components of SOM (Simpson et al., 2007). Overwhelming spectroscopic evidence of the presence of biorefractory peptidoglycan in degraded microbial biomass was previously reported in ***Chapter 3***. It may also be postulated that the high abundances of other amino acids surviving degradation were derived from membrane proteins and/or proteins surviving degradation in the form of glycoproteins (Yamashita and Tanoue, 2004). The acid hydrolysates of clay-microbial complexes (initial and degraded) were generally lower in amino acid composition than those of the un-complexed biomass. This variation in composition is most likely due to the fact that proteins are strongly adsorbed to clay minerals and have been demonstrated to remain intact even after acid hydrolysis of clay-microbial complexes (***Chapter 4***). We surmized that the urea detected in the hydrolysates of the microbial biomass degraded under ambient and UV conditions is indicative of protein degradation (Sakami and Harrington, 1963). This is further supported by the presence of the nonproteinogenic amino acid ornithine, a co-product of urea resulting from arginase catalysed hydrolysis of arginine, and the nonprotein amino acids such as β-alanine and γ-aminobutyric (Voet and Voet, 1990). Conclusive evidence of protein degradation is presented in ***Chapter 6***.

Pyroglutamic acid and hydroxyproline, two amino acids rarely observed in biological systems (Podell and Abraham, 1978) were detected in the extracts (initial and degraded) or the un-reacted biomass. The former has been found in proteins such as bacteriorhodopsin (membrane protein), and the latter in diatom cell walls and has been linked to Si deposition (Nakajima and Volcani, 1969). This observation is significant and seems to support our previous interpretation (***Chapter 3***) that soil microorganisms are capable of accumulating stable amounts of silicon and may play a more vital role in silicon cycling and ultimately C sequestration than currently thought. It is not surprising to detect strong evidence of heterocyclic nitrogen, such as purines/pyrimidine in the extracts of the degraded samples as these compounds have been previously linked to the refractory amide-N in microbially derived OM (***Chapter 3***) and soils (Knicker et al., 1996; Zang et al., 2001). Ethanolamine is the second most abundant head group for phospholipids, and its detection in the samples may be due to its liberation from the rapid degradation of phospholipids (***Chapter 3***) as is characteristic in senescent microbial cells.

Glucosamine, a stable microbial component was detected at approximately twice the concentration of galactosamine and represented the major amino sugar in the starting materials and some degraded samples, while the latter was not detected in other degraded samples. This is somewhat surprising considering that amino sugars of microbial origin (Glaser et al., 2004) have been reported to be relatively stable to microbial attacks in soils (Liang et al., 2007). It should also be noted that we failed to detect the presence of mannosamine and/or muramic acid. Carbohydrates behaved variably in the degraded samples; however, myo-inositol appeared recalcitrant to photochemical and biological degradation. This is expected, because recalcitrant soil P is known to contain orthophosphate monoesters dominated by inositol phosphates (Turner et al., 2002). However, we failed to detect orthophosphate monoesters beyond six weeks degradation and attributed this to NaOH degradation during sample preparation and data acquisition (***Chapter 3***).

5.5 Conclusions

In this study, we investigated the decomposition of lipids and amino acids from microbial biomass and clay-microbial complexes and their leachates degraded under ambient and UV conditions. Although strong compositional differences were observed between the starting material and the degraded samples, and the biomass and their leachates, no significant differences were observed between the ambient and UV degraded samples. However, the organic solvent extracts and acid hydrolysates of clay-microbial complexes (un-degraded and degraded) were generally lower in amino acid composition than those of the clay-free biomass. This variation in composition is most likely due to the fact that lipids and proteins are strongly adsorbed to clay minerals and have been demonstrated to remain intact even after acid hydrolysis of clay-microbial complexes, suggesting that they are protected by clay (***Chapters 3*** and ***4***). The *n*-C_{16} and *n*-C_{18} saturated fatty acids were the dominant components detected in our samples, while other components behaved variably. Based on our findings, it would be logical to conclude that molecular structure, particularly unsaturation and chain length were important factors controlling fatty acid lability under ambient and UV conditions. Several other mechanisms including β-oxidation, decarboxylation, demethylation and hydroxylation of unsaturated fatty acids may be implicated in both ambient and UV degraded samples, while heterolytic and allylic cleavage were probably important photodegradation mechanisms. In many cases we failed to detect photo-products that

may be used as tracers of UV-degradation. In future work, the degradation of microbial biomass should be carried out in such a way that would allow for the collection of volatile photoproducts for headspace analysis.

5.6 References

Abraham, W.-R., Hesse, C., and Pelz, O. 1998. Ratios of carbon isotopes in microbial lipids as an indicator of substrate usage. *Applied and Environmental Microbiology* 64, 4202–4209.

Ambles, A., Jambu, P., Parlanti, E., Joffre, J., and Riffe, C. 1994. Incorporation of natural monoacids from plant residues into an hydromorphic forest podzol. *European Journal of Soil Science* 45, 175–82.

Amelung, A., Zhang, X., and Flach, K. W. 2006. Amino acids in grassland soils: climate effects on concentrations and chirality. *Geoderma* 130, 207–217.

Bremner, J. M. 1950. The Amino-acid composition of protein material in soil. *Science* 47, 538–542.

Bull, I. D., Nott, C. J., van Bergen, P. F., Poulton, P. R., and Evershed, R. P. 2000b. Organic geochemical studies of soils from the Rothamsted classical experiments-VI. The occurrence and source of organic acids in an experimental grassland soil. *Organic Geochemistry* 32, 1367–1376.

Bull, I. D., van Bergen, P. F., Nott, C. J., Poulton, P. R., and Evershed, R. P. 2000a. Organic geochemical studies of soils from the Rothamsted classical experiments-V. The fate of lipids in different long-term experiments. *Organic Geochemistry* 31, 389–408.

Christodoulou, S., Marty, J.-C., Miquel, J.-C., Volkman, J. K., and Rontani, J.-F. 2009. Use of lipids and their degradation products as biomarkers for carbon cycling in the northwestern Mediterranean Sea. *Marine Chemistry* 113, 25–40.

Colombini, M. P., Giachi, G., Modugno, F., and Ribechini, E. 2005a. Characterization of organic residues in pottery vessels of the roman age Antinoe (Egypt). *Microchemical Journal* 79, 83–90.

Colombini, M. P., Modugno, F., and Ribechini, E. 2005b. Organic mass spectrometry in archaeology: evidence for *Brassicaceae* seed oil in Egyptian ceramic lamps. *Journal of Mass Spectrometry* 40, 890–898.

Daniel, R. 2005. The metagenomics of soil. *Nature Reviews Microbiology* 3, 470–478.

Doménech-Carbó, M. T., Osete-Cortina, L., de la Cruz Cañizares, J., Bolívar-Galiano, F., Romero-Noguera, J., Fernández-Vivas, M. A., and Martín-Sánchez, I. 2006. Study of the microbiodegradaton of terpenoid resin-based varnishes from easel painting using pyrolysis-gas chromatography-mass spectrometry and gas chromatography-mass spectrometry. *Analytical and Bioanalytical Chemistry* 385, 1265–1280.

Fang, C., Smith, P., Moncrieff, J. B., and Smith, J. U. 2005. Similar response of labile and resistant soil organic matter pools to changes in temperature. *Nature* 433, 57–59.

Feng, X., Simpson, A. J., and Simpson, M. J. 2005. Chemical and mineralogical controls on humic acid sorption to clay mineral surfaces. *Organic Geochemistry* 36, 1553–1566.

Feng, X., Simpson, A. J., and Simpson, M. J. 2006. Investigating the role of mineral-bound humic acid in phenanthrene sorption. *Environmental Science and Technology* 40, 3260–3266.

Franchi, M., Bramanti, E., Morassi Bonzi, L., Luigi Orioli, P., Vettori, C., and Gallori, E. 1999. Clay-nucleic acid complexes: characterization and implications for the preservation of genetic materials in primeval habitats. *Origins of Life and Evolution of the Biosphere* 29, 279–315.

Frankel, E. N. 1998. *Lipid oxidation*. The Oily Press, Dundee pp. 1–302.

Gillan, F. T., Nichols, P. D., Jhons, R. B., and Bavor, H. J. 1983. Phytol degradation by marine bacteria. *Applied and Environmental Microbiology* 55, 2888–2893.

Glaser, B., Turrión, M.-B., and Alef, K. 2004. Amino sugars and muramic acid-biomarkers for soil microbial community structure analysis. *Soil Biology & Biochemistry* 36, 399–407.

Grasset, L., and Amblés, A. 1998. Structure of humin and humic acid from an acid soil as revealed by phase transfer catalysed hydrolysis. *Organic Geochemistry* 29, 881–891.

Grossi, V., Caradec, S., and Gilbert, F. 2003. Burial and reactivity of sedimentary microbial lipids in bioturbated Mediterranean coastal sediments. *Marine Chemistry* 81, 57–69.

Haddad, R. I., Martens, C. S., and Farrington, J. W. 1992. Quantifying early diagenesis of fatty acids in rapidly accumulating coastal marine sediments. *Organic Geochemistry* 19, 205–216.

Hartgers, W. A., Schouten, S., Lopez, J. F., Sinninghe Damsté, J. S., and Grimalt, J. O. 2000. ^{13}C-contents of sedimentary bacterial lipids in shallow sulfidic monomictic lake (Lake Cisó, Spain). *Organic Geochemistry* 31, 777–786.

Hurst, J. R., Wilson, S. I., and Schuster, G. B. 1985. The ene reaction of singlet oxygen: kinetics and product evidence in support of a perepoxide intermediate. *Tetrahedron* 41, 2191–2197.

Hylemon, P. B., and Harder, J. 1999. Biotransformation of monoterpenes, bile acids, and other isoprenoids in anaerobic ecosystems. *FEMS Microbiology Reviews* 22, 475–488.

Jandl, G., Schulten, H.-R., and Leinweber, P. 2002. Quantification of long-chain fatty acids in dissolved organic matter and soils. *Journal of Plant Nutrition and Soil Science* 165, 133–139.

Johnson, D., Campbell, C. D., Lee, J. A., Callaghan, T. V., and Gwynn-Jones, D. 2002. Artic microorganisms respond more to elevated UV-B radiation than CO_2. *Nature* 416, 82–83.

Kawamura, K., and Gagosian, R. B. 1987. Implications of ω-oxocarboxylic acids in the remote marine atmosphere for photo-oxidation of unsaturated fatty acids. *Nature* 325, 330–332.

Kawamura, K., Handa, N., and Nozaki, Y. 1990. ω-Oxocarboxylic acids in the sediment trap and sediment samples from the North Pacific: implication for the transport of photo-oxidation products to deep-sea environments. *Geochemical Journal* 24, 217–222.

Knicker, H., Scaroni, A. W., and Hatcher, P. G. 1996. ^{13}C and ^{15}N NMR spectroscopic investigation on the formation of fossil algal residues. *Organic Geochemistry* 24, 661–669.

Kögel-Knabner, I. 2002. The molecular organic composition of plant and microbial residues as inputs in soil organic matter. *Soil Biology & Biochemistry* 34, 139–162.

Liang, C., Zhang, X., Rubert IV, K. F., and Balser, T. C. 2007. Effect of plant materials on microbial transformation of amino sugars in three soil microcosms. *Biology and Fertility of Soils* 43, 631–639.

Marchand, D., and Rontani, J.-F. 2001. Characterization of photo-oxidation and autoxidation products of phytoplanktonic monounsaturated fatty acids in marine particulate matter and recent sediments. *Organic Geochemistry* 32, 287–304.

Michaels, B. C., Ruettinger, R. T., and Fulco, A. J. 1980. Hydration of 9,10-epoxypalmitic acid by a soluble enzyme from *Bacillus megaterium*. *Biochemical and Biophysical Research Communications* 92, 1189–1195.

Naafs, D. F. W., van Bergen, P. F., de Jong, M. A., Oonincx, A., and de Leeuw, J. W. 2004. Total lipid extracts from characteristic soil horizons in a podzol profile. *European Journal of Soil Science* 55, 657–669.

Nakajima, T., and Volcani, B. E. 1969. 3,4-Dihydroxyproline: a new amino acid in diatom cell walls. *Science*, 164, 1400–1401.

Nguyen, R. T., Harvey, H. R., Zang, X., van Heemst, J. D. H., Hetényi, M., and Hatcher, P. G. 2003. Preservation of algaenan and proteinaceous material during oxic decay of *Botryococcus braunii* as revealed by pyrolysis-gas chromatography/mass spectrometry and ^{13}C NMR spectroscopy. *Organic Geochemistry* 34, 483–497.

O'Leary, W. M. 1962. The fatty acids of bacteria. *Bacteriological Reviews* 26, 421–447.

Otto, A., and Simpson, M. J. 2005. Degradation and preservation of vascular plant-derived biomarkers in grassland and forest soil from Western Canada. *Biogeochemistry* 74, 377–409.

Otto, A., and Simpson, M. J. 2007. Analysis of soil organic matter biomarker by sequential chemical degradation and gas chromatography-mass spectrometry. *Journal of Separation Science* 30, 272–282.

Otto, A., Chubashini, S., and Simpsom, M. J. 2005. A Comparison of plant and microbial biomarkers in grassland soils from the Prairie Ecozone of Canada. *Organic Geochemistry* 36, 425–448.

Oursel, D., Loutelier-Bourhis, C., Orangr, N., Chevalier, S., Norris, V., and Lange, C. M. 2007. Identification and relative quantification of fatty acids in *Escherichia coli* membranes by gas chromatography/mass spectrometry. *Rapid Communications in Mass Spectrometry* 21, 3229–3233.

Pereira, M. A., Pires, O. C., Mota, M., and Alves, M. M. 2002. Anaerobic degradation of oleic acid by suspended and granular sludge: identification of palmitic acid as a key intermediate. *Water Science and Technology* 45, 139–144.

Podell, D. N, and Abraham, G. N. 1978. A technique for the removal of pyroglutamic acid from the amino terminus of proteins using calf liver pyroglutamate amino peptidase. *Biochemical and Biophysical Research Communications* 81, 176–85.

Rhead, M. M., Eglinton, G., and Draffan, G. H. 1971. Conversion of oleic acid to saturated fatty acids in seven estuary sediments. *Nature* 232, 327–330.

Rontani, J.-F. 1998. Photodegradation of unsaturated fatty acids in sescent cells of phytoplankton: photoproduct structural identification and mechanistic aspects. *Journal of Photochemistry and Photobiology A*: *Chemistry* 114, 37–44.

Rontani, J.-F., Bonin, P. C., and Volkman, J. K. 1999. Biodegradation of free phytol by bacterial communities isolated from marine sediments under aerobic and denitrifying conditions. *Applied and Environmental Microbiology* 65, 5484–5492.

Rontani, J.-F., Koblížek, M., Beker, B., Bonin, P., and Kolber, Z. S. 2003. On the origin of *cis*-Vaccenic acid photodegradation products in the marine environment. *Lipids* 38, 1085–1092.

Rontani, J.-F., Zabeti, N., and Wakeham, S. G. 2009. The fate of marine lipids: biotic vs. abiotic degradation of particulate sterols and alkenones in the Northwestern Mediterranean Sea. *Marine Chemistry* 113, 9–18.

Ruettinger, R. T., and Fulco, A. J. 1981. Epoxidation of unsaturated fatty acids by a soluble cytochrome P-450-dependent system from *Bacillus megaterium*. *The Journal of Biological Chemistry* 256, 5728–5734.

Sakami, W., and Harrington, H. 1963. Amino acid metabolism. *Annual Review of Biochemistry* 32, 355–98.

Schulze, W. X. 2005. Protein analysis in dissolved organic matter: what proteins from organic debris, soil leachate and surface water can tell us – a prospective. *Biogeosciences* 2, 75–86.

Shevchenko, A., Loboda, A., Shevchenko, A., Ens, W., and Standing, K. G. 2000. MALDI quadrupole time-of-flight mass spectrometry: a powerful tool for proteomics research. *Analytical Chemistry* 72, 2132–2141.

Simpson, A. J., Simpson, M. J., Kingery, W, L., Lefebvre, B. A., Moser, A., Williams, A. J., Kvasha, M., and Kelleher, B. P. 2006. The application of ^{1}H high-resolution magic-angle spinning NMR for the study of clay–organic associations in natural and synthetic complexes. *Langmuir* 22, 4498–4508.

Simpson, A. J., Simpson, M. J., Smith, E., and Kelleher, B. P. 2007. Microbially derived inputs to soil organic matter: are current estimates too low? *Environmental Science and Technology* 41, 8070–8076.

Stephanou, E. G. 1992. α,ω-Dicarboxylic acid salts and α,ω-dicarboxylic acids photooxidation products of unsaturated fatty acids present in marine aerosols and marine sediments. *Naturwissenschaften* 79, 128–131.

Stephanou, E. G., and Stratigakis, N. 1993. Oxocarboxylic and α,β-dicarboxylic acids: photooxidation products of biogenic unsaturated fatty acids present in urban aerosols. *Environmental Science and Technology* 27, 1403–1407.

Sun, M.-Y., and Wakeham, S. G. 1994. Molecular evidence for degradation and preservation of organic matter in the anoxic Black Sea Basin. *Geochimica et Cosmochimica Acta* 58, 3395–3406.

Sun, M.-Y., Shi, Y., and Lee, R. F. 2000. Lipid-degrading enzyme activities associated with distribution and degradation of fatty acids in the mixing zone of Altamaha estuarine sediments. *Organic Geochemistry* 31, 889–902.

Sun, M.-Y., Wakeham, S. G., and Lee, C. 1997. Rates and mechanisms of fatty acid degradation in oxic and anoxic coastal marine sediments of Long Island Sound, New York, USA. *Geochimica et Cosmochimica Acta* 61, 341–355.

Turner, B. L., Paphazy, M. J., Haygarth, P. M., and McKelvie, I. A. 2002. Inositol phosphates in the environment. *Phylosophical transactions of the Royal Society of London B* 357, 449–469.

van Bergen, P. F., Bull, I, D., Poulton, P. R., and Evershed, R. P. 1997. Organic geochemical studies of soils from the Rothamsted Classical Experiments-I. Total lipid extracts, solvent insoluble residues and humic acid from Broadbalk Wilderness. *Organic Geochemistry* 26, 117–135.

Voet, D., and Voet, J. G. 1990. *Biochemistry*. John Wiley & Sons, New York.

Wakeham, S. G., Hedges, J. I., Lee, C., Peterson, M. L., and Herns, P. J. 1997. Compositions and transport of lipid biomarkers through the water column and surficial sediments of the equatorial Pacific Ocean. *Deep-Sea Research II* 44, 2131–2162.

Wakeham, S. G., Pease, T. K., and Benner, R. 2003. Hydroxy fatty acids in marine dissolved organic matter as indicators of bacterial membrane material. *Organic Geochemistry* 34, 857–868.

Wilson, K., and Walker, J. (Eds). 2000. *Principles and techniques of practical biochemistry*. Cambridge University Press, UK. 2000.

Yamashita, Y., and Tanoue, E. 2004. Chemical characteristics of amino acid-containing dissolved organic matter in seawater. *Organic Geochemistry* 35, 679–692.

Zang, X., Nguyen, R. T., Harvey, H. R., Knicker, H., and Hatcher, P. G. 2001. Preservation of proteinaceous material during the degradation of green alga *Botryococcus braunii*: a solid-state 2D ^{15}N ^{13}C NMR spectroscopy study. *Geochimica et Cosmochimica Acta* 65, 3299–3305.

Chapter 6

Protein Degradation and Peptide Mass Fingerprinting

Protein degradation and peptide mass fingerprinting

6.1 Introduction

Proteins are by far the most abundant components in bacterial cells (Zang et al., 2001). They are an important link between the soil C cycle and the soil N cycle, both of which are key factors in soil fertility and microbial activity in soil (Kindler et al., 2009). They represent the largest organic N pool in soil and account for up to 85% of the organic N found in SOM (Tanoue, 1995; Simpson et al., 2007). The two main categories of amino-N compounds in soils are intact proteins released for various extracellular functions and detrital proteins and polypeptides–plant and microbial constituents in various stages of transformation (Murase et al., 2003; Rillig et al., 2007). Other N-containing compounds in the soil are amino sugars and compounds formed by abiotic interactions, such as protein–tannin complexes and Maillard reaction products, as well as various heterocyclic pyrolysis products (Knicker, 2006).

Proteins have traditionally been considered inherently labile biomolecules in the environment with poor preservation potential (Nguyen and Harvey, 2003). This lability is conferred by the high sensitivity of the amide linkages present in peptides (Derenne and Largeau, 2001; Roth and Harvey, 2006). However, several studies have provided evidence of high molecular mass proteinaceous materials or at least proteinaceous moieties in soil-aquatic environments, citing various mechanisms for their preservation (Nguyen and Harvey, 1997; Knicker and Hatcher, 1997; Michalzik and Matzner, 1999; Kelleher et al., 2007). In soils, the degradation of proteins is an important process in the turnover of organic N. This degradation is assumed to occur independently of the source origin of proteins, but proteins of scarce organisms may be harder to detect as they may be dilited in the bulk of proteins from more abundant organisms (Schulze et al., 2005). Despite this limitation, the analysis of protein identity can improve our understanding of the functional protein composition of organic C and N, and at the same time yield clues to the phylogenetic groups contributing to the refractory protein pool in the environment (Schulze, 2005; Schulze et al., 2005).

Proteins have been reported to be relevant for the stabilization of SOM by sorption to mineral surfaces (Kleber et al., 2007). They are particularly versatile in

attaching to all kinds of surfaces, because they contain both cationic and anionic functional groups as well as both hydrophilic and hydrophobic residues (Kleber et al., 2007). The strong interactions of proteins with minerals make them a stable base layer for the sorption and stacking of other organic compounds to mineral surfaces. The fate of proteins in soil may therefore be a key to understanding SOM stabilization (Miltner et al., 2009). Previously, we demonstrated the selective preservation of polymeric protein structures and determined that amide-N is the most refractory organic N in microbial biomass and leachates using advanced NMR spectroscopy (***Chapter 3***). We also provided unambiguous evidence of a strong association between microbial proteins and clay minerals using XRD, SEM-EDS and advanced NMR approaches (***Chapter 4***).

Since the data presented in ***Chapters 3*** and ***5*** indicated considerable stabilization of microbially derived proteins in a clay-free environment, we reasoned that these proteins are most likely of a structural nature. Further to the findings of clay-microbial complexes studied in ***Chapters 4*** and ***5***, we also hypothesize that clay minerals are capable of stabilizing greater quantities of microbially derived proteins than chemical recalcitrance alone. Therefore, the objectives of this work were to determine the composition of the refractory protein pool of soil microbial biomass in a degradation study (involving microbial biomass, clay-microbial complexes and microbial leachates; ***Chapter 3***), and at the same time evaluate their phylogenetic origin using peptide mass fingerprinting (PMF).

Currently, PMF is the most common method used to identify proteins and is based on the comparison of a list of experimental peptide masses with theoretical peptide masses. The experimental masses are generated from the MS measurement of an enzymatically digested protein sample, while the theoretical masses are obtained from and *in silico* (computer simulated) digestion of all sequences in a database. The goal is to find the protein(s) whose peptide masses show the best match with the experimental fingerprint (Bienvenut et al., 1999). The method can be divided into threes steps, the first step involving the selection of the most relevant masses for protein identification from the mass spectra. The second step is the comparison of the selected experimental peptide mass values to all protein sequences in a database, which were theoretically cleaved by applying the cleavage rule corresponding to the enzyme used for the sample digestion. Finally, a similarity rule (score) should provide a measure of quality of fit of the matched values, in order to select the best matching protein (Bienvenut et al., 1999).

6.2 Materials and Methods

6.2.1 Protein extraction

Soluble proteins were extracted from initial microbial biomass and clay-microbial complexes (kaolinite- and montmorillonite-) as well as, ambient and UV degraded microbial biomass, clay-microbial complexes and microbial leachates. The clay-microbial complexes used for the extraction of soluble proteins were prepared as previously described in ***Section 4.2.1***. All degraded samples (microbial biomass, clay-microbial complexes and microbial leachates) used for the extraction of soluble proteins were prepared as previously described in ***Section 3.2.2***. Protein extractions were carried out on all samples according to a modified version of previously published protocols (Ogunseitan, 1993; Singleton et al., 2003) as described in ***Section 4.2.2***. Note, all samples considered in this chapter were unlabelled.

6.2.2 Protein separation

Extracted proteins were separated by one-dimensional SDS-PAGE according to Bienvenut et al. (1999). The proteins were solubilised in SDS-PAGE sample buffer (Tris-HCl: 60 mM, [pH 6.8], β-mercaptoethanol: 3% [v/v], glycerol: 10% [v/v], SDS: 2% [w/v], bromophenol blue: 0.002% [w/v] and then reduced at 95ºC for 5 min before being loaded on the gel (4% stacking gel, 12% separating gel) for one-dimensional electrophoresis migration. The dimensions of the gel were 7 cm x 10 cm with a thickness of 1 mm. Migration was carried out using the Mini-Protean II electrophoresis apparatus (Bio-Rad) operated at 200 V constant for 45 min. The gel was stained in Coomassie Brilliant Blue R250 (0.2% w/v), water (60% v/v), methanol (30% v/v) and acetic acid (10% v/v) for 1 h and destained with repeated washes of water (50% v/v) methanol (40% v/v) and acetic acid 10% v/v). A Sigma Wide Range Marker or a PageRuler™ Plus Prestained Protein Ladder (Fermentas Life Sciences) was used as references for SDS-PAGE.

6.2.3 In-gel protein digestion

Selected protein bands were excised from the 1-DE gels and then digested with trypsin using previously published procedures (Bienvenut et al., 1999) modified as described below. Gel pieces were destained in 100 µl of 50 mM ammonium bicarbonate, 30% acetonitrile by incubation at 37ºC for 30 min. The procedure was repeated until destaining was complete. The destaining solution was removed and the

gel pieces dried in a vacuum centrifuge. The gel pieces were subsequently reswollen and the proteins in-gel reduced with 25 mM NH_4HCO_3 containing 10 mM 1,4-dithio-DL-threitol (DTT; Sigma) at 60ºC for 30 min. After cooling to room temperature, the DTT solution was removed and the proteins in-gel alkylated with 55 mM iodoacetamide (Thermo) in the dark at room temperature for 30 min. After reduction and alkylation, the gel pieces were washed with 100 µl of 100 mM NH_4HCO_3 for 10 min, and dehydrated with acetonitrile. The gel pieces were rehydrated in digestion buffer containing 50 mM NH_4HCO_3 and 12.5 ng/µL of sequencing-grade modified trypsin (Thermo) at 4ºC for 30 min. A further 10 µl aliquot of 50 mM NH_4HCO_3 was added to each tube and protein digestion carried out overnight at 37ºC. The resulting peptides were extracted twice (20 min per extraction) using 0.1% formic acid in 50% acetonitrile at room temperature and dried down under high vacuum. One microlitre (1 µl) of the concentrated peptides was mixed with 1 µl of acetonitrile:methanol (50:50; v/v) containing 3.70 mg/mL of MALDI-MS matrix, α-cyano-4-hydroxycinnamic acid (ACCA) for MALDI-Qq-TOF peptide analysis.

6.2.4 MALDI-Q-ToF MS analysis

Mass spectra were acquired using a Micromass® Q-ToF Ultima™ MALDI mass spectrometer equipped with a 337 nm nitrogen laser in the positive ion reflectron mode (Waters, Milford, MA, USA). Laser pulses of 250 µJ were delivered to the target through a 0.2-mm core diameter fused-silica optic fibre. The laser beam was focused at the target into a spot about 0.3 mm x 1 mm. A 10-kV acceleration voltage was used in the TOF part of the instrument. The orthogonal injection pulse repetition rate was set at 8.5 kHz. An aliquot of approximately 0.3–0.5 µl of the tryptic peptide-ACCA mix was loaded on the MALDI stainless steel sample plate and the mixture allowed to air dry. MALDI-MS spectra were acquired at a laser repetition pulse rate of 5–10 Hz for time interval at 1.5 min. The instrument was calibrated externally using the ProteoMass™ MALDI Calibration Kit (Sigma) and no postacquisition recalibration of MS spectra was performed.

6.2.5 Database interrogation

Measured masses were submitted for PMF interrogations using the MASCOT software package v.2.1.03 (Matrix Science, London, UK; http://www.matrixscience.com/). Peak harvesting was done automatically using MassLynx software (Waters). Peak resolution was calculated, with baseline correction,

smoothing and peak centre being applied to the raw data. The query was made for each sample with a minimum number of matches set at 4. The maximum tolerance for masses was set at ±1.2 Da, at most one missed cleavage for tryptic peptides was allowed. Monoisotopic peptides and possible carbamidomethylation of cysteine was considered as fixed modification, while oxidation of methionine, acrylamidated cysteine and pyroglutamate formation at N-terminal glutamine and glutamic acid were considered as artifactual modifications for PMF analysis. No limitations on protein molecular weights and species origin were imposed. No p*I* limits were used to restrict the search of the samples. Searches were conducted against *SWISS*-PORT (Release 57.4), NCBI and MSDB databases. Positive identification was accepted when the data satisfied the following criteria: (i) targets were obtained with statistically significant scores (>95% confidence intervals, equivalent to the MASCOT expect value <0.05); or (ii) the molecular weights of the targets were consistent with those observed in the SDS-PAGE gel.

6.2.6 Molecular weight analysis by LC-ESI-TOF-MS

The mixture of intact proteins was precipitated by adding four volumes of cold 80% (v/v) acetone to the sample and incubation on dry ice for 3 h. The sample was then centrifuged at 14,000 x g at 4ºC for 10 min and the supernatant carefully removed. The pellet was washed twice with cold acetone (100%), air dried, and the dried sample resuspended in acetonitrile:water (50:50, v/v) containing 0.2% (v/v) formic acid, using a volume equivalent to 1/3 the starting volume of the mixture of intact proteins. The sample was vortexed for 2 min, and then incubated at 60ºC for 5 min. Vortexing was repeated and the sample incubated for a further 10 min at 60ºC until the pellet was completely dissolved.

Mass determination measurements were performed using the Agilent 6200 series time of flight mass spectrometer with an electrospray ionization interface. The concentrated proteins were infused at 200 µl mL^{-1}, using a mobile phase of acetonitrile:water (50:50, v/v) with 0.2% (v/v) formic acid. Alternatively, the masses of concentrated proteins were verified using a LC-ESI-TOF MS system in positive ionization mode. The mixture was separated by a RP-HPLC system (Agillent Technologies 1100 Series LC/MSD, Germany) equipped with a quaternary pump, micro vacuum degasser, an autosampler equipped with a 100 µl-loop, a diode-array and multiple wavelength UV-VIS detector (DAD), and a multitray fraction collector.

Separation was performed using a Jupiter, 5 µ C18 300Å column (250 x 2.0 mm), with a safety guard (4 x 3 mm) installed ahead of it (Phenomenex, Torrance, CA). Fractions (10 µl) were autoinjected and eluted using a binary mobile phase of 0.1% formic acid in water as mobile phase A and 0.1% formic acid v/v in acetonitrile as mobile phase B. The initial mobile phase comprised of 5% B for 5 min, followed by a linear gradient to 65% B in 30 min at a flow rate of 0.2 mL min^{-1}. The HPLC system was coupled to a TOF mass spectrometer (Agilent Technologies, USA) operating under the following conditions: desolvation gas flow, 8 L min^{-1}; desolvation gas temperature, 350ºC; source temperature, 100ºC; nebulizer gas pressure, 50 psi; VCap, 4000 V; and fragmentor, 200V. Spectra were acquired in profile scan mode over the *m/z* 100–3000 range at a scan range of 0.05s/spectrum. Bovine serum albumen (BSA; 10 ng mL^{-1}) was used as reference. Because proteins are multiple-charged compounds, they acquire a range of charge states yielding a series of masses for an individual compound. The employment of Deconvolution software (Agilent Technologies) allowed statistical transformation of the envelope of multiple-charged products into a singly charged parent spectrum for molecular weight determination. The entire mass spectra were processed using MassHunter software (Agilent technologies).

6.3 Results and Discussion

6.3.1 Analysis of proteins from microbial biomass and microbial leachates

Proteins recovered from initial and degraded microbial biomass, and degraded microbial leachates were separated by 1-D SDS-PAGE, and visualized by Coomassie Brilliant Blue staining (***Figures 6.3.1.1-6.3.1.3***). Copious distinct proteins exhibiting a large range of molecular weights: from approximately 6.5 to 250 kDa were recovered from the initial microbial biomass (***Figure 6.3.1.1***). In contrast, only 5 distinct protein bands were present at detectable levels in the ambient degraded biomass, indicating that a small number of refractory proteins exist at relatively high concentrations in the degraded samples. These proteins were distributed over a large range of molecular masses: from approximately 20 to 250 kDa. On the other hand, no discernable bands were detected in the smear of stained material for the UV degraded biomass (***Figure 6.3.1.2***). A characteristic electrophoretic pattern of proteins with apparent molecular masses of ~250, 110, 50, 36 and 32 kDa was observed for all ambient degraded biomass (6, 14 and 26 weeks). A relatively large number of discrete (well separated) proteins

(numbering ~20) were observed as major bands in all microbial leachates (***Figure 6.3.1.3***) regardless of the conditions of degradation (see comparable signals, regions 1 and 2; ***Figure 3.3.8.1***). These proteins were distributed over a large range of molecular masses: from approximately 11 to 250 kDa. The distribution of molecular masses of refractory proteins in the degraded samples was quite similar, indication that the same proteins were selectively preserved across all the samples (***Figures 6.3.1.1-6.3.1.3***).

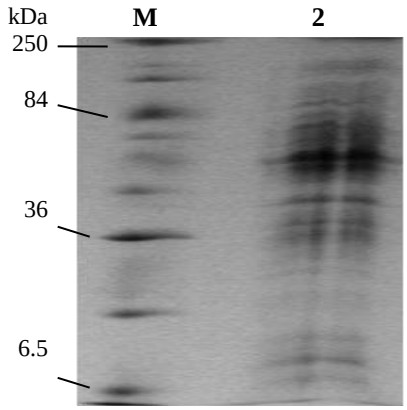

Figures 6.3.1.1: Electrophoretogram of a Coomassie Brilliant Blue-stained SDS-PAGE gradient gel (12%-4%) form a one-dimensional gel separation of a fraction of proteins isolated from initial soil microbial biomass. The lanes identified are as follows: M, Sigma Wide Range Molecular Marker and 2, protein extract of the initial microbial biomass (starting material).

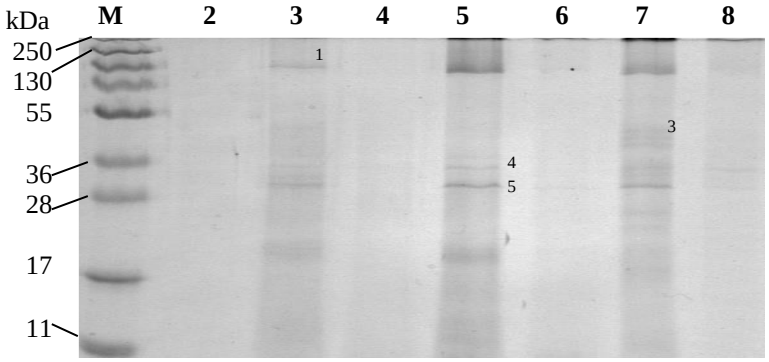

Figures 6.3.1.2: Electrophoretogram of a Coomassie Brilliant Blue-stained SDS-PAGE gradient gel (12%-4%) form a one-dimensional gel separation of a fraction of proteins isolated from degraded soil microbial biomass. The lanes are as follows: M, PageRuler™ Plus Prestained Protein Ladder; Lane Lanes 3, 5 & 7, microbial biomass degraded under ambient conditions for 6, 14 & 26 weeks, respectively; Lanes 4, 6 & 8, microbial biomass degraded under UV irradiation (300 – 350 nm) for 6, 14 and 26 weeks, respectively. Labelled bands were exised for identification.

The major refractory proteins did not vary spatially, and the protein with apparent molecular masses of 130, 36 and 30 kDa were clearly visible as the major refractory proteins in the differentially degraded biomass and microbial leachates. The remaining refractory proteins were detected in faint but distinct bands. A low-level background, presumably, less concentrated proteins and degradation products (Powell et al., 2005) was particularly noticeable for the UV degraded biomass but also observed for all other samples. From the electrophoretograms (***Figures 6.3.1.1-6.3.1.3***), it would appear that degradation of the less recalcitrant proteins was a stepwise process resulting in the loss of whole macromolecules as previously discussed (***Chapter 5***).

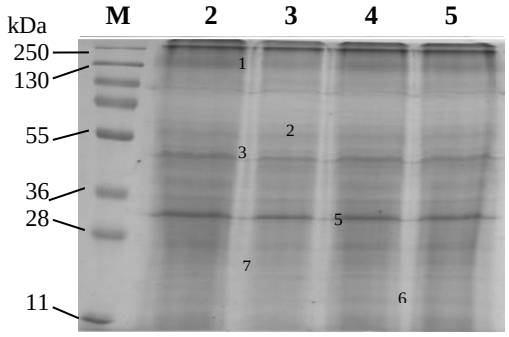

Figures 6.3.1.3: Electrophoretogram of a Coomassie Brilliant Blue-stained SDS-PAGE gradient gel (12%-4%) form a one-dimensional gel separation of a fraction of proteins isolated from soil microbial biomass leachates. The lanes are as follows: M, PageRuler™ Plus Prestained Protein Ladder; Lanes 2 & 4, microbial biomass leachate degraded under UV irradiation (300 – 350 nm) for 6, & 14 weeks, respectively; Lanes 3 & 5, microbial biomass leachate degraded under ambient conditions for 6 and 14 weeks, respectively. Labelled bands were exised for peptide map fingerprinting.

6.3.2 Analysis of proteins isolated from clay-microbial complexes

To further investigate the protective influence of montmorillonite and kaolinite clay minerals against biodegradation and photocatalysis of proteins, the electrophoretograms of proteins recovered from initial clay-microbial complexes and degraded clay microbial-complexes (***Section 6.2.1***) were compared in ***Figure 6.3.2.1A-C***. Except for differences in apparent concentrations, the electrophoretic patterns of proteins isolated from kaolinite-microbial complexes at different stages of degradation are largely similar with a molecular mass distribution ranging between 17 and 250 kDa. A discrete banding pattern (17 to 250 kDa), previously not detected in the UV irradiated biomass, and is now clearly observed in the extracts of the UV irradiated kaolinite-microbial complexes. Proteins extracted from montmorillonite-complexes were slightly less variable, ranging from 30 to 250 kDa. It is interesting to note that while several faint but distinct bands were observed after 26 weeks degradation under ambient

conditions, only four distinct proteins (approximately 30 and 250 kDa) survived UV degradation beyond 14 weeks (***Figure 6.3.2.1B***). As expected, these findings correlate with the data reported in ***Chapters 4*** and ***5***, showing that clay minerals are capable of stabilizing significant quantities of microbially derived proteins even under the harshest possible conditions (acid hydrolysis).

The persistence of microbial proteins in the degraded biomass is of critical importance in the context of soil C and N sequestration. This is especially significant as numerous gaps in our knowledge of the role of proteins in C and N stabilization have been highlighted (Kleber et al., 2007; Miltner et al., 2009). One of the most fundamental gaps of knowledge is our ability to quantify soil protein or peptidic N (Rillig et al., 2007). It is not immediately clear, whether specific proteins from the un-reacted biomass are resistant to degradation through their protein structure, as has been suggested for bacterial porin proteins (Yamashita and Tanoue, 2004), or stabilization was achieved through interaction with other biomolecules. However, noncovalent forces such as hydrophobic and hydrogen-bond interactions between proteinaceous materials and nonprotein components have been suggested as major mechanisms for the stabilization and preservation of proteins (Nguyen and Harvey, 2001; Yamashita and Tanoue, 2004). The stability of structural materials of other biomolecules has been previously studied. Membrane proteins of bacteria (Nagata et al., 1998) are reportedly more stable than cytoplasmic ones under kinetic studies of bacterial degradation, and structural carbohydrates are reportedly more refractory than storage carbohydrates (Derenne et al., 1993, 1996). These findings would appear consistent with our observation of intact membrane protein in the degraded samples and reinforce the fact that structural biomolecules are inherently more recalcitrant than their storage counterparts.

The stability of membrane proteins is likely to result from association with other organic compounds such as phospholipids (Nagata et al., 1998). Phospholipids are unique organic compounds in that they contain both hydrophobic and hydrophilic polarities, making them capable of forming hydrophobic, hydrogen and covalent bonds with other organic compounds (Alberts et al., 1994). In addition, the proteins observed could have survived degradation by being encapsulated by lipids (Nguyen and Harvey, 2003), covalently bonded to sugar molecules in the form of glycoproteins (Yamada and Tanoue, 2003), or possible modifications under abiotic conditions (Keil and Kirchham,

1993). Complementary evidence of the stabilization of microbially derived proteins by other organic molecules was previously reported in ***Chapters 3*** and ***4***. In addition, the bio-refractory proteins detected may simply be proteins which have unfolded after cellular disruption, with the exposure of hydrophobic polypeptide regions leading to various inter- and intra-molecular associations (Nguyen and Harvey, 2001).

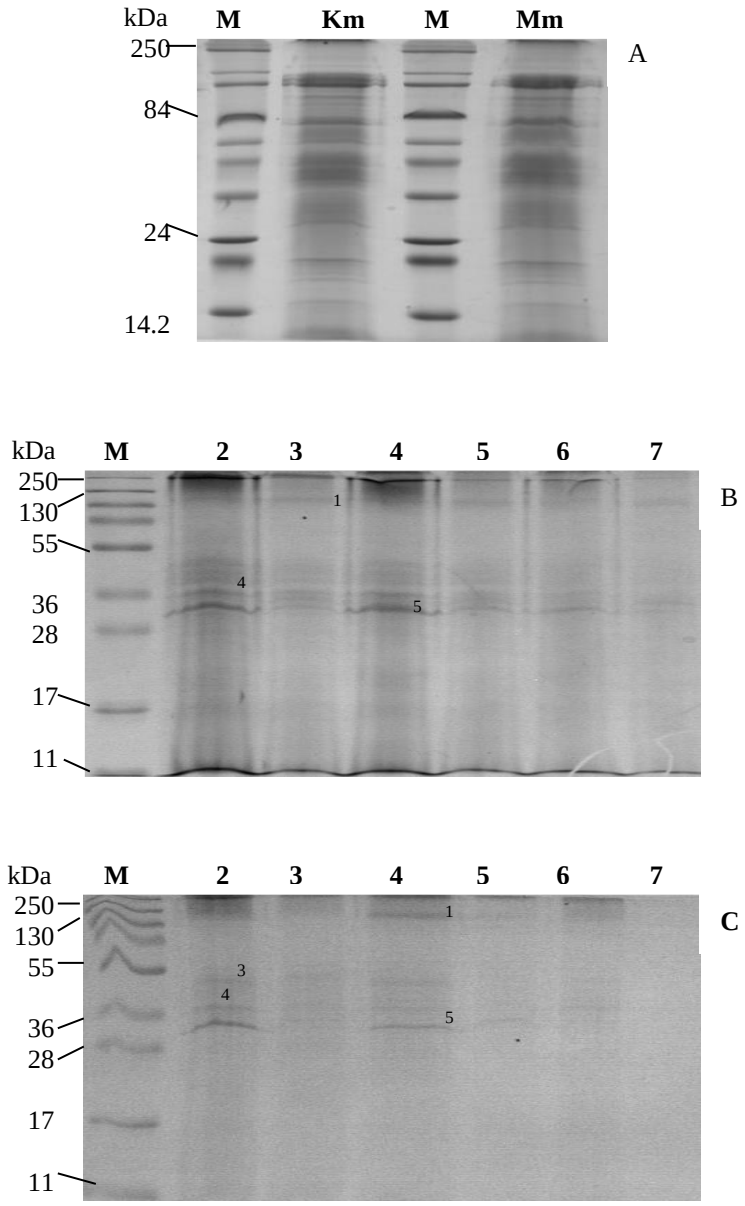

Figures 6.3.2.1: Electrophoretograms of Coomassie Brilliant Blue-stained SDS-PAGE gradient gels (12%-4%) of protein fractions isolated from a) initial clay-microbial complexes (starting material), b) kaolinite-microbial complexes and c) montmorillonite-microbial complexes degraded under ambient and UV conditions. The lanes are as follows: M, PageRuler™ Plus Prestained Protein Ladder; Lanes Km & Mm, initial kaolinite- and momtmorillonite-microbial complex, respectively; Lanes 2, 4 & 6, microbial-complexes degraded under ambient conditions for 6, 14 & 26 weeks, respectively; Lanes 3, 5 & 7, microbial-complexes degraded under UV irradiation (300 – 350 nm) for 6, 14 & 26 weeks, respectively.

There are other protective mechanisms that may participate in the preservation of proteins in degraded samples at the molecular level. For example, the selective preservation or physical protection of proteins through the presence of highly conserved sequences is one such possibility (Powell et al., 2005). The amino acid sequence of a protein encodes its physiological location and structure that provide inherent protection from degradation processes (Nunn et al., 2003). Thus, for proteins, physical protection is strongly linked to primary sequence, because the sequence of the protein is critical in determining if it could remain part of a cellular fragment or partition into a particular pore. Therefore, physical protection and selective preservation are not mutually exclusive survival mechanisms, but rather these two models are very dependent upon one another for explaining the survival of refractory proteins in the environment (Powell et al., 2005). Amino acid modifications are known to impart protection from degradation by enzymes by altering the protein structure so that it fits imperfectly into the active site of the enzyme (West, 1986), and should be considered as an important molecular level mechanism involved in the preservation of proteins over the course of the degradation.

Considering the electrophoretic evidence, the near complete loss of proteins from the biomass incubated under UV irradiation (relative to those degraded under ambient conditions) is most probably due to photochemical conversion of the bio-refractory protein molecules into biologically labile and/or volatile compounds (Mopper et al., 1991). This hypothesis is supported by the observation that UV-B radiation results in direct photochemical modification of proteins, particularly those associated with membranes (Caldwell, 1993). The peptide backbone, tryptophan (Trp), tyrosine (Tyr), phenylalanine (Phe) and cysteine (Cys–Cys disulfide bonds) have been demonstrated to be the primary targets of photodegradation in proteins (Kerwin and Remmele, 2006). Furthermore, it has been suggested that Trp photodegradation could directly alter protein structure or modify membrane lipids and proteins through the production O_2^- and H_2O_2 (Caldwell, 1993). There is also evidence to suggest that tryptophanyl residues in relatively hydrophilic environments are more susceptible to photodegradation (Caldwell, 1993) and may further explain the massive loss of proteins in the UV degraded samples.

The stabilization of microbially derived proteins by clay minerals was clearly demonstrated in ***Figure 6.3.2.1B*** and ***C***, and previously in ***Chapter 5***. Threfore, we

deduced that the relatively large number of discrete proteins observed in the leachates (***Figure 6.3.1.3***) is a result of their association with soil particles and clay minerals as they are leached through the soil (although their survival may also be due to structural stability). Survival is illustrated by the presence of bands characteristic of intact proteins and are often of relatively higher concentration (brighter bands) in the extracts of degraded clay-microbial complexes (***Figure 6.3.2.1B*** and ***C***) when compared with the extracts of the degraded biomass (***Figure 6.3.1.2***). Moreover, FT-IR spectroscopy demonstrated clear amide I and amide II bands (data not shown) in protein extracted clay-microbial residues. This method cannot be used to identify proteins, only characteristic band vibration patterns. However, these data are consistent with other data supporting the presence of proteinaceous material still tightly bound and preserved on clay minerals after acid hydrolysis (***Figure 4.3.5.1***). The stabilizing effect of silicate-type minerals has been previously reported for the protein-silica complex of diatom cell walls (Hecky et al., 1973). Our findings are consistent with this and subsequent suggestion that the presence of mineral particles are capable of protecting organic material, perturbing the progression from less to more chemically recalcitrant material during decomposition.

The stabilization of microbial proteins by montmorillonite may be attributed in part to intercalation of the interlamellar regions of montmorillonite by these molecules. Supporting evidence of the intercalation of montmorillonite by proteins was previously presented (***Chapter 4***; ***Figure 4.3.3.1***). The intercalation of montmorillonite clay mineral by proteins may protect these macromolecules against decomposition due to: (i) reduced access to microbes and their enzymes; (ii) and restricted aerobic decomposition due to reduced diffusion of oxygen (Lützow et al., 2006). Other mechanisms such as hydrophobicity may be implicated in the protection of proteins from degrading enzymes. While pure clays demonstrate hydrophilic properties, the association of organic material with clay minerals increases their hydrophobicity (Doerr et al., 2000).

N-containing compounds, particularly those derived from microorganisms have been reported to adsorbe strongly to mineral surfaces (Feng et al., 2006; Simpson et al., 2006). These interactions appear to confer greater stability than chemical recalcitrance and may explain the greater preservation potential of proteinaceous materials in the degraded clay-microbial complexes. The adsorption of macromolecules to mineral surfaces is associated with conformational changes that render them unavailable to

activity of extracellular enzymes (Khanna et al., 1998). However, the adsorption of degrading enzymes to clay minerals rather than adsorption of the substrate may also be significant in the preservation of otherwise labile proteinaceous materials (Demaneche et al., 2001). It is tempting to hypothesize that some proteins in microbial leachates and degraded clay-microbial complexes were preserved as glycoproteins as previously suggested (***Chapter 3***). This suggestion is also supported by previous evidence linking the stabilization of glycoproteins to increased sorption to soil particles consequently decreasing their accessibility to degrading enzymes (Keil and Kirchman, 1993; Yamada and Tanoue, 2003).

6.3.3 Validation of peptide mass fingerprinting

PMF is recognised as the most common method used to identify proteins in a sample, and is applied in this study to identify the refractory protein pool and their taxonomic origins from a mixed culture of soil microbial biomass degraded under ambient and UV conditions. However, to test the method (peptide separation and resolution), a MALDI peptide map of BSA (Sigma) obtained from a freshly prepared gel allowed comparison (***Figure 6.3.3.1***). The spectrum was acquired on the same instrument and the sample prepared using the same in-gel tryptic digestion protocol. There are 55 potential fragments that can be produced by complete digestion of BSA with trypsin, assuming no missed cleavage sites (Nunn et al., 2003). A total of 24 peptide fragments were identified, and their sequences were matched to BSA. Nineteen of those fragments could be assigned to peptides from the primary structure with no missed cleavages (35% of the predicted peptide fragments). The *m/z* peaks at 1250 (Phe35 – Lys45), 1245 (Glu267 – Lys285), 1350 (Arg360 – Arg371), 1355 (Lys437 – Arg451) and 1441 (Cys581 – Lys597) all possessed one missed cleavage. From the spectrum, only a few minor peaks were not matched to BSA sequence. Cumulatively, the MALDI-MS peptide map of BSA accounted for 43% peptide coverage of the entire BSA sequence. These results are typical for controlled trypsin digests of BSA; it is rare for trypsin to achieve greater than 40% coverage (Nunn et al., 2003). The oxidation of methionine and tryptophan residues and S-acrylamidation of cysteine residues were the major artefactual modification observed for tryptic digested BAS. Four major types of artefactual protein modifications (mono- and di-oxidation of methionine residues, pyroglutamation of N-terminal glutamic acid, and acrylamidation of cysteine residues) frequently encountered in sequencing of proteins from conventional polyacrylamide gels (Clauser et al., 1995; Thiede et al., 2000) were observed for the proteins analysed.

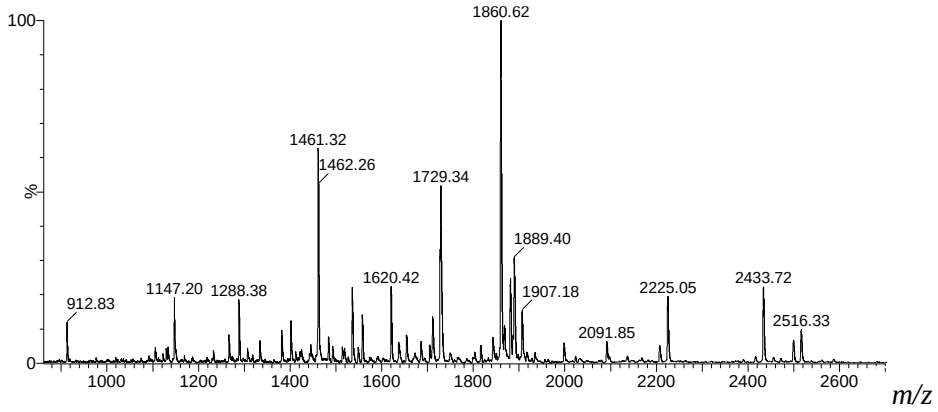

Figure 6.3.3.1: MALDI-TOF mass spectra of in-gel tryptic digested BSA used for method validation. All the conditions of digestion, MALDI peptide mapping used for the proteins analysed were applied.

6.3.4 Limitations of peptide mass fingerprinting

Protein identification techniques using either PMF or MS/MS data are still inherently limited to the availability of the protein in the databases. Furthermore, the source of the refractory proteins in the samples is likely to be bacteria whose genomes and proteomes have yet to be sequenced. If the sequence database does not contain the unknown protein, then the aim is to identify those entries which exhibit the closest homology, often equivalent proteins from related species (Perkins et al., 1999). Therefore, it is not surprising that greater scores were not obtained from database matches by computer automated correlation software. If the protein cannot be identified by such techniques, *de novo* sequencing becomes a valuable tool through which a short sequence tag can be identified (Bienvenut, 2005).

The minimum number of peptides required for a protein match is strongly dependent on the possible number of cleavage sites and generally varies with the mass of the protein. Nevertheless, the value can be kept relatively low because of the fact that the difference to randomly scored peptides and the sequence coverage is more important than the number of peptides matched to estimate the result of a database search. Other crucially important parameters used to rate the result of mass search are; the matching of the main peaks, the mass accuracy and the difference in numbers of matched masses to randomly matched proteins (Thiede et al., 2000). At best, all peptide masses of a peptide mass fingerprint can be attributed to the protein with the highest score. This is frequently not possible due to, for example, incomplete purification of the protein, modification of amino acids, and genetic variations (Thiede et al., 2000). In-gel or in situ (on the surface of PVDF or nitrocellulose membranes) digestion with trypsin is

probably the most widely used protein cleavage method in proteomics research. However, tryptic digestion is not very efficient for very hydrophobic proteins and very basic proteins, since too long and too short peptides are generated, respectively (Shevchenko et al., 2000).

Post-translational modifications, and modifications due to chemical derivatization, contribute greatly to the complexity of mass-based searching. Often, there is uncertainty as to whether a particular modification is present or not. Even if present, a modification may not be quantitative. For example, a peptide may contain oxidised and nonoxidised methionine residues (Perkins et al., 1999). Although only a percentage of the experimental peptides matched against the theoretical peptides from the database, it is important to note that there are significant matches for peptides of some of the most intense peaks. This does not mean that the remaining peptides are noise. It may be that the matching peptides gave the lowest probability (Perkins et al., 1999).

6.3.5 Peptide mass fingerprinting of refractory proteins

Following PMF validation, we attempted to identify the more prominent intact proteins observed in degraded soil microbial biomass, clay-microbial complexes and microbial leachates. This was accomplished by in-gel trypsinolysis of the selected proteins followed by MALDI peptide mass mapping. It should be noted that a number of intense peaks in the MALDI peptide maps of the in-gel digested samples were not assigned to protein sequences even at a mass tolerance exceeding 1.2 Da (Shevchenko et al., 2001). Furthermore, the sequence coverage of peptide maps acquired from in-gel digestion of proteins from degraded samples was lower than the corresponding spots excised from an initial sample (starting material). Taken together, these observations would suggest that there was some degree of loss or degradation during the experiments, first demonstrated in ***Chapter 3***. Several attempts were made to fragment intense peptide ions that could not be matched to the sequence of proteins already identified (Shevchenko et al., 2001). However, no meaningful fragmentation pattern was obtained from the MALDI-MS/MS data. It should be emphasized here that MS analysis and database searching leads to a probability of identity, not an absolute identification.

During database interrogations of the MALDI peptide maps, homologues of 7 dominant refractory proteins common to all degraded samples were identified (***Figures***

6.3.1.2-3 and ***6.3.2.1***). The mass spectra of the protein homologues are presented in ***Figure 6.3.5.1-7***. A major theme of protein homologues was observed for two categories of proteins: membrane proteins and enzymes, including several synthases and transferases (***Table 6.3.5.1***). These data confirmed our previous hypothesis that refractory proteins were of a structural nature. They also agree with the findings of Yamashita and Tanoue (2004) who identified enzymes as a major theme of dissolved proteins recovered from sea water. Protein synthesis (i.e. ribosomes) and energy metabolism (i.e. metabolic enzymes) are also two of the most abundant categories of protein function in living organisms (Schulze, 2005).

Among the protein molecules detected in the current study is a protein of apparent molecular mass of approximately 130 kDa commonly observed as one of the major refractory proteins in all microbial samples (***Figures 6.3.1.2-3*** and ***6.3.2.1***). A homology search of the protein database indicated that this protein is a homologue of a subunit of the bacterial membrane protein, ATP-synthase of *Pseudomonas fluorescence*, the mass spectrum of which is presented in (***Figure 6.3.5.1***). Similar discoveries were made in DOM and soil leachate (Schulze, 2005). The ambient concentration of proteins in an environment would be a balance of the synthesis and degradation of that protein. Therefore, the detection of ubiquitous proteins such as aspartate carbamoyltransferase (***Figure 6.3.5.4***) may be due to a higher rate of synthesis rather than degradation, an equilibrium which favours net accumulation (Powell et al., 2005), or that these proteins are selectively preserved (by chemical or physical means) in the environment.

PMF results indicate protein homologues from two different taxonomic groups of bacteria. Proteins from the γ-proteobacteria were the most dominant in the samples (accounting for 6 samples), compared to a single protein homologue from the less well represented *firmicutes*. Interestingly, using 16S rRNA amplification and sequencing, we previously demonstrated that members of the *Proteobacteria* and *Firmicutes* sub-groups dominanted the culturable biomass of the source soil used in this study (***Chapter 2***). These results also demonstrate that protein analysis may be a suitable tool to study the contribution of microbial communities contributing to the refractory soil organic nitrogen (Schulze, 2005). However, it should be made clear that the results presented in this chapter do not quantify the number of species, but would more appropriately reflect the potential contribution of different phylogenetic groups to the refractory soil organic N pool, and the degradation dynamics of proteins.

We would like to argue that as a result of their vast biochemical significance, membrane protein and the enzymes identified in this study rendered them resistant to biodegradation and allowed them to persist over the degradation process. For example, the enzymes identified are versatile molecular switches, involved in the control of a wide range of biological processes - protein synthesis, signal transduction pathways, growth and differentiation. Moreover, they exhibit a variety of molecular structural features important for preservation. These include the presence of multiple complex sub-units with tight 3-D structures, highly conserved domains and motifs (consensus amino acid sequences), conserved aromatic amino acid residues (Phe) and large numbers of hydrophobic residues (e.g., Cys, Trp and Leu). It is also interesting to note, that some of these enzymes are associated with membrane lipids which may enhance their stability in the environment. Paradoxically, it would appear that some of these structural features (for example, the presence of Phr, Try and Cys) render theses proteins susceptible to UV degradation.

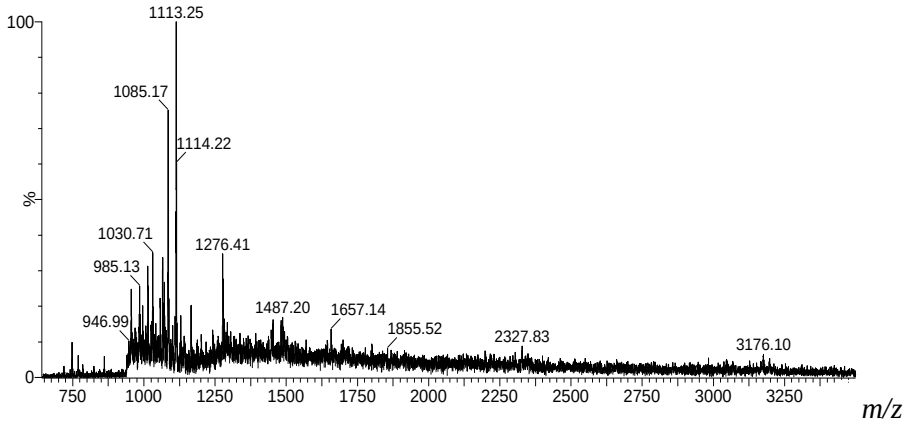

Figure 6.3.5.1: MALDI-TOF mass spectra of in-gel tryptic digested bio-refractory soil microbial (fragment 1; ***Figure 6.3.1.2***). The MALDI-peptide map of the fragment was subsequently identified as a homologue of the 130 kDa membrane protein ATP synthase alpha chain of *Pyrococcus abyssi* (***Table 6.3.5.1***).

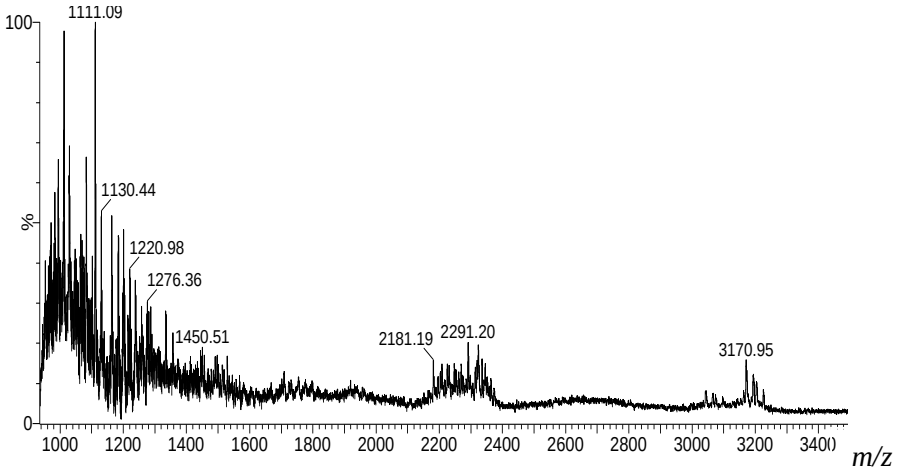

Figure 6.3.5.2: MALDI-TOF mass spectra of in-gel tryptic digested bio-refractory soil microbial (fragment 2; ***Figure 6.3.1.3***). The MALDI-peptide map of the fragment was subsequently identified as a homologue of the 66 kDa prtotein, Prolyl-tRNA synthetase of Gammaproteobacteria (***Table 6.3.5.1***).

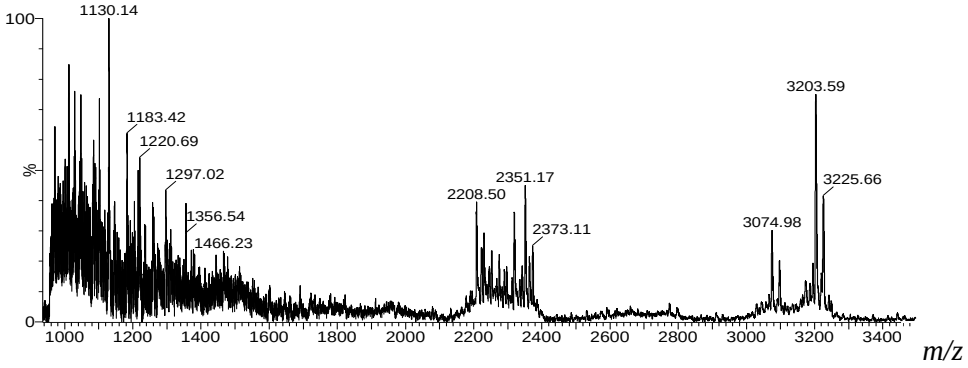

Figure 6.3.5.3: MALDI-TOF mass spectra of in-gel tryptic digested bio-refractory soil microbial (fragment 3; ***Figure 6.3.1.2***). The MALDI-peptide map of the fragment was subsequently identified as a homologue of the 50 kDa GTP-binding protein of Gammaproteobacteria (***Table 6.3.5.1***).

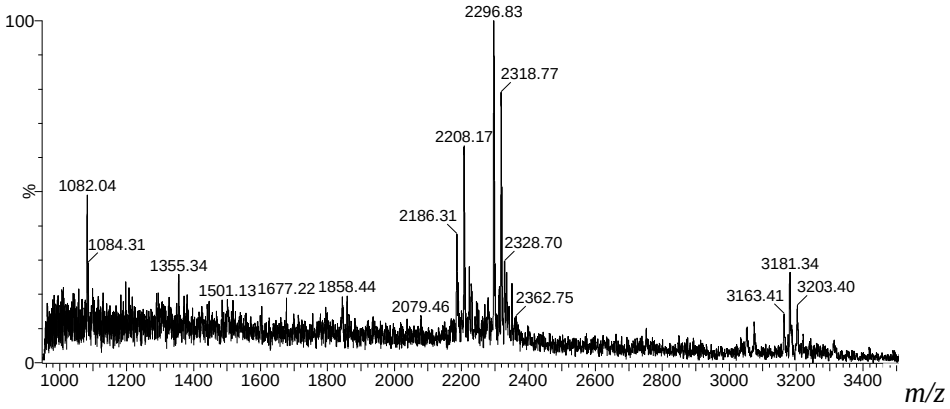

Figure 6.3.5.4: MALDI-TOF mass spectra of in-gel tryptic digested bio-refractory soil microbial (fragment 4; ***Figure 6.3.1.2***). The MALDI-peptide map of the fragment was subsequently identified as a homologue of the 36 kDa Aspartate carbamoyltransferase of Gammaproteobacteria (***Table 6.3.5.1***).

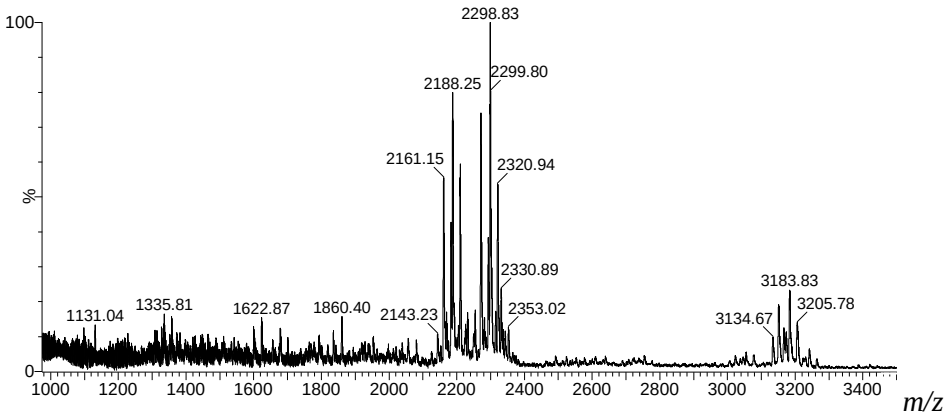

Figure 6.3.5.5: MALDI-TOF mass spectra of in-gel tryptic digested bio-refractory soil microbial (fragment 5; ***Figure 6.3.1.2***). The MALDI-peptide map of the fragment was subsequently identified as a homologue of the 30 kDa Indole-3-glycerol phosphate synthase of Gammaproteobacteria (***Table 6.3.5.1***).

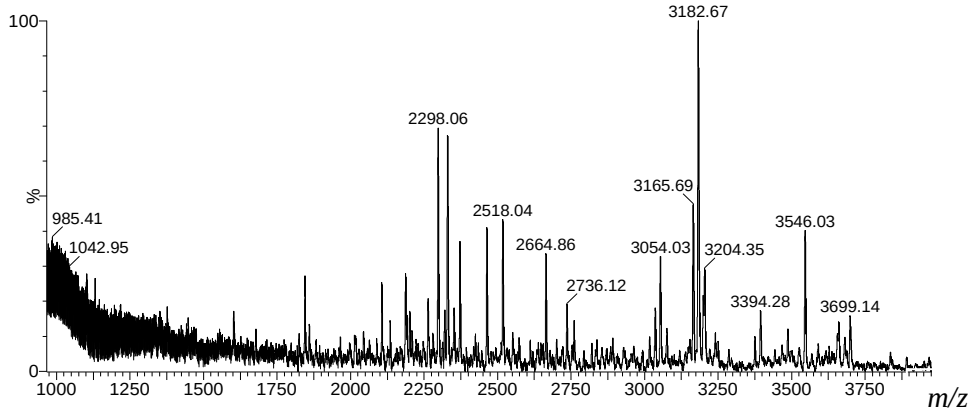

Figure 6.3.5.6: MALDI-TOF mass spectra of in-gel tryptic digested bio-refractory soil microbial (fragment 6; ***Figure 6.3.1.3***). The MALDI-peptide map of the fragment was subsequently identified as a homologue of the 17 kDa UPF0178 protein Mlg_1612 of Gammaproteobacteria (***Table 6.3.5.1***).

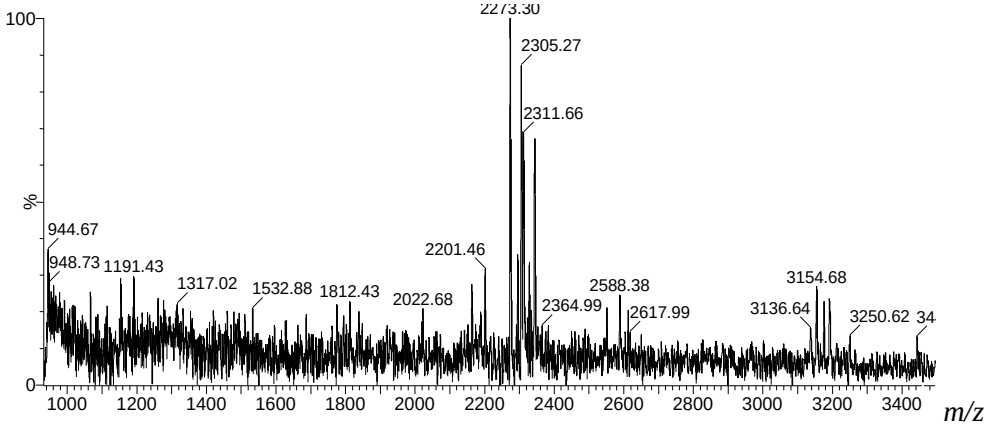

Figure 6.3.5.7: MALDI-TOF mass spectra of in-gel tryptic digested bio-refractory soil microbial (fragment 7; ***Figure 6.3.1.3***). The MALDI-peptide map of the fragment was subsequently identified as a homologue of the 17 kDa UPF0178 protein Mlg_1612 of Gammaproteobacteria (***Table 6.3.5.1***).

The minimum number of matching peptide masses required to unequivocally identify a protein in a database is 5 (Bienvenut, 2005). Although the peptide map of band number 6 (***Figure 6.3.1.3*** and ***Figure 6.3.5.6***) matched only 4 peptide masses of a protein in the database, it was judged to be a positive identification for the following reasons: (i) the match retrieved in the database was a bacterial protein, (ii) the apparent molecular mass of 16 kDa on the gel matched the calculated mass of 16.4 kDa of the protein (***Table 6.3.5.1***) and is within the mass accuracy of measurement from the gel, and (iii) all four matching peptides deviated from the calculated values 0.1 Da or less. Accurate mass determination of individual proteins in the protein mixtures yielded three distinct refractory proteins of molecular weights 31.1, 50.4 and 66.4 kDa (data not shown), and are in agreement the apparent molecular weights observed on 1-D SDS-PAGE. The deconvoluted mass of BSA used as reference was also confirmed to be 66.4 kDa (***Figure 6.3.5.8***).

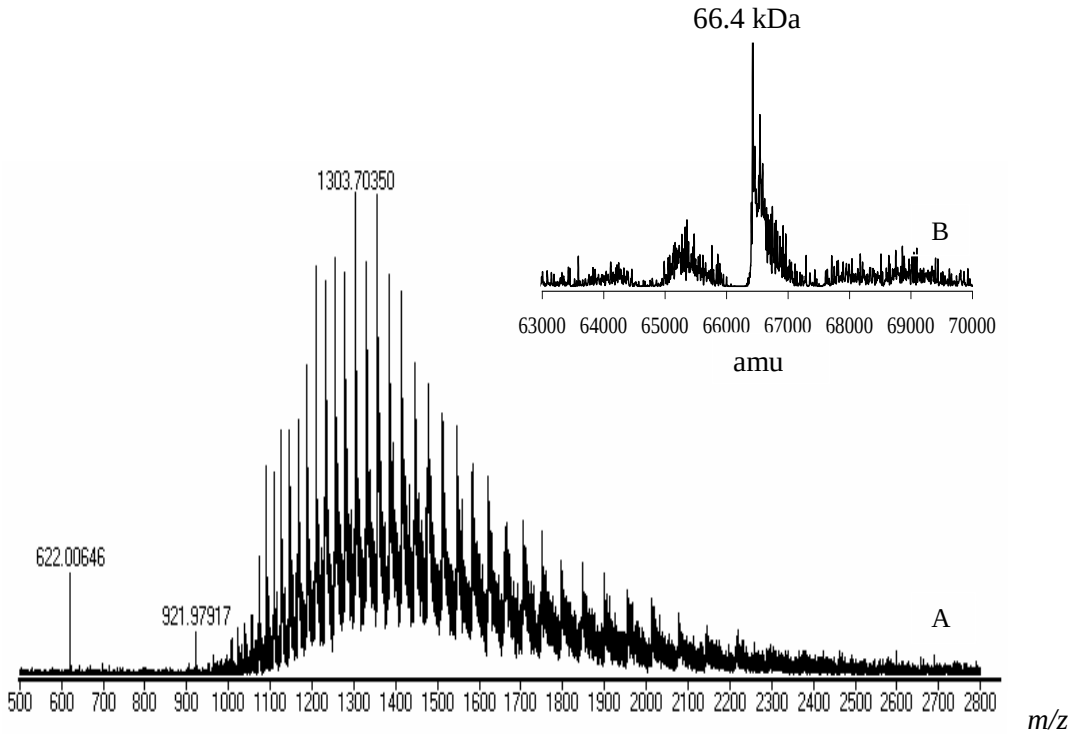

Figure 6.3.5.8: LC-ESI-TOF/MS mass spectra (A) and deconvoluted mass (B) of bovine serum albumen (BSA) used as reference in the mass determination of intact proteins studied. The 'envelope' observed (A) is typical of intact proteins, with peaks at lower *m/z* positioned at closer intervals. The deconvoluted mass of BSA was calculated 66.4 kDa.

Table 6.3.5.1: Identification of intact proteins from an ambient degradation study.

Band	Apparent MW, kDa	Protein Identified	MW calcd	Peptide matches	Coverage (%)
1	130	ATP synthase alpha chain (Pyrococcus)	114282	20	13
2	66	Prolyl-tRNA synthetase (γ-pb)	64607	16	28
3	50	GTP-binding protein (γ-pb)	49677	19	36
4	36	Aspartate carbamoyltransferase (γ-pb)	35328	12	35
5	30	Indole-3-glycerol phosphate synthase (γ-pb)	29695	13	39
6	17	UPF0178 protein Mlg_1612 (γ-pb)	16450	4	43
7	26	oxidoreductase (*Rhodococcus* spp)	26684	6	52

[a]Band numbers correspond to the gels in ***Figures 6.3.1.2-6.3.1.3***.
γ-pb = gama-proteobacteria.

Our results clearly demonstrate that there was rapid biodegradation of proteins in the microbial biomass and that the bulk of the microbial proteins were susceptible to biodegradation within the first six weeks of decomposition. This would suggest that there is the potential for rapid mineralization of microbially derived proteins (that are not physically protected) in soils. However, after six weeks the remaining proteins in the degraded microbial biomass appeared to be intrinsically stabilized. The presence of polymeric protein structures (enzymes and a single membrane protein) surviving the degradation process points to the intrinsic stability of microbially derived proteins within the non-living SOM. These results imply that microbially derived proteins represent an important fraction of the major stable N-compounds such as those found in HS. Identical NMR experiments revealed that there was no significant difference between the spectra of humic substances and a theoretical combination of plant and microbial biomolecules and their degradation products (Kelleher and Simpson, 2006). Similarly, evidence of enzymes and other protein-types have been found to survive over extended time spans in soil (Kincker, 2004).

There is also considerable evidence showing that photodegradation of microbial proteins within the first six weeks of the degradation process was rapid. However, unlike the ambient degraded biomass, we failed to detect distinct proteins (protein bands) stabilized as polymeric structures. This implies that microbially derived proteins void of physical protection in the top few millimeters of sparsely vegetated, arid and/or semi-arid soils are susceptible to rapid photomineralization. However, based on our findings**,** we deduced that clay minerals are capable of stabilizing microbially derived

proteins in SOM even under conditions of sustained UV degradation. This is consistent with the stabilizing effects of montmorillonite clay mineral on microbially derived OM, previously demonstrated in ***Section 4.3.5***. Furthermore, clay minerals are known to have catalytic properties (Hazen, 2001) and may catalyze the formation of HS in soil. Undoubtedly, one of the most significant findings is the large quantity of distinct intact proteins detected in the ambient and UV degraded microbial leachates (***Figure 6.3.1.3***). These findings support our previous interpretation of NMR spectroscopic data (***Chapter 3***) demonstrating the relative stability of significant quantities of microbially derived proteins in the leached materials.

There is clearly scope to consider the wider implications of these findings; however, our initial assessment is that clay minerals and the leaching of OM from the top surface of the soil to the subsoil are key factors in the sequestration and stabilization of microbially derived C and N. The significance of these results is amplified by the fact that microbially derived proteins play a more significant role in the soil C and N biogeochemical cycles than plant derived proteins because the protein content of microbes is about ten times higher than plants. Moreover, the stability of microbial proteins as well as bulk microbial-C in soil, which contains an abundance of microbial proteins, may be critical to understanding SOM stability as suggested by Miltner et al. (2009).

The biorefractory protein pool was dominated by proteins of the enzyme class, while the origin of the refractory proteins identified was predominantly gama-proteobacteria. This is not surprising since these organisms dominated our cultures (***Chapter 2***). Furthermore, these organisms are capable of utilizing a broad spectrum of growth substances and can grow well in the presence of other organisms and dominate most soils (Palleroni, 1992). The presence of a membrane protein among the identified proteins, as well as the protein size distribution indicate that the proteins in the samples are products of natural cell lysis as it occurs when cells and organisms die (Schulze, 2005). An important question surrounding the detection of proteins with enzymatic function in the degraded samples is whether these proteins are actually functional and could become actively involved in geochemical processes. The results of this and related studies could be applicable in the area of bio-prospecting. For example, it is possible that proteins and enzymes identified in soil microbial biomass may be linked to different biochemical pathways such as those involved in lignocellulosic decomposition.

Based on the ability of PMF to potentially identify different taxonomic groups of bacteria, the identified enzymes can be used to discern a particular microbial profile involved in lignocellulosic decomposition. Lignocelluloses decomposition is of huge importance since these compounds are highly refractory and are a major component in HS (Simpson et al., 2007). Moreover, microbes potentially involved in the degradation of these compounds have attracted particular interest in the production of biofuels.

7.4 Conclusions

The results presented in this study provide an insight into the fate of proteins from a mixed culture of soil microbial biomass, microbial leachates and clay microbial-complexes degraded under ambient and UV conditions. Vital clues about the composition of the refractory protein pool and their phylogenetic origin were also obtained. Here, we showed that a large proportion of the proteins in the microbial biomass were susceptible to biodegradation, while only a small number of proteins (5 proteins) survived the biodegradation process (membrane protein and enzymes). The stabilization of proteins may be due to selective preservation (stability conferred by 3-D structure of the protein) or chemical modification (for example through the association with carbohydrates and lipids). The primary structure (amino acid sequence) of the proteins is important in conveying protection imparted by the micro environment, supporting the hypothesis of selective preservation (Tanoue et al., 1996). Furthermore, outer membrane proteins may have an inherent natural protection to external degradation processes in order to survive exposure to the external environment and perform their physiological function (Powell et al., 2005).

In contrast, we did not observe any evidence of polymeric proteinaceous structures in the biomass following UV irradiation. Virtually all proteins were lost after only 6 weeks degradation. This would suggest that microbial proteins are highly vulnerable to photodegradation. However, it is interesting to note that extracts from clay-microbial complexes and microbial leachates degraded under ambient and UV conditions yielded several intact proteins of varying molecular weight, indicating that clay minerals and soil matrices are capable of protecting labile biomolecules from intense UV degradation. Moreover, the lower turnover rates of proteins from clay-microbial complexes and microbial leachates would suggest a greater contribution from

proteins to the formation of SOM in a clay environment, when compared to a clay-free environment. This discrepancy further underlines the importance of physical protection in the stabilization of the labile SOM pool. Greater quantities of proteins were detected in the leachates compared to the other degraded samples these results would suggest that the leachable C and N pools were not highly labile. This observation may have significant implications for the turnover of OM in the sub-soil.

6.5 References

Alberts, B., Barry, D., Lewis, J., Raff, M., Roberts, K., and Watson, J. D. 1994. *Molecular Biology of the Cell*, third Ed. Garland Publishing Inc., New York.

Baldock, J. A., and Skjemstad, J. O. 2000. Role of the soil matrix and minerals in protecting natural organic materials against biological attack. *Organic Geochemistry* 31, 697–710.

Bienvenut, W. V. (Ed). 2005. *Acceleration and improvement of protein identification by mass spectrometry*. Springer, Netherlands, pp. 189–224.

Bienvenut, W. V., Sanchez, J.-C., Karmime, A., Rouge, V., Rose, K., Binz, P-A., and Hochstrasser, D. F. 1999. Toward a clinical molecular scanner for proteome research: Parallel protein chemical processing before and during western blot. *Analytical Chemistry* 71, 4800–4807.

Caldwell, C. R. 1993. Ultraviolet-induced photodegradation of cucumber (*Cucumis sativus* L.) microsomal and soluble protein tryptophanyl residues in vitro. *Plant Physiology* 101, 947–953.

Clauser, K. R., Hall, S. C., Smith, D. M., Webb, J. W., Andrews, L. E., Tran, H. M., Epstein, L. B., and ALMA L. Burlingame, A. L. 1995. Rapid mass spectrometric peptide sequencing and mass matching for characterization of human melanoma proteins isolated by two-dimensional PAGE. *Proceedings of the National Academy of Science USA* 92, 5072–5076.

Demaneche, S., Jocteur-Monrozier, L., Quiquampoix, H., and Simonet, P. 2001. Evaluation of biological and physical protection against nuclease degradation of clay-bound plasmid DNA. *Applied and Environmental Microbiology* 67, 293–299.

Derenne, S., and Largeau, C. 2001. A review of some important families of refractory macromolecules: composition, origin, and fate in soils and sediments. *Soil Science* 166, 833–847.

Derenne, S., Largeau, C. and Berkaloff, C. 1996. First example of an algaenan yielding an aromatic-rich pyrolysate. Possible geochemical implications on marine kerogen formation. *Organic Geochemistry* 24, 617–627.

Derenne, S., Largeau, C. and Taulelle, F. 1993. Occurrence of non-hydrolysable amides in the macromolecular constituent of *Scenedesmus quadricauda* cell wall as revealed by ^{15}N NMR: origin of N-alkylnitriles in pyrolysates of ultralaminae-containing kerogens. *Geochimica et Cosmochimica Acta* 57, 851–857.

Doerr, S. H., Shakesby, R. A., and Walsh, R. P. D. 2000. Soil water repellency: its causes, characteristics and hydro-geomorphological significance. *Earth Science Reviews* 51, 33–65.

Feng, X., Simpson, A. J., and Simpson, M. J. 2006. Investigating the role of mineral-bound humic acid in phenanthrene sorption. *Environmental Science and Technology* 40, 3260–3266.

Hazen, R.M. 2001. Life's rocky start. *Scientific American*, April, 77–85.

Hecky, R. E., Mopper, K., Kilham, P., and Degens, E. T. 1973. The amino acid and sugar composition of diatom cell walls. *Marine Biology* 19, 323–331.

Keil, R. G., and Kirchman, D. L. 1993. Dissolved combined amino acids: chemical form and utilization by marine bacteria. *Limnology and Oceanogr*aphy 38, 1256–1270.

Kelleher, B. P., Simpson, A. J., Rogers, R. E., Dearman, J., and Kingery, W. L. 2007. Effects of organic matter from sediments on the growth of marine gas hydrates. *Marine Chemistry* 103, 237–249.

Kerwin, B. A., and Remmele, R. L. Jr. 2006. Protect from light: photodegradation and protein biologics. *Journal of Pharmaceutical Sciences* 96, 1468–1479.

Khanna, M., Yoder, M., Calamai, L., and Stotzky, G. 1998. X-ray diffractometry and electron microscopy of DNA bond to clay minerals. *Sciences of Soils* 3, 1–10.

Kindler, R., Miltner, A., Thullner, M., Richnow, H.-H., and Kästner, M. 2009. Fate of bacterial biomass derived fatty acids in soil and their contribution to soil organic matter. *Organic Geochemistry* 40, 29–37.

Kleber, M., Sollins, P., and Sutton, R. 2007. A conceptual model of organo-mineral interactions in soils: self-assembly of organic molecular fragments into zonal structures on mineral surfaces. *Biogeochemistry* 85, 9–24.

Knicker, H. 2004. Stabilization of N-compounds in soil and organicmatter-rich sediments – what is the difference? *Marine Chemistry* 92, 167–195.

Knicker, H. 2007. Vegetation fires and burnings: how do they affect the nature and stability of soil organic nitrogen and carbon? – a review. *Biogeochemistry* 85, 91–118.

Knicker, H., and Hatcher, P. G. 1997. Survival of protein in an organicrich sediment: possible protection by encapsulation in organic matter. *Naturwissenschaften* 84, 231–234.

Michalzik, B., and Matzner, E. 1999. Dynamics of dissolved organic nitrogen and carbon in a Central European Norway spruce ecosystem. *European Journal of Soil Science* 50, 579–590.

Miltner, A., Kindler, R., Knicker, K., Richnow, H-H, and Kästner, M. 2009. Fate of microbial biomass-derived amino acids in soil and their contribution to soil organic matter. *Organic Geochemistry* 40, 978–985.

Mopper, K., Zhou, X., Kieber, R. J., Kieber, D. I., Sikorski, R. J., and Jones, R. D. 1991. Photochemical degradation of dissolved organic carbon and its impact on oceanic carbon cycle. *Nature* 353, 60–62.

Murase, A., Yoneda, M., Ueno, R., and Yonebayyashi, K. 2003. Isolation of extracellular proteins from greenhouse soil. *Soil Biology & Biochemistry* 35, 733–736.

Nagata, T., Fukuda, R., Koike, I., Kogure, K., Kirchman, D. L. 1998. Degradation by bacteria of membrane and soluble protein in seawater. *Aquatic Microbiology Ecology* 14, 29–37.

Nguyen, R. T., and Harvey, H. R. 1997. Protein and amino acid cycling during phytoplankton decomposition in oxic and anoxic waters. *Organic Geochemistry* 27, 115–128.

Nguyen, R. T., and Harvey, H. R. 2001. Protein preservation in marine systems: hydrophobic and other non-covalent associations as major stabilizing forces. *Geochimica et Cosmochimica Acta* 65, 1467–1480.

Nguyen, R. T., and Harvey, H. R. 2003. Preservation via macromolecular associations during *Botryococcus braunii* decay: proteins in the Pula Kerogen. *Organic Geochemistry* 34, 1391–1403.

Nunn, B. L., Norbeck, A., and Keil, R. G. 2003. Hydrolysis patterns and the production of peptide intermediates during protein degradation in marine systems. *Marine Chemistry* 83, 1-2, 59–73.

Ogunseitan, O. A. 1993. Direct extraction of proteins from environmental samples. *Journal of Microbial Methods* 17, 273–281.

Palleroni, N. J. 1992. Introduction to the family Pseudomonadaceae. In: Balows, W., Trüper, H. G., Drowkin, M., Harder, W., and Schleifer, K.-H. (Eds.), *The prokaryotes*. Springer-Verlag, New York, N.Y., pp. 3071–3085.

Perkins, D. N., Pappin, D. J., Creasy, D. M., and Cottrell, J. S. 1999. Probability-based protein identification by searching sequence databases using mass spectrometry data. *Electrophoresis* 20, 3551–3567.

Powell, M. J., Sutton, J. N., Del Castillo, C. E., and Timperman, A. T. 2005. Marine proteomice: generation of sequence tags for dissolved proteins in sea water using tandem mass spectrometry. *Marine Chemistry* 95, 183–198.

Rillig, M. C., Caldwell, B. A., Wösten, H. A. B., and Sollins, P. 2007. Role of proteins in soil carbon and nitrogen storage: controls of persistence. *Biogeochemistry* 85, 25–44.

Roth, L. C., and Harvey, R. 2006. Intact protein modification and degradation in estuarine environments. *Marine Chemistry* 102, 33–45.

Schulze, W. X. 2005. Protein analysis in dissolved organic matter: what proteins from organic debris, soil leachate and surface water can tell us – a prospective. *Biogeosciences* 2, 75–86.

Schulze, W. X., Gleixner, G., and Kaiser, K. 2005. A proteomic fingerprint of dissolve organic carbon of soil particles. *Oecologia* 142, 335–343.

Shevchenko, A., Loboda, A., Ens, W., Schraven, B., Standing, K. G., and Shevchenko, A. 2001. Archived polyacrylamide gels as a resource for proteome characterization by mass spectrometry. *Electrophoresis* 22, 1194–1203.

Shevchenko, A., Loboda, A., Shevchenko, A., Ens, W., and Standing, K. G. 2000. MALDI quadrupole time-of-flight mass spectrometry: A powerful tool for proteomics research. *Analytical Chemistry* 72, 2132–2141.

Simpson, A. J., Simpson, M. J., Kingery, W, L., Lefebvre, B. A., Moser, A., Williams, A. J., Kvasha, M., and Kelleher, B. P. 2006. The application of ^{1}H high-resolution magic-angle spinning NMR for the study of clay–organic associations in natural and synthetic complexes. *Langmuir* 22, 4498–4508.

Simpson, A. J., Simpson, M. J., Smith, E., and Kelleher, B. P. 2007. Microbially derived inputs to soil organic matter: are current estimates too low. *Environmental Science and Technology* 41, 8070–8076.

Singleton, I., Merrington, G., Colvan, S., and Delahunty, J. S. 2003. The potential of soil protein-based methods to indicate metal contamination. *Applied Soil Ecology* 23, 25–32.

Spence, A., and Kelleher, B. P. 2008. Soil microbes and soil microbial proteins: interactions with clay minerals. *FEBS Journal* 275, Suppl. 1, 281.

Tanoue, E. 1995. Detectionof dissolved protein molecules in oceanic waters. *Marine Chemistry* 51, 239–252.

Tanoue, E., Ishir, M., and Midorikawa, T. 1996. Discrete dissolved and particulate proteins in oceanic waters. *Limnology and Oceanogr*aphy 41, 1334–1343.

Thiede, B., Lamer, S., Mattow, J., Siejak, F., Dimmler, C., Rudel, T., and Jungblut, P. R. 2000. Analysis of missed cleavage sites, tryptophan oxidation and N-terminal pyroglutamylation after in-gel tryptic digestion. *Rapid Communication in Mass Spectrometry* 14, 496–502.

von Lützow, M., Kögel-Knabner, I., Ekschmitt, K., Matzner, E., Guggenberger, G., Marschner, B., and Flessa, H. 2006. Stabilization of organic matter in temperate soils: mechanisms and their relevance under different soil conditions—a review. *European Journal of Soil Science* 57, 426–445.

West, C. M. 1986. Current ideas on the significance of protein glycosylation. *Molecular and Cellular Biochemistry* 72, 3–20.

Yamada, N., and Tanoue, E. 2003. Detection and partial characterization of dissolved glycoproteins in oceanic waters. *Limnology and Oceanogr*aphy 48, 1037–1048.

Yamashita, Y., and Tanoue, E. 2004. Chemical characteristics of amino acid-containing dissolved organic matter in seawater. *Organic Geochemistry* 35, 679–692.

Zang, X., Nguyen, R. T., Harvey, H. R., Knicker, H., and Hatcher, P. G. 2001. Preservation of proteinaceous material during the degradation of the green alga *Botryococcus braunii*: a solid state 2D ^{15}N ^{13}C NMR spectroscopy study. *Geochimica et Cosmochimica Acta* 65, 3299–3305.

Chapter 7

General Conclusions

7.1 General conclusions

In this project, we propagated isotopically enriched (^{13}C and ^{15}N) soil microbial biomass and characterized the community diversity and richness of the culturable biomass using 16S rRNA coupled with other molecular tools. We fully acknowledge that it is unlikely that cultivation-based diversity studies will reflect the true microbial community structure present *in situ* because of inherent qualitative and quantitative biases. However, Simpson et al. (2007) have demonstrated that the microbial signature of cultivable biomass is similar to that of microbes extracted from soils, and although only a small fraction of the total population can be cultured, the cultivable fraction is representative (at the biochemical input level) of the microbes that cannot be cultured. Moreover, Barbieri et al. (2007) suggested that the culturable soil microbial fraction can be considered as, and provide relative measures of the natural bacterial diversity in soils. Enriched microbial biomass, clay-microbial complexes and microbial leachates were incubated under ambient and intensive UV-A/UV-B radiation and the degradation dynamics of major biochemical components investigated. It is hoped that the results presented in this study will provide further understanding of the contribution of soil microbial biomass to key processes such as carbon and nitrogen cycling, OM adsorption and stabilization by clay minerals and their associated impacts on climate change and agricultural productivity. Due to the huge contribution of microbial input in soils, ultimately we want to know if its degradation pathways are different from that of plant materials.

Isotopic enrichment of biomass leachates combined with HR-MAS significantly enhances the detection limits, and provides a great deal of information that is unattainable by any other method. Through the application of 1-D and 2-D NMR approaches, we were able to identify specific structural units and determine how the different biochemical categories change structurally with time. The chemical compositions of the initial and degraded microbial biomass showed that bacterial carbon was dominated by alkyl-C (aliphatic), but also contained substantial amounts of carbonyl-C and O-alkyl-C attributed to carbohydrates. It is evident that as degradation of the biomass proceeded, the amount of aliphatic-C increased relative to other biochemical classes, suggesting that these compounds were selectively preserved. Proteins/peptides were significantly degraded under both conditions (complementary evidence provided by SDS-PAGE); however, the detection of intact proteinaceous

materials in the ambient degraded biomass is indicative of selective preservation, possibly from chemical modifications such as phosphorylation or glycosylation. The possibility also exists that protein/peptide materials are simply a component of microbial biomass feeding on the degraded material. The major form of organic N detected in all samples was by protonated amide-N which has been demonstrated to be highly refractory (Knicker et al., 1996; Knicker, 2000).

These results are consistent with plant decomposition studies carried out by Kelleher et al. (2006) who demonstrated that proteinaceous materials and carbohydrate-C are either mineralised or assimilated at a faster rate than the more recalcitrant aliphatic-C and aromatic species during the decomposition process. Protonated amide-N was the major form of organic ^{15}N in the fresh and degraded plant materials and exhibited a high degree of recalcitrance throughout the degradation process. Based on these findings, it is tempting to suggest that there is a degree of similarity between the degradation pathways of plant materials and soil microbial biomass, or at least the major biochemical classes. Furthermore, the conventional view that soil microbial biomass is often associated with the labile and readily degradable components was recently challenged and it has been demonstrated that much larger contributions of microbial peptide/protein are found in the HS fraction of soil OM than was previously thought (Simpson et al., 2007).

It has been demonstrated that intact and degraded microbial biomass account for more than half of the organic material in soils (Simpson et al., 2007). Furthermore, the chemical dynamics of OM in the subsoil where leached materials often accumulate has not been investigated in detail and it has become clear that OM in these strata may represent a significant proportion of the total amount of carbon sequestered in soils. As a consequence, the study of microbial leachates provided an important opportunity to expand our knowledge of this area. The chemical composition of the degraded microbial leachates showed that bacterial carbon was dominated by aliphatic-C after 6 weeks, with substantial contributions from carbohydrates and carbonyl-C. The carbohydrate and carbonyl biochemical pools are particularly significant as these compounds have the tendency to be more mobile in the soil environment and thus are more susceptible to leaching from soil down to the groundwater. However, the ability of carboxyl groups to interact with solutes, colloids and soil, may strongly resist their mobility in soil under conditions favourable for sorption onto soil surfaces (Kaiser et al., 2001). Interestingly,

after 14 weeks degradation, the microbial leachates were dominated by carbohydrate-C (increasing relatively after 6 weeks), and a simultaneous decrease in aliphatic-C by approximately 19%. These findings are not consistent with the general literature on carbohydrate and lipid degradation, and may be explained by the stabilization (physically and chemically) and microbial synthesis of O-alkyl-C (carbohydrates) and the degradation of labile lipids.

Another very intriguing observation is the amount of intact proteinaceous materials detected in both the ambient and UV degraded leachates. This is consistent with literature reports of a significant microbial contribution to peptide/protein in HS fractions from soils (Simpson et al., 2007). The fact that these labile biomolecules survived microbial and UV degradation may be due to selective preservation, most likely from long-term protein-dissolved OM, encapsulation or physical protection from interactions with clay mineral during leaching. The detection of natural silicate species in the NMR spectra of microbial leachates is also of huge significance, suggesting that soil microorganisms are capable of accumulating stable amounts of silicon and may play a more vital role in silicon cycling than currently thought. This is particularly important from the standpoint that carbon sequestration in the ocean has been linked with the global cycling of silicon (Tréguer et al., 1995). Novel degradation products in the form of peptides were observed in the leachate after 14 weeks under UV degradation, which is an indication of the possible effects of increased UV-radiation reaching the Earth's surface. Undoubtedly, the results of these and future studies will be useful proxies in understanding SOM turnover, C and N cycling. This is possible as different stages of SOM degradation can be used to extract yields of organic components and this information can then be extrapolated to predict degradation pathways and differences in OM composition as a result of climate change (Otto et al., 2005).

The importance of the study of the cycling of microbially derived P compounds has been previously mentioned. In this study, two major P forms; inorganic P dominated by orthophosphate P (the dominant P form in all samples) and organic P dominated by orthophosphate monoesters were detected in the initial and degraded biomass. Another form of microbial organic P is orthophosphate diesters (composed of DNA, RNA and phospholipids) which were found to be highly susceptible to microbial and photolytic degradation and alkaline hydrolysis during sample preparations and acquisition. It is believed that the decomposition of labile diesters such as RNA may contribute to the

signals assigned to orthophosphate monoesters (observed only at 6 weeks of decomposition). Unfortunately, alkaline extraction is necessary for the extraction of P compounds for solution ^{31}P-NMR spectroscopy. A consequence of the chemical lability of some organic P compounds is that it adds a degree of complexity to any quantitative investigation of these compounds. It should be noted that there was no apparent difference in the degradation dynamics of the ^{31}P-NMR of alkaline extracts of the samples degraded under ambient conditions when compared with those degraded under UV conditions. While we were able to make a clear distinction between the refractory and labile microbial P pool, to improve our understanding of the P cycle, separate investigations are now required to probe the coupled C-P biogeochemical cycles.

It is generally accepted that soil minerals provide extensive surface area that strongly influences the adsorption and stabilization of SOM. However, the exact mechanisms of adsorption and stabilization are not clear. As a result, there is a greater need for a mechanistic understanding of the sorption of OM (the largest C fraction of the global C pool) which is critical to predict the response of the soil C pool to the increase atmospheric CO_2. Different types of clays exhibit different sorption characteristics. For example, in this study, montmorillonite adsorbed greater quantities of microbes and microbial proteins than kaolinite clay mineral. These findings are in agreement with Feng et al. (2005) who showed that montmorillonite displayed a higher uptake of peptide/proteins when compared with kaolinite. There is also evidence to suggest that microbial products and proteins intercalated, but did not saturate the interlamellar layers of montmorillonite, while adsorption was restricted to the external surfaces of kaolinite.

The application of advanced NMR approaches and FT-IR spectroscopy (data not shown) provided vital clues into the mechanisms of sorption of OM to clays. There is evidence to suggest that aliphatic groups (especially long-chained polymethylene [$(CH_2)n$] groups) preferentially bind to montmorillonite surfaces in the presence of carbohydrates and proteins as has been suggested by other studies (Feng et al., 2006; Simpson et al., 2006). We believe that cation bridging followed by hydrophobic interactions between the $RCOO^-$ groups of aliphatic-C with Al ions in clay, were the primary mechanisms involved in the formation of clay-organo complexes. However, no single mechanism can adequately explain the formation of clay-organo complexes, suggesting the involvement of other mechanisms such as multilayer sorption of fatty

acids, hydrogen bonding between the carboxylic groups of free fatty acids and by van der Waals attraction. Carbohydrates were also strongly adsorbed to clay and were probably facilitated by bacterial EPS and hydrogen bonding. Proteins were also critical in the formation of clay-complexes. However, given the diversity of the functional groups in a protein molecule, several mechanisms including electrostatic interactions, ligand exchange and physisorption may be involved. The 'zonal effect' phenomenon was also observed as a possible mechanism of sorption.

Individual microbial biomolecules (lipids, amino acids and proteins) were extracted from the initial and degraded samples to provide further insights into the transformation dynamics of soil microbial biomass. A broad range of extractable fatty acid methyl esters of varying chain lengths and chemistry were obtained for the initial and degraded biomass. The samples revealed a dominance of saturated, even-carbon-number fatty acids, particularly hexadecanoic and octadecanoic acids. Some polysaccharides and phytol were also extracted. Our results suggest that the solvent extractable organic compounds present in the source biomass undergo various degradation processes and most of the lipid classes and carbohydrates were rapidly degraded. The *n*-alkanes, alkenes and PUFAs were the most labile lipids, most showing near complete degradation after 6 weeks. Some of the mechanisms emphasized include hydroxylation and cleavage of double bonds via radical reactions and the migration of radicals to positions nearer to carboxylic groups. Some oxidation reactions may also be involved in the process. Several factors were implicated in the observed degradation of fatty acid methyl esters, including molecular structure, degree of unsaturation and chain length. A degree of homogeneity in the characteristic distribution of fatty acids, amino acids and amino sugars was observed between ambient and UV degraded biomass. However, few important differences have been noted between the compositions of the samples degraded under the above conditions. These observations suggest that one or several of the following processes are occurring under UV degradation: (i) complete mineralization; (ii) photochemical alteration to form modified compounds; or (iii) condensation of these compounds to form non-volatile constituents that are intractable by GC-analyses.

We speculate that oxidation and heterolytic cleavage are likely to be two of the major mechanisms involved in the auto- and photoxidation of microbial biomass and clay-microbial complexes leading to the production of several degradation products.

However, we failed to detect a number of oxidation products in the degraded samples corresponding to some of the fatty acids detected in the un-degraded samples. This is possibly due to (i) the instability of the hydroperoxides formed, (ii) the involvement of cross-linking reactions (after homolytic cleavage) leading to the formation of maromolecular structures non-amenable to gas chromatography, or (iii) the protective influence of clay minerals against auto- and photooxidation processes. These findings will undoubtedly add to our understanding of the contributions of soil microbial biomass to SOM and its contribution to global C cycling. This is particularly important in the light of global warming as an increase in auto- and photoxidation coupled with a high degree of unsaturation will lead to a considerable amount of microbial oxidation products in soil environments. It is clear that a mixture of photoxidation and autoxidation products are present in the solvent extracts of UV degraded microbial biomass and microbial leachates. It should also be noted that the bio-degraded and UV-irradiated profiles were not easily discriminated, and no unique degradation products were identified that could be used as indicators of elevated photo-exposure.

Protein degradation is an important process in the turnover of nitrogen in soils. The degradation of proteins in the environment is assumed to occur independently of the source origin of proteins, but proteins of scarce organisms may be harder to detect as they may be diluted in the bulk of proteins from more abundant organisms (Schulze et al., 2005). Despite this limitation, the analysis of protein identity can improve our understanding of the functional protein composition of organic carbon and nitrogen, and at the same time yield clues to the phylogenetic groups contributing to the refractory protein pool in the environment (Schulze, 2005; Schulze et al., 2005).

In this study, the rate of protein degradation appeared to be rapid over the first six weeks, but was significantly slower over the remainder of the degradation period, and the pattern of degradation also appeared to be uniform across the ambient degraded microbial biomass. A characteristic electrophoretic pattern revealed that proteins with apparent molecular masses of ~250, 110, 50, 36 and 32 kDa were selectively preserved across these samples. A number of mechanisms of preservation have been suggested previously. In contrast, no distinct protein was observed in the UV degraded samples. However, it should be noted that proteins extracted from clay-microbial complexes degraded under UV conditions revealed distinct protein molecules, which is suggestive of their stability. Equally, a number of discrete proteins were observed in the ambient

and UV degraded microbial leachates, most likely stabilized by mineral particles during leaching. Proteins with apparent molecular masses of 130, 36 and 30 kDa were clearly visible as the major refractory proteins in the differentially degraded biomass and microbial leachates. Our results further demonstrate that photochemical degradation has an important role in the cycling of biologically refractory soil microbial components. This role is likely to become more important in the future as depletion of atmospheric ozone increases the solar UV-B flux (Mopper et al., 1991). PMF investigations revealed that the selectively preserved proteins belong to the enzymatic and membrane protein classes.

7.2 References

Barbieri, E., Guidi, C., Bertaux, J., Frey-Klett, P., Garbaye, J., Ceccaroli, P., Saltarelli, R., Zambonelli, A., and Stocchi, V. 2007. Accurance and diversity of bacterial communities in *Tuber magnatum* during truffle maturation. *Environmental Microbiology* 9, 2234–2246.

Feng, X., Simpson, A. J., and Simpson, M. J. 2005. Chemical and mineralogical controls on humic acid sorption to clay mineral surfaces. *Organic Geochemistry* 36, 1553–1566.

Feng, X., Simpson, A. J., and Simpson, M. J. 2006. Investigating the role of mineral-bound humic acid in phenanthrene sorption. *Environmental Science and Technology* 40, 3260–3266.

Kaiser, K., Guggenberger, G., Haumaier, L., and Zech, W. 2001. Seasonal variation in the chemical composition of dissolved organic matter in organic forest floor layer leachates of old-growth Scots pine (*Pinus sylvestris* L.) and European beech (*Fagus sylvatica* L.) stands in northeastern Bavaria, Germany. *Biochemistry* 55, 103–143.

Kelleher, B. P., Simpson, M. J., and Simpson, A. J. 2006. Assessing the fate and transformation of plant residues in the terrestrial environment using HR-MAS NMR Spectroscopy. *Geochimica et Cosmochimica Acta* 70, 4080–4094.

Knicker, H. 2000. Biogenic nitrogen in soils as revealed by solidstate carbon-13 and nitrogen-15 nuclear magnetic resonance spectroscopy. *Journal of Environmental Quality* 29, 715–723.

Knicker., H., Scaroni, A. W., and Hatcher, P. G. 1996. ^{13}C and ^{15}N NMR spectroscopic investigation on the formation of fossil algal residues. *Organic Geochemistry* 24, 661–669.

Mopper, K., Zhou, X., Kieber, R. J., Kieber, D. I., Sikorski, R. J., and Jones, R. D. 1991. Photochemical degradation of dissolved organic carbon and its impact on oceanic carbon cycle. *Nature* 353, 60–62.

Otto, A., Chubashini, S., and Simpsom, M. J. 2005. A comparison of plant and microbial biomarkers in grassland soils from the Prairie Ecozone of Canada. *Organic Geochemistry* 36, 425–448.

Schulze, W. X. 2005. Protein analysis in dissolved organic matter: what proteins from organic debris, soil leachate and surface water can tell us – a prospective. *Biogeosciences* 2, 75–86.

Schulze, W. X., Gleixner, G., and Kaiser, K. 2005. A proteomic fingerprint of dissolve organic carbon of soil particles. *Oecologia* 142, 335–343.

Simpson, A. J., Simpson, M. J., Kingery, W, L., Lefebvre, B. A., Moser, A., Williams, A. J., Kvasha, M., and Kelleher, B. P. 2006. The application of ^{1}H high-resolution magic-angle spinning NMR for the study of clay–organic associations in natural and synthetic complexes. *Langmuir* 22, 4498–4508.

Simpson, A. J., Simpson, M. J., Smith, E., and Kelleher, B. P. 2007. Microbially derived inputs to soil organic matter: are current estimates too low? *Environmental Science and Technology* 41, 8070–8076.

Tréguer, P., Nelson, D. M., and Van Bennekom, A. J. 1995. The silica balance in the world ocean: a reestimate. *Science* 268, 375–379.

Appendix

List of abbreviations

$(^{15}NH_4)_2SO_4$	heavy nitrogen isotope labelleg ammonium sulphate
(*E*)	trans
(*Z*)	cis
$[(CH_2)_n]$ C	polymethylenic carbon
~	approximately
°2θ	two degrees theta
‰	per mil
1°2θ/min	one degree two theta per minute
^{13}C HSQC	heavy carbon isotope Heteronuclear Single-Quantum Correlation spectroscopy
^{13}C	heavy carbon isotope
^{13}C-^{13}C	^{13}C-^{13}C Chemical Shift
^{14}C	radiogenic carbon isotope
1525r	1525 reverse
^{15}N	heavy nitrogen isotope
16S rRNA	16S ribosomal ribonucleic acid
1-D ^{13}C NMR	one-dimensional carbon Nuclear Magnetic Resonance
1-D ^{1}H	one-dimensional proton Nuclear Magnetic Resonance
^{1}H HR-MAS	proton High resolution Magic Angle Spinning
^{1}H NMR	proton Nuclear Magnetic Resonance
^{1}H-^{13}C	^{1}H-^{13}C Chemical Shift
^{1}H-^{15}N	^{1}H-^{15}N Chemical Shift
$^{1}O_2$	singlet oxygen
1x TAE	1x concentration Tris-acetate-EDTA
1x	1x concentration
27f	27 forward
2-D ^{13}C NMR	two-dimensional carbon Nuclear Magnetic Resonance
2-D ^{15}N NMR	two-dimensional nitrogen Nuclear Magnetic Resonance

2-D HSQC	two-dimensional Heteronuclear Single-Quantum Correlation spectroscopy
3'-	3 prime
^{31}P NMR	phosphorus Nuclear Magnetic Resonance
3-D	three dimensional
5'-	5 prime
Å	Angstrom
ACCA	α-cyano-4-hydroxycinnamic acid
ACD	Advanced Chemistry Development
ADEQUATE	Abundance Double Quantum Transfer Experiment
ADP	adenosine diphosphate
AHY	acid hydrolysis
Arg (R)	argentine
ATP	adenosine triphosphate
BLAST	Basic Local Alignment Search Tool
BSA	Bovine Serum Albumen
BSTFA	*N*,*O*-*bis*-(trimethylsilyl)trifluoroacetamide
Bt	*Bacillus thuringiensis*
c	cis
C=O	carbonyl group
CEC	cationic exchange capacity
CH_2	methylene
CH_3	methyl
C_{max}	carbon maximum
CMS	Clay Mineral Society
COO^-	carboxylate ion
CP MAS	Cross Angle Polymerization Magic Angle Spinning
C-P	carbon-phosphorus linkage
Cu-K_α	cupper-K_{alpha}
Cys (C)	cysteine
Cys–Cys	cysteine
$d_{(001)}$	basal reflection
D_2O	deuterated water
D-Asp (D)	D-aspartic acid
DE-NMR	Diffusion Edited Nuclear magnetic Resonance

D-Glu (E)	D-glutamic acid
D-Gly (G)	D-glycine
D-His (H)	D-histidine
D-Ile (I)	D-isoleucine
D-Leu (L)	D-leucine
D-Lys (K)	D-lysine
DMSO-d_6	deuterated Dimethyl sulfoxide
DNA	deoxyribonucleic acid
DNB	dilute nutrient broth
dNTPs	deoxynucleotides
DOC	dissolved organic carbon
DOM	dissolved organic matter
D-Phe (F)	D-phenylalanine
D-Pro (P)	D-proline
D-Ser (S)	D-serine
D-Thr (T)	D-threonine
DTT	1,4-dithio-DL-threitol
D-Tyr (Y)	D-tyrosine
D-Val (V)	D-valine
EDTA	ethylenediaminetetraacetic acid
$EDTANa_2 \cdot H_2O$	sodium ethylenediaminetetraacetic acid·monohydrate
EI	electron ionization
EPS	extracellular polymeric substances
ESI	electrospray ionization
EU	European Union
eV	electron voltave
Fe^{2+}	ferrous ion
FT-IR	Fourier Transform Infrared
GC-IR-MS	gas chromatography isotope ratio mass spectrometry
GC-MS	gas chromatography mass spectrometry
Glu (E)	glutamic acid
Gt	gigatons
HMQC	Heteronuclear Multiple-Quantum Correlation spectroscopy
HS	humic substances
HSQC	Heteronuclear Single Quantum Coherence

i.d.	identification
INADEQUATE	Incredible Natural Abundance Double Quantum Transfer Experiment
IPCC	Intergovernmental Panel on Climate Change
Kb	Kilo base
kDa	kilo Dalton
keV	electron voltage
kV	kilo voltage
LB	Lysogeny broth/Luria broth/Luria-Bertani broth
LC-TOF/MS	liquid chromatography time of flight mass spectrometry
Lys (K)	lysine
m/z	mass-to-charge ration
mA	milliamps
MALDI-TOF/MS	matrix assisted laser desorption ionization time of flight mass spectrometry
MS	mass spectra
MS/MS	mass spectrometer coupled mass spectrometer
MSD	mass selective detector
MSDB	Mass Spectra Database
n-	normal
N	number of replicates
Na_2SO_4	sodium sulphate
NaOH-EDTA	sodium hydroxide- ethylenediaminetetraacetic acid
NCBI	National Centre for Biotechnology Information
NIST	National Institute of Standards and Technology
NJ	Neighbour Joining
NMR	Nuclear Magnetic Resonance
OM	organic matter
PAUP	Phylogenetic Analysis Using Parsimony
PCR	Polymerase Chain Reaction
PG	N-acetyl peptidoglycan
Phe (F)	phenylalanine
Pi	inorganic orthophosphate
p*I*	isoelectric point
PL	phospholipids

PLFAs	phospholipid fatty acids
PMF	peptide mass fingerprinting
POM	particulate organic matter
PPE	terminal phosphorus in the polyphosphate chain
PUFA	poly unsaturated fatty acid
PVDF	Polyvinylidene Fluoride
RDP	Ribosomal Database Project
RNA	ribonucleic acid
RP-HPLC	Reversed Phase High Performance Liquid Chromatography
RT	room temperature
S	sulfer
S_ab	binary association coefficient
SDS-PAGE	sodium dodecyl sulfate polyacrylamide gel electrophoresis
SEM-EDS	scanning electron microscopy energy dispersive X-ray s pectrometer
SOM	soil organic matter
spp.	species
T	Telsa
t	trans
THCL	Teagasc heavy clay-loam
TIC	total ion chromatogram
TlCL	Teagasc light clay-loam
TMS	Tetra Methyl Silane
TMS	trimethylsilyl
TOCSY	Total Correlation Spectroscopy
TPPI	Time-Proportional Phase Incrementation
Tris-HCL	Tris-hydrochloric acid
Trp (W)	tryptophan
Tyr (Y)	tyrosine
U	units
UV-A	ultraviolet-A
UV-B	ultraviolet-B
v/v	volume to volume
wt/vol	weight to volume
xg	gravity

XRD	X-ray diffraction
α-	alpha
β -	beta
γ-	gama
Δ	double bon position as enumerated from the carboxyl end
$\delta^{13}C$	isotopic signature/delta notation
ω-	omega